Végétation, climat et sociétés humaines du bassin Méditerranéen du Tardiglaciaire à l'Holocène : approche multi-proxy (pollen, NPP, brGDGT, XRF) de l'Italie (Lac Matese) à l'Arménie (Lac Sevan)

Mary Robles

THÈSE POUR OBTENIR LE GRADE DE DOCTEUR DE L'UNIVERSITÉ DE MONTPELLIER

En EERGP – Ecologie, Evolution, Ressources Génétiques, Paléobiologie

École doctorale GAIA – Biodiversité, Agriculture, Alimentation, Environnement, Terre, Eau

Unité de recherche – Institut des Sciences de l'Évolution de Montpellier – UMR 5554

En partenariat international avec l'Université de Molise, Campobasso, Italie

Végétation, climat et sociétés humaines du bassin méditerranéen du Tardiglaciaire à l'Holocène : approche multi-proxy (pollen, NPP, brGDGT, XRF) de l'Italie (lac Matese) à l'Arménie (lac Sévan)

Présentée par Mary ROBLES

Le 12 juillet 2022

Sous la direction d'Odile PEYRON, Elisabetta BRUGIAPAGLIA, Sébastien JOANNIN et Guillemette MENOT

Devant le jury composé de

Mr. Vincent LEBRETON, Professeur, Muséum national d'Histoire naturelle	Rapporteur
Mme. Laura SADORI, Professeure, Università di Roma "La Sapienza"	Rapportrice
Mr. Gonzalo JIMENEZ-MORENO, Professeur assistant, Universidad de Granada	Examinateur
Mme. Marie-Alexandrine SICRE, Directrice de recherche CNRS, Sorbonne Université	Examinatrice
Mr. Giuseppe MAIORANO, Professeur, Università degli Studi del Molise	Examinateur
Mme. Odile PEYRON, Directrice de recherche CNRS, Université de Montpellier	Co-directrice
Mme. Elisabetta BRUGIAPAGLIA, Professeure associée, Università degli Studi del Molise	Co-directrice
Mr. Sébastien JOANNIN, Chargé de Recherche CNRS, Université de Montpellier	Co-encadrant

UNIVERSITÉ DE MONTPELLIER

UNIVERSITÀ DEGLI STUDI DEL MOLISE

Department of Agricultural, Environmental and Food Sciences

PhD Course in:

AGRICULTURE TECHNOLOGIES AND BIOTECHNOLOGIES

(CURRICULUM: SUSTAINABLE PLANT PRODUCTION AND PROTECTION)

In cotutelle with the University of Montpellier

CYCLE (XXXIV)

Related Disciplinary Scientific Sector: BIO/03

PhD Thesis

Vegetation, climate, and human history of the Mediterranean basin: A Lateglacial to Holocene reconstruction from Italy (Lake Matese) to Armenia (Lake Sevan) inferred from a multi-proxy approach (pollen, NPPs, brGDGTs, XRF)

Coordinator of the PhD course: Prof. Giuseppe MAIORANO

Supervisors: Prof. Elisabetta BRUGIAPAGLIA and Prof. Odile PEYRON

Co-supervisors: Prof. Sébastien JOANNIN and Prof. Guillemette MENOT

PhD Student: Mary ROBLES
164235

Academic Year 2020/2021

ACKNOWLEGMENTS

Je souhaite dans un premier temps remercier les membres du jury d'avoir accepté d'évaluer mes travaux de thèse et pour les riches discussions lors de la soutenance de thèse. Je remercie également les membres de mon comité de suivi de thèse pour les différents échanges toujours très constructifs, pour votre écoute et votre bienveillance.

Je voudrais tout particulièrement remercier mes directeurs et encadrants de thèse, Odile Peyron, Sébastien Joannin, Elisabetta Brugiapaglia, Guillemette Ménot qui m'ont donné l'opportunité d'étudier l'histoire des montagnes dans la zone méditerranéenne, un milieu qui m'est cher. Merci de m'avoir donné l'opportunité d'apprendre et de comprendre un peu plus le monde qui nous entoure. J'ai eu un sujet passionnant et j'ai adoré mener ce projet au cours de ces trois dernières années. Merci de m'avoir permis de mener à bien ce sujet, merci pour votre suivi, vos soutiens et vos encouragements tout au long de mon parcours. Sébastien, merci de m'avoir formé à la paléoécologie (terrain, datation, pollen, NPP, géochimie, sédimentologie), pour ton recul sur les données, pour ton soutien indéfectible, pour ton coaching pour respecter les plannings et éviter mon côté perfectionniste, pour ta bienveillance, pour nos échanges scientifiques. Odile, merci de m'avoir formé aux fonctions de transfert et à l'interprétation des données climat, merci pour ta bienveillance, pour ton soutien indéfectible, pour nos échanges, pour ta confiance et d'avoir su gérer d'une main de fer les nombreux problèmes administratifs. Elisabetta, merci de m'avoir formé à l'identification des pollen, pour nos échanges, pour ton soutien et d'avoir su patiemment gérer tout le côté administratif du côté italien. Guillemette, merci de m'avoir formé aux GDGTs, de m'avoir accueilli dans ton laboratoire, pour ton soutien et pour nos nombreux échanges scientifiques. Je n'aurais pas pu imaginer mieux comme encadrement, merci à vous !

Je tiens aussi à remercier toute l'équipe de l'ISEM ! Merci de m'avoir fait découvrir la paléoécologie en L3 avec l'UE ORPAL et avec le master CEPAGE, merci tout particulièrement à Jean-Fred, et Vincent. Merci à Laurent de m'avoir donné l'opportunité de travailler sur les savanes du Gabon au cours de deux stages (L2, M1), et à Serge de m'avoir fait découvrir l'étude des pollen au cours d'ORPAL et d'un stage en L3. Merci d'avoir contribué à ce que mes années universitaires soient si passionnantes et de m'avoir donné l'envie de continuer en paléoécologie ! Merci à toutes les personnes de l'ISEM qui m'ont aidé au cours de ces dernières années à l'ISEM ! Merci tout particulièrement à Bertrand qui a été toujours été là pour moi depuis 2015 à chacun de mes stages, d'abord au CBAE puis à l'ISEM, merci pour ta

bienveillance, pour ta gentillesse, pour nos échanges et pour ta bonne humeur !! Merci à Laurent et Isabel, merci pour votre aide lors de la préparation des échantillons pour les datations, pour nos discussions et nos échanges. Merci Séverine de m'avoir aidé lors de mes multiples problèmes administratifs, merci pour ta bienveillance et ton soutien ! Merci à Alloween, Lucie, Christelle pour nos discussions et nos échanges ! Merci à Sarah de m'avoir aidé de multiples fois, pour ta bonne humeur et ton enthousiasme ! Merci à Chantal d'avoir dû gérer mes innombrables missions, toujours avec le sourire et la bonne humeur ! Merci à Benoit et Thierry de m'avoir aidé à préparer le terrain en Italie ! Merci à Sylvie de toujours faire le maximum pour les étudiants avec bienveillance, respect et enthousiasme !

Je tiens tout particulièrement à remercier, mes amis, mes co-bureaux, doctorants et post-doctorants que j'ai pu rencontrer au cours de ma thèse. Merci à la « première génération » de doctorants, merci à Chéïma, Gwen, Marion, Boris, Dorian, Lucas, Marine D., Stéphanie, Marianne, merci pour toutes les discussions, les rires, les moments de complicité, les soirées jeux, le bozendo, le yoga, pour votre soutien et votre bienveillance. Merci à vous d'avoir rendu mon quotidien si joyeux ! Merci à Amy pour nos échanges et ton soutien au moment du labo ! Merci à la « nouvelle génération » de doctorants, merci à Angèle, Marine J., Cyprien, Betty, Juliette, Mathieu, merci pour toutes les discussions, pour votre bonne humeur, votre sincérité, votre soutien, votre bienveillance et pour nos échanges ! Merci de me faire rire, pour l'ambiance si joyeuse au bureau et de m'apporter de la bonne humeur tous les jours ! Merci aux doctorants et post-doctorants du 22, merci à Eleonora pour nos échanges, ta bienveillance, ton soutien, et pour ton aide pour les multiples galères administratives ! Merci aussi à Nagham, Katy, Paola, Sergio, Rudney, Marion, Olga pour nos échanges et votre bonne humeur ! Merci aussi à Delphine de Lyon, merci pour ta gentillesse, pour ta bienveillance de m'avoir intégré au labo, pour nos échanges ! Merci aussi à tous les doctorants (Auguste, Prianka, Sam et plein d'autres) que j'ai pu rencontrer lors de mon séjour à Lyon, pour les soirées jeux, pour nos échanges, pour l'ambiance au bureau !

Merci à mes amis qui m'ont soutenu tout au long de cette thèse ! Merci tout particulièrement à Fanny pour ta bienveillance, pour nos discussions, pour ton aide, pour ton soutien pendant ma thèse, surtout pendant mes/nos galères de thèse, merci d'avoir été là tout le temps et en toute circonstance !! Merci à Vivek pour tes multiples relectures pendant ma thèse, merci pour ton soutien, ta bienveillance, ta bonne humeur et ton optimisme ! Merci à July et Dorine, mes amies d'enfance qui ont toujours été là pour me soutenir et m'encourager, merci d'être là d'avoir toujours été là pour moi ! Merci aussi à Maë, Momo, Marine, pour votre soutien et pour nos échanges !

Merci à ma famille qui a toujours été là pour moi en toute circonstance et qui m'a soutenu au cours de cette thèse même s'ils n'ont jamais totalement compris ce que je faisais !! Merci à mes grands-parents et à ma marraine pour leur soutien indéfectible et leur encouragement ! Merci à mon père pour son soutien et son amour ! Merci à ma maman pour son soutien inconditionnel, pour son amour, pour sa présence, pour son aide, de m'avoir supporté, encouragé et soutenu à chaque moment, pour avoir cru en moi ! Merci à Peio, (et aussi Chipie, Boubou, Craquotte, Cocotte) pour son amour, pour son soutien, pour m'avoir accompagné dans cette folle aventure, et d'avoir été à mes côtés durant ces 3 dernières années !

ABSTRACT

The Mediterranean area is a key region to study relationships between vegetation dynamics, climate changes and human practices along the time. This region is characterized by high biodiversity, a significant sensitivity to climate changes and a complex and long human history. The Mediterranean Basin is thus a key region for understanding the respective impact of climate changes and human activities on ecosystems since the Holocene. The actual climate and biodiversity crisis raises this topic as a current and major issue that needs to be investigated and debated. This PhD study proposes to document environmental dynamics, climate changes and human practices during the last 15,000 years around the Mediterranean Basin through a multiproxy approach including sediment geochemistry (XRF), pollen, Non-Pollen Palynomorphs (NPPs) and biomarkers molecular (branched Glycerol Dialkyl Glycerol Tetraethers or brGDGTs). Two mountainous areas poorly documented have been studied: the Lesser Caucasus with the Vanevan peat (Armenia) and the Apennines in Southern Italy with the Lake Matese. We investigated (1) modern pollen-vegetation relationships in Armenia and in the Matese Massif, (2) changes in vegetation and human activity around the Vanevan peat and the Lake Matese, (3) climate changes with water-level changes, molecular biomarkers "brGDGTs", and pollen transfer functions (multi-method approach: Modern Analogue Technique, Weighted Averaging Partial Least Squares regression, Random Forest, and Boosted Regression Trees) and (4) relationships between vegetation dynamics, climate changes and human activities during the Lateglacial and the Holocene.

At Vanevan, steppic taxa dominated during the last 9700 years and few trees have grown on shores of the Lake Sevan, even during the Mid-Holocene. At Matese, the vegetation was mainly steppic during the Lateglacial and the Early Holocene, although an increase of deciduous arboreal taxa was recorded during the Bølling–Allerød and finally *Fagus* and Mediterranean taxa develop during the Mid-Late Holocene. The Younger Dryas is well recorded in the Matese pollen assemblages. Climate reconstructions based on pollen and brGDGTs are complementary and they each have their advantages and biases. At Vanevan, climate reconstructions show an arid and cold Early Holocene, a more humid and warmer Mid Holocene, and a more arid and cooler Late Holocene. Several abrupt events have been detected at 6.2 ka, 5.2 ka, 4.2 ka, 2.8 ka and allow us to highlight the atmospheric processes in the Caucasus and the Near East. At Matese, the Bølling–Allerød is characterized by warm and humid conditions whereas the Younger Dryas is marked by cold conditions. The Holocene is

firstly characterized by humid and warmer conditions followed by a slight decrease of precipitation and temperatures during the Mid-Late Holocene. Our study reveals a significant impact of abrupt climate changes on populations in the Near East and the Caucasus even for the recent periods. In the South Caucasus, the arid climate events are consistent with the population abandonment phases and changes in the agricultural practices around the Lake Sevan. In Southern Italy, anthropogenic indicators are less important, and the opening of forests is detected during the last 2800-2600 years and seem associated to human practices.

Keywords: Paleoecology; Paleoclimate quantitative reconstructions; Pollen; Molecular biomarkers brGDGTs; Water level changes; Anthropogenic impacts; Agriculture; Abrupt climate events; Lateglacial; Holocene

RIASSUNTO

L'area mediterranea è una regione chiave per studiare le relazioni tra le dinamiche della vegetazione, i cambiamenti climatici e le pratiche umane nel corso del tempo. Questa regione è caratterizzata da un'elevata biodiversità, una notevole sensibilità ai cambiamenti climatici ed una storia umana complessa e lunga. Per il bacino del Mediterraneo, la comprensione dell'impatto dei cambiamenti climatici e delle attività umane sugli ecosistemi dall'Olocene a tutt'oggi, è ancora oggetto di ricerca e di dibattito. Questa tesi di dottorato si propone di documentare le dinamiche ambientali, i cambiamenti climatici e le pratiche umane durante il Tardiglaciale e l'Olocene negli ultimi 15,000 anni intorno al bacino del Mediterraneo attraverso un approccio multiproxy che include la geochimica dei sedimenti (XRF), il polline, i palinomorfi non pollinici (NPP) e I biomarcatori molecolari (glicerolo ramificato dialchil glicerolo tetraeteri o brGDGT). In particolare sono state studiate due aree montuose scarsamente documentate: la torbiera di Vanevan nel Piccolo Caucaso, in Armenia, e il Lago del Matese nell'Italia meridionale. La ricerca ha riguardato: (1) le moderne relazioni polline-vegetazione in Armenia e nel Massiccio del Matese, (2) i cambiamenti nella vegetazione e nell'attività umana intorno alla torbiera di Vanevan e al Lago del Matese, (3) i cambiamenti climatici attraverso i cambiamenti del livello dell'acqua, i biomarcatori molecolari " brGDGTs", le funzioni di transfert (approccio multi-metodo: Modern Analogue Technique, Weighted Averaging Partial Least Squares regression, Random Forest e Boosted Regression Trees) e (4) le relazioni tra le dinamiche della vegetazione, i cambiamenti climatici e le attività umane durante il tardiglaciale e l'Olocene.

I risultati della torbiera di Vanevan mostrano che la vegetazione steppica era dominante negli ultimi 9700 anni e che la vegetazione circostante il lago Sevan era scarsamente boscosa, anche durante l'Olocene medio. Per il Matese, la vegetazione è stata principalmente steppica durante il Tardiglaciale e l'Olocene inferiore, sebbene sia stato registrato un aumento dei taxa arborei decidui durante il Bølling–Allerød e che *Fagus* e i taxa mediterranei si sono sviluppati durante l'Olocene medio e finale. Il Dryas recente è ben registrato negli assemblaggi pollinici del Matese. Le ricostruzioni climatiche basate su polline e brGDGT sono complementari e ciascuna ha i suoi vantaggi e problematiche. A Vanevan, le ricostruzioni climatiche mostrano un Olocene inferiore arido e freddo, un Olocene medio più umido e più caldo e un Olocene finale più arido e più fresco. Diversi bruschi eventi sono stati rilevati a 6,2 ka, 5,2 ka, 4,2 ka, 2,8 ka che ci consentono di evidenziare i processi atmosferici nel Caucaso e nel Vicino Oriente.

Al Matese, il Bølling–Allerød è caratterizzato da condizioni calde e umide mentre lo Dryas recente è caratterizzato da condizioni fredde e aride. Per questo sito, l'Olocene è inizialmente caratterizzato da condizioni umide e più calde seguite da una leggera diminuzione delle precipitazioni e delle temperature durante l'Olocene medio-finale. Il nostro studio rivela un impatto significativo dei bruschi cambiamenti climatici sulle popolazioni del Vicino Oriente e del Caucaso anche per i periodi recenti. Nel Caucaso meridionale, i diversi eventi climatici sono coerenti con le fasi di abbandono della popolazione e le pratiche agricole intorno al lago Sevan. Nell'Italia meridionale gli indicatori antropogenici sono meno importanti e l'apertura di foreste è rilevata negli ultimi 2800-2600 anni e sembra associata alle pratiche umane.

Parole chiave: Paleoecologia ; Ricostruzioni paleoclimatiche quantitative ; Polline; Marcatori molecolari brGDGTs; Cambiamenti livello idrico; Impatto antropogenico; Agricoltura; Bruschi cambiamenti climatici; Tardiglaciale; Olocene.

RÉSUMÉ

La région méditerranéenne est une région clé pour étudier les relations entre les dynamiques de végétation, les changements climatiques et les pratiques humaines au cours du temps. Cette région est caractérisée par une grande biodiversité, une sensibilité importante aux changements climatiques et une histoire humaine complexe et longue. Comprendre l'impact respectif des changements climatiques et des activités humaines sur les écosystèmes depuis l'Holocène est une question d'actualité qui doit être étudiée et débattue autour du bassin méditerranéen. L'objectif de cette thèse est de documenter les dynamiques environnementales, les changements climatiques et les activités humaines au cours des 15,000 dernières années autour du bassin méditerranéen par une approche multiproxy incluant la géochimie des sédiments (XRF), les pollen, les Palynomorphes Non-Polliniques (NPP) et les biomarqueurs moléculaires (Glycerol Dialkyl Glycerol Tetraethers ramifiés ou brGDGT). Deux zones montagneuses peu documentées ont été étudiées : le Petit Caucase avec la tourbière Vanevan (Arménie) et les Apennins en Italie du Sud avec le Lac Matese. Nous avons étudié (1) les relations modernes pollen-végétation en Arménie et dans le massif du Matese, (2) les changements de végétation et d'activités humaines autour de la tourbière Vanevan et du lac Matese, (3) les changements climatiques issus des changements de niveau d'eau, des biomarqueurs moléculaires "brGDGT", et des fonctions de transfert appliquées sur les pollen (approche multi-méthodes : Modern Analogue Technique, Weighted Averaging Partial Least Squares regression, Random Forest, and Boosted Regression Trees) et (4) les relations entre la dynamique de la végétation, les changements climatiques et les activités humaines pendant le Tardiglaciaire et l'Holocène.

À Vanevan, les taxons steppiques ont dominé la végétation pendant les 9700 dernières années et peu d'arbres étaient présents sur les rives du lac Sévan, même pendant l'Holocène moyen. À Matese, la végétation était principalement steppique pendant le Tardiglaciaire et l'Holocène inférieur, bien qu'une augmentation des taxons arborés décidus ait été enregistrée pendant le Bølling-Allerød et finalement, *Fagus* ainsi que des taxons méditerranéens se développent pendant l'Holocène moyen-supérieur. Le Dryas récent a été bien enregistré dans les assemblages polliniques de Matese. Les reconstructions climatiques basées sur les pollen et les brGDGTs sont complémentaires et ont chacun leurs avantages et leurs biais. À Vanevan, les reconstructions climatiques montrent un Holocène inférieur aride et froid, un Holocène moyen plus humide et plus chaud, et un Holocène supérieur plus aride et plus frais. Plusieurs

événements climatiques abrupts ont été détectés à 6.2 ka, 5.2 ka, 4.2 ka, 2.8 ka et nous permettent de mettre en évidence les processus atmosphériques dans le Caucase et le Proche-Orient. À Matese, le Bølling-Allerød est caractérisé par des conditions chaudes et humides alors que le Dryas récent est marqué par des conditions froides. L'Holocène est d'abord caractérisé par des conditions humides et plus chaudes, suivies d'une légère diminution des précipitations et des températures au cours de l'Holocène moyen-supérieur. Notre étude révèle un impact significatif des changements climatiques abrupts sur les populations du Proche-Orient et du Caucase, même pour les périodes récentes. Dans le Petit Caucase, les événements climatiques arides sont cohérents avec des phases d'abandon des populations et des changements dans les pratiques agricoles autour du lac Sévan. Dans le sud de l'Italie, les indicateurs anthropiques sont moins importants, et l'ouverture des forêts est détectée au cours des 2800-2600 dernières années et semble associée aux pratiques humaines.

Mots-clés : Paléoécologie ; Reconstitutions quantitatives des paléoclimats ; Pollen ; Biomarqueurs moléculaires brGDGTs ; Changements de niveau d'eau ; Impacts anthropiques ; Agriculture ; Événements climatiques abrupts ; Tardiglaciaire ; Holocène

TABLE OF CONTENTS

LIST OF FIGURES

LIST OF TABLES

LIST OF ABBREVIATIONS

AMOC *: Atlantic Meridional Overturning Circulation*
AMS *: Accelerator Mass Spectrometry*
AP *: Arboreal Pollen*
B/A *: Bølling–Allerød*
brGDGT *: Branched Glycerol Dialkyl Glycerol Tetraether*
BRT : *Boosted Regression Forest*
cal BP *: calibrated Before Present*
CBT *: cyclization of branched GDGTs*
COST *: cold steppe*
CPT *: Common Pollen Types*
EH *: Early Holocene*
GDGT *: Glycerol Dialkyl Glycerol Tetraethers*
GI *: Greenland Interstadial*
GS *: Greenland Stadial*
HPLC-APCI-MS *: High-Performance Liquid Chromatography Mass Spectrometry*
MAAT *: mean annual air temperature*
MAF : *mean temperature of months above freezing*
MAT : *Modern Analogue Technique*
MBT *: methylation of branched GDGTs*, *: methylation of branched GDGTs*
MC *: mastercore*
MS *: Magnetic Susceptibility*
MTCO *: temperature of the coldest month*
MTWA *: temperature of the warmest month*
NAO : *North Atlantic Oscillation*
NAP : *non arboreal pollen*
NPP : *Non-Pollen Palynomorph*
NPPAZ *: Non-Pollen Palynomorph Assemblage Zones*
OD *: Oldest Dryas*
PANN *: mean annual precipitation*
PAZ *: Pollen Assemblage Zones*
P_{summer} *: summer precipitation*
P_{winter} *: winter precipitation*
RF : *Random Forest*
RMSE *: Root Mean Square Error*
RPT *: Rare Pollen Types*
SIM *: selective ion monitoring*
SST *: Sea-Surface Temperatures*
TEDE *: temperature deciduous*
WAMX *: warm mixed forest*
WAPLS : *Weighted Averaging Partial Least Squares regression*
XRF *: X-ray Fluorescence*
YD *: Younger Dryas*

CHAPTER I - INTRODUCTION

Lake Sevan, Armenia, M.Robles

1. The Mediterranean region: a key area

The Mediterranean is a hot spot for biodiversity. The Mediterranean region is characterized by a high diversity in landscapes, due to the complexity of its relief and its climatic influences. Mediterranean mountains thus play an important part in the conservation of global biodiversity. In total, they cover some 1,7 million km², corresponding to 50 % of the land in Mediterranean countries. Seven of which are in the top 20 mountainous countries in the world (Vogiatzakis, 2012).

The Mediterranean is a hot spot for climate-related issues. The climate of the Mediterranean region (its past evolution, present variability, trends and changes simulated for the future) has been the object of many research studies (e.g. Tzedakis, 2007; Lionello, 2012). The location of the Mediterranean area in a transitional band between subtropical and mid-latitude regimes produces a large climate variability at multiple timescales. Southern part of the Mediterranean is particularly vulnerable to this climate variability and to the irregular water availability. In addition, in the next decades, climate simulations performed by GCMs show an extension and an intensification of drought periods (IPCC 2017) in many regions of the Mediterranean. These changes may contribute to a loss of biodiversity of terrestrial biomes due to their significant sensitivity (Quereda Sala et al., 2000).

The Mediterranean is also a key area for present-day societies and past human civilizations. Through the Holocene (last 11,700 years cal BP), the Mediterranean region has contributed significantly to the development of important human civilizations. The complexity of the Mediterranean Basin history has been reinforced by the increase of this human impact on the ecosystems since the last 10,000 years in the eastern part of the Mediterranean and 7500-7000 years in the western part of the Mediterranean (e.g. Guilaine, 2003; Jalut et al., 2009). Pre-industrial societies were also highly sensitive to the environment and climate changes and present-day societies are also dependent on variation in the climate and natural environment.

The Mediterranean region is thus characterized by close interactions between ecosystems, climate and human societies in the past and for the next decades. Disentangle the climate signal in ecosystems potentially impacted by human practices is still a research challenge. In this context, it is important to better understand the variability of the climatic changes since the last 15,000 years and its impact on Mediterranean ecosystems and more specifically agroecosystems.

2. The Mediterranean area: geological context, climate, vegetation and human societies

2.1 Geological context

Mediterranean mountains cover some 1,7 million km², corresponding to 50 % of land in Mediterranean countries and seven of which are in the top 20 mountainous countries in the world. Mountains are generally situated around the Mediterranean Basin at a short distance from the sea, inducing unique geographical and climatological characteristics (Vogiatzakis, 2012).

The development of the Mediterranean Sea began with the separation of African and European plates and the increase of the Tethys Sea around 150 million years ago during the Jurassic. Both of the plates then converged, shrinking the Tethys Sea and forming the Mediterranean Sea between 100 million and 60 million years ago, during the Cretaceous. Many marine sediments present in the ancient Tethys Ocean formed the uplands bordering on the Mediterranean Sea due to the collision between the African and the Eurasian plates (Vogiatzakis, 2012). The ranges Atlas, Rif, Baetic Cordillera, Cantabrian Mountains, Pyrenees, Alps, Apennines, Dinaric Alps, Hellenide, Balkan, Taurus are the result of the Alpine orogeny and the Caucasian Mountains were formed with the Alpine and Himalayan orogeny (Vogiatzakis, 2012; Sharkov et al., 2015).

2.2 Climate

Mediterranean climate is characterized by marked seasonality with dry summers and wet winters, high evaporation, low annual precipitation and high interannual variability (Lionello et al., 2006; Lionello, 2012). Nevertheless, the presence of different mountains, basins, gulfs and peninsulas, of various sizes and orientation, leads to different climatic conditions in the Mediterranean regions. In addition, mountains located around the Mediterranean Sea produce contrasted climatic features than without them (Lionello et al., 2006). Climate in the Mediterranean, including atmospheric circulation, and hydrology, is principally controlled by latitude (Rhanem, 2008) and strongly determined by the relief.

Mediterranean region is located in a transitional zone between mid-latitude and subtropical climate (Lionello et al., 2006; Lionello, 2012). Northwestern Mediterranean is principally influenced by the North Atlantic Oscillation (NAO), mainly winter precipitations with a negative correlation (Hurrell, 1995; Trigo et al., 2004; Lionello et al., 2006; López-Moreno et al., 2011). NAO is determined by the difference in pressure, at sea level, between Icelandic and Azores (Wallace and Gutzler, 1981). However, some studies indicate that winter

temperatures are mostly controlled by the Eastern Atlantic (EA) pattern (Sáenz et al., 2001). Central and Eastern Mediterranean is under the influence of Asian and African monsoons, linked to tropical and subtropical circulation. When NAO is weak, winter precipitations can be controlled by El Niño–Southern Oscillation (ENSO) (Lionello et al., 2006).

2.3 Vegetation

Mediterranean vegetation is principally composed by evergreen shrubs, as *Arbustus*, *Erica* and *Pistacia*, and sclerophyllous trees at low and middle elevations. The favorable growing seasons are the spring, with the moist soil and an increase of temperatures, and the autumn after the first rains (Roberts et al., 2011). Western and central parts of the basin are dominated by *Quercus ilex, Quercus suber, Quercus coccifera, Ceratonia siliqua, Pistacia lentiscus* and *Olea europaea* var. *sylvestris*. In the Eastern parts, *Q. suber* is absent and *Q. coccifera* subsp. *calliprinos* is more present (Quézel and Médail, 2003). However, when precipitation is high or the soil is deep and wet, deciduous forests can be present with *Quercus faginea*, *Q. infectoria*, *Q. cerris*, *Q. ithaburensis* and sub-Mediterranean forests with *Quercus pubescens*, *Q. fraineto* and *Q. trojana* are present. Mountainous forests, in particular between 1200 m and 1600 m are dominated by coniferous species with a majority of Pines as *Pinus nigra, P. halepensis, P. brutia* and *P. pinaster* in the western Mediterranean and *P. brutia* in the eastern Mediterranean. Other important coniferous can be found, as cedars in the Atlas Mountains, Cyprus, Lebanon and Turkey, junipers in the Spanish Sierras and the Atlas Mountains, and firs in Turkey, Lebanon and Spain (Vogiatzakis, 2012).

2.4 Human impact

In the Mediterranean region, human practices are widespread since the Neolithic. Human societies begin to modify the environment, about 10,000 years ago, in the eastern Mediterranean in the Fertile Crescent with the beginning of the domestication of plant and animal species. The cultivation of wild cereals and pulses began about 11,500 cal BP in several sites currently present in Turkey (Zeist and Roller, 1994), Syria (Van Zeist and Bakker-Heeres, 1984; Hillman et al., 2001; Willcox et al., 2009), West Bank (Weiss et al., 2006) and Jordan (Edwards et al., 2004; Kuijt and Finlayson, 2009; White and Makarewicz, 2012) The morphological characteristics of domestic wheat and barley appear about 10,000 cal BP and the first domestic cereals are confirmed about 10,500 cal BP (Colledge et al., 2004; Fuller, 2007). The Holocene climate, more stable, has allowed the emergence of agriculture and the apparition of archeological developments (Willcox et al., 2009). Then, agro-pastoral activities extend

around the Mediterranean Basin and the first human impacts in the Western Mediterranean appear about 7500-7000 years ago (e.g. Guilaine, 2003; Jalut et al., 2009). In the mountains different human practices have modified the environment, as wood cutting for construction and fuel (including mining), pastoralism, fires to open forest and transform them to grazing land and agriculture (Vogiatzakis, 2012).

3. Paleoecology: a tool to understand past ecosystems and past climate

Studying past environments allows us to have a better understanding of current ecosystem dynamics and anticipate future changes. Paleoecology is the study of past environments and can be used to understand the history of biodiversity, and its link with human societies, and climate. Evidences of past environmental or climatic conditions are commonly preserved in natural archives such as lacustrine, peat and marine sediments, cave deposits (speleothems), ice cores, trees, loess, and in geomorphological features (glacial deposits) (Bradley, 2015).

Paleoenvironmental or paleoclimatic indicators, named "proxies", can be used to reconstruct past environments and climate. Paleoenvironmental reconstructions also depend on our knowledge of present day ecosystems (Roberts, 2013) because some of these proxies are calibrated on modern data. Understanding the sources (local, extralocal, or regional) and deposition patterns of these indicators is necessary to properly interpret the fossil records. Various proxies are used to reconstruct the paleoenvironment changes from terrestrial or marine sediments: pollen, oxygen isotopes, beetles, chironomids, speleothems and more recently molecular biomarkers as alkenones or brGDGTs (e.g. Coope, 2004; Peyron et al., 2005; Sicre et al., 2013; Heiri et al., 2015; Regattieri et al., 2014; Moreno et al., 2014; Martin et al., 2020).

In this study, we propose a multiproxy approach (pollen, Non-Pollen-Palynomorphs, molecular biomarkers…) to reconstruct the environments and climate changes of the Mediterranean Basin through the last 15,000 years. The use of independent and complementary proxies is more reliable than approaches based on single proxies because it is possible to understand the bias associated to each proxy and to better document the paleoenvironmental changes of a region.

3.1 Pollen

Palynology, the study of pollen and spores, is widely used to reconstruct past ecosystems. Pollen grains are male gametophyte of plant and are necessary for plant

reproduction. Pollen grains range in size from 10-150 µm and their morphology varies according to the plant families, the genus or the species. Pollen grains are distinguished according to their size, shape of exine, type and a number of apertures (Faegri et al., 1989). Pollen grains and spores are well preserved in anoxic environment such as lake or peatland (Jacobson and Bradshaw, 1981). The exine of pollen grains is largely composed of sporopollenin, which is highly resistant to degradation.

The production of pollen by plants varies according to the taxa. The pollination type influences the productivity, which will be much greater for wind-pollinated in comparison with insect-pollinated taxa. The dispersion of pollen also varies according to the taxa. The pollen of some taxa can be carried over long distances, such as conifers whose pollen grains have sacs to help to keep them airborne. The deposition of pollen in sediments depends on several factors, including the size of the wetland, the surrounding vegetation, the topography of the site and the microclimatic parameters (Jacobson and Bradshaw, 1981). The larger the diameter of a lake, the more regional vegetation it records. For sites of one hectare, local and extralocal pollen is predominantly recorded and when sites are larger than five hectares, regional pollen is dominant (Jacobson and Bradshaw, 1981). The presence of an open or closed environment around the deposition site also determines the source area (Jacobson and Bradshaw, 1981). The transport distance of pollen within a closed forest did not exceed 20-30 m. However, the generalization of transport distance is not applicable to all types of pollen.

Palynology allows us to determine the relative importance of taxa (with a level of identification precision corresponding to the species, genus or families) to give information about the main ecological factors (Jacobson and Bradshaw, 1981). Pollen can also be used to reconstruct paleoclimate changes (e.g. Peyron et al., 2013), however, it is sometimes difficult to distinguish human impact and climate forcing on the environment in palynology studies (Roberts et al., 2011). Therefore, we use here two other independent proxies: Non-Pollen-Palynomorph which help to characterize the human impact, and the molecular biomarkers (brGDGTs) which help to reconstruct quantitatively the past temperature.

3.2 Non-Pollen-Palynomorphs (NPPs)

Non-pollen palynomorphs (NPPs) are palynomorphs other than pollen material (pollen grains and embryophyte spores). Their natures (taxonomy) and forms (types of remains) are numerous, and they vary from one site to another. The most studied NPPs to reconstruct past ecosystems are algae and fungi (Van Geel, 2002). They are generally produced in situ in the wetland or provided from the catchment area (Van Geel, 2002). Algae are produced in situ and

they are principally used to understand the changes in hydrology and trophic conditions (Van Geel, 2002). The most common algae are *Pediastrum* and *Botryococcus* species which are colonial green algae (Chlorophyceae) that is commonly found among the plankton of freshwater lakes (Van Geel, 2002; Sarmaja-Korjonen et al., 2006). Considering fungi, they are generally transported by air or runoff and can provided from the local vegetation (mycorrhizae or parasites associated with the roots of plants) (Van Geel and Andersen, 1988; Van Geel, 2002). For example, *Glomus* spores is part of the arbuscular mycorrhizal fungi and they can be indicators of erosion in the area around the wetland (Van Geel, 2002). The size of its spores is extremely variable from 18 to 138 µm (Van Geel, 2002). Other spores are part of the coprophilous groups, and they are used to detect the presence of herbivores domesticated associated to pastoralism (López-Merino et al., 2009; Cugny et al., 2010) or sometimes wild herbivores (Aptroot and van Geel, 2006). The most common coprophilous fungi are *Sporormiella* (HdV-113) and *Sordaria* (HdV-55).

3.3 Branched Glycerol Dialkyl Glycerol Tetraethers (brGDGTs)

Branched Glycerol Dialkyl Glycerol Tetraethers (brGDGTs) are ubiquitous organic compounds from membrane lipids produced by bacteria (Weijers et al., 2006a). They consist of tetra- (I), penta- (II) or hexa- (III) methylated components with none (suffix a), one (b) or two (c) cyclopentyl moieties, and with methyl groups on the 5-methyl (X), 6-methyl (X') or 7-methyl (X") carbon position of their alkyl chain (Sinninghe Damsté et al., 2000; Weijers et al., 2006a; De Jonge et al., 2014; Ding et al., 2016). The alkyl structure and stereochemistry of the glycerol group strongly suggest a bacterial source (Weijers et al., 2006a). The phylum Acidobacteria was identified as precursor organisms for the production of brGDGTs (Sinninghe Damsté et al., 2018). BrGDGTs can be found in a variety of environments such as soil (e.g. Weijers et al., 2006b; Naafs et al., 2017a; Dearing Crampton-Flood et al., 2020), peat (e.g. Weijers et al., 2006a; Naafs et al., 2017b, 2019; Dearing Crampton-Flood et al., 2020), lake sediments (e.g. Russell et al., 2018; Sun et al., 2011; Martínez-Sosa et al., 2021; Raberg et al., 2021), marine sediments (e.g. Dearing Crampton-Flood et al., 2018), loess (e.g. Lu et al., 2019) and fossil bones (e.g. Zhao et al., 2020). The brGDGTs distribution can be different according to the type of samples (Martin et al., 2019). For example, the brGDGTs distribution of peat and soil samples are closed, however, their distribution differs with samples of lake sediments mainly when the in situ production is important (Loomis, 2011; Dearing Crampton-Flood et al., 2018; Martínez-Sosa et al., 2021). Bacteria that synthetized brGDGTs are still largely unknown, however, the relationship between brGDGT distribution and environmental changes, in

particular the pH and the temperature, is well established (Naafs et al., 2017b, 2017a; Dearing Crampton-Flood et al., 2020; Martínez-Sosa et al., 2021; Raberg et al., 2021). The degree of methylation of brGDGTs (MBT; methylation of branched GDGTs) varies depending on the mean annual air temperature (MAAT) and higher fractional abundance of hexa- (III) and penta- (II) methylated brGDGTs are recorded in colder environments (Weijers et al., 2007). BrGDGTs are an emerging proxy and they are increasingly used as a temperature proxy, such as in Europe and more particularly in Switzerland (Blaga et al., 2013) and France (Martin et al., 2020). However, the association between brGDGTs and other proxies, such as pollen, for climate reconstructions are still rare (Watson, 2018; Martin et al., 2020; Dugerdil et al., 2021a, 2021b).

4. Objectives of this study: reconstruct the paleoenvironmental changes in the Mediterranean area since the last 15,000 years

Over the last million years, the variability of the climate changes in the Mediterranean region is not yet fully understood (e.g. Tzedakis, 2007). For recent period as the Lateglacial and Holocene, more proxies are available to document the climate changes. During the Holocene, different climate patterns are suggested between East/West and North/South of the Mediterranean region and contrasted precipitation patterns have been reconstructed between the South-Western Mediterranean and the South-Central and South-Eastern Mediterranean regions (e.g. Roberts et al., 2011, 2012; Mauri et al., 2015; Magny et al., 2013; Di Rita et al., 2018; Bini et al., 2019; Azuara et al., 2020; Marriner et al., 2022). These different patterns are linked to Westerly activity and NAO changes (Joannin et al., 2014). However, these climate processes are not yet fully understood (Mauri et al., 2014) and more studies need to be added in various sub-regions (North-West Africa, Zielhofer et al., 2017; South-West Europe, Sabatier et al., 2012; Central Mediterranean, Peyron et al., 2013, 2017; Near East, Joannin et al., 2014; Middle East, Sorrel and Mathis, 2016).

Many regions of the Mediterranean Basin are still understudied; this is the case for the Lesser Caucasus and the semi-arid Near East, where paleoclimate changes are mainly inferred from pollen-based vegetation record (Wick et al., 2003; Connor and Kvavadze, 2008; Djamali et al., 2010; Joannin et al., 2014; Leroyer et al., 2016; Messager et al., 2017; Cromartie et al., 2020) and by sparse lake hydrological studies (Stevens et al., 2001, 2006; Roberts et al., 2011; McCormack et al., 2019) derived from geochemical and geophysical proxies ($\delta^{18}O$, XRF). These methods strongly disagree when tracking past precipitation seasonality (Litt et al., 2009; Stockhecke et al., 2016). This emphasizes the need for new climate reconstruction targeting

methodologies and sedimentary archives able to echo regional climate, such as the lake Sevan in Armenia.

As the Lesser Caucasus, the Southern Italy is also a key region of the Mediterranean Basin which is still understudied. In Central/Southern Italy for example, recent studies reveal a very complex picture of climate variability within this region for the Holocene. Indeed, the northern and southern regions of Italy have been under the prevalent influence of different climate patterns (around 40°N), producing opposite hydrological regimes and consequent vegetation dynamics (Magny et al., 2013; Peyron et al., 2013). Moreover, recurrent forest declines and dry events are recorded in the south-central Mediterranean (Italy) while an opposite pattern is suggested for the south-western Mediterranean, suggesting that different expressions of climate modes occurred in the two regions at the same time (Di Rita et al., 2018). The Holocene also exhibits a millennial-scale climate variability (Azuara et al, 2020; Marriner et al., 2022) and abrupt events as the 7.5 ka (Joannin et al., 2012) or the 4.2 ka (e.g. Di Rita et al, 2019; Bini et al., 2019, Kaniewski et al., 2019). These spatio-temporal patterns and underlying processes during the Holocene are not fully deciphered yet. More regional studies are needed to document and better understand these complex climate patterns.

Our study focuses on these two areas. We propose here a multi-proxy approach to document the Holocene and if possible, the Lateglacial in Southern Italy and Lesser Caucasus, in order to better understand the links between climate, vegetation and human societies in these key areas of the Mediterranean region. Two high-altitude lakes have been selected: Lake Matese (1002 m a.s.l. Province of Caserta) in the Southern Apennines in Italy and the Vanevan peat (1919 m a.s.l.) located south-west of Lake Sevan in the Lesser Caucasus of Armenia. Lake Matese is the highest karstic lake in Matese mountains, and Lake Sevan is the largest lake in Armenia and one of the highest freshwater lakes in Eurasia. Both sites are comparable because they are approximately on the same latitude but, are under different climate influences. They also have different cultural and agroecosystems histories and chronologies.

In this frame, our study investigates (1) modern pollen-vegetation relationships and (2) changes in vegetation, human activity and climate in the records of Vanevan peat and Lake Matese, using a multiproxy approach including sediment geochemistry (XRF), pollen, Non-Pollen Palynomorphs (NPPs), and branched Glycerol Dialkyl Glycerol Tetraethers (brGDGTs). Climate reconstructions will be provided by (1) water-level changes, (2) brGDGTs, and (3) pollen transfer functions (multi-method approach: Modern Analogue Technique, Weighted Averaging Partial Least Squares regression, Random Forest, and Boosted Regression Trees). To date, the comparative study between brGDGTs and other proxies for climate reconstructions

is rare (Watson, 2018; Martin et al., 2020; Dugerdil et al., 2021) and no study are still available for the continental Mediterranean Basin.

5. Objectifs de cette étude : reconstruire les changements paléoenvironnementaux dans la région méditerranéenne depuis les 15,000 dernières années.

Au cours du dernier million d'années, la variabilité des changements climatiques dans la région méditerranéenne n'est pas encore totalement comprise (par exemple, Tzedakis, 2007). Pour les périodes récentes comme le Tardiglaciaire et l'Holocène, de nombreux proxies sont disponibles pour documenter les changements climatiques. Au cours de l'Holocène, différentes tendances climatiques sont suggérées entre l'est/ouest et le nord/sud de la région méditerranéenne et les précipitations reconstruites sont contrastées entre le sud-ouest de la Méditerranée et les régions du centre-sud et du sud-est de la Méditerranée (par exemple Roberts et al., 2011, 2012 ; Mauri et al., 2015 ; Magny et al., 2013 ; Di Rita et al., 2018 ; Bini et al., 2019 ; Azuara et al., 2020 ; Marriner et al., 2022). Ces différentes tendances sont liées aux variations de l'activité des vents d'Ouest et aux changements de la NAO au cours du temps (Joannin et al., 2014). Cependant, ces processus climatiques ne sont pas encore totalement compris (Mauri et al., 2014) et d'autres études doivent être menées dans diverses sous-régions (Afrique du Nord-Ouest, Zielhofer et al., 2017 ; Europe du Sud-Ouest, Sabatier et al., 2012 ; Méditerranée centrale, Peyron et al., 2013, 2017 ; Proche-Orient, Joannin et al., 2014 ; Moyen-Orient, Sorrel et Mathis, 2016).

De nombreuses régions du bassin méditerranéen sont encore peu étudiées ; c'est le cas du Petit Caucase et du Proche-Orient semi-aride, où les changements paléoclimatiques sont principalement issus des enregistrements de végétation basés sur les pollen (Wick et al., 2003 ; Connor et Kvavadze, 2008 ; Djamali et al, 2010 ; Joannin et al., 2014 ; Leroyer et al., 2016 ; Messager et al., 2017 ; Cromartie et al., 2020) et par des études hydrologiques lacustres éparses (Stevens et al., 2001, 2006 ; Roberts et al., 2011 ; McCormack et al., 2019) basées sur des proxies géochimiques et géophysiques ($\delta^{18}O$, XRF). Ces méthodes sont cependant en désaccord lorsqu'il s'agit de reconstruire la saisonnalité des précipitations passées (Litt et al., 2009 ; Stockhecke et al., 2016). Cela souligne le besoin de nouvelles reconstructions climatiques ciblant des méthodologies et des archives sédimentaires capables de faire écho au climat régional, comme le lac Sévan en Arménie.

Comme le Petit Caucase, l'Italie du Sud est également une région clé du bassin méditerranéen qui est encore peu étudiée. En Italie centrale et méridionale, par exemple, des

études récentes révèlent une image très complexe de la variabilité climatique dans cette région au cours de l'Holocène. En effet, les régions du nord et du sud de l'Italie ont été sous différentes influences climatiques prédominantes (autour de 40°N), produisant des régimes hydrologiques et des dynamiques de végétation opposés (Magny et al., 2013 ; Peyron et al., 2013). En outre, des déclins forestiers et des événements secs récurrents sont enregistrés dans le centre-sud de la Méditerranée (Italie) tandis qu'un schéma opposé est suggéré pour le sud-ouest de la Méditerranée, suggérant que différentes expressions des modes climatiques se sont produites dans les deux régions à la fois. (Di Rita et al., 2018). L'Holocène présente également une variabilité climatique à l'échelle millénaire (Azuara et al., 2020 ; Marriner et al., 2022) et des événements abrupts comme le 7.5 ka (Joannin et al., 2012) ou le 4.2 ka (par exemple Di Rita et al., 2019 ; Bini et al., 2019 ; Kaniewski et al., 2019). Ces modèles spatio-temporels et les processus sous-jacents au cours de l'Holocène ne sont pas encore entièrement déchiffrés. Des études plus régionales sont nécessaires pour documenter et mieux comprendre ces schémas climatiques complexes.

Notre étude se concentre sur ces deux régions. Nous proposons ici une approche multi-proxy pour documenter l'Holocène et si possible le Tardiglaciaire en Italie du Sud et dans le Petit Caucase afin de mieux comprendre les liens entre le climat, la végétation et les sociétés humaines dans ces zones clés de la région méditerranéenne. Deux lacs de haute altitude ont été sélectionnés : le lac Matese (1002 m d'altitude, province de Caserta) dans les Apennins méridionaux en Italie et la tourbière Vanevan (1919 m d'altitude) située au sud-ouest du lac Sévan dans le Petit Caucase en Arménie. Le lac Matese est le plus haut lac karstique des montagnes Matese, et le lac Sévan est le plus grand lac d'Arménie et l'un des plus hauts lacs d'eau douce d'Eurasie. Les deux sites sont comparables, car ils se trouvent approximativement à la même latitude, mais ils sont soumis à des influences climatiques différentes. Ils ont également des histoires et des chronologies culturelles et agro-écosystémiques différentes.

Dans ce cadre, notre étude examine (1) les relations pollen-végétation modernes et (2) les changements dans la végétation, l'activité humaine et le climat dans les enregistrements de la tourbe du Vanevan et du lac Matese, en utilisant une approche multiproxy comprenant la géochimie des sédiments (XRF), le pollen, les palynomorphes non polliniques (NPP) et les tétraéthers ramifiés de glycérol dialkyle (brGDGT). Les reconstructions climatiques seront fournies par (1) les changements de niveau d'eau, (2) les brGDGTs, et (3) les fonctions de transfert du pollen (approche multi-méthodes : Modern Analogue Technique, Weighted Averaging Partial Least Squares regression, Random Forest, and Boosted Regression Trees). A ce jour, l'étude comparative entre les brGDGTs et d'autres proxies pour les reconstructions

climatiques est rare (Watson, 2018 ; Martin et al., 2020 ; Dugerdil et al., 2021) et aucune étude n'est encore disponible pour le bassin méditerranéen continental.

CHAPTER II - IMPACT OF CLIMATE CHANGES ON VEGETATION AND HUMAN SOCIETIES DURING THE HOLOCENE IN THE SOUTH CAUCASUS (VANEVAN, ARMENIA): A MULTIPROXY APPROACH INCLUDING POLLEN, NPPS AND BRGDGTS

Mary Robles[1,2], Odile Peyron[2], Elisabetta Brugiapaglia[1], Guillemette Ménot[3], Lucas Dugerdil[2,3], Vincent Ollivier[4,5], Salomé Ansanay-Alex[3], Anne-Lise Develle[6], Petros Tozalakyan[7], Khachatur Meliksetian[7], Kristina Sahakyan[7], Lilit Sahakyan[7], Bérengère Perello[8], Ruben Badalyan[9], Claude Colombié[10], Sébastien Joannin[2]

1 - Univ. Molise, Department Agriculture, Environment and Alimentation, Italy
2 - Univ. Montpellier, CNRS, IRD, EPHE, UMR 5554 ISEM, Montpellier, France
3 - Univ. Lyon, ENSL, UCBL, UJM, CNRS, LGL-TPE, F-69007 Lyon, France
4 - Aix-Marseille Univ., CNRS, MCC, UMR 7269 LAMPEA, Aix-en-Provence, France
5 - Aix-Marseille Univ., CNRS, FR ECCOREV, Aix-en-Provence, France
6 - Univ. Savoie Mont Blanc, CNRS, UMR 5204 EDYTEM, Le Bourget-du-Lac, France
7 - National Academy of Sciences of Armenia, Institute of Geological Sciences, Yerevan, Armenia
8 - Univ. Lyon, CNRS, UMR 5133 'Archéorient', Maison de l'Orient et de la Méditerranée, Lyon, France
9 - National Academy of Sciences of Armenia, Institute of Archaeology and Ethnography, Yerevan, Armenia
10 - Univ. Lyon, UCBL, ENSL, UJM, CNRS, LGL-TPE, F-69622, Villeurbanne, France


Lake Sevan, Armenia, M.Robles

Published in
Quaternary Science Reviews
doi.org/10.1016/j.quascirev.2021.107297

Abstract

Relationships between steppe vegetation, human practices and climate changes in the past are crucial to disentangle human development in Eurasia. In this frame, our study investigates (1) modern pollen-vegetation relationships and (2) changes in vegetation, human activity and climate in the Holocene record of Vanevan peat (south-eastern shore of Lake Sevan, Armenia), using a multiproxy approach including sediment geochemistry (XRF), pollen, Non-Pollen Palynomorphs (NPPs), and branched Glycerol Dialkyl Glycerol Tetraethers (brGDGTs). Climate reconstructions are provided by (1) water-level changes, (2) brGDGTs, and (3) pollen transfer functions (multi-method approach: Modern Analogue Technique, Weighted Averaging Partial Least Squares regression, Random Forest, and Boosted Regression Trees). Modern pollen assemblages are selected along an altitudinal transect in Armenia. They show a dominance of Chenopodiaceae in semi-desert/steppe regions while meadows steppes, subalpine, and alpine meadows are dominated by Poaceae. Past vegetation is characterized by steppes dominated by Poaceae surrounded during the Mid-Holocene (8200-4200 a cal BP) by scarce open woodlands. Humans have influenced the local vegetation, mainly through their agricultural practices present since 5200 a cal BP with several intensification steps. Our reconstruction indicates a climate shift from a cold and arid Early Holocene toward a warmer and more humid Mid-Late Holocene. An aridification trend marks the last 5000 years causing a drop in water level, which allowed humans to live and cultivate on Lake Sevan shores. Arid events are recorded at 6.2 ka, 5.2 ka, 4.2 ka and 2.8 ka a cal BP, which are commonly related to multi-centennial-scale variations of Westerlies activity (North Atlantic Oscillation). Through our temperature reconstruction, we can assign (1) the 5.2 and 2.8 ka events as being cold and probably related to a strong Siberian High, and (2) the 4.2 ka event as being warm associated with high Arabian subtropical pressures in the South Caucasus and the Near East. Our study suggests a significant impact of these arid events on the Lake Sevan shore populations and they are consistent with cultural phases in the South Caucasus, thus showing the impact of climatic variations on cultural, land use and occupation mode development in this crossroad region between Europe, Africa and Asia.

Keywords: Vegetation dynamics; Human impact; Agriculture; Water level changes; Paleoclimate; Arid climate events; Transfer functions; XRF

Résumé

Les relations entre la végétation steppique, les pratiques humaines et les changements climatiques du passé sont cruciales afin de comprendre le développement des Hommes en Eurasie. Dans ce cadre, notre étude examine (1) les relations pollen-végétation modernes et (2) les changements de végétation, les activités humaines et le climat dans l'enregistrement de la toubière Vanevan (rive sud-est du lac Sévan, Arménie), datant de l'Holocène, en utilisant une approche multi-proxy comprenant la géochimie des sédiments (XRF), le pollen, les palynomorphes non polliniques (NPP) et les tétraéthers glycéroliques ramifiés (brGDGT). Les reconstructions climatiques sont fournies par (1) les changements de niveau d'eau, (2) les brGDGT, et (3) les fonctions de transfert du pollen (approche multi-méthodes : Modern Analogue Technique, Weighted Averaging Partial Least Squares regression, Random Forest, and Boosted Regression Trees). Les assemblages polliniques modernes sont sélectionnés le long d'un transect altitudinal en Arménie. Ils montrent une dominance de Chenopodiaceae dans les régions semi-désertiques/steppiques tandis que les prairies steppiques, subalpines et alpines sont dominées par les Poaceae. La végétation passée est caractérisée par des steppes dominées par des Poaceae entourées, pendant l'Holocène moyen (8200-4200 a cal BP), par de rares forêts ouvertes. Les Hommes ont influencé la végétation locale, principalement à travers leurs pratiques agricoles présentes depuis 5200 a cal BP et au cours de plusieurs étapes d'intensification. Nos reconstructions indiquent un changement climatique d'un Holocène inférieur froid et aride vers un Holocène moyen et supérieur plus chaud et plus humide. Une tendance à l'aridification marque les 5000 dernières années, provoquant une baisse du niveau de l'eau, et permettant aux Hommes de vivre et de cultiver sur les rives du lac Sévan. Des événements arides sont enregistrés à 6.2 ka, 5.2 ka, 4.2 ka et 2.8 ka a cal BP, et sont généralement liés à des variations à l'échelle multi-centennale de l'activité des vents d'Ouest (oscillation nord-atlantique). Grâce à nos reconstructions de températures, nous pouvons attribuer (1) les événements du 5.2 et 2.8 ka comme étant froids et probablement liés à un fort anticyclone Sibérien, et (2) l'événement du 4.2 ka comme étant chaud et associé à des pressions subtropicales arabes élevées dans le Sud du Caucase et le Proche-Orient. Notre étude suggère un impact significatif de ces événements arides sur les populations riveraines du lac Sévan et ils concordent avec les phases culturelles du Sud du Caucase, montrant ainsi l'impact des variations climatiques sur le développement culturel, l'utilisation des terres et les modes d'occupation dans cette région carrefour entre l'Europe, l'Afrique et l'Asie.

Mots-clés : Dynamique de la végétation ; Impact humain ; Agriculture ; Changements de niveau d'eau ; Paléoclimat ; Événements climatiques arides ; Fonctions de transfert ; XRF

1. Introduction

Understanding relationships between vegetation, climate, and anthropogenic impact over long time periods is a major goal to stress out human development in arid and steppe environments of Eurasia. Paleoecology is therefore a mandatory approach for the regions characterized by a strong human impact such as the Mediterranean Basin or the Near East. The Caucasus is among the areas that have been influenced by humans the longest, since the Neolithic, which witness the rise of agriculture and animal husbandry (ca. around 6000 BC) (Badalyan et al., 2004; Chataigner et al., 2014). The variety of landscapes of the region also resulted from its complex orography, geology, and climate (Volodicheva, 2002). The Caucasus is recognized as a "hotspot" of biodiversity (Connor and Kvavadze, 2008; Solomon et al., 2014) and was an important tree refugium during glacial periods (Connor and Kvavadze, 2008). The current vegetation of the South Caucasus is mainly dominated by steppe or desert (Bohn et al., 2000) and only 8% of Armenia's area is covered by exploited or deteriorated forests (Sayadyan, 2011). In contrast, in the 18th century, the forest covered 18% (Sayadyan, 2011), thus questioning the afforestation rate during the Holocene, either before or after the increasing impact of human societies on the environment and the respective impact of climate and humans on ecosystems.

Paleoecological studies of the South Caucasus have recorded forested phases during the Holocene (e.g. Connor et al., 2018; Messager et al., 2013; 2017). In Armenia however, the vegetation dynamic is more complex and suggests steppes dominance throughout the Holocene (Joannin et al., 2014; Leroyer et al., 2016; Cromartie et al., 2020). At Vanevan, on Lake Sevan's shores, Leroyer et al. (2016) also revealed steppes expansion but, as their core only covers the Mid-Holocene (from 7800 to 5100 a cal BP), this vegetation dynamic cannot be extrapolated for the whole Holocene. Old studies based on palynological records with low temporal resolution have suggested that broadleaf deciduous forests existed around 6000 uncalibrated years on the slopes of Lake Sevan (Takhtajyan, 1941; Tumanyan, 1971; Tumajanov and Tumanyan, 1973; Sayadyan et al., 1977; Sayadyan, 1978, 1983; Moreno-Sanchez and Sayadyan, 2005); archaeological sites have revealed animal remains and statues of animals (deer, bears, wolf and foxes) associated with deciduous forests (Lalayan, 1931; Mnatsakanyan, 1952; Mezhlumyan, 1972) but their chronological frame is not precise enough. Further investigations are required to better understand the history of forest and steppes in the South Caucasus over the Holocene and to connect to nowadays issues with aridification and land use impact on soil erosion.

Several studies suggest that humans have an impact on their environment since the Early Holocene in the Near East, by fostering the maintenance of steppic vegetation with fires (Roberts et al., 2002; Turner et al., 2008, 2010). However, in the South Caucasus the regional fire activities do not increase at this period (Messager et al., 2017; Joannin et al., 2014) and climate seems to play an important role in the delayed regional postglacial reforestation in the Near East and the South Caucasus (Wright et al., 2003; Stevens et al., 2001; Djamali et al., 2010; Leroy et al., 2013; Joannin et al., 2014; Messager et al., 2013, 2017; Leroyer et al., 2016). On the shores of Lake Sevan, humans have a long history and agriculture is attested since 5500 a cal BP (Biscione et al., 2002; Parmegiani and Poscolieri, 2003; Hovsepyan, 2013, 2017). As human activities (e.g. agriculture and deforestation) modify the vegetation structure, composition and diversity, a major challenge is to identify and to distinguish the relationships between climate, human, and vegetation. This issue is particularly difficult to address in places (1) where human neolithization already took place during the Early to Mid-Holocene, (2) where the openness of the landscape is not primarily determined by human pressure, and (3) when the technological advancement (e.g. water management systems, winery and fishery) preserves societies from climate and environmental sudden changes (Lawrence et al., 2016; McGovern et al., 2017; Ollivier et al., 2018; Roberts et al., 2019; Ritchie et al., 2021). Human influence is generally detected in paleoecological records during the Early Bronze Age and becomes obvious during the last 3000 years (e.g. Wick et al., 2003; Cromartie et al., 2020). Moreover, wild cereals and other Poaceae produce pollen grains of *Cerealia*-type pollen, which may have biased the interpretation of anthropogenic pollen occurrence (Van Zeist et al., 1975).

Climate role on vegetation during the Holocene is not very well understood in the Caucasus region because of its complexity, mainly due to seasonality influence and climate mechanisms. Few climate reconstructions based on pollen data are available (Connor and Kvavadze, 2008; Joannin et al., 2014; Leroyer et al., 2016; Cromartie et al., 2020) and the climate of Armenia during the Holocene is poorly documented (Joannin et al., 2014; Cromartie et al., 2020). The abrupt climate changes are difficult to detect and until now the 4.2 ka event, a major climate event around the Mediterranean Basin (e.g. Bini et al., 2019), has not yet been detected in the South Caucasus. The climate mechanisms are not totally understood although the role of the North Atlantic Oscillation and the Siberian High is undeniable in this region (e.g. Joannin et al., 2014; Bini et al., 2019). Moreover, human impact can substantially influence pollen-climate relationships even if the impact of this influence on climate reconstructions is often difficult to quantify (Chevalier et al., 2020). Accordingly, pollen-based climate reconstructions from records characterized by a strong human influence need to be evaluated

carefully, by comparison with independent climate reconstructions based on other proxies. Molecular biomarkers are an emerging proxy that allow quantitative reconstruction of paleotemperature changes from lake or peat sediments. Specifically, brGDGTs (branched Glycerol Dialkyl Glycerol Tetraethers) or glycerol tetraethers are ubiquitous organic compounds synthesized by bacteria (Weijers et al., 2006; Dearing Crampton-Flood et al., 2020). Although bacteria that produce brGDGTs are still unknown (Sinninghe Damsté et al., 2018), the relationship between brGDGTs assemblages and temperature is well established (Weijers et al., 2004; Schouten et al., 2007) and this new proxy allows annual paleotemperature reconstructions (e.g. Dearing Crampton-Flood et al., 2020; Dugerdil et al., 2021; Stockhecke et al., 2021). To date, there are very few studies based on comparative approaches including pollen and molecular biomarkers to quantify climate variability over time and more particularly abrupt climate events (Watson et al., 2018; Martin et al., 2020; Dugerdil et al., 2021).

This study aims to document vegetation and climate changes around Lake Sevan in Armenia for the Holocene period. Based on a multi-proxy approach, we provide Holocene high-resolution sediment geochemistry, pollen, Non-Pollen Palynomorphs (NPPs), and molecular biomarkers records from a newly retrieved core in the Vanevan peat, located on the south-eastern shore of Lake Sevan. Our study goals are to:

1) based on a collection of new modern samples from Armenia, understand the modern relationships between pollen and vegetation and reinforce the reliability of pollen-based climate reconstructions by the addition of new samples.
2) reconstruct the Holocene wetland dynamics and water level changes based on XRF data, aquatic pollen taxa and NPPs.
3) reconstruct the Holocene vegetation dynamics and identify the existence of deciduous forests or the persistence of steppes on the slopes of Lake Sevan.
4) identify human activity traces on vegetation records by distinguishing the "agricultural" practices present on the south-eastern shore of Lake Sevan.
5) provide a reliable climate reconstruction for the South Caucasus based on a multi-proxy approach including both brGDGTs and pollen (multi-method approach: MAT (Modern Analogue Technique), WAPLS (Weighted Averaging Partial Least Squares regression), RF (Random Forest) and BRT (Boosted Regression Forest)).
6) finally infer relationships between vegetation dynamics, climate changes, and human practices at a local scale and discuss these results at a regional scale (South Caucasus and Near East).

2. Study site

2.1 Geological and geographical setting

The Caucasus Mountains are situated at the eastern edge of the Near East, between the Black Sea and the Caspian Sea (Fig. 1A). They were formed by the Alpine and Himalayan orogeny with the collision between the Arabian and Eurasian plates (Volodicheva, 2002). Located in the Lesser Caucasus (i.e. a geological structure of the South Caucasus), Lake Sevan has a volcano-tectonic origin. Its northeastern shore is characterized by an ophiolitic structure dating from the Middle Jurassic to Early Cretaceous while the western and southern shores are defined by volcanic ridges dating from the Quaternary (Karakhanian et al., 2000; Sosson, et al., 2010). The lava flows from Porak volcano, located in the southeast, spread towards Lake Sevan and Vanevan peat (40°12'8.83"N, 45°40'24.03"E, Fig. 1AB). Several lava flows may date from the Holocene (Karakhanian et al., 2002). The most important fault system in Armenia, the Pambak-Sevan-Syunik fault system extends through the Porak volcano and Lake Sevan. Seven strong earthquakes on this fault are attested during the Holocene (Karakhanian et al., 2017).
The hydrological system of Lake Sevan has a negative water balance and a slow turnover (50 years) due to higher evaporation (800 mm/year) than precipitation (360 mm/year) (Leroyer et al., 2016). During the Soviet period, its water was intensively used for irrigation and electricity (Jenderedjian, 2005). Consequently, its level dropped approximately 20 m and its volume decreased by more than 40%. The lake passed from oligotrophic to eutrophic conditions, accompanied by changes in the flora and fauna (Lind and Taslakyan, 2005). Among the 28 rivers draining the lake catchment (3650 km²), the Masrik River is located in the South-East. Prior to the lake lowering and field management during the Soviet time, it crossed a wetland area named Gilli (Jenderedjian, 2005). After the drying of the wetland, the area was used for agricultural (mainly wheat and barley), pastoralism (sheep and cattle), and peat exploitation for fuel.

2.2 Modern climate and vegetation

The climate of Armenia is dominated in winter by dry and cold air masses from Siberian High. However, when these masses are weak, they are replaced by the Westerlies (associated with North Atlantic Oscillation, NAO) with snowfall in winter and rainfall in spring. In summer, the climate is warm and dry, and it is linked to Arabian subtropical high pressure in the west and Asian depression in the east (Volodicheva, 2002; Joannin et al., 2014). In the north of Lake Sevan, the annual precipitation is about 500 mm and the annual temperature is 3°C, with a

minimum in January of -8°C and a maximum in August of 15°C (Sevan City meteorological station). The coastal belt of the lake receives between 350 and 450 mm of annual precipitation while the mountain zones receive around 800 mm (Baghdasaryan, 1958). Thunderstorms are common around the lake in late spring, particularly in May-June.

The Armenian vegetation is dominated by steppes and only 8% are represented by forests (Sayadyan, 2011). Armenia has a rich biodiversity and a high level of endemism (Fayvush et al., 2013). The mountainous relief favors very different ecological environments (Stanyukovich, 1973; Volodicheva, 2002; Fayvush et al., 2017). The lower landscapes (480–1200 m a.s.l.) are covered by semi-desert vegetation, dominated by *Artemisia fragrans*. The middle mountains (1200-1800 m a.s.l.) are covered by steppes, mainly dominated by *Stipa* spp., or sparse arid woodland composed by *Pistacia atlantica* subsp. *mutica, Amygdalus fenzliana* and *Rhamnus pallasii*. On the slopes (1700-2300 m a.s.l.) arid woodland may develop with *Juniperus* spp. The upper mountains (1900-2300 m a.s.l.) are characterized by meadow steppe, rich in Poaceae. The subalpine mountains (2300-2900 m a.s.l.) are covered by subalpine meadows, generally dominated by *Festuca varia*, and some *Quercus macranthera* woodlands. The alpine mountains (2700-3700 m a.s.l.) are covered by alpine meadows rich in Poaceae (such as *Poa alpina*) and including *Taraxacum stevenii*, *Alchemilla* spp., *Potentilla* spp., *Primula* spp., *Geranium* spp., *Campanula* spp. and *Pedicularis* spp. The vegetation around Lake Sevan is mostly composed of meadow steppes dominated by Poaceae. Only the borders of the lake have trees, principally pines planted during the 1980s and some arid woodland on north-facing slopes. In the southeast slopes of Lake Sevan, some *Juniperus* spp. are also present. The detailed description of potential vegetation of Bohn et al. (2000) around Lake Sevan is presented in Leroyer et al. (2016). At a local scale, the vegetation of Vanevan peat is dominated by Poaceae, Cyperaceae and Juncaceae.

2.3 Archeology and modern human activities

During the Holocene, the first signs of human occupation (hunter-gatherers) in Armenia have been recorded during the Mesolithic in the lower Kasakh valley (Arimura et al., 2012). Agriculture is established during the Late Neolithic (8000-7500 a cal BP) on the Ararat plain (Badalyan et al., 2004; Hovsepyan and Willcox, 2008; Badalyan and Harutyunyan, 2014) where cereals, vetch and lentil have all been recorded along with the presence of sheep (*Ovis aries*), goat (*Capra hircus*), cattle (*Bos taurus*) and scant evidence of pigs (*Sus domesticus*) (Hovsepyan and Willcox, 2008). On the shore of Lake Sevan, the first traces of agriculture date around 5500 a cal BP during the Early Bronze Age (Hovsepyan, 2013, 2017). During the Early,

Mid-, and Late Bronze Ages, Early Iron Age, and medieval period, cereals are the primary subsistence crop in the southeast of Lake Sevan around Gilli wetland (Biscione et al., 2002; Parmegiani and Poscolieri, 2003; Hovsepyan, 2013, 2017). The long-term occupation of this area is also attested by the presence of many tombs in Gilli wetland (Fig. 1C). Several empires including the Persians (Achaemenids and Sassanids), Arabs, and Mongols and states including Urartu, Ottoman Turkey, Imperial Russia, and the USSR have succeeded in Armenia (Lindsay and Smith, 2006). The Urartian Empire was present during the Iron Age and centered around Lake Sevan (Biscione et al., 2002; Parmegiani and Poscolieri, 2003). During this period subsistence focused on the cultivation of cereals, vines, fruit trees, and pastoralism. Today, the activities are centered around agriculture and extensive pastoralism. To date, no pollen study has been able to compare pollen indicators of human activities with archeological findings in the Sevan area. In the work done by Leroyer et al. (2016) at Vanevan, the pollen sequence does not cover the last 5700 years BP.

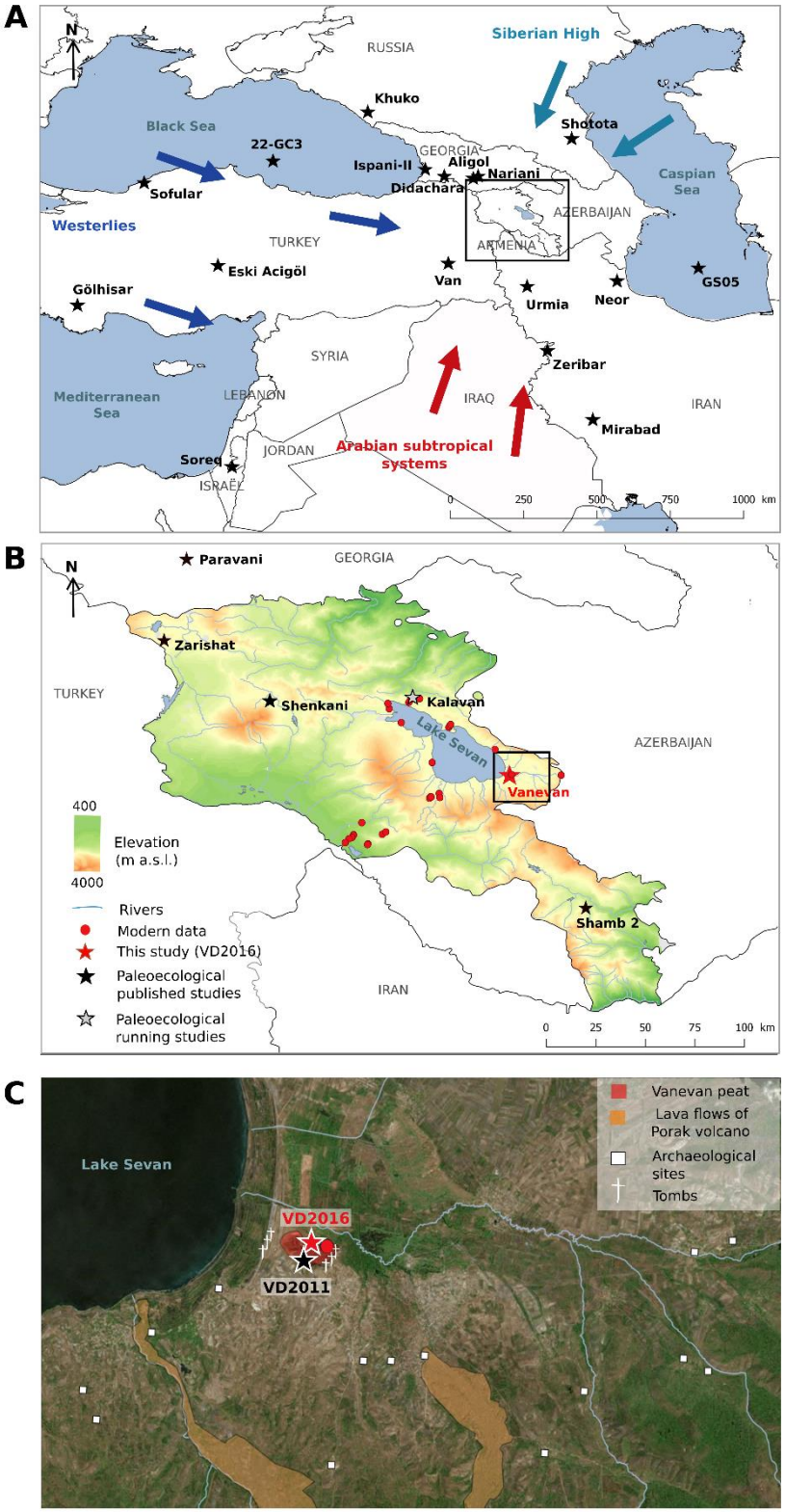

Figure II-1. A) East Mediterranean region with selected paleoenvironmental studies: Lake Khuko (Grachev et al., 2020), Shotota swamp (Ryabogina et al., 2018), 22-GC3 (Shumilovskikh et al., 2012), Ispani-II mire (Connor and Kvavadze, 2008), Lake Aligol (Connor and Kvavadze, 2008), Didachara Mire (Connor et al., 2018), Nariani wetland (Messager et al., 2017), Sofular cave (Göktürk et al., 2011), Lake Van (Wick et al., 2003), Eski Acigöl (Roberts et al., 2001), Lake Neor (Sharifi et al., 2015), Lake Urmia (Djamali et al., 2008), Lake Gölhisar (Eastwood et al., 2007), GS05 (Leroy et al., 2013), Lake

Zeribar (Stevens et al., 2001), Lake Mirabad (Stevens et al., 2006), Soreq cave (Bar-Matthews et al., 1997). B) Topography of Armenia with the location of Vanevan peat and modern samples (mosses, soils and botanical records). Black and gray stars represent published and ongoing paleoecological studies, respectively: Lake Paravani (Messager et al., 2013; 2073 m), Zarishat fen (Joannin et al., 2014; 2116 m), Lake Shenkani (Cromartie et al., 2020; 2193 m), Lake Kalavan (Joannin et al., in prep; 1603 m), Shamb 2 (Ollivier et al., 2011). C) Southeastern shore of Lake Sevan with the location of Vanevan peat (VD2016 core, this study; VD2011 core, Leroyer et al., 2016) and archeological sites (Biscione et al., 2002; Parmegiani and Poscolieri, 2003; Hovsepyan, 2013, 2017). Image modified from Google Earth (Image © 2020 CNES/Airbus, © 2019 Google, © 2019 Basarsoft).

3. Material and methods

3.1 Field campaign

3.1.1 Core retrieval

The present study focuses on a new core VD2016 (40°12'8.83"N, 45°40'24.03"E, 1916 m a.s.l.) retrieved from approximately 850 meters north of the previous Vanevan study (Fig. 1C). Two parallel cores (cores A and B) were taken with a 1 m Russian corer with a 6.3 cm diameter chamber. The mastercore (MC), was built from sections of both cores using the lithology and XRF data for correlation. The complete continuous sequence measures 601 cm in total.

3.1.2 Modern samples

A total of 28 modern pollen samples along an altitudinal transect from the Ararat plain (808 m a.s.l.) to the mountains of Lake Sevan (2699 m a.s.l.) were collected in May 2016, 2017, and 2019 (Fig. 1B and Supplementary Table S1). This transect records the vegetation in semi-desert steppes, meadow steppes, subalpine, and alpine meadows in Armenia (Stanyukovitch, 1973; Volodicheva, 2002). Several sampling sites are located around Lake Sevan and three altitudinal transects were performed in the mountains around it (Mount Artanish, Mount Armaghan, and Mount Katarajayr). In each sampling site, 2-5 moss polsters or soil were collected within a radius of 5 m and then combined into one sample. The vegetation within a radius of 10 m, representing the local vegetation, was recorded by visual estimation of percentage cover for 19 sites (adaptation of the Braun-Blanquet method; Braun-Blanquet and Schoenichen, 1964). For the other sites, the local vegetation was not quantitatively identified but qualitatively estimated. The vegetation within a radius of 100 m is considered as the extra-local vegetation and beyond this distance as the regional vegetation. The modern climate data

were calculated with the *New_LocClim 1.10* software (Grieser et al., 2006) and then corrected according to the site elevation.

3.2 Age model, lithology, and geochemistry

3.2.1 Age model and lithology

The core chronology is based on 12 accelerator mass spectrometry (AMS) ^{14}C dates (Table 1). For seven samples, plant macrofossils (plant fibers, seeds) and charcoal were selected for dating. In addition, bulk sediment was used for another set of 5 samples in which the quantity of macrofossils was insufficient. Radiocarbon ages were calibrated in years cal BP using *Calib 8.2* software with the IntCal20 calibration curve (Reimer et al., 2020) and the median calibrated ages with the 2 σ confidence intervals (95%) are reported in Table 1. The age-depth model was constructed using an interpolated linear curve with the R 'Clam' program with 95% confidence intervals (Blaauw, 2010). Three zones were defined upon visual differences in lithology.

Table II-1. AMS-radiocarbon dates (Radiocarbon Laboratory, Poznań), calibrated median ages, with 2 σ range of calibration from Vanevan peat A and B cores. *: Age rejected

Sample ID	Depth MC (cm)	Lab code	Material	AMS 14C age (a BP)	Age (a cal BP) (2 σ)	Median age (a cal BP)
A0 15-17	15	Poz-111218	Plant fibers	875 ± 30	692-903	768
A0 42-43	42	Poz-88797	Plant fibers	1860 ± 50	1623-1916	1773
A1 16-17	59	Poz-110035	Plant fibers, seeds	2355 ± 35	2326-2665	2377
A1 55-57	98	Poz-89222	Plant fibers	4380 ± 40	4848-5255	4943
A2 16-17	126	Poz-110036	Plant fibers, seeds	4400 ± 35	4859-5263	4966
A2 56-57	165	Poz-119280	Plant fibers, charcoals, seeds	4450 ± 30	4885-5284	5112
A2 86-87*	195	Poz-122005	Bulk	6605 ± 35	7429-7568	7495
A3 39-40	247	Poz-122006	Bulk	6690 ± 35	7479-7651	7554
A3 81-82	289	Poz-119285	Bulk	6920 ± 40	7670-7842	7746
A5 80-81	486	Poz-119281	Bulk	7980 ± 50	8646-8998	8844
B5 29-31	534	Poz-89221	Plant fibers	8230 ± 40	9026-9401	9197
A6 91-92*	597	Poz-121074	Bulk	6980 ± 50	7690-7931	7810

3.2.2 Geochemistry

The running chemical composition of the sediment cores was performed using an Avaatech XRF (EDYTEM Laboratory) core scanner at a 0.5 cm interval (elements presented here: Si, K, Ti, Al, S, Fe, Ca, Mg, P). XRF measurements were carried out on split cores with a duration step of 10 s. A 10 kV voltage and a 1000 µA current was applied to detect elements. Because of the influences of variable water content and grain size on the sediment matrix, the

XRF scanner provides an estimate of the geochemical composition, and the acquired counts are semi-quantitative. The selected elements are indicative of the sediment geochemistry itself depending on erosive and deposit conditions, and of sources in the catchment (Croudace and Rothwell, 2015). Principal component analysis (PCA) was performed on XRF data with *FactoMineR 2.4* package (Lê et al., 2008). Titanium (Ti) content is considered as a terrigenous indicator because it is weakly affected by weathering and redox conditions (Arnaud et al., 2012). Silicon (Si) content may be derived from diatoms, radiolaria, siliceous sponges, or from phytoliths contained in aquatic and terrestrial plants. The ratio Si/Ti allows to understand the respective role of organic production or terrigenous inputs (Brown et al., 2007).

3.3 Pollen, NPP analysis, and pollen-inferred climate reconstruction

3.3.1 Pollen, NPP extraction, and counting

A total of 28 modern and 94 fossil pollen samples from the Vanevan core (2 cm resolution between 43-99 cm, 4 cm resolution between 99-170 cm, 10 cm resolution between 170-600 cm) were extracted for analysis. For each sample, 1 cm^3 of sediment was processed and 3 *Lycopodium* tablets were added to calculate the absolute abundance of pollen grains. The core samples were treated with the standard procedure (Fægri et al., 1989; Moore et al., 1991) including HCl, KOH, acetolysis and HF. The pollen and NPP counts were carried out with a Leica DM1000 LED microscope at a standard magnification of 400x. Pollen and NPP taxa were identified using photo atlases (Reille, 1992–1998; Komárek and Jankovská, 2001; Van Geel, 2002; Beug, 2004) and a modern reference collection (ISEM, University of Montpellier). A minimum of 300 or 200 pollen grains of terrestrial taxa (excluding aquatic plants, mainly Cyperaceae) was counted by slide for the richest and the poorest samples, respectively, to obtain a representative assessment of pollen types (Lytle and Wahl, 2005; Djamali and Cilleros, 2020). Grass pollen grains greater than 40 µm were classified as *Cerealia*-type (Beug, 2004). Aquatic taxa, fern spores, and NPPs (algae and fungal spores) were counted alongside pollen. The pollen diagrams were constructed with the R package *Rioja* (Juggins, 2020).

3.3.2 Pollen-inferred climate reconstruction

To reconstruct climate parameters from pollen data, currently available methods have their own set of advantages and limitations and the selection of the most appropriate technique to be used on the fossil pollen record can be complex. A multi-method approach is the best

choice to increase the reliability of the climate reconstruction (e.g. Brewer et al., 2008; Peyron et al., 2013; Salonen et al., 2019). Four methods have been selected here among the most accurate (Chevalier et al., 2020): the Modern Analog Technique (MAT; Guiot, 1990), Weighted Averaging Partial Least Squares regression (WAPLS; Ter Braak and Van Dam, 1989; Ter Braak et al., 1993), and regression Trees: Random Forest (RF; Breiman, 2001; Prasad et al., 2006) and Boosted Regression Trees (BRT; De'ath, 2007; Elith et al., 2008). The MAT and the WAPLS are often selected to reconstruct past climate changes while RF and BRT have been developed recently to reconstruct palaeoclimate changes (Salonen et al., 2016, 2019) and have never been tested on Caucasus pollen records. Based on machine learning, these classification trees are used to partition the data by separating the pollen assemblages based on the relative pollen percentages. RF is based on a large number of regression trees, each tree being estimated from a randomized ensemble of different subsets of the modern pollen dataset by bootstrapping. BRT is also based on regression trees and differs from RF in the definition of the random modern datasets. In RF, each sample gets the same probability of being selected, while in BRT the samples that were insufficiently described in the previous tree get a higher probability of being selected. This approach is called 'boosting' and increases the performance of the model over the elements that are least well predicted.

The modern pollen dataset used here (382 samples) is part of the large Eurasian/Mediterranean dataset compiled by Peyron et al., (2013, 2017) which include more than 3200 modern pollen samples (moss polster, soils and top-cores). A recent study showed that (1) large databases are not reliable for the reconstruction of steppic environment/climate and (2) local calibrations including data from steppe and desert–steppe sites are necessary to better calibrate arid environments (Dugerdil et al., 2021). Therefore, the large database has been cropped to optimize the selection of surface samples consistent with our paleosequence environment: we used here a reduced dataset of 382 "cold steppe" samples, including new samples from Mongolia (Peyron et al., 2013, 2017; Dugerdil et al., 2021), Georgia (Connor et al., 2004) and Armenia (seventy-five new modern samples, this study). We applied here a biome constraint (Guiot et al., 1993), which is essential to define steppe environments and to distinguish between cold and warm steppes. Therefore, we have finally used for the calibration of each method the samples attributed to the biomes "cold steppes" following the biomization procedure (Prentice et al., 1996; Peyron et al., 1998). The location of these 382 cold steppe samples is given in the Supplementary Fig. S2. The surface calibration methods and datasets to reconstruct paleoclimate in arid environments are discussed in Dugerdil et al., (2021). In order to estimate the performance of each method, the transfer functions have been tested on the

modern "cold steppe" dataset, 60% of the dataset has been used to calibrate and 40% to test the transfer functions, thereby preventing a circular reasoning. Correlations have been realized between the current climate parameters extracted from WorldClim 2 (Fick and Hijmans, 2017) and the estimated climate parameters reconstructed by each method (Supplementary Fig. S3). Then, the performance of each method and each calibration training was statistically tested with a bootstrap technique (for more details, see Dugerdil et al., 2021). The transfer functions have been applied 500 times on the modern "cold steppe" dataset, thereby obtaining the Root Mean Square Error (RMSE) and the R^2 and determining if modern samples are suitable for quantitative climate reconstructions (Supplementary Table S4). Thereafter, the function transfers have been applied on the Vanevan core samples with the modern "cold steppe" dataset. Four climate parameters were reconstructed, mean annual air temperature (MAAT), mean annual precipitation (MAP), mean temperature of the warmest month (MTWA), and summer precipitation (P_{summer}) including July, August, and September. For each climate parameter, the methods fitting with the higher R^2 and the lower RMSE were selected. The WAPLS and the MAT methods were applied with the R package Rioja (Juggins, 2020), the RF with the R package randomForest (Liaw and Wiener, 2002) and the BRT with the R package dismo (Hijmans et al., 2020). Cyperaceae and ferns of Vanevan record have been excluded because they indicate local dynamics in Armenia (Joannin et al., 2014; Cromartie et al., 2020).

3.4 GDGT analysis and annual temperature reconstruction

3.4.1 BrGDGT analyses

A total of 46 core samples (4-20 cm resolution) were used for GDGT analysis. After freeze-drying and grounding, a subsample (0.8 g for soil, 1 g for clay and 0.6 g for peat sediments) was extracted using a Microwave oven (MARS 6; CEM) with a mix of dichloromethane and methanol (3:1). The total lipid extract was split on a silica SPE cartridge, using hexane: DCM (1:1) and DCM:MeOH (1:1). GDGTs were analyzed using a High-Performance Liquid Chromatography Mass Spectrometry (HPLC-APCI-MS, Agilent 1200) with detection via selective ion monitoring (SIM) of m/z 1050, 1048, 1046, 1036, 1034, 1032, 1022, 1020, and 1018 for brGDGTs (Hopmans et al., 2016; Davtian et al., 2018). GDGT concentrations were calculated based on the internal standard (C_{46} GDGT, Huguet et al., 2006). The linearity and analytic reproducibility were assessed based on an internal standard sediment.

3.4.2 brGDGT-based proxy calculation and global calibration datasets

The formulae for the brGDGT indexes are presented in Table 2. The proportions of tetra- (I), penta- (II) and hexa- (III) methylated brGDGTs were calculated with the fractional abundances of brGDGTs including the 5-methyl (X), the 6-methyl (X') and the 7-methyl brGDGT (X_7) (Ding et al., 2016). The ΣIIIa/ΣIIa ratio proposed by Xiao et al. (2016) was calculated according to the equation modified by Martin et al. (2019) including the 5-, 6- and 7-methyl brGDGTs. The CBT and MBT indexes were developed by Weijers et al. (2007) and the MBT'$_{5me}$, only based on the 5-methyl brGDGTs, by De Jonge et al. (2014). The mean annual temperature was calculated with the global soil calibration developed by Naafs et al. (2017a) and the global lacustrine calibration developed by Sun et al. (2011). The calibrations are applied according to the sediment types in paleorecords (e.g. Martin et al., 2019) and can be homogenized using a ΔMAAT based on the mean value of each sediment type. The analytic reproducibility corresponds to 0.005 for CBT, 0.006 for MBT, 0.008 for MBT'$_{5me}$, 0.3 for $MAAT_{soil5me}$ and 0.2 for $MAAT_{lake}$.

Table II-2. Synthesis of the formulae for the main brGDGT indices

Indice	Formula	Reference
$\%tetra$	$\frac{Ia + Ib + Ic}{\Sigma brGDGTs}$	Ding et al., 2016
$\%penta$	$\frac{IIa + IIa' + IIa_7 + IIb + IIb' + IIb_7 + IIc + IIc' + IIc_7}{\Sigma brGDGTs}$	Ding et al., 2016
$\%hexa$	$\frac{IIIa + IIIa' + IIIa_7 + IIIb + IIIb' + IIIb_7 + IIIc + IIIc' + IIIc_7}{\Sigma brGDGTs}$	Ding et al., 2016
$\Sigma IIIa/\Sigma IIa$	$\frac{IIIa + IIIa' + IIIa_7}{IIa + IIa' + IIa_7}$	Martin et al., 2019
CBT	$-log\frac{Ib + IIb}{Ia + IIa}$	Weijers et al., 2007
MBT	$\frac{Ia + Ib + Ic}{\Sigma brGDGTs}$	Weijers et al., 2007
MBT'_{5me}	$\frac{Ia + Ib + Ic}{Ia + Ib + Ic + IIa + IIb + IIc + IIIa}$	De Jonge et al., 2014
$MAAT_{soil5me}(°C)$	$39.09 \times MBT'_{5me} - 14.50 (n = 177, R^2 = 0.76, RMSE = 4.1°C)$	Naafs et al., 2017a
$MAAT_{lake}(°C)$	$3.949 - 5.593 \times CBT + 38.213 \times MBT (n = 100, R^2 = 0.73, RMSE = 4.27°C)$	Sun et al., 2011

4. Results

4.1 Sediment analysis

4.1.1 Age-depth model

The Clam age-depth model (Fig. 2B) is based on ten calibrated ^{14}C dates (Table 1). Two ^{14}C dates (A2 86-87 at depth 195 cm and A6 91-92 at depth 597) were excluded from the age-depth model. The age-depth model constructed with the R 'Bacon' program (Blaauw and Christen, 2011; not shown) has rejected the two dates and the same information was used with the 'Clam' program. The VC2016 record extends from 9700 a cal BP to 800 a cal BP. The age-depth model has an error of ~50–260 years between 15-550 cm and ~210–470 years for the base of the core (550-600 cm) (Fig. 2B and Supplementary Table S5). The age–depth curve shows a sedimentation rate (16.7 cm.100 yr^{-1}) that decreases at 7560 a cal BP (3.3 cm.100 yr^{-1}) except between 5100 and 4950 a cal BP (43.5 cm.100 yr^{-1}). From the base of the core to 43 cm depth, an average temporal resolution of 77 years was achieved for pollen records and 202 years for brGDGTs.

4.1.2 Lithology changes

The core lithology is divided into 3 units (Fig. 2B). Unit 1 (600-558 cm) is characterized by a light gray clay and sand sediment. Unit 2 (558-170 cm) is composed of a gray clay sediment. Unit 3 (170-15 cm) is divided into 4 subzones. Unit 3a (170-144 cm) is composed of a brown peat silt sediment. Unit 3b (144-125 cm) is characterized by alternating yellow and dark peat silt sediments. Unit 3c (125-113 cm) is marked by a gray clay sediment. Unit 3d (113-15 cm) is composed of a peat silt sediment with brown, dark and orange colors. The clay sediments are interpreted as open underwater environments while the peat sediments indicate the accumulation of plant remains growing in place in restricted underwater or near-surface environments.

4.1.3 Geochemical composition

A principal component analysis (PCA) was conducted on XRF elements (Fig. 2B) and the sample map was colored according to the lithology units. The first two dimensions (PCA 1_{XRF} and PCA 2_{XRF}) explain 80% of the variability (64% and 16% respectively). Two major geochemical end-members are identified: the first one represents terrigenous inputs (K, Al, Mg,

Si, Ti, Fe) and are positively correlated with PCA 1_{XRF}. Terrigenous elements are associated with clay sediments (Units 1 and 2) deposited in open underwater environments, and are opposed to organic sediments (Unit 3) mainly composed of peat sediments formed in restricted underwater or near-surface environments.

The second end-member represents carbonate components (Ca), sulfur (S) and phosphorus (P) and are positively correlated with PCA 2_{XRF}. Calcium is abundant at the base of the core (Unit 1) and in the first organic levels (Units 3a, 3b, 3c). Sulfur and phosphorus are only abundant in the first organic levels (Units 3a, 3b, 3c). The upper part of the core (Unit 3d) is distinguished by a biogenic silica production, visible in the ratio Si/Ti (Brown et al., 2007).

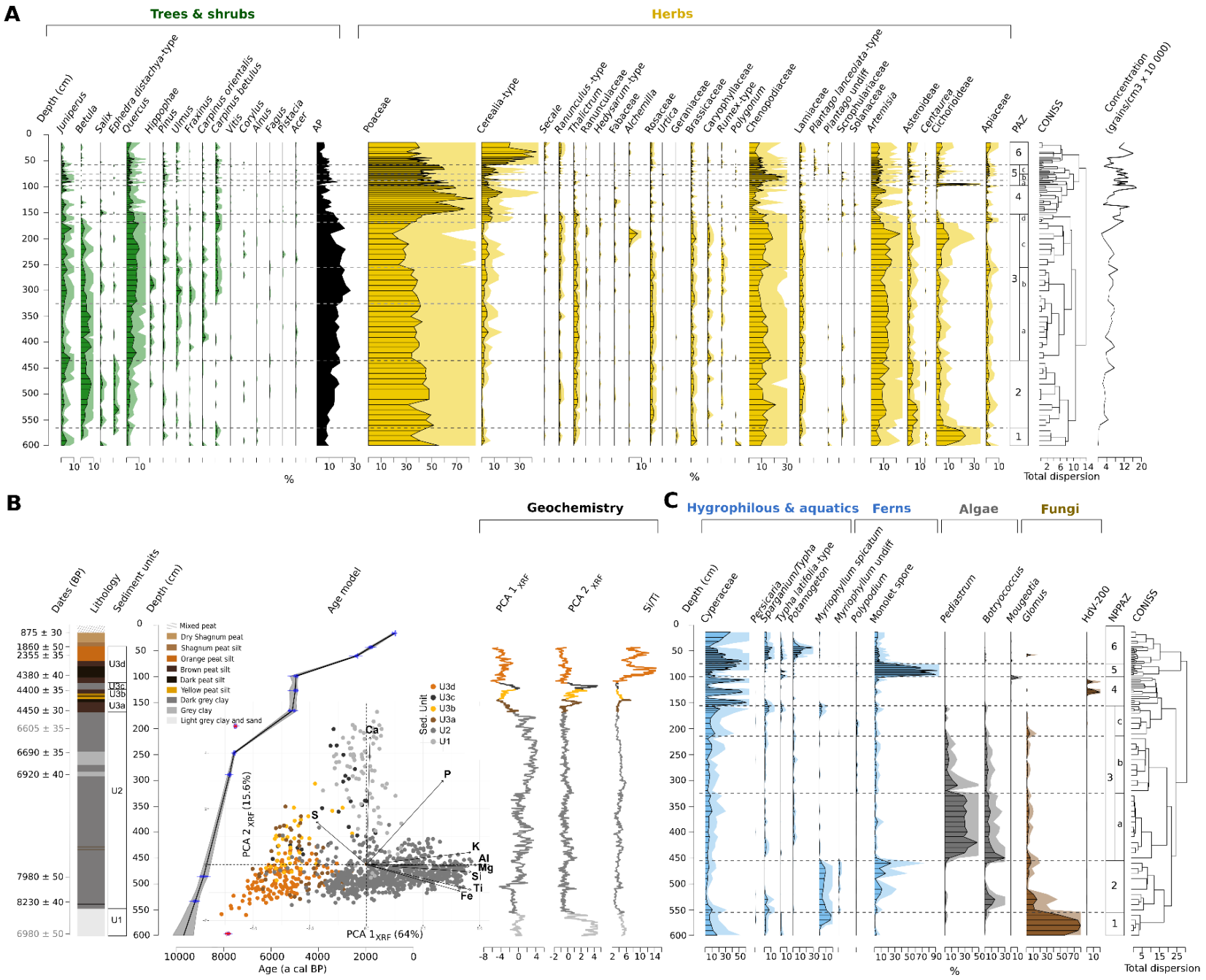
A
Trees & shrubs
Herbs
Depth (cm)
Juniperus
Betula
Salix
Ephedra distachya-type
Quercus
Hippophae
Pinus
Ulmus
Fraxinus
Carpinus orientalis
Carpinus betulus
Vitis
Corylus
Alnus
Fagus
Pistacia
Acer
AP
Poaceae
Cerealia-type
Secale
Ranunculus-type
Thalictrum
Ranunculaceae
Hedysarum-type
Fabaceae
Alchemilla
Rosaceae
Urtica
Geraniaceae
Brassicaceae
Caryophyllaceae
Rumex-type
Polygonum
Chenopodiaceae
Lamiaceae
Plantago lanceolata-type
Plantago undiff
Scrophulariaceae
Solanaceae
Artemisia
Asteroideae
Centaurea
Cichorioideae
Apiaceae
PAZ
CONISS
Concentration (grains/cm3 x 10 000)
%
Total dispersion
B
Geochemistry
Dates (BP)
Lithology
Sediment units
Depth (cm)
Age model
Mixed peat
Dry Shagnum peat
Shagnum peat silt
Orange peat silt
Brown peat silt
Dark peat silt
Yellow peat silt
Dark grey clay
Grey clay
Light grey clay and sand
Sed. Unit
U3d
U3c
U3b
U3a
U2
U1
PCA 1 XRF
PCA 2 XRF
SiTi
Ca
P
S
K
Al
Mg
Si
Ti
Fe
PCA 1XRF (64%)
PCA 2 XRF (15.6%)
Age (a cal BP)
C
Hygrophilous & aquatics
Ferns
Algae
Fungi
Cyperaceae
Persicaria
Sparganium/Typha
Typha latifolia-type
Potamogeton
Myriophyllum spicatum
Myriophyllum undiff
Polypodium
Monolet spore
Pediastrum
Botryococcus
Mougeotia
Glomus
HdV-200
NPPAZ
Total dispersion

Figure II-2. Pollen and sedimentology of Vanevan peat against core depth. A) Selected terrestrial pollen taxa. Tree, shrub, and herb pollen taxa are expressed in percentages of total terrestrial pollen. AP: Arboreal Pollen. PAZ: Pollen Assemblage Zones. B) Sediment lithology, age-depth model and geochemical data. The age–depth model is based on calibrated radiocarbon ages (with 2 σ errors) (AMS, see Table 1). Principal component analysis (PCA) was done on XRF data according to the lithological units. The first two dimensions (PCA 1_{XRF} and PCA 2_{XRF}) of PCA are arranged by depth. C) Selected hygrophilous and aquatic pollen taxa and NPPs. Hygrophilous and aquatic pollen taxa are expressed in percentages of total pollen. Fern spores, algae and fungi are expressed in percentages of total terrestrial pollen and NPPs. NPPAZ: Non-Pollen Palynomorph Assemblage Zones.

4.2 Pollen analysis and pollen-based climate reconstruction

4.2.1 Surface samples, vegetation, and climate

The modern pollen assemblages (Fig. 3) are dominated by herbaceous pollen taxa, including Poaceae, Chenopodiaceae and *Artemisia*. By comparing the pollen data with the vegetation, it appears that Poaceae is well associated with the local vegetation, while Chenopodiaceae, *Artemisia*, Asteroideae and Cichorioideae are over-represented. Arboreal taxa such as *Hippophae* is well associated with the local vegetation while *Quercus* and *Pinus* are over-represented.

The altitudinal vegetation gradient is well recorded in the modern pollen rain. The lower and middle elevations (800-1900 m) are dominated by pollen of Chenopodiaceae (33%), Poaceae (19%), *Artemisia* (16%), and indicate a semi-desert or steppe vegetation. A few pollen grains of *Pistacia* and *Salix* are also recorded. These levels are distinguished by high percentages of Chenopodiaceae and *Artemisia* and by low percentages of arboreal pollen taxa (7%). The upper elevations (1900-2300 m) record high percentages of Poaceae (30%), characteristic of meadow steppes, except when trees or shrubs are present in the local (*Hippophae, Salix, Juniperus, Acer, Viburnum*) or extra-local vegetation (*Pinus*). *Pinus* was present in the extralocal vegetation of sites number 13 and 18. However, only site number 13 records *Pinus* pollen. *Quercus*, *Carpinus betulus* and *Fagus* are recorded with low percentages (<4%). *Artemisia* and Chenopodiaceae represent only 7% and 4%, respectively. The subalpine and alpine environments are dominated by Poaceae pollen (38%) and few arboreal pollen taxa, such as *Quercus* (7%), *Betula* (6%), *Ulmus* (3%), are recorded. At these elevations, *Artemisia* and Chenopodiaceae represent 7% each.

Although the modern sites are distant from agricultural areas, pollen of *Cerealia*-type are recorded, reaching up to 11%. Pollen indicator of pastoralism activities, such as *Plantago lanceolata*-type or *Rumex*-type, represent less than 1% on average and a maximum of 6%.

Otherwise, the pollen rain shows correspondence to climatic gradients (Fig. 3). The highest percentages of Chenopodiaceae and *Artemisia* pollen correspond to high temperature (>5°C) and low precipitation (MAP<500 mm). The limit between cool and warm steppe biomes correspond to a change in Chenopodiaceae percentages and in MAP. In contrast, percentages of Poaceae pollen increase when MAAT decreases.

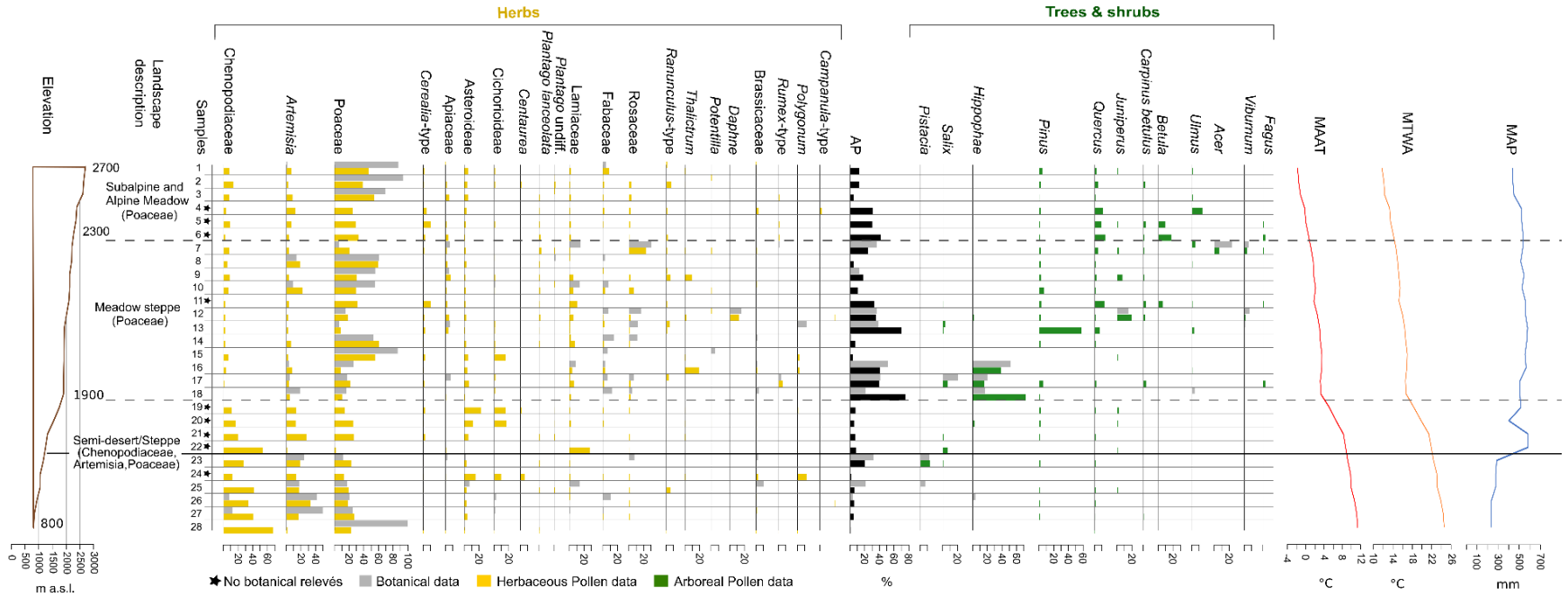

Figure II-3. Selected modern pollen assemblages, botanical relevés and climate values along an altitudinal transect in Armenia. MAAT=mean annual air temperature, MTWA= mean temperature of the warmest month, MAP= mean annual precipitation.

Table II-3. Inventory of pollen assemblage zones (PAZ), depth, estimated ages, total of arboreal pollen (AP_t), common and rare pollen types (CPT, RPT) for arboreal and herbaceous taxa, Non-Pollen Palynomorph assemblage zones (NPPAZ) and main hygrophilous pollen taxa and Non-Pollen Palynomorphs (NPPs). Common pollen types (CPT) include pollen taxa with percentages > 5% and rare pollen types (RPT) percentages < 5%

PAZ	Depth (cm) *Age (a cal BP)*	Total of Arboreal Pollen %	Arboreal and herbaceous pollen Common pollen types (CPT) Rare pollen types (RPT)	NPPAZ	Hygrophilous pollen NPPs
6	58-15 *2350-790*	AP_t 7	CPT: Poaceae, *Cerealia*-type, Chenopodiaceae, *Artemisia* RPT: Cichorioideae, Asteroideae, Apiaceae Rosaceae, *Ranunculus*-type, *Quercus, Carpinus betulus, Juniperus*	**6**	Cyperaceae, *Potamogeton, Sparganium/Typha*, Cyperaceae
5c	76-58 *3500-2350*		CPT: Poaceae, Chenopodiaceae, *Cerealia*-type, *Artemisia* RPT: Cichorioideae, Asteroideae, Apiaceae; *Quercus, Juniperus, Carpinus betulus, Pinus*		
5b	88-76 *4300-3500*		CPT: Poaceae, Chenopodiaceae, *Artemisia*, *Cerealia*-type RPT: Asteroideae, Cichorioideae, Apiaceae, *Juniperus, Quercus, Pinus, Carpinus betulus*		
5a	98-88 *4950-4300*		CPT: Poaceae, Cichorioideae, Chenopodiaceae, *Artemisia* RPT: *Cerealia*-type, Asteroideae, Lamiaceae, *Thalicthrum; Quercus, Juniperus, Pinus, Carpinus betulus*		
5	98-58 *4950-2350*	AP_t 9		**5**	Monolete spores, *Typha latifolia*-type, Cyperaceae
4	153-98 *5100-4950*	AP_t 8	CPT: Poaceae, *Cerealia*-type, Chenopodiaceae, *Artemisia* RPT: Lamiaceae; *Quercus, Juniperus, Carpinus betulus*	**4**	Alternating episodes with or without Cyperaceae accompanied by *Sparganium/Typha, Myriophyllum spicatum*, fungi HdV-200, *Mougeotia*
3d	256-153 *5200-5100*		CPT: Poaceae, Chenopodiaceae, *Cerealia*-type, *Artemisia* RPT: Cichorioideae, Asteroideae, *Quercus, Carpinus betulus, Juniperus, Carpinus orientalis*		
3c	256-169 *7600-5200*		CPT: Poaceae Chenopodiaceae, *Artemisia, Cichorioideae, Quercus, Alchemilla* RPT: *Cerealia*-type, Asteroideae, *Thalictrum*, Brassicaceae, Lamiaceae, Rosaceae, *Ranunculus*-type, *Caryophyllaceae, Rumex*-type; *Betula, Juniperus, Carpinus betulus*		
3b	326-256 *8000-7600*		CPT: Poaceae, *Artemisia*, Chenopodiaceae, *Quercus* RPT: *Cerealia*-type, *Thalictrum*, Cichorioideae, Brassicaceae, Apiaceae, Lamiaceae, Rosaceae, Asteroideae, *Caryophyllaceae*, *Ranunculus*-type, *Rumex*-type*; Betula, Juniperus,Ulmus, Fraxinus, Hippophae, Carpinus betulus, Carpinus orientalis*		
3a	436-326 *8600-8000*		CPT: Poaceae, *Artemisia*, Chenopodiaceae RPT: *Cerealia*-type, *Thalictrum*, Cichorioideae, Brassicaceae, Apiaceae, Lamiaceae, Rosaceae, Asteroideae, *Caryophyllaceae*; *Betula, Quercus, Ulmus, Fraxinus, Carpinus orientalis, Hippophae, Pinus*		
3	436-153 *8600-5100*	AP_t 17	Maximum of arboreal pollen percentages and diversity. Progressive decrease in Poaceae and trees until 5900 a cal BP.	**3**	Planktonic algae (*Pediastrum, Botryococcus*), Cyperaceae
2	566-436 *9400-8600*	AP_t 13	CPT: Poaceae Chenopodiaceae, *Artemisia* RPT: *Cichorioideae*, Asteroideae, *Thalictrum*, Brassicaceae, Apiaceae, Lamiaceae, Rosaceae; *Betula, Quercus, Juniperus, Ephedra distachya*-type, *Salix, Hippophae*	**2**	*Myriophyllum spicatum*, Monolete spores. At 9200 a cal BP, peak of Botryococcus *Glomus, Sparganium/Typha*

1	600-566 *9700-9400*	AP_t 8	CPT: Poaceae, Cichorioideae, Chenopodiaceae *Artemisia* RPT: Asteroideae, *Polygonum, Thalictrum*, Brassicaceae, Apiaceae; *Juniperus, Quercus, Betula, Carpinus betulus*	**1**	*Glomus*, Cyperaceae, *Myriophyllum spicatum*

4.2.3 Comparison between surface and core samples

A classification by hierarchical cluster analysis was conducted on Armenian surface samples and core VD2016 samples (Fig. 4). The surface samples are well distributed within the core samples: the surface samples dominated by Poaceae (n. 1-3, 8, 14, 15), are close to core samples which record a large percentage of Poaceae (PAZ 1, 2, 4, 5) whereas those recording regional arboreal taxa (n. 4-7, 9-12, 17) approach the core samples of PAZ 3 representing the most forested phase. At lower and middle elevations, the surface samples with a large percentage of Cichorioideae (19, 20, 24) are close to the PAZ 1 core samples recording a large proportion of this taxon whereas those dominated by Chenopodiaceae, Artemisia and Poaceae (n. 13, 16, 18, 21-23, 25-28; i.e. mainly lowland samples) seem more different of the core samples.

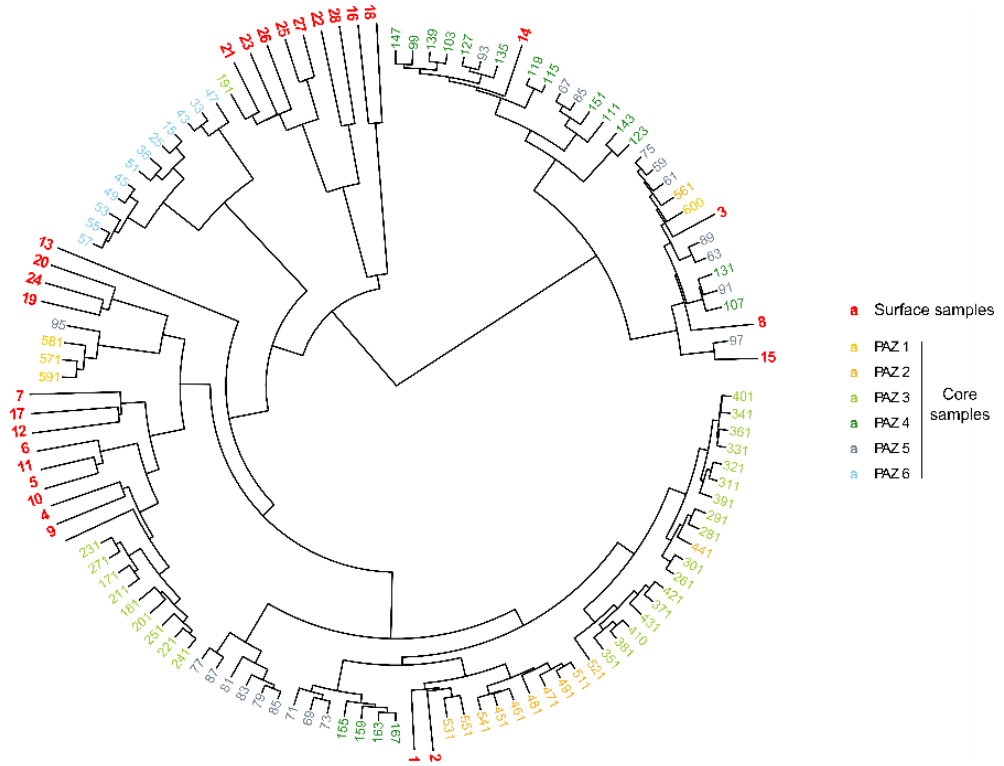

Figure II-4. Classification by hierarchical cluster analysis on surface samples of Armenia (presented in Fig. 3) and core samples of VD2016 expressed in depth (presented in Fig. 2). The color of core samples corresponds to the six pollen assemblage zones (PAZ) defined with the CONISS method. The distance matrix was calculated using Euclidean distance and Ward's algorithm was applied for clustering.

4.2.4 Pollen-inferred climate reconstruction

Climate changes at Vanevan are estimated using four methods: MAT, WAPLS, RF, and BRT (Fig. 5). The climate patterns reconstructed are consistent and do not seem method-dependent. The MAT and the BRT appear as the most sensitive methods and the results show important sample-to-sample variability; the WAPLS method shows large variations along the Holocene and the inferred values are significantly higher than the modern values; the RF is the less sensitive method (Fig. 5). Correlations between current and estimated climate parameters show the maximum R^2 for the RF and BRT methods (Supplementary Fig. S3). However, the RF method does not reconstruct correctly the high or the low current climate values. Statistical results of the model performances are presented in Supplementary Table S4; the BRT method presents the maximum R^2 and the minimum RMSE for all climatic parameters.

Based on the multi-method approach, the Vanevan climate reconstruction (Fig. 5) shows remarkably consistent trends during the Holocene, except for the most recent periods. Five climatic phases have been defined and are described below.

Phase 1 (9700 – 8200 a cal BP) is first characterized by warm and wet conditions. For temperature and annual precipitation, all methods show the same trend although the reconstructed values can be different. Then, the reconstructions show a drop in temperature and precipitation with a minimum between 8600 and 8200 a cal BP.

Phase 2 (8200 – 5500 a cal BP) is marked by warmer conditions than previously. Temperatures increase and reach an optimum around 6000 a cal BP (2.5-6°C for MAAT and 17-19°C for MTWA). Considering precipitation, it first increases and then declines around 6000 a cal BP (350-530 mm/year for MAP and 130-150 mm/year for P_{summer}).

Phase 3 (5500 – 4300 a cal BP) shows cooler and wetter conditions than previously. Precipitation increases for all methods reaching 460-550 mm/year for MAP and 130-170 mm/year for P_{summer}.

Phase 4 (4300 - 3500 a cal BP) is mainly characterized by a drop in annual precipitation and particularly in P_{summer} with a minimum at 4100 a cal BP (90-150 mm/year).

Phase 5 (3500 - 800 a cal BP) is marked by divergent trends according to the methods. The MAT, RF, and BRT methods record a decrease of temperature and precipitation. In contrast, the WAPLS method shows the warmest and the wettest conditions of the Holocene. At 2800 a cal BP, a decrease in temperature and precipitation are recorded by WAPLS and RF methods.

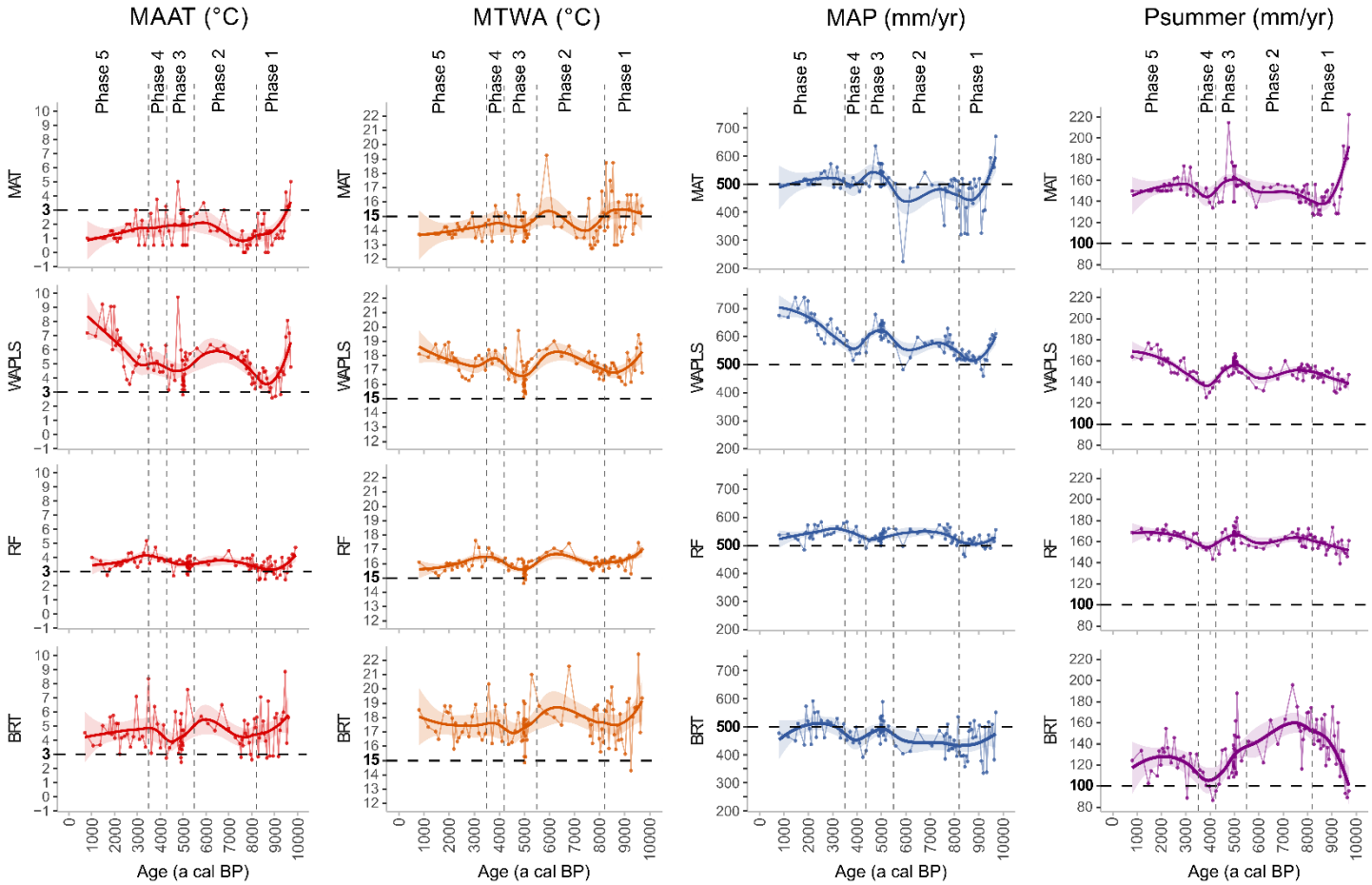

Figure II-5. Pollen-inferred climate changes estimated using four methods: MAT (Modern Analogue Technique), WAPLS (Weighted Averaging Partial Least Squares regression), RF (Random Forest) and BRT (Boosted Regression Trees). Dotted lines correspond to modern values (Sevan city meteorological station). MAAT: mean annual air temperature. MTWA: mean temperature of the warmest month. MAP: mean annual precipitation. P_{summer}: summer precipitation.

4.3 GDGT analysis

4.3.1 Distribution of brGDGTs

The concentration of brGDGTs (Fig. 6D) ranges from 0.04 to 11.6 µg/g dry sediment. The fractional abundances of brGDGTs (Fig. 6A) show a dominance of pentamethylated brGDGTs (II, 49%) in particular brGDGT IIa (20%), brGDGT IIa' (11%), and brGDGT IIb (9%). The relative abundance of tetramethylated brGDGTs (III, 26%) is explained by the abundance of brGDGT Ia (14%) and brGDGT Ib (10%). Finally, the relative abundance of hexamethylated brGDGTs (III, 25%) can be explained by the presence of brGDGT IIIa (11%) and brGDGT IIIa' (9%). The relative abundances of tetra, penta- and hexamethylated brGDGTs

(Fig. 6B) differ according to the type of sediment in the core. The peat sediment samples are close to global soils and peats, whereas the clay sediment samples are closer to global lakes.

A principal component analysis (PCA) and a hierarchical clustering on principal components (HCPC) were conducted on the fractional abundances of brGDGTs with *FactoMineR 2.4* package (Lê et al., 2008) (Fig. 6C). The first two dimensions (PCA 1 and PCA 2) explain 86% of the variability (54% and 32% respectively). Three groups are identified by HCPC: the first one is associated with tetramethylated brGDGTs and the samples are negatively correlated with PCA 1. This group is composed of peat sediment samples. The second one is associated with brGDGTs ΣIIa and the samples are negatively correlated with PCA 1 and PCA 2. The group is composed of samples mainly located in the lithological transition zone of the core between peat and clay sediments. The third one is associated with hexamethylated brGDGTs, brGDGTs ΣIIb and brGDGTs ΣIIc and the samples are positively correlated with PCA 1. The group is mainly composed of lake-type sediment samples.

4.3.2 Ratio and indices

The ΣIIIa/ΣIIa ratio shows a general decreasing trend from the beginning to the end of the core (Fig. 6D). From 9700 to 5100 a cal BP (lake sediment), the average ΣIIIa/ΣIIa ratio is equal to 0.83 and then from 5100 a cal BP to today (peat sediment), the average ratio is equal to 0.52. The MBT and the MBT'5Me show similar variations but different absolute values (Fig. 6D). The MBT varies between 0.15 and 0.40 and the MBT'5Me between 0.30 and 0.51. From 9700 to 7300 a cal BP, the index values increase and then remain relatively stable. From 7300 a cal BP, they decline and from 5000 a cal BP they largely increase. From 4200 to 3000 a cal BP, the index values progressively decrease and then remain stable except at 1800 a cal BP. The CBT index shows variation between 0.17 and 0.42 except at 9200, 8900 and 5000 a cal BP where the values vary from 0.5 to 0.71 (Fig. 6D).

4.3.3 Temperature reconstructions

The reconstructed mean annual air temperature (MAAT) using soil (Naafs et al., 2017a) and lake calibrations (Sun et al., 2011) show similar trends but different absolute values (Fig. 6D). For soil, the average MAAT is equal to 0.66 °C during the Holocene and for lake the average MAAT is equal to 11.9 °C. Between 9700 to 7300 a cal BP, MAAT reconstructed values increase and then remain relatively stable. For this period, the average MAAT is equal to 10.4 °C for lake calibration. From 7300 a cal BP, the MAAT reconstructed values decline, reaching

9.6°C for lake calibration at 6200 a cal BP. Then shifting to soil calibration, a large increase is recorded from 5000 a cal BP and the MAAT reaches 5.7°C. From 4200 to 3000 a cal BP, the MAAT progressively decrease and then remains stable until the present at around 0.86°C for soil calibration except at 1800 a cal BP when a peak is recorded. The ΔMAAT records low temperatures between 9700 and 8700 a cal BP and a plateau until 7400 a cal BP followed by a continuous decrease onward. Inner variability in this last trend occurs at 4900-3600 a cal BP and a single peak at 1800 a cal BP.

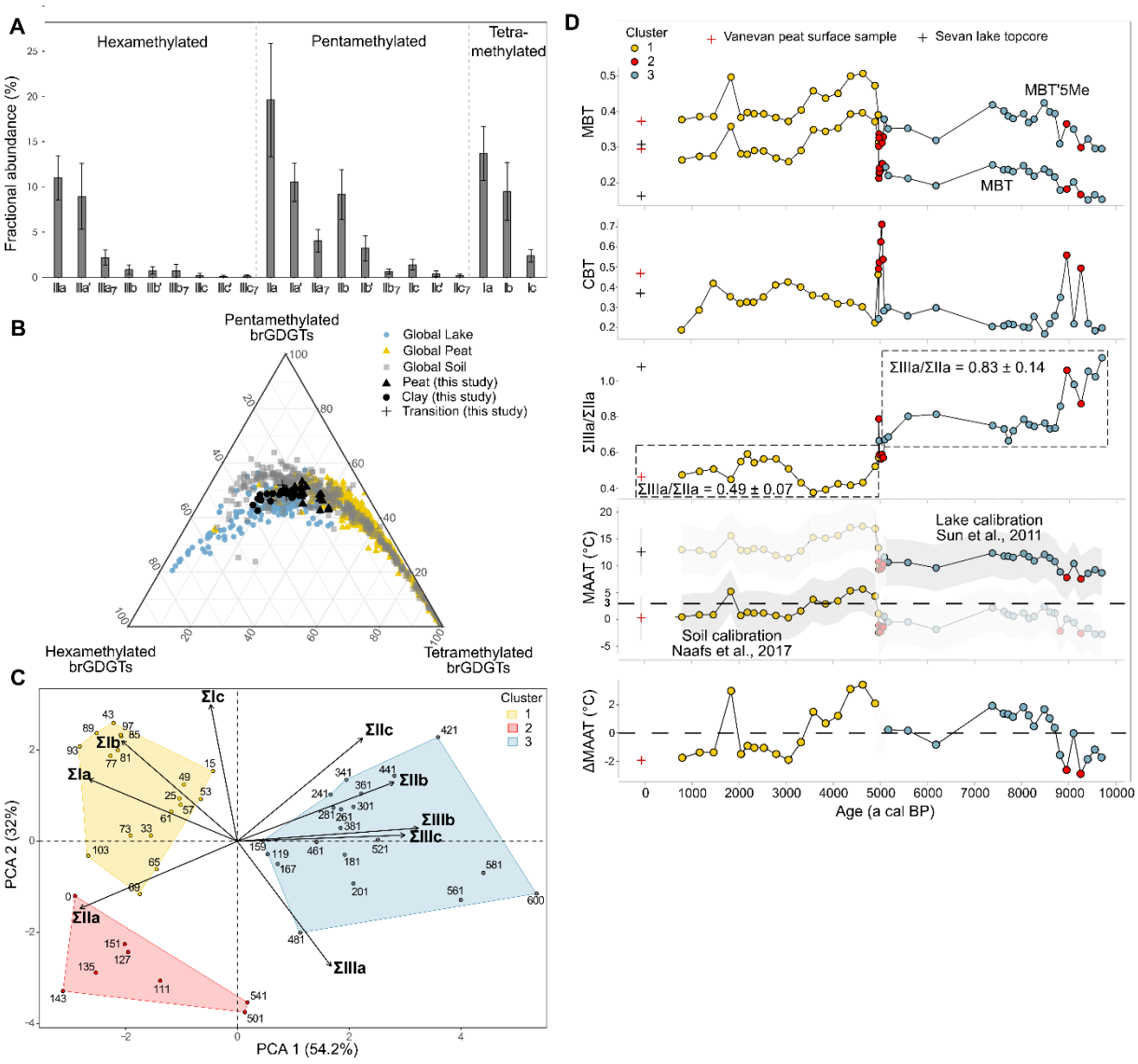

Figure II-6. A) Average fractional abundance of individual brGDGT, B) Ternary diagram showing the fractional abundances of tetra-, penta-, and hexamethylated brGDGTs. The dataset of Vanevan core are plotted against that of lakes (Wang et al., 2012; Günther at al., 2014; Li et al., 2016; Zink et al., 2016; Dang et al., 2018; Weber et al., 2018; Martin et al., 2019; Ning et al., 2019), of global peat (Naafs et al., 2017b), and of soils (Yang et al., 2014; Naafs et al., 2017a). C) Principal component analysis (PCA) and hierarchical clustering on principal components (HCPC) with fractional abundances of brGDGTs.

Labels correspond to sample depth. D) Degree of methylation (MBT, MBT'5Me), Cyclisation ratio (CBT), ΣIIIa/ΣIIa ratio, Mean annual air temperature values (MAAT) based on Naafs et al., 2017a and Sun et al., 2011, Difference of temperature (ΔMAAT) against age. ΔMAAT corresponds to the centered values based on the mean value of the two sediment types (peat and lake).

5. Discussion

5.1 Pollen representation in modern vegetation and relationship with climate variables

The relationship between pollen assemblages and modern vegetation depends on various factors, including pollen production, type of pollination, dispersion mechanisms, surrounding vegetation, topography and microclimatic parameters (Jacobson and Bradshaw, 1981). Pollen rain integrates local to regional vegetation (Jacobson and Bradshaw, 1981; Prentice, 1985). In Armenia, the vegetation is largely open which contributes to a greater pollen dispersion, but topography and microclimatic parameters may also play significant roles. Understanding the representation of pollen and their origins are important for the reliability of the fossil record in vegetation and climate reconstructions.

In our study (Fig. 3), the modern vegetation shows the dominance of herbaceous taxa whose pollen representation largely depends on the type of pollination. The insect-pollinated nature of Fabaceae and Rosaceae explain their under-representation whereas the wind-pollinated nature of Asteraceae (*Artemisia*, Asteroideae and Cichorioideae) and Chenopodiaceae explain their over-representation (Fig. 3). These results are consistent with previous studies in semi-arid regions of the Caucasus where Chenopodiaceae represent 30% to 80 % of the pollen signal (Connor et al., 2004). In the desert regions of East Asia, Chenopodiaceae is the most abundant taxa and represents more than 60% of the pollen signal in China (e.g. Zhao and Herzschuh, 2009; Wei and Zhao, 2015; Zhang et al., 2018) and Mongolia (Ma et al., 2008). *Artemisia,* another taxa characterizing the semi desert-steppe environments of Armenia, is associated with the local vegetation along our sample gradient but is also present without local presence (Fig. 3), indicating over-representation. This is consistent with observations from the arid and semi-arid areas of Iran (up to 80% of the pollen signal in Djamali et al., 2009), China (e.g. Li et al., 2005; Xu et al., 2007, 2009; Zhang et al., 2018), and Mongolia (Ma et al., 2008) where *Artemisia* is the dominant taxa in steppe regions. In contrast, in Georgia (Connor et al., 2004) and Armenia, *Artemisia* is never the dominant taxa in modern pollen assemblages, although it is well recorded in semi desert-steppe environments of Armenia. According to previous studies in East Asia (e.g. Li et al., 2008; Zheng et al., 2008),

the over-representation of Chenopodiaceae and *Artemisia* could be explained by wind transport dispersal, their long-distance transport capacity and a high pollen production. In our study, Chenopodiaceae and *Artemisia* are registered in all modern samples although they are not necessarily present in the local vegetation. Chenopodiaceae is even well registered in subalpine and alpine meadows whereas they do not appear in the vegetation, confirming the previous assumptions.

In steppes, subalpine and alpine meadows of Armenia, Poaceae is the dominant taxa and it is reliably associated with the local vegetation (Fig. 3). In East Asia, Poaceae is very common in the semi-desert and steppe vegetation, even though it is generally not the dominant taxa in pollen assemblages due to under-representation (e.g. Ma et al., 2008; Xu et al., 2014). However, in protected areas of Mongolia, Poaceae is better recorded in pollen assemblages (Ma et al., 2008). Anthropogenic activities, such as overcultivation and overgrazing, may prevent the flowering of Poaceae plants (Ma et al., 2008; Wei and Zhao, 2015). The rapid deterioration of Poaceae pollen after their deposition may also contribute to the low representation of Poaceae in pollen assemblages of soils and mosses (Cao et al., 2007). In general, Poaceae is under-represented in pollen assemblages and often represents a quarter of vegetation (Ge et al., 2017). However, our study and Connor et al. (2004) show that in Georgia and Armenia, Poaceae is well associated with the vegetation. In our case, the p/v ratio (average pollen percentages/average vegetation cover percentages) is equal to 0.99, indicating a good correspondence between pollen and local vegetation. The reliable representation of Poaceae could be explained by the abundance of Poaceae in Armenia and a limited anthropogenic pressure with extensive pastoralism.

Anthropogenic indicators, such as *Plantago lanceolata* and *Rumex*-type are present in very low proportion even with extensive pastoralism which is not easily detectable in the modern pollen assemblages. Considering *Cerealia*-type, the pollen percentages are low and no relationship was found between pollen and vegetation. These results are consistent since the selection of modern sites was done in areas remote from agricultural zones.

Arboreal pollen taxa are registered in all modern samples, but they are mainly present at mid- and high elevations (Fig. 3). In meadow steppes, trees and shrubs come primarily from local or extra-local vegetation whereas in subalpine and alpine meadows, trees come from regional vegetation. The long-distance component varies depending on the location and the elevation of modern sites and it also favored by the vegetation openness in Armenia. Arboreal pollen taxa representative of the local vegetation are *Hippophae, Pistacia, Salix, Juniperus, Acer* and *Viburnum*. In semi desert-steppe environments, *Pistacia* can be present in areas close

to sparse arid woodlands. In meadow steppes, *Hippophae* is present in areas close to humid zones (Lake Sevan, rivers), *Salix* in riparian areas and *Juniperus* on south-facing slopes. In the sample from the Lake Sevan surrounding, *Hippophae* is well associated with the local vegetation even if it is a wind-pollinated tree (Li et al., 2005).

Other trees (*Pinus, Quercus, Carpinus betulus*, *Betula, Ulmus* and *Fagus)* recorded in our samples come from regional vegetation. Their over-representation may be partly explained by a wind pollination. *Pinus* pollen is registered at all elevations even if it is not present in the vegetation, except around Lake Sevan. There, *Pinus* was planted during afforestation program of USSR in the eighties. However, these pine plantations do not seem to produce pollen, as indicated by the low percentages of *Pinus* for the sample 18. A similar result occurs around the Mount Aragats in Armenia where *Pinus* is poorly registered despite the presence of planted pine trees for approximately 40 years (Cromartie et al., 2020). *Pinus* is considered as a high pollen producer and it has a good pollen dispersion by wind (Connor et al., 2004). In subalpine and alpine meadows, *Quercus* pollen averages 7% when oak forests are not present. Interestingly, oak pollen is recorded at the same elevations inhabited by oaks on the reverse slopes of the northeast mountains of Armenia and Azerbaijan. The over-representation of *Quercus* is also reported from Georgia (Connor et al., 2004) and Iran (Ramezani et al., 2013) although *Quercus* has a good pollen representation in the eastern part of Iran (Djamali et al., 2009). *Quercus* is a high pollen producer and it is often well represented in the modern pollen assemblages of the Near East (Connor et al., 2004). Our study confirms that *Quercus* pollen can be transported over long distance, even where topographic barriers are high.

The relationship between modern pollen assemblages and climate variables is marked across the altitudinal transect. Chenopodiaceae and *Artemisia* pollen dominate in semi desert-steppe vegetation of Armenia when MAAT is high and MAP is low whereas Poaceae are dominant in meadow steppes, subalpine and alpine meadows when MAAT decreases. Chenopodiaceae and *Artemisia* are indicators of continental climate characterized by cold winters and dry summers (El-Moslimany, 1990). In the Near East and Asia, the *Artemisia*/Chenopodiaceae (A/C) ratio is used as an aridity index for desert and steppe environments (e.g. Herzschuh, 2007; Zhao and Herzschuh, 2009). However, in Georgia a low relationship between A/C ratio and precipitation is observed compared to Chenopodiaceae percentages alone (Connor et al., 2004). In our study, Chenopodiaceae dominance also has higher relationship to MAP (R^2=0.40) and MAAT (R^2=0.58) than A/C ratio to MAP (R^2=0.02) and MAAT (R^2=0.16). In the South Caucasus, Chenopodiaceae changes seem to be a better aridity index than the A/C ratio.

5.2 Holocene reconstruction at a local scale: wetland dynamics and human activities at Vanevan

5.2.1 Validation of age-depth model

The comparison of the vegetation dynamics with that of the closest site (Shenkani, Cromartie et al., 2020) validates the age model. Similar trends are observed in both sites: occurrence of *Carpinus betulus* from 9700 to 9300 a cal BP, *Betula* beginning at 9600 a cal BP (Fig. 7), an arboreal taxa maximum at 7800 a cal BP, and a drop of *Betula* at 5000-4700 a cal BP.

At Vanevan, however, the trends evidenced in cores VD2016 (this study) and VD2011 (Leroyer et al., 2016) are closely related but changes are not simultaneously (Supplementary Fig. S6). For example, the maximum of arboreal pollen dates to 7800 and 6800 a cal BP for VD2016 and VD2011, respectively. Similarly, both sequences end with a peak of arboreal pollen at 5900 and 5600 a cal BP for VD2011 and VD2016 followed by an increase of Poaceae, Cyperaceae, and then ferns at 5100 and 4900 a cal BP for VD2011 and VD2016. This comparison therefore reveals a temporal gap between the two cores ranging from 2200 years at the base to 300 years at the top of the VD2011 sequence. Underestimation of the ages in the VD2011 sequence could be explained by an age model based on plant macrofossils imbedded in clay sediments. It should, moreover, be noted that the most basal date of VD2011 core, rejected by the authors, is consistent with the older ages of the VD2016 core.

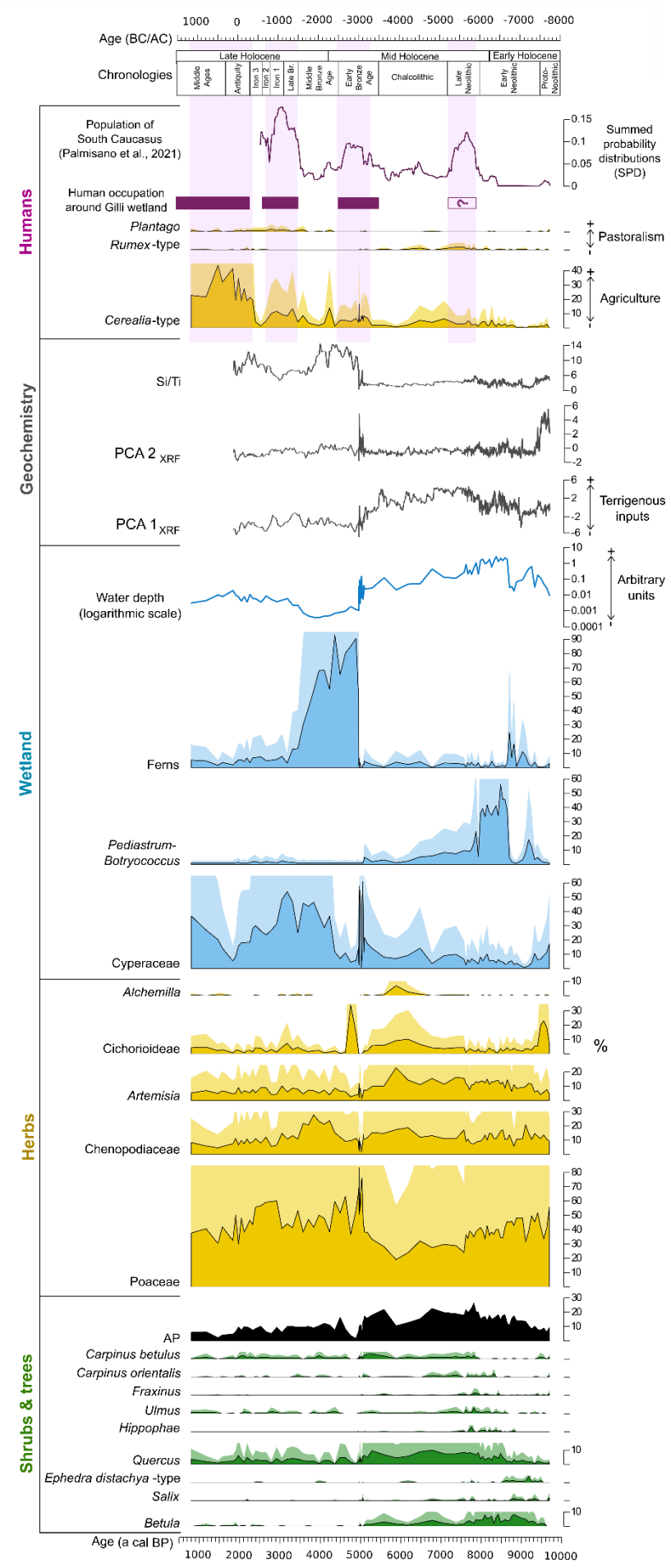
Age (BC/AC)
1000 0 -1000 -2000 -3000 -4000 -5000 -6000 -7000 -8000
Chronologies
Late Holocene
Mid Holocene
Early Holocene
Middle Ages
Antiquity
Iron 3
Iron 2
Iron 1
Late Br.
Middle Bronze Age
Early Bronze Age
Chalcolithic
Late Neolithic
Early Neolithic
Proto-Neolithic
Humans
Population of South Caucasus (Palmisano et al., 2021)
Summed probability distributions (SPD)
Human occupation around Gilli wetland
Plantago
Rumex-type
Pastoralism
Cerealia-type
Agriculture
Geochemistry
Si/Ti
PCA 2 XRF
PCA 1 XRF
Terrigenous inputs
Wetland
Water depth (logarithmic scale)
Arbitrary units
Ferns
Pediastrum-Botryococcus
Cyperaceae
Herbs
Alchemilla
Cichorioideae
Artemisia
Chenopodiaceae
Poaceae
%
Shrubs & trees
AP
Carpinus betulus
Carpinus orientalis
Fraxinus
Ulmus
Hippophae
Quercus
Ephedra distachya -type
Salix
Betula
Age (a cal BP)
1000 2000 3000 4000 5000 6000 7000 8000 9000 10000

Figure II-7. Selected Pollen taxa, NPPs, XRF, and archeological data of Vanevan peat against age. Water depth = (Algae+1)/(semi-aquatic plants+1))/(ferns +1) plotted on a logarithmic scale. Algae: Pediastrum, Botryococcus. Semi-aquatic plants: Cyperaceae, Sparganium, Typha. Ferns: Monolote spore, Botrychium, Polypodium, Selaginella, Asplenium.

5.2.2 Wetland dynamics and water-level changes

Aquatic taxa, fern spores, and NPP variations are environmental indicators of the type of wetland, the openness of the waterbody, and its water depth. Following Joannin et al. (2012), a ratio between such environmental indicators is used to estimate changes in water-level (Fig. 7), and for comparison with the conditions indicated by the lithology and XRF data. The ratio increases from 9700 to 8600 a cal BP, progressively decreases until 5100 a cal BP and remains low afterwards.

From 9700 to 5100 a cal BP, the Vanevan sequence is characterized by clay sediments formed by inputs of detrital elements (PCA 1_{XRF}, Fig. 7). The poorly developed semi-aquatic vegetation and the presence of freshwater algae suggest a lake system seen in the water-depth reconstruction. This is consistent with a transgression of Lake Sevan reported in Sayadyan's works (1977-1983). Within this period, however, we can distinguish a low water-level phase from 9700 to 9400 a cal BP consistent with the regressive phase reported by Sayadyan (1977-1983) at the same period. Such conditions would create an erosional context and may explain both the dominance of the mycorrhizal root-fungi *Glomus* (Fig. 2C) and high calcium concentrations (PCA 2_{XRF}, Fig. 7). *Glomus* is often interpreted as an indicator of close distance soil-related input (Wünnemann et al., 2010; Mudie et al., 2011) and the proportion of calcium may be derived from evaporative concentration, biogenic production (Cohen, 2003) or dissolution of the basaltic outcrops around or in the lake (detrital or in situ; Gudbrandsson et al., 2011). This raises the question of whether the calcium recorded in Vanevan was produced during the regression phase or produced before and washed down during this phase. According to Sayadyan (2009), Lake Sevan was high at the onset of the Holocene and it could have been connected with the Gilli wetland. As calcium concentrations were high in Lake Sevan before the Soviet lowering (Alekin and Ulyanova, 1986), it could be due to the remobilization of previous carbonates formed during a high stand of the paleoSevan. The high percentages of Cichorioideae also fit in a regression scenario as it is not connected to known regional vegetation development and therefore suggest local development or taphonomic processes in erosive conditions leading to an over-representation of this resistant pollen taxa (Lebreton et al., 2010).

A transitional phase is recorded between 5100 and 4950 a cal BP and shows large variations in Cyperaceae percentages. Succesive peaks of the saprophyte fungi HdV-200 may indicate alternating drying conditions followed by aquatic phases (Kuhry, 1985; van Geel et al., 1989). A peak of the green algae *Mougeotia* (Zygnemataceae) is recorded and may indicate changes in the trophic conditions and could play a role in the water-plant succession (Van Geel and van der Hammen, 1978; Van Geel and Grenfell, 1996). This phase is also characterized by high proportions of calcium, sulfur and phosphorus (PCA 2, Fig. 7) and corresponds to high fire activity (core VD2011, Leroyer et al., 2016; Supplementary Fig. S6). The macrocharcoals reported in Leroyer et al. (2016) are assumed to reconstruct local scale fires and the chemistry of the fire byproducts is likely recorded through the XRF data (Smith, 1969). The fire activity seems to have burned Cyperaceae sedges or grassland and favored developments of ferns and Poaceae. The same vegetation dynamic after fire events is recorded at Shenkani (Cromartie et al., 2020). In the Vanevan wetland, the ecological perturbation of fire also results in a brief but massive peak of Cichorioideae recorded at 4800 a cal BP. Again, the presence of this taxa suggests a local development on perturbed soil or a drying phase leading to an over-representation of the resistant pollen taxa (Lebreton et al., 2010). The relative impact of human activities and climate changes on the rapid water-level fluctuations between 5100 and 4800 a cal BP remains to be determined because agricultural activities are present around Gilli wetland and climate changes are recorded at this period in the region.

After 4800 a cal BP, the Vanevan wetland then evolves towards a peatland characterized by peat deposits produced by a semi-aquatic vegetation, primarily Cyperaceae. The water level is low until 4500 a cal BP before the development of semi-aquatic vegetation. Abundant ferns are associated with the increase of the ratio Si/Ti. The biogenic silica production is likely due to phytoliths associated with the ferns (Brown et al., 2007). The water-level remains low and the wetland is dominated by Cyperaceae, except from 2300 to 1800 a cal BP when *Potamogeton*, *Sparganium* and *Typha* dominated the signal (Fig. 2C). This corroborates the Lake Sevan transgression (through underground influence) dating from 2350 to 1700 a cal BP (Sayadyan et al., 1977; Sayadyan, 1978, 1983). In Armenia, a water-level rise is also registered at Shenkani between 2200 and 1500 a cal BP (Cromartie et al., 2020).

5.2.3 Human impact

Agriculture

In our record, human activities are principally expressed through agricultural practices identified by *Cerealia*-type pollen. Although, *Cerealia*-type pollen may come from Poaceae species or wild cereals commonly present in the Near East (Van Zeist et al., 1975), our record matches the estimates of the population in the South Caucasus (Fig. 7) (Palmisano et al., 2021).

Low percentages of *Cerealia*-type pollen are recorded between 8300 and 6300 a cal BP (Late Neolithic-Chalcolithic). However, there is limited evidence of a Neolithic presence around Vanevan during this period evidenced only by an obsidian source, (Khorapor) located ~20 km away from the Vanevan peatland, which may have been used by Neolithic populations (Chataigner and Gratuze, 2014). Some evidence of Neolithic occupations is also recorded in the Kasakh valley, ~50 km from Lake Sevan (Colonge et al., 2013) and agriculture during this period is primarily recorded on the Ararat plain at an elevation of 850 m a.s.l. (Badalyan et al., 2004; Hovsepyan and Willcox, 2008; Badalyan and Harutyunyan, 2014). During the Early and Middle Chalcolithic, the archeological site of Getahovit-2 in north-eastern Armenia shows the presence of cereals (Chataignier et al., 2020). According to Chataignier et al., 2020, cereals were not locally cultivated however, such a transport of cereals at this period is not evidenced around the Lake Sevan. The presence of *Cerealia*-type pollen in our record questions the conservation of archeological remains on the shores of Lake Sevan. The high degree of mobility of Neolithic population (Ricci et al., 2018) has certainly not helped to the conservation of archeological material.

Since 5200 a cal BP, archeological remains and *Cerealia*-type pollen occur simultaneously when the environmental conditions shift from a lake to a peatland due to an abrupt drop of water level.

Percentages of *Cerealia*-type pollen are more important from 5200 to 4500 a cal BP during the Early Bronze Age, a period marked by an increase of the population in the South Caucasus (Fig. 7) and the first archeological evidence of agriculture around Gilli wetland (Hovsepyan, 2013, 2017). During this period, the Kura-Araxes culture is present in the South Caucasus and archeological data show the development of permanent village communities and agro-pastoral systems at any elevation in Armenia (Badalyan, 2014).

Then, a maximum of *Cerealia*-type pollen is recorded at 4300 a cal BP followed by a strong decrease from 4100 to 3700 a cal BP. The decline of agricultural practices at Vanevan is consistent with few archeological remains around Gilli wetland and with a decline of the

population in the South Caucasus (Hovsepyan, 2013, 2017; Palmisano et al., 2021). However, very little is known about the Middle Bronze Age and archeological sites for this period are scarce. According to Smith (2015), this period is characterized by a shift to more mobile lifeways and not necessarily accompanied by a decline of the population. Our record indicates that agriculture, which was present at the beginning of the Middle Bronze Age on the Sevan shores, became less important around the 4.2 ka climate event, which is characterized by arid conditions around the Mediterranean Basin (e.g. Kaniewski et al., 2018; Bini et al., 2019).

From 3600 to 2600 a cal BP (Late Bronze Age, Iron Age I and II), an increase of *Cerealia*-type pollen is recorded and is consistent with the large quantity of archeological sites located on the shores of Lake Sevan and an increase of the population in the South Caucasus (Biscione et al., 2002; Parmegiani and Poscolieri, 2003; Hovsepyan, 2013, 2017; Palmisano et al., 2021). At this period, the Lchashen-Metsamor culture is present around the Lake Sevan and the Urartu empire appears during the Iron Age II. The conception of forts, territory, politics and the development of agriculture, irrigation systems and pastoralism characterized this period (Badalyan et al., 2003).

From 2700 to 2400 a cal BP (Iron Age II and III), a strong decline of *Cerealia*-type pollen is recorded (Fig. 7) probably connected to the end of the Urartu empire and Lchashen-Metsamor culture centered on the north-west of Lake Sevan at 2600 a cal BP (Smith, 2015). At the scale of the Lesser Caucasus, a decline of population seems to occur at around 2700 a cal BP although the data from Palmisiano et al. (2021) are rather incomplete for this period. This period is also marked by the arrival of domination of the Persian Achaemenid Empire in Armenia between 2540 and 2281 a cal BP (Briant, 1996).

From 2300 to 800 a cal BP, *Cerealia*-type pollen strongly increase during the Antiquity and Medieval Period and are consistent with the presence of archeological sites located on the shores of Gilli wetland and Lake Sevan (Parmegiani and Poscolieri, 2003; Hovsepyan, 2013, 2017). *Cerealia* percentages up to 40% suggest crops close or within the wetland. If located in the wetland, a drainage system would have been required in conjunction with fire utilization to suppress semi-aquatic vegetation. At this period, increase of fire activity is recorded in Armenia (Joannin et al., 2014; Cromartie et al., 2020) and Georgia (Connor, 2011). This period is also consistent with the conquest of Alexander the Great in 2281 a cal BP (Briant, 1996) and the foundation of the Kingdom of Armenia, which contributed to a change of human practices.

Pastoralism

Pastoral activities are complex to detect in pollen records (Fig. 7). Similarly to the modern pollen samples, anthropogenic indicators such as *Plantago lanceolata* and *Rumex*-type (Behre, 1981) are present in very low proportion whereas extensive pastoralism existed since the Neolithic in Armenia (Badalyan et al., 2004; Hovsepyan and Willcox, 2008; Badalyan and Harutyunyan, 2014). During the Late Neolithic and the Chalcolithic (7900-6000 a cal BP), the occurrence of *Rumex*-type suggests two phases of grazing (Behre, 1981), corresponding to increases in cereal cultivation and population in the South Caucasus (Fig. 7) and was already observed by Leroyer et al. (2016).

From 4100 to 3700 a cal BP (Middle Bronze Age), no pollen indicators of pastoralism are recorded. At Vanevan, the decline of agriculture is not accompanied by a shift to more mobile lifeways centered on pastoralism as mentioned by Smith (2015). Several studies show a significant impact of the 4.2 ka climate event on Near East societies, hypothesize population decline or migration (Kaniewski et al., 2018; Palmisano et al., 2021). Our data seem to agree for a decline of local population around Lake Sevan.

During the last 3700 a cal BP, pollen of *Plantago lanceolota,* are continuously recorded at Vanevan, although in low percentages. This pollen may be an indicator of pastoralism activities (Behre, 1981). Since the Early Bronze Age (5500 a cal BP), bones of domestic animals are recorded in archaeological materials and confirm the presence of herds of cattle around Gilli wetland (Hovsepyan, 2017). At Zarishat, the last 3000 a cal BP are also marked by a continuous record for *Plantago* and *Rumex*-type (Joannin et al., 2014).

The succession of *Rumex*-type then *Plantago* along the Holocene raises questions about pastoral practices and particularly livestock types for each period (cow, sheep, goat, horse). However, these anthropogenic taxa are also common in mountain steppe environment and it is difficult to unequivocally associate them with specific practices.

5.3 Holocene vegetation dynamics for the Lesser Caucasus

Steppe grassland vegetation with pioneer trees during the Early Holocene (9700-8000 a cal BP)

The Vanevan sequence covers most of the Holocene but does not document the Chenopodiaceae steppe recorded before 10,000 a cal BP when it got replaced by grassland steppes (Wick et al., 2003; Messager et al., 2013; Joannin et al., 2014; Cromartie et al., 2020). From 9700 to 8000 a cal BP, the steppe vegetation is primarily dominated by Poaceae and secondarily by Chenopodiaceae and *Artemisia* (Fig. 7). During this period, open vegetation is

also recorded in the Southern Caucasus and the Near East mainly, although the dominant steppic taxa varies from (1) Poaceae (this study; Roberts et al., 2001; Stevens et al., 2001; Wick et al., 2003; Stevens et al., 2006;Ryabogina et al., 2018; Cromartie et al., 2020), to (2) *Artemisia,* (Djamali et al., 2008; Joannin et al., 2014; also in Central Asia: Chen et al., 2008; Zhao et al., 2009, 2020) or (3) Chenopodiaceae (Leroy et al., 2013; Messager et al., 2013). In contrast, the sites north-west of Armenia document forested phases during the same part of the Early Holocene (Connor, 2011; Shumilovskikh et al., 2012; Messager et al., 2017; Connor et al., 2018; Grachev et al., 2020). At Vanevan, a low proportion of arboreal pollen taxa is recorded (Fig. 7). There, the occurrence of *Carpinus betulus*, *Betula* and *Quercus* observed is also recorded at Shenkani (Cromartie et al., 2020), suggesting that these taxa mostly represent regional vegetation. From 9500 to 8500 a cal BP, *Ephedra distachya*-type, *Hippophae,* and *Betula* expand. *Ephedra*, which has a long-distance dispersal by wind (Herzschuh, 2007; Djamali et al., 2009), is indicative of dry climate conditions and is also observed at Lake Van during the Early Holocene (Wick et al., 2003). *Hippophae,* according to the modern relationship between pollen and vegetation, represents the local vegetation bordering Gilli wetland (Fig. 3). *Betula*, which is simultaneously recorded at Shenkani (Cromartie et al., 2020) and Lake Van (Wick et al., 2003), is a pioneer taxon. After this pioneer phase, the arboreal taxon richness increases from 8500 a cal BP with the appearance of several deciduous trees that represent the regional vegetation such as *Carpinus orientalis* and *Carpinus betulus*.

Mixed steppe and open woodlands during a truncated Mid Holocene (8000-5100 a cal BP)

During the Mid Holocene, the vegetation remains steppic but becomes more mixed with Poaceae, *Artemisia*, Chenopodiaceae and Cichorioideae (Fig. 7). From 5900 a cal BP, Poaceae decrease progressively with the same dynamic recorded at Shenkani (Cromartie et al., 2020). The arboreal pollen are dominated by *Quercus* (<10%) and the percentages remain low with a maximum recorded at 7800 a cal BP. Older palynological studies have suggested the presence of deciduous forests on the slopes of Lake Sevan during the Middle Holocene in particular around 6000 years (e.g. Sayadyan et al., 1977; Sayadyan, 1978, 1983; Moreno-Sanchez and Sayadyan, 2005). However, modern pollen-vegetation relationships demonstrated that *Quercus* pollen could represent up to 15% even if no trees were present in the catchment (Fig. 3). More likely, a *Quercus* forest was not present on the slopes of Lake Sevan during the Mid-Holocene. In contrast, *Juniperus* is also well recorded at this period. According to Figure 3, *Juniperus* is mainly an indicator of the local vegetation and could have lived on the slopes such as today

where it grows as open woodland. Therefore, the Vanevan's landscape, with nearby grasslands and scarce open woodlands, resembles similar pollen assemblages from Armenia (Joannin et al., 2014; Cromartie et al., 2020) and Iran (Djamali et al., 2008) during the Mid-Holocene. However, Vanevan's pollen record differs by an abrupt drop of arboreal taxa between 6300-5700 a cal BP. The increase of *Artemisia*, Chenopodiaceae, Cichorioideae and *Alchemilla* can be an indicator of both dry climate and pastoralism activities.

Steppe grassland and limited tree diversity (5100-700 a cal BP)

The major vegetation change, initiated at 5400 and which fully settled after 5100 a cal BP, is characterized by an increase of Poaceae, a drop of arboreal taxa (*Quercus, Betula)* and wetland changes (Fig. 7*)*. The decrease of *Betula* is also recorded in Armenia (Cromartie et al., 2020), Turkey (Wick et al., 2003), and at a larger scale in East Asia (Qian et al., 2019). At Vanevan, the vegetation changes around 5100 a cal BP can be discussed in light of the presence of important fires (detected by macro-charcoals) that have affected the landscape and the wetland itself (Leroyer et al., 2016). Several hypotheses explain the ignition of fires: (1) an anthropogenic cause with the lighting of fires by the local population living around Gilli wetland; (2) a volcanic origin due to nearby lava flows from Porak volcano dated to the Mid-Holocene (Fig. 1C, Karakhanian et al., 2017; Meliksetian et al., 2021) or (3) a climatic driver linked with the aridification period around 5000 a cal BP recorded in Armenia (Joannin et al., 2014), Georgia (Connor and Kvadadze, 2008; Connor, 2011), Turkey (Wick et al., 2003), Iran (Stevens et al., 2001, 2006) and in Israel (Bar-Matthews et al., 1997). Although this event could be multifactorial, the regional scale of the changes points towards a climatic cause.

From 4200 to 800 a cal BP, the steppe vegetation continues to dominate the landscape with Poaceae (Fig. 7) in accordance with the Zarishat (Joannin et al., 2014) and Shenkani records (Cromartie et al., 2020). According to the modern pollen-vegetation relationships (Fig. 3), Chenopodiaceae is better recorded in pollen assemblages at low and mid-elevations in Armenia (<1900 m) where the climate conditions are more arid. The increase of Chenopodiaceae between 4400-3500 a cal BP may therefore be an indicator of aridification. A decline of agriculture is also highlighted around 4000 a cal BP and abandoned crops may have favored the expansion of Chenopodiaceae. However, this dynamic is not visible during other agriculture abandonments at Vanevan, therefore the climate appears as the main driver of vegetation change at 4.2 cal yr BP (e.g. Kaniewski et al., 2018; Bini et al., 2019).

5.4 Holocene climate reconstructions for the Lesser Caucasus

5.4.1 Pertinence and reliability of climate reconstructions

Pollen-based climate reconstructions

The results of the four quantitative pollen-based climate reconstructions are consistent (Fig. 5), whether for commonly-used transfer functions/assemblages methods (WAPLS, MAT) or recent "machine-learning" methods (RF, BRT). The minor discrepancies observed in the climate reconstructions at Vanevan can be method-dependent. For the MAT, a major limitation can be the occurrence of no-analogs, however, at Vanevan, it is clearly not the case because the fossil assemblages mainly correspond to the modern Armenian analogs added in this study, as demonstrated by the comparison of modern and core samples (Fig. 4). This method also tends to select analogs that are geographically close to each other (spatial autocorrelation; Telford and Birks, 2005, 2009, 2011), however, at Vanevan the spatial autocorrelation is relatively low (Moran's I<0.26, p-value<0.01). The MAT shows a high variability among the reconstructed values of close samples, and this variability is linked to the high degree of sensitivity of the method (Brewer et al., 2008) but is probably overestimated for the Holocene period (Fig. 5). The WAPLS performs well and this method is particularly useful for local to regional scale reconstructions (Chevalier et al., 2020); its main disadvantage is the overestimation of the values (Fig. 5) linked to the implicit inverse regression in WAPLS that "pulls" the predicted values toward the mean of the training set (Birks, 1998). The reconstructed values of the RF show low amplitude variations in contrast to the values of other methods. The BRT include the "boosting' which increases the performance of the model, however the curves present a high sample-to-sample variability. The BRT results are preferred for the regional climate comparison (Fig. 8) since this method is the most performant (maximum R^2 and the minimum RMSE values for all climatic parameters - Supplementary Table S4).

At Vanevan, the pollen-based climate reconstructions are problematic for two periods: (1) between 9700 to 9400 a cal BP, the high temperature and precipitation trends are contradictory to all other climate reconstructions available in the South Caucasus (Fig. 8) and to the brGDGT results, suggesting that this overestimation is probably due to the low pollen taxa diversity and the dominance of Cichorioideae , a very resistant pollen grain (Lebreton et al., 2010); (2) From 2300 a cal BP onwards, the climate trends of the different methods diverge, when the percentages of *Cerealia*-type become important (19-44%). There, it is expected that human activities (agriculture, pastoralism) modified the vegetation structure, composition, and

diversity, influencing the paleoclimate reconstructions (St Jacques et al., 2015). Therefore, the pollen-based climate reconstructions for these two periods (9700-9400, and 2300-800 a cal BP) are not considered in the comparison of climate reconstructions and in the climate synthesis (Fig. 8).

BrGDGT temperature reconstructions

At Vanevan, the wetland dynamic changes along the Holocene with a lake system from 9700 a cal BP, a drying phase at 5000 a cal BP and finally the development of a peatland. The type of wetland, the water level and the surrounding vegetation may influence the brGDGT distribution and origins (catchment soils, rivers, in situ production in waters or sediments) (Martin et al., 2019; Martinez-Sosa et al., 2021). The water level and aquatic plant community changes of the wetland may have largely impacted the brGDGT distribution. For example, between 4800 and 3000 a cal BP, the high ΔMAAT is associated with a low water-level and a switch to ferns. The peak of ΔMAAT at 1820 a cal BP is also associated to a change in plant aquatic distribution, Cyperaceae largely decrease whereas *Potamogeton* and *Sparganium/Typha* increase. The local dynamic has therefore largely impacted the brGDGT distribution and could overprint the climate signal. The type of sediment has also impacted the distribution of brGDGTs. The tetramethylated brGDGTs are more abundant in peat sediments whereas the hexamethylated brGDGTs, brGDGTs ΣIIb and brGDGTs ΣIIc are more abundant in lake sediments (Fig. 6BC), confirming the distributions of brGDGTs reported in lakes, peats and soils (Naafs et al., 2018; Russell et al., 2018). Due to the difference in brGDGT distributions and the in-situ production in lakes, if a soil-based MBT-CBT calibration is applied on lake samples, the reconstructed temperatures are generally underestimated (e.g. Sun et al., 2011; Loomis et al., 2011, 2012; Russel et al., 2018).

In the Vanevan core, the difference in the distribution of brGDGTs according to the type of sediment is well identified (Fig. 6C), for this reason a lake calibration was applied from 9700 to 5100 a cal BP whereas a soil calibration was applied from 4900 to 790 a cal BP (Fig. 6D). A soil calibration is applied because the peat samples of Vanevan core are closer to global soils than global peats (Fig. 6B). Moreover, the temperature reconstructed for the surface sample of Vanevan peat is closer to modern temperatures when soil calibration is applied. The ΣIIIa/ΣIIa values suggest important terrigenous sources of brGDGTs in the Vanevan peat (Xiao et al., 2016; Martin et al., 2020).

Global lake calibrations applied to our modern lake samples (Sevan core top and Vanevan surface sample) tend to overestimate the reconstructed temperatures, with values close

to warmest month mean (MTWA). The overestimation of reconstructed temperatures has already been evidenced in middle- and high-latitude lakes and could be linked to a seasonal bias (e.g. Foster et al., 2016; Dang et al., 2018; Cao et al., 2020). Both higher brGDGT production during warm seasons (Pearson et al., 2011; Shanahan et al., 2013) or winter ice formation on lake surfaces limiting air/lake water exchanges (Cao et al., 2020) could explain this seasonal bias. To account for the overestimated temperature values in our sequence, they were normalized to their mean values on each part of the record in the following discussion (ΔMAAT, Fig. 6D). The development of local and regional calibrations

Comparison of climate reconstructions based on pollen and brGDGTs (Fig. 8)

The Early Holocene is characterized by cold and dry conditions as indicated by pollen and brGDGT climate reconstructions. The Mid-Holocene (8200-5500 a cal BP) shows warmer conditions associated with a decrease in precipitation by pollen and in temperature by brGDGTs at 6000 a cal BP. Between 5100 and 4800 a cal BP, an important change in wetland dynamic and a drying phase are recorded and have largely impacted the distribution of brGDGTs and the pollen conservation. Therefore, this part will not be considered for climate reconstructions. Then, the climate reconstructions based on pollen and brGDGTs during the last 5000 a cal BP differ because of (1) the change in water level and aquatic plant which impact the bacterial community and therefore the brGDGT distribution and (2) the strong human impact during the last 3000 a cal BP which biased the climate reconstruction based on pollen. However, both climate reconstructions based on pollen and brGDGTs recorded a decrease in temperature between 6300-5700 a cal BP and 4200-3700 a cal BP.

5.4.2 Millennial-scale climate changes in the Lesser Caucasus

A cold and arid Early Holocene (9700-8200 a cal BP)

Vanevan climate reconstructions clearly indicate low annual temperature and precipitation during the Early Holocene (Fig. 8), followed by a rise from 8700 a cal BP. This climate improvement is also accompanied by the increase in water level in Vanevan wetland. This climate pattern is echoed in Armenia and in Georgia: due to time resolution difference between these archives, the climate change goes from more progressive in Georgia (Connor and Kvavadze, 2008) to more abrupt in Armenia (Joannin et al., 2014; Cromartie et al., 2020). In Arid Central Asia, the Early Holocene is also characterized by arid conditions (Chen, et al., 2008). In contrast, in the Near and Middle East (Iran, Turkey and Israel), low values of the

oxygen isotopes are generally interpreted as responding to higher water levels, suggesting higher precipitation during the Early Holocene (Roberts et al., 2001; Stevens et al., 2001, 2006; Wick et al., 2003; Bar-Matthews et al., 2003). However, the openness of the vegetation recorded at such a large extent (South Caucasus, Near East, Central Asia) brings into question this climate interpretation. Therefore, our study brings a new argument to attribute cold and dry conditions during the Early Holocene for the whole Near East region. Going into details, several studies in Armenia (Joannin et al., 2014), Iran (Stevens et al., 2001), and Turkey (Wick et al., 2003) attributed the vegetation changes to low spring precipitation, a limiting factor for the plants' growing season, controlled by the Siberian High (Wick et al., 2003). This is not contradictory with the wet Early Holocene identified by isotope data of the Near East if it is the result of high winter precipitation, a parameter typical of the Mediterranean climate (Stevens et al., 2001, 2006; Djamali et al., 2010). Indeed, the winter snows have lower $\delta^{18}O$ values leading to more negative values and a lower total precipitation (Stevens et al., 2001, 2006). Moreover, according to Messager et al. (2017), the winter snow accumulated can melt during spring and summer, generating higher water level in lakes. However, isotopic and lake-level studies are rarely conducted together rendering this interpretation difficult to extrapolate for the Early Holocene. In addition, lake variations depicted in Sevan by our study and Sayadyan's works (1977-1983) do not corroborate a high lake level during the second half of the Early Holocene.

Abrupt installation of warm and humid Mid Holocene progressively shifting to cooler and drier conditions

The Mid Holocene starts with high precipitation and temperature suggested by brGDGTs, pollen and water-level changes (Fig. 8). This agrees well with the warm and humid Mid-Holocene documented in Armenia and Georgia (Connor and Kvavadze, 2008; Joannin et al., 2014; Cromartie et al., 2020), and in Arid Central Asia (Chen et al., 2008). In contrast, the isotopic curves of the Near East show a progressive decrease of precipitation throughout this period (Roberts et al., 2001; Stevens et al., 2001, 2006; Wick et al., 2003; Bar-Matthews et al., 2003). Our study thus records a mid-Holocene climatic optimum and supports an increase of spring precipitation linked to the Westerlies (Wick et al., 2003; Joannin et al., 2014). This change marks the installation of the present-day climate dominated by late spring rainfall over the East Anatolia and North Iran. Since 5100 a cal BP, pollen and low water levels suggest a large decrease in precipitation, while brGDGTs shows a temperature decrease (Fig. 8). This trend agrees with Georgian and Central Asia records for declining precipitation. At the scale of the Near East, our study clarifies the climate pattern with conditions becoming colder, and

aridification (Roberts et al., 2001; Stevens et al., 2001, 2006; Wick et al., 2003; Bar-Matthews et al., 2003). Since this period, humans were able to live and cultivate nearer Gilli wetland thanks to the water level drop.

5.4.3 Rapid/abrupt climate events in the Lesser Caucasus

6.2 and 5.2 ka arid events

At Vanevan, the Mid-Holocene is marked by two arid events. The first one is recorded at 6300-5700 a cal BP and appears both in pollen and brGDGT reconstructions (Fig. 8). In the South Caucasus, the fire frequence history and abundance variations of sedge at Zarishat in Armenia show a drier phase at 6400 a cal BP (Joannin et al., 2014). At a larger scale, a drop in rainfall occurs at Lake Zeribar (Iran) at 6200 a cal BP (Stevens et al., 2006), at Sofular cave (Turkey) at 6200-6000 a cal BP (Zanchetta et al., 2014) and in East Asia at 6.2 ka, linked to an abrupt monsoon event (Yu et al., 2006; Wu et al., 2018). Considering temperature, there is no clear trends according to our results (Fig. 8) and the other studies carried out in the South Caucasus and the Near East.

The second arid event recorded at Vanevan occurs at 5100-4800 a cal BP and is marked by a drop in arboreal trees, a drying wetland phase, high fire activity, and changes in brGDGT distribution (Fig. 8). Major changes are also recorded in Armenia: at Zarishat, by fire frequence history and sedge changes, which show a dry phase at 5300-4900 a cal BP (Joannin et al., 2014); at Shenkani, by an increase of fire activity for the same period (Cromartie et al., 2020); and in Georgia at Lake Aligol, by an increase of fires accompanied by a drop in rainfall at 5000-4500 a cal BP (Connor and Kvavadze, 2008). In the Caucasus, glacier advances are recorded at 5000-4500 a cal BP, supporting the hypothesis of a colder climate in the Caucasus (Solomina et al., 2015). In the Near East, an arid phase is visible in isotopic data at Lake Mirabad and Zeribar in Iran at 5200 a cal BP (Stevens et al., 2001, 2006), at Gölhisar in Turkey at 4900 a cal BP (Eastwood et al., 2007) and at Soreq cave in Israël at 5200 a cal BP (Bar-Matthews et al., 1997; Bar-Matthews and Ayalon, 2011). Magny et al. (2006) define the '5.2 ka event' as a global climate event, characterized by drier conditions around the Mediterranean Basin. Although agriculture practices are present around Gilli wetland since 5200 a cal BP, the changes of vegetation and fire between 5300 and 4800 a cal BP are regional and seem to be largely affected by the aridification event.

The 4.2 ka arid event

At Vanevan, a period of aridity between 4200 and 3700 a cal BP is recorded by the pollen climate reconstruction, water-level, and brGDGT changes. This event is characterized by a drop in annual and summer precipitation and an increase in summer temperature. The brGDGT reconstructions confirm warm conditions for this period (Fig. 8). In the South Caucasus, the other pollen sequences do not clearly record this arid event, except at Shenkani where an increase of the Br/Ti ratio indicates a decrease in terrigenous inputs between 4300 and 4100 a cal BP (Cromartie et al., 2020). In the Near East, the isotopic data of Lake Zeribar in Iran (Stevens et al., 2001), Eski Acigöl in Turkey and Soreq cave in Israel (Bar-Matthews et al., 2003) show a climate aridification around 4000 a cal BP. At Lake Van in Turkey, arid conditions at 4200-4000 a cal BP are expressed through the increase of fire, the decrease of *Quercus* and low lake-level (Wick et al., 2003). This arid event is also characterized by an increase of dust deposits in the Near East (Ön et al., 2021) as at Lake Van in Turkey (Lemcke and Sturm 1997) and at Lake Neor in Iran (Sharifi et al., 2015). However, this dust event is not recorded in the South Caucasus (Cromartie et al., 2020). The 4.2 ka event is defined by a severe and prolonged drought around the Mediterranean Basin (global "megadrought", Weiss, 2016). It was first proposed by Weiss et al. (1993) for the Near East and is recorded at a global scale although not evidenced in all records (Cullen et al., 2000). The 4.2 ka event is today considered as the formal boundary of Late and Middle Holocene. This event is often characterized as a cold event (Cullen et al., 2000; Dixit et al., 2014), however for the Eastern Mediterranean the records show warmer conditions (this study; Bini et al., 2019). In this region, the 4.2 ka event is defined by climatic and environmental changes that extend between 4.3 and 3.8 ka (Bini et al., 2019). In the South Caucasus, the Vanevan sequence is the first to report the impact of a warm and arid 4.2 ka event. The concordance between the 4.2 ka event and the decline of agricultural practices is easily linkable to the decline of local population but cannot tell whether it is due to societal collapse or migrations of population in the South Caucasus and the Near East (Kaniewski et al., 2018; Palmisano et al., 2021).

The 2.8 ka climate event

Between 2900 and 2400 a cal BP, a cold and arid event appears at Vanevan, mainly with the WAPLS method (Fig. 8). This pattern is consistent with the glacier advances recorded in the Greater Caucasus at 2900-2800 a cal BP (Solomina et al., 2015) and the drop in rainfall at Lake Van, in Turkey (Wick et al., 2003) and Soreq Cave, in Israël (Bar-Matthews et al., 2003). The 2.8 ka event is defined by cold conditions at a global scale and several studies have also

identified its impact in East Asia (Fukumoto et al., 2012) and Europe (Ivy-Ochs et al., 2009; Van Geel et al., 2014). In the South Caucasus, our climate reconstructions marked the impact of the 2.8 ka event, which is accompanied by a decline of agricultural practices around Lake Sevan, certainly due to a decline of local population (Fig. 8). This climate event may have contributed to the decline of the Urartian empire centered around Lake Sevan and it coincides with the arrival of the Persians in Armenia. At the scale of the Caucasus, Palmisiano et al. (2021) also showed a decline of population at 2700 a cal BP although the data are limited for this period. According to several studies focused on the Near East, the demographic trends become dissociated from climate from 4000-3500 a cal BP because populations are more resilient due to the technological advancement (Lawrence et al., 2016; Roberts et al., 2019). This hypothesis might need to be revisited in the light of the present study, at least for the South Caucasus.

Atmospheric processes

The abrupt climate events described here are all characterized by arid conditions in the Caucasus and the Near East. Temperature shows colder conditions for the 5.2 ka and 2.8 ka events whereas the 4.2 ka event is characterized by warmer conditions. Several studies indicate that the North Atlantic Oscillation (NAO) is the main driver of precipitation variability in the Near East and the Caucasus during the Mid- and Late Holocene (Joannin et al., 2014; Jones et al., 2019). Therefore, arid events in the Eastern Mediterranean can be caused by a weak westerly flow associated to multi-centennial cyclicity of the NAO system (e.g. Magny et al., 2013; Zielhofer et al., 2017; Bini et al., 2019). Many studies suggest that the Westerlies decreasing influence is accompanied by the reinforcement and latitudinal expansion of the Siberian High and subtropical systems (Djamali et al., 2008; Joannin et al., 2014; Zanchetta et al., 2016; Bini et al., 2019; Ön et al., 2021). The southward expansion of the Siberian High provides the incursion of cold-dry air masses in southern Europe (Zanchetta et al., 2016; Perşoiu et al., 2019). We hypothesize that the 5.2 ka and 2.8 ka events are mainly under the influence of the winter Siberian High as cold conditions are recorded in the South Caucasus and the Near East. According to Perşoiu et al. (2019), the 4.2 ka event is also characterized by a dominance of the winter Siberian High in Europe, however, the records of the South Caucasus and the Near East show warm conditions (this study; Bini et al., 2019). Other atmospheric systems could come into play in these regions during the 4.2 ka event. According to Ön et al. (2021), precipitation of the southeastern Mediterranean is mainly controlled by the latitudinal migration of the Intertropical Convergence Zone and the subtropical high pressure belt but the model does not specify clear trends on the aridity or temperature in the Near East. Noteworthy, the study of

Sharifi et al. (2015) evidences the arrival of dust from the Middle East coming from the south, but does not identify the origins. We hypothesize that the 4.2 ka event in the South Caucasus and the Near East is influenced by the northward migration of subtropical systems providing warm and arid conditions. This migration is also reflected through the arrival of dust from the Near East but not reaching the South Caucasus. Considering the 6.2 ka event, it is also linked to the NAO variations (Joannin et al., 2014), however, the contradicting temperature reconstructions from Vanevan do not allow us to hypothesize whether the 6.2 ka arid event is due to polar or Arabian subtropical influences.

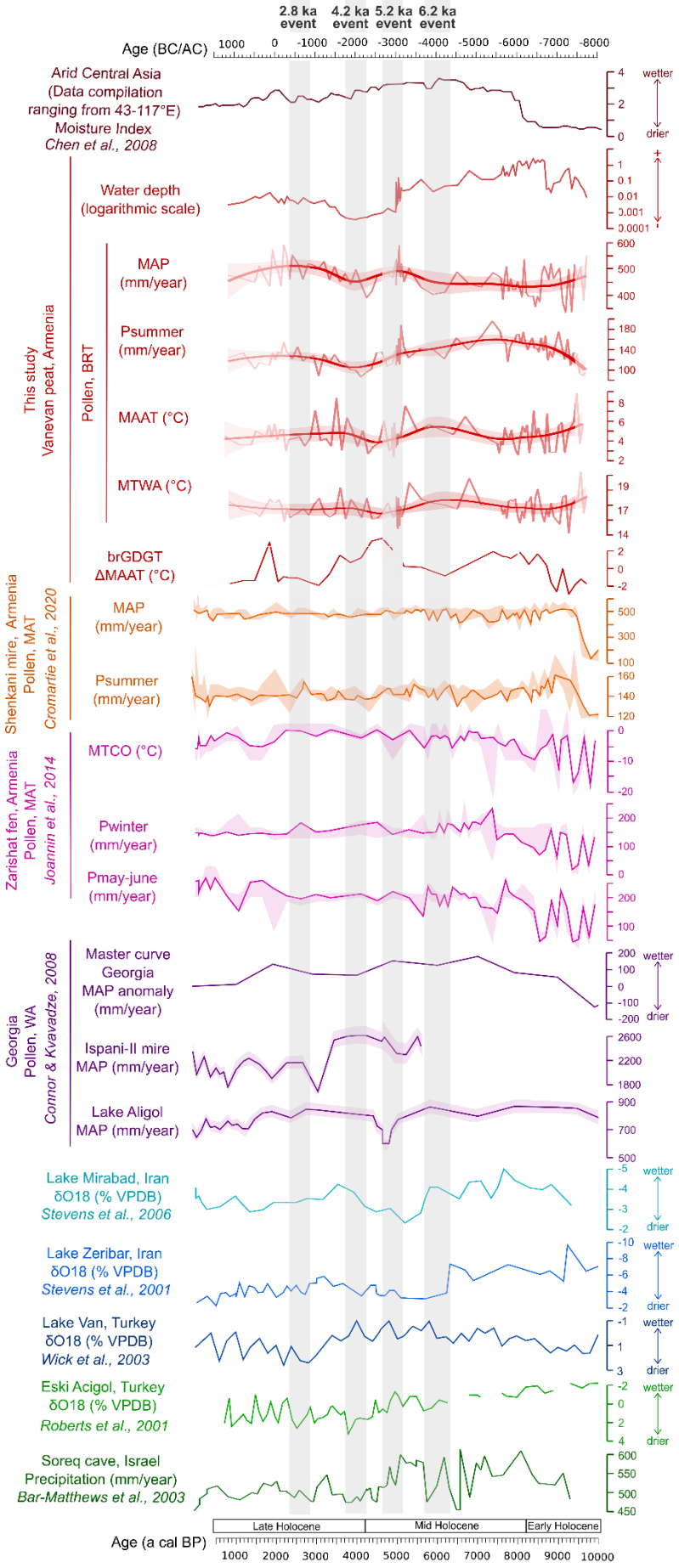
2.8 ka event
4.2 ka event
5.2 ka event
6.2 ka event
Age (BC/AC)
1000 0 -1000 -2000 -3000 -4000 -5000 -6000 -7000 -8000
Arid Central Asia (Data compilation ranging from 43-117°E) Moisture Index
Chen et al., 2008
wetter
drier
This study
Vanevan peat, Armenia
Pollen, BRT
Water depth (logarithmic scale)
MAP (mm/year)
Psummer (mm/year)
MAAT (°C)
MTWA (°C)
brGDGT ΔMAAT (°C)
Shenkani mire, Armenia
Pollen, MAT
Cromartie et al., 2020
MAP (mm/year)
Psummer (mm/year)
Zarishat fen, Armenia
Pollen, MAT
Joannin et al., 2014
MTCO (°C)
Pwinter (mm/year)
Pmay-june (mm/year)
Georgia
Pollen, WA
Connor & Kvavadze, 2008
Master curve Georgia MAP anomaly (mm/year)
Ispani-II mire MAP (mm/year)
Lake Aligol MAP (mm/year)
Lake Mirabad, Iran δO18 (‰ VPDB)
Stevens et al., 2006
Lake Zeribar, Iran δO18 (‰ VPDB)
Stevens et al., 2001
Lake Van, Turkey δO18 (‰ VPDB)
Wick et al., 2003
Eski Acigol, Turkey δO18 (‰ VPDB)
Roberts et al., 2001
Soreq cave, Israel Precipitation (mm/year)
Bar-Matthews et al., 2003
Late Holocene
Mid Holocene
Early Holocene
Age (a cal BP)
1000 2000 3000 4000 5000 6000 7000 8000 9000 10000

Figure II-8. Synthesis of paleoenvironmental records over the last 10,000 yrs based on pollen, brGDGTs and $\delta^{18}O$ data. Gray vertical shading represents abrupt climate events. MAAT: mean annual air temperature. MTWA: mean temperature of the warmest month. MAP: mean annual precipitation. P_{summer}: summer precipitation. For location, refer to Fig. 1.

6. Conclusions

Environmental dynamic, climate changes and human practices are reconstructed using multi-proxies at Vanevan peat in Armenia during the last 9700 years. This study extends the Mid-Holocene record documented at Vanevan peat by Leroyer et al. (2016) and proposes new proxies as brGDGTs.

- For the first time in the South Caucasus and the Near East, our study provides climate reconstructions based on brGDGTs and pollen coupled with a multimethod approach (MAT, WAPLS, RF, BRT). The climate reconstructions are complementary and show a good correspondence between the proxies and the methods used. However, our results reveal that it is essential to understand the local dynamic of the wetland to properly interpret the climate reconstructions based on brGDGTs and pollen. The results show an arid and cold Early Holocene, a more humid and warmer Mid Holocene, and a more arid and cooler Late Holocene. Several abrupt events are detected at 6.2 ka, 5.2 ka, 4.2 ka, 2.8 ka and allow us to highlight the atmospheric processes in the Caucasus and the Near East. The four climate events are arid and seem linked to weak westerlies associated to multi-centennial cyclicity (NAO-like). The 5.2 ka and 2.8 ka are characterized by cold conditions and could be associated to a strong Siberian High. On the contrary, the 4.2 ka is characterized by warm conditions and would be influenced by the northward migration of Arabian subtropical systems.
- This study is also the first to investigate the modern relationship between vegetation and pollen in Armenia. It complements the study of Connor and Kvavadze (2008) for Georgia. The results show an abundance of Chenopodiaceae in semi-desert/steppe regions and Poaceae in steppes, subalpine and alpine meadows. Chenopodiaceae and *Artemisia* are over-represented whereas Poaceae is reliably associated with the local vegetation. In the South Caucasus, Chenopodiaceae percentages seem to be a better aridity index than A/C ratio.
- The vegetation during the last 9700 years shows a dominance of steppes predominantly composed of Poaceae. The surrounding vegetation of Lake Sevan was poorly forested, even during the Mid-Holocene and contrasts with the previous hypotheses which suggested the

occurrence of a deciduous forest. This result brings into question the existence of open woodland around Lake Sevan and new studies are necessary to better estimate the vegetation around the entire lake and the relationship to open woodland.

- Humans have been able to live and cultivate when the Gilli wetland level dropped at around 5200 a cal BP. The expansion and decline phases of agricultural practices are remarkably correlated with the occupation and abandonment phases of archeological sites of Lake Sevan but also with demographic trends of the South Caucasus (Palmisano et al., 2021).
- Major changes in paleohydrological conditions are recorded by abundances of aquatic plants and algae at Vanevan during the last 9700 a cal BP. A lake system is initially present following by a drying phase at 4950 a cal BP associated with fire and finally a peatland dominated by Cyperaceae appears. The water level changes are consistent with the previously established variations of Lake Sevan in Sayadyan's works (1977-1983) and they are congruent with our climate reconstructions proposed for the South Caucasus.
- Contrary to several studies, which conclude to the dissociation between demographic trends and climate from 4000-3500 a cal BP in the Near East, our study suggests a significant impact of abrupt climate changes on populations. The different events are consistent with the population abandonment phases and question the human enfranchisement in the face of climate changes due to their technological advancements. In our study, climate changes appear as one of the main drivers of vegetation and demographic changes in the South Caucasus. However, further research is needed to understand all the social complexities related to these changes although our study clearly shows links between climatic changes and demographic shifts.

In the line with the previous studies of Joannin et al. (2014), Leroyer et al. (2016) and Cromartie et al. (2020) for Armenia, this new study brings a better understanding of vegetation dynamics and the respective role of climate and humans in the South Caucasus. The multiproxy approach provided a robust chronicle of climate changes occurring during the Holocene.

Funding

This research was co-founded by the International PhD course in "Agriculture Technologies and Biotechnologies" (34° Cycle, Code: DOT1339335). Financial support for this study was provided by the French–Armenian International Associated Laboratory HEMHA "Humans and Environments in Mountainous Habitats, the case of Armenia" supervised by C. Chataigner and P. Avetisyan. This programme between Armenia and France was founded by

the French National Centre for Scientific Research (CNRS). Field trip campaigns and analyses were founded by CNRS program INSU INTERRVIE (PI: C. Colombié) and Labex OT Med and ECCOREV program from Aix-Marseille University through the GeoArT and SoCCER project (PI: V. Ollivier). For the analytical work completed at LGLTPE-ENS de Lyon, this research was funded by Institut Universitaire de France funds to G. Ménot. The travels between Italy and France were financed by VINCI founding. The conference funding was provided by the Association des Palynologues de Langue Française (APLF).

Author contributions

M. Robles: Conceptualization, Field work, Laboratory work, Formal analysis, Writing draft manuscript, Review, Funding acquisition. S. Joannin: Project administration, Conceptualization, Field work, Supervision, Review, Funding acquisition; O. Peyron: Conceptualization, Formal analysis, Supervision, Review, Funding acquisition. G. Ménot: Conceptualization, Supervision, Review, Funding acquisition; E. Brugiapaglia: Conceptualization, Supervision, Review. L. Dugerdil: Formal analysis, Review. V. Ollivier: Field work, Review, Funding acquisition. S. Ansanay-Alex and A.-L. Develle: Laboratory work. P. Tozalakyan and K. Sahakyan: Field work. K. Meliksetian and L. Sahakyan: Field supervision. R. Badalyan and B. Perello: Field supervision, Review. C. Colombié: Field work, Review, Funding acquisition.

Declaration of competing interest

The authors declare that they have no known competing financial interests or personal relationships that could have appeared to influence the work reported in this paper.

Acknowledgements

The authors would like to express their appreciation to David Etienne for the NPP identification help, to Laurent Bouby and Isabelle Figueiral for seed or wood identifications used for radiocarbon datings, and to Sandrine Canal for the preparation of moss samples. We would like to thank Amy Cromartie for the proofreading and comments on the manuscript.

References

Alekin, O., Ulyanova, D., 1986. Super-saturation of Sevan water with CaC03. Water Resources Moscow I, 117-122 (in Russian).

Arimura, M., Gasparyan, B., Chataigner, C., 2012. Prehistoric sites in Northwest Armenia: Kmlo-2 and Tsaghkahovit, in: Matthews, R.J., Curtis, J. (Eds.), Proceedings of the 7th International Congress of the Archaeology of the Ancient Near East. Volume 3: Fieldwork and Recent Research e Posters. Harrasowitz, Wiesbaden, pp. 135-150.

Arnaud, F., Révillon, S., Debret, M., Revel, M., Chapron, E., Jacob, J., Giguet-Covex, C., Poulenard, J., Magny, M., 2012. Lake Bourget regional erosion patterns reconstruction reveals Holocene NW European Alps soil evolution and paleohydrology. Quaternary Science Reviews 51, 81–92. https://doi.org/10.1016/j.quascirev.2012.07.025

Badalyan, R.S., Smith A.T., Avetisyan P.S., 2003. The Emergence of Socio-Political Complexity in Southern Caucasia: An Interim Report on the Research of Project ArAGATS, in: Smith, A.T. and Rubinson K.S. (Eds.), Archaeology in the Borderlands: Investigations in Caucasia and Beyond. The Cotsen Institute of Archaeology, Los Angeles, pp. 144-166.

Badalyan, R., Lombard, P., Chataigner, C., Avetisyan, P., 2004. The Neolithic and Chalcolithic phases in the Ararat Plain (Armenia): The view from Aratashen, in: Sagona, A. (Eds.), A View from the Highlands-Archaeological Studies in Honour of Charles Burney. Ancient Near Eastern Studies Supplement 12, Peteers, pp. 399-420.

Badalyan, R.S., 2014. New data on the periodization and chronology of the Kura-Araxes culture in Armenia. Paléorient 40, 71–92. https://doi.org/10.3406/paleo.2014.5636

Badalyan, R., Harutyunyan, A., 2014. Aknashen-the Late Neolithic Settlement of the Ararat Valley: Main Results and Prospects for the Research, in : Gasparyan, B., Arimura, M. (Eds.), Stone age of Armenia. Kanazawa University, Kanazawa, pp. 161-177.

Baghdasaryan, A.B., 1958. Klimat Armyanskoy, SSR, Yerevan, pp. 108-118.

Bar-Matthews, M., Ayalon, A. and Kauffman, A., 1997. Late Quaternary paleoclimate in the eastern Mediterranean region from stable isotope analysis of speleothems at Soreq Cave, Israel. Quaternary Res. 47, 155–168. https://doi.org/10.1006/qres.1997.1883

Bar-Matthews, M., Ayalon, A., Gilmour, M., Matthews, A., Hawkesworth, C.J., 2003. Sea–land oxygen isotopic relationships from planktonic foraminifera and speleothems in the Eastern Mediterranean region and their implication for paleorainfall during interglacial intervals. Geochimica et Cosmochimica Acta 67, 3181–3199. https://doi.org/10.1016/S0016-7037(02)01031-1

Bar-Matthews, M., Ayalon, A., 2011. Mid-Holocene climate variations revealed by high-resolution speleothem records from Soreq Cave, Israel and their correlation with cultural changes. The Holocene 21, 163–171. https://doi.org/10.1177/0959683610384165

Behre, K.E., 1981. The interpretation of anthropogenic indicators in pollen diagrams. Pollen et spores, 23(2), 225-245.

Beug, H.-J, 2004. Leitfaden der Pollenbestimmung fur Mitteleuropa und angrenzende Gebeite, Pfeil, Munchen.

Bini, M., Zanchetta, G., Perşoiu, A., Cartier, R., Català, A., Cacho, I., Dean, J.R., Di Rita, F., Drysdale, R.N., Finnè, M., Isola, I., Jalali, B., Lirer, F., Magri, D., Masi, A., Marks, L., Mercuri, A.M., Peyron, O., Sadori, L., Sicre, M.-A., Welc, F., Zielhofer, C., Brisset, E., 2019. The 4.2 ka BP Event in the Mediterranean region: an overview. Clim. Past 15, 555–577. https://doi.org/10.5194/cp-15-555-2019

Birks, H.J.B., 1998. Numerical tools in palaeolimnology-progress, potentialities, and problems. J. Paleolimnol. 20, 307–332.

Biscione, R., Hmayakyan, S., Parmegiani, N., 2002. The North-Eastern frontier: Urartians and Non-Urartians in the Sevan Lake Basin, The Southern Shores. CNR istituto di studi sulle civilt`a dell'Egeo e del Vicino Oriente, Rome.

Blaauw, M., 2010. Methods and code for "classical" age-modelling of radiocarbon sequences. Quat. Geochronol. 5, 512–518. https://doi.org/10.1016/j.quageo.2010.01.002

Blaauw, M., Christen, J.A., 2011. Flexible paleoclimate age-depth models using an autoregressive gamma process. Bayesian analysis 6, 457–474. https://doi.org/10.1214/11-BA618

Bohn, U., Gollub, G., Hettwer, C., 2000. Karte der natürlichen Vegetation Europas, Bundesamt für Naturschutz, Bonn.

Bottema, S., 1992. Prehistoric cereal gathering and farming in the Near East: the pollen evidence. Rev. Palaeobot. Palynol. 73, 21–33.

Braun-Blanquet, J., Schoenichen, W. 1964.Grundzüge der Vege-tationskunde, Springer, Vienna.

Breiman, L., 2001. Random forests. Machine learning 45, 5–32.

Brewer, S., Guiot, J., Sánchez-Goñi, M.F., Klotz, S., 2008. The climate in Europe during the Eemian: a multi-method approach using pollen data. Quaternary Science Reviews, 27, 2303-315. https://doi.org/10.1016/j.quascirev.2008.08.029

Briant, P., 1996. Histoire de l'Empire perse de Cyrus à Alexandre. Fayard, Paris, 1247p.

Brown, E., Johnson, T., Scholz, C., Cohen, A., King, J., 2007. Abrupt change in tropical African climate linked to the bipolar seesaw over the past 55,000 years. Geophys. Res. Lett., 34, L20702. https://doi.org/10.1029/2007GL031240

Cao, X., Tian, F., Xu, Q.H., Li, Y.C., Zhang, Z.Q., Jia, H.J., Zhang, L.Y., Wang, X., 2007. Pollen influx and comparison with surface pollen in the east part of Yinshan Mountains. Acta Palaeontologica Sinica, 46(4), 418 (in Chinese).

Cao, J., Rao, Z., Shi, F., Jia, G., 2020. Ice formation on lake surfaces in winter causes warm-season bias of lacustrine brGDGT temperature estimates. Biogeosciences 17, 2521–2536. https://doi.org/10.5194/bg-17-2521-2020

Chataigner, C., Gratuze, B., 2014. New data on the exploitation of obsidian in the Southern Caucasus (Armenia, Georgia) and eastern Turkey, Part 2: obsidian procurement from the Upper Palaeolithic to the Late Bronze Age. Archaeometry 56 (2), 569-577. https://doi.org/10.1111/arcm.12007

Chataigner, C., Gratuze, B., Tardy, N., Abbès, F., Kalantaryan, I., Hovsepyan, R., Chahoud, J., Perello, B., 2020. Diachronic variability in obsidian procurement patterns and the role of the cave-sheepfold of Getahovit-2 (NE Armenia) during the Chalcolithic period. Quaternary International 550, 1–19. https://doi.org/10.1016/j.quaint.2020.02.010

Chen, F., Yu, Z., Yang, M., Ito, E., Wang, S., Madsen, D.B., Huang, X., Zhao, Y., Sato, T., John B. Birks, H., Boomer, I., Chen, J., An, C., Wünnemann, B., 2008. Holocene moisture evolution in arid central Asia and its out-of-phase relationship with Asian monsoon history. Quat. Sci. Rev. 27, 351–364. https://doi.org/10.1016/j.quascirev.2007.10.017

Chevalier, M., Davis, B.A.S., Heiri, O., Seppä, H., Chase, B.M., Gajewski, K., Lacourse, T., Telford, R.J., Finsinger, W., Guiot, J., Kühl, N., Maezumi, S.Y., Tipton, J.R., Carter, V.A., Brussel, T., Phelps, L.N., Dawson, A., Zanon, M., Vallé, F., Nolan, C., Mauri, A., de Vernal, A., Izumi, K., Holmström, L., Marsicek, J., Goring, S., Sommer, P.S., Chaput, M., Kupriyanov, D., 2020. Pollen-based climate reconstruction techniques for late Quaternary studies. Earth-Science Reviews 210, 103384. https://doi.org/10.1016/j.earscirev.2020.103384

Cohen, A.S., 2003. Paleolimnology: the history and evolution of lake systems. Oxford University Press, New York, 528p.

Connor, S.E., Thomas, I., Kvavadze, E.V., Arabuli, G.J., Avakov, G.S., Sagona, A., 2004. A survey of modern pollen and vegetation along an altitudinal transect in southern Georgia, Caucasus region. Review of Palaeobotany and Palynology 129, 229–250. https://doi.org/10.1016/j.revpalbo.2004.02.003

Connor, S.E., Kvavadze, E.V., 2008. Modelling late Quaternary changes in plant distribution, vegetation and climate using pollen data from Georgia, Caucasus. Journal of Biogeography 36, 529–545. https://doi.org/10.1111/j.1365-2699.2008.02019.x

Connor, S.E., 2011. A promethean legacy: late quaternary vegetation history of southern Georgia, the Caucasus. Peeters, Leuven.

Connor, S.E., Colombaroli, D., Confortini, F., Gobet, E., Ilyashuk, B.P., Ilyashuk, E.A., van Leeuwen, J.F.N., Lamentowicz, M., van der Knaap, W.O., Malysheva, E., Marchetto, A., Margalitadze, N., Mazei, Y., Mitchell, E.A.D., Payne, R.J., Ammann, B., 2018. Long-term population dynamics: Theory and reality in a peatland ecosystem. J. Ecol. 106, 333–346. https://doi.org/10.1111/1365-2745.12865

Cromartie, A., Blanchet, C., Barhoumi, C., Messager, E., Peyron, O., Ollivier, V., Sabatier, P., Etienne, D., Karakhanyan, A., Khatchadourian, L., Smith, A.T., Badalyan, R., Perello, B., Lindsay, I., Joannin, S., 2020. The vegetation, climate, and fire history of a mountain steppe: A Holocene reconstruction from the South Caucasus, Shenkani, Armenia. Quat. Sci. Rev. 246, 106485. https://doi.org/10.1016/j.quascirev.2020.106485

Croudace, I.W., Rothwell, R.G., 2015. Micro-XRF Studies of Sediment Cores: Applications of a Non-destructive Tool for the Environmental Sciences. Springer, Dordrecht.

Cullen, H.M., deMenocal, P.B., Hemming, S., Hemming, G., Brown, F.H., Guilderson, T., Sirocko, F., 2000. Climate change and the collapse of the Akkadian empire: Evidence from the deep sea. Geology 28, 379–382. https://doi.org/10.1130/0091-7613

Dang, X., Ding, W., Yang, H., Pancost, R.D., Naafs, B.D.A., Xue, J., Lin, X., Lu, J., Xie, S., 2018. Different temperature dependence of the bacterial brGDGT isomers in 35 Chinese lake sediments compared to that in soils. Organic Geochemistry 119, 72–79. https://doi.org/10.1016/j.orggeochem.2018.02.008

Davtian, N., Bard, E., Ménot, G., Fagault, Y., 2018. The importance of mass accuracy in selected ion monitoring analysis of branched and isoprenoid tetraethers. Org. Geochem. 118, 58–62. https://doi.org/10.1016/j.orggeochem.2018.01.007

Dearing Crampton-Flood, E., Tierney, J.E., Peterse, F., Kirkels, F.M.S.A., Sinninghe Damsté, J.S., 2020. BayMBT: A Bayesian calibration model for branched glycerol dialkyl glycerol tetraethers in soils and peats. Geochimica et Cosmochimica Acta 268, 142–159. https://doi.org/10.1016/j.gca.2019.09.043

De'ath, G., 2007. Boosted trees for ecological modeling and prediction. Ecology 88, 243-251. https://doi.org/10.1890/0012-9658(2007)88[243:BTFEMA]2.0.CO;2

De Jonge, C., Hopmans, E.C., Zell, C.I., Kim, J.-H., Schouten, S., Sinninghe Damsté, J.S., 2014. Occurrence and abundance of 6-methyl branched glycerol dialkyl glycerol tetraethers in soils: implications for palaeoclimate reconstruction. Geochem. Cosmochim. Acta 141, 97–112. https://doi.org/10.1016/j.gca.2014.06.013

Ding, S., Schwab, V.F., Ueberschaar, N., Roth, V.-N., Lange, M., Xu, Y., Gleixner, G., Pohnert, G., 2016. Identification of novel 7-methyl and cyclopentanyl branched glycerol dialkyl glycerol tetraethers in lake sediments. Org. Geochem. 102, 52–58. https://doi.org/10.1016/j.orggeochem.2016.09.009

Dixit, Y., Hodell, D.A., Petrie, C.A., 2014. Abrupt weakening of the summer monsoon in northwest India ~4100 yr ago. Geology 42, 339–342. https://doi.org/10.1130/G35236.1

Djamali, M., de Beaulieu, J.-L., Shah-hosseini, M., Andrieu-Ponel, V., Ponel, P., Amini, A., Akhani, H., Leroy, S.A.G., Stevens, L., Lahijani, H., Brewer, S., 2008. A late Pleistocene long pollen record from Lake Urmia, Nw Iran. Quat. res. 69, 413–420. https://doi.org/10.1016/j.yqres.2008.03.004

Djamali, M., de Beaulieu, J.-L., Campagne, P., Andrieu-Ponel, V., Ponel, P., Leroy, S.A.G., Akhani, H., 2009. Modern pollen rain–vegetation relationships along a forest–steppe transect in the Golestan National Park, NE Iran. Review of Palaeobotany and Palynology 153, 272–281. https://doi.org/10.1016/j.revpalbo.2008.08.005

Djamali, M., Akhani, H., Andrieu-Ponel, V., Braconnot, P., Brewer, S., de Beaulieu, J.-L., Fleitmann, D., Fleury, J., Gasse, F., Guibal, F., Jackson, S.T., Lézine, A.-M., Médail, F., Ponel, P., Roberts, N., Stevens, L., 2010. Indian Summer Monsoon variations could have affected the early-Holocene woodland expansion in the Near East. The Holocene 20, 813–820. https://doi.org/10.1177/0959683610362813

Djamali, M., Cilleros, K., 2020. Statistically significant minimum pollen count in Quaternary pollen analysis; the case of pollen-rich lake sediments. Rev. Palaeobot. Palynol., 275, 104156. https://doi.org/10.1016/j.revpalbo.2019.104156

Dugerdil, L., Joannin, S., Peyron, O., Jouffroy-Bapicot, I., Vannière, B., Bazartseren, B., Unkelbach, J., Behling, H., Ménot, G., 2021. Climate reconstructions based on GDGT and pollen surface datasets from Mongolia and Siberia: calibrations and applicability to extremely cold-dry environments over the Late Holocene. Climate of the Past Discussions, pp.1-39. https://doi.org/10.5194/cp-2020-154

Eastwood, W.J., Leng, M.J., Roberts, N., Davis, B., 2007. Holocene climate change in the eastern Mediterranean region: a comparison of stable isotope and pollen data from Lake Gölhisar, southwest Turkey. J. Quaternary Sci. 22, 327–341. https://doi.org/10.1002/jqs.1062

El-Moslimany, A., 1990. Ecological significance of common non-arboreal pollen: examples from drylands of the Middle East. Review of Palaeobotany and Palynology 69, 343-350.

Elith, J., Leathwick, J.R., Hastie, T., 2008. A working guide to boosted regression trees. J. Anim. Ecol. 77, 802-813

Fægri, K., Iversen, J., Kaland, P.E., Krzywinski, K., 1989. Textbook of pollen analysis, IV, John Wiley & Sons, Chichester.

Fayvush, G., Tamanyan, K., Kalashyan, M., Vitek, E., 2013. Biodiversity Hotspots in Armenia. Annalen des Naturhistorischen Museums Wien B 115, 11–20.

Fayvush, G., Aleksanyan, A., Bussmann, R.W., 2017. Ethnobotany of the Caucasus – Armenia, in: Bussmann, R.W. (Eds.), Ethnobotany of the Caucasus, European Ethnobotany. Springer International Publishing, Cham, pp. 21–36. https://doi.org/10.1007/978-3-319-49412-8_18

Fick, S.E., Hijmans, R.J., 2017. Worldclim 2: new 1-km spatial resolution climate surfaces for global land areas: New climate surfaces for global land areas. International Journal of Climatology 37, 4302–4315. https://doi.org/10.1002/joc.5086

Fletcher, W.J., Debret, M., Goñi, M.F.S., 2013. Mid-Holocene emergence of a low-frequency millennial oscillation in western Mediterranean climate: Implications for past dynamics of the North Atlantic atmospheric westerlies. The Holocene 23, 153–166. https://doi.org/10.1177/0959683612460783

Foster, L.C., Pearson, E.J., Juggins, S., Hodgson, D.A., Saunders, K.M., Verleyen, E., Roberts, S.J., 2016. Development of a regional glycerol dialkyl glycerol tetraether (GDGT)–temperature calibration for Antarctic and sub-Antarctic lakes. Earth and Planetary Science Letters 433, 370–379. https://doi.org/10.1016/j.epsl.2015.11.018

Fukumoto, Y., Kashima, K., Orkhonselenge, A., Ganzorig, U., 2012. Holocene environmental changes in northern Mongolia inferred from diatom and pollen records of peat sediment. Quaternary International 254, 83–91. https://doi.org/10.1016/j.quaint.2011.10.014

Ge, Y., Li, Y., Bunting, M.J., Li, B., Li, Z., Wang, J., 2017. Relation between modern pollen rain, vegetation and climate in northern China: Implications for quantitative vegetation reconstruction in a steppe environment. Science of The Total Environment 586, 25–41. https://doi.org/10.1016/j.scitotenv.2017.02.027

Göktürk, O.M., 2011. Climate on the southern Black Sea coast during the Holocene: implications from the Sofular Cave record. Quaternary Science Reviews 30, 2433-2445. https://doi.org/10.1016/j.quascirev.2011.05.007

Grachev, A.M., Novenko, E.Y., Grabenko, E.A., Alexandrin, M.Y., Zazovskaya, E.P., Konstantinov, E.A., Shishkov, V.A., Lazukova, L.I., Chepurnaya, A.A., Kuderina, T.M., Ivanov, M.M., Kuzmenkova, N.V., Darin, A.V., Solomina, O.N., 2020. The Holocene

paleoenvironmental history of Western Caucasus (Russia) reconstructed by multi-proxy analysis of the continuous sediment sequence from Lake Khuko. The Holocene 31, 368–379. https://doi.org/10.1177/0959683620972782

Grieser, J., Giommes, R., Bernardi, M., 2006. New LocClim – theLocal Climate Estimator of FAO, Geophys. Res. Abstr., 8, 08305.

Grimm, E., 1987. CONISS: a Fortran 77 Program for stratigraphically constraint cluster analysis by the 655 method of incremental squares. Computers and Geosciences 13, 13-35.

Gudbrandsson, S., Wolff-Boenisch, D., Gislason, S.R., Oelkers, E.H., 2011. An experimental study of crystalline basalt dissolution from 2⩽pH⩽11 and temperatures from 5 to 75°C. Geochimica et Cosmochimica Acta 75, 5496–5509. https://doi.org/10.1016/j.gca.2011.06.035

Guiot, J., 1990. Methodology of the last climatic cycle reconstruction in France from pollen data. Palaeogeography, Palaeoclimatology, Palaeoecology 80, 49–69.

Guiot, J., de Beaulieu, J. L., Cheddadi, R., David, F., Ponel, P., Reille, M., 1993. The climate in Western Europe during the last Glacial/Interglacial cycle derived from pollen and insect remains.Palaeo-geography, Palaeoclimatology, Palaeoecology 103, 73–93.

Günther, F., Thiele, A., Gleixner, G., Xu, B., Yao, T., Schouten, S., 2014. Distribution of bacterial and archaeal ether lipids in soils and surface sediments of Tibetan lakes: Implications for GDGT-based proxies in saline high mountain lakes. Organic Geochemistry 67, 19–30. https://doi.org/10.1016/j.orggeochem.2013.11.014

Herzschuh, U., 2007. Reliability of pollen ratios for environmental reconstructions on the Tibetan Plateau. J. Biogeography 34, 1265–1273. https://doi.org/10.1111/j.1365-2699.2006.01680.x

Hijmans, R.J., Phillips, S., Leathwick, J., Elith, J., 2020. Dismo: Species Distribution Modeling. R package version 1.3-3. https://cran.r-project.org/web/packages/dismo/

Hopmans, E.C., Schouten, S., Sinninghe Damsté, J.S., 2016. The effect of improved chromatography on GDGT-based palaeoproxies. Org. Geochem. 93, 1-6. https://doi.org/10.1016/j.orggeochem.2015.12.006

Hovsepyan, R., Willcox, G., 2008. The earliest finds of cultivated plants in Armenia: evidence from charred remains and crop processing residues in pisé from the Neolithic settlements of Aratashen and Aknashen. Vegetation History and Archaeobotany, 17(1), 63-71. https://doi.org/10.1007/s00334-008-0158-6

Hovsepyan, R. 2013. First archaeobotanical data from the basin of Lake Sevan. Archäologie in Armenien II 67, 93-108.

Hovsepyan, R. 2017. New data on archaeobotany of the Lake Sevan basin. Iran and the Caucasus 21(3), 251-276.

Huguet, C., Hopmans, E.C., Febo Ayala, W., Thompson, D.H., Sinninghe Damsté, J.S., Schouten, S., 2006. An improved method to determine the absolute abundance of glycerol dibiphytanyl glycerol tetraether lipids. Org. Geochem. 37, 1036-1041. https://doi.org/10.1016/j.orggeochem.2006.05.008

Ivy-Ochs, S., Kerschner, H., Maisch, M., Christl, M., Kubik, P.W., Schlüchter, C., 2009. Latest Pleistocene and Holocene glacier variations in the European Alps. Quat. Sci. Rev. 28, 2137–2149. https://doi.org/10.1016/j.quascirev.2009.03.009

Joannin, S., Brugiapaglia, E., de Beaulieu, J.-L., Bernardo, L., Magny, M., Peyron, O., Goring, S., Vannière, B., 2012. Pollen-based reconstruction of Holocene vegetation and climate in southern Italy: the case of Lago Trifoglietti. Clim. Past. 8, 1973–1996. https://doi.org/10.5194/cp-8-1973-2012

Joannin, S., Ali, A.A., Ollivier, V., Roiron, P., Peyron, O., Chevaux, S., Nahapetyan, S., Tozalakyan, P., Karakhanyan, A., Chataigner, C., 2014. Vegetation, fire and climate history of the Lesser Caucasus: a new Holocene record from Zarishat fen (Armenia). J. Quat. Sci. 29, 70–82. https://doi.org/10.1002/jqs.2679

Joannin, S., in prep.

Jacobson, G. L., Bradshaw, R. H., 1981. The selection of sites for paleovegetational studies. Quaternary research 16, 80-96.

Jenderedjian, K., 2005. Peatlands of Armenia, in: Steiner, G.M. (Eds.), Moore von Sibirien bis Feuerland / Mires-from Siberia to Tierra Del Fuego. Biologiezentrum/ Oberösterreichische Landesmuseen, Linz, pp. 323-333.

Jones, M.D., Abu-Jaber, N., AlShdaifat, A., Baird, D., Cook, B.I., Cuthbert, M.O., Dean, J.R., Djamali, M., Eastwood, W., Fleitmann, D., Haywood, A., Kwiecien, O., Larsen, J., Maher, L.A., Metcalfe, S.E., Parker, A., Petrie, C.A., Primmer, N., Richter, T., Roberts, N., Roe, J., Tindall, J.C., Ünal-İmer, E., Weeks, L., 2019. 20,000 years of societal vulnerability and adaptation to climate change in southwest Asia. WIREs Water 6. https://doi.org/10.1002/wat2.1330

Juggins, S., 2020. Rioja: Analysis of Quaternary Science Data. R package version 0.9-26. https://cran.r-project.org/package=rioja

Kaniewski, D., Marriner, N., Cheddadi, R., Guiot, J., Van Campo, E., 2018. The 4.2 ka BP event in the Levant. Clim. Past 14, 1529-1542. https://doi.org/10.5194/cp-14-1529-2018

Karakhanian, A., Tozalakyan, P., Grillot, J.C., Philip, H., Melkonyan, D., Paronyan, P., Arakelyan, S., 2000. Tectonic impact on the Lake Sevan environment (Armenia). Environmental geology 40(3), 279-288.

Karakhanian, A., Djrbashian, R., Trifonov, V., Philip, H., Arakelian, S., Avagian, A., 2002. Holocene-historical volcanism and active faults as natural risk factors for Armenia and adjacent countries. Journal of Volcanology and Geothermal Research 113, 319–344. https://doi.org/10.1016/S0377-0273(01)00264-5

Karakhanian, A., Arakelyan, A., Avagyan, A., & Sadoyan, T., 2017. Aspects of the seismotectonics of Armenia: New data and reanalysis. Tectonic evolution, collision, and seismicity of Southwest Asia, in: Sorkhabi, R. (Eds.), Honor of Manuel Berberian's Forty-Five Years of Research Contributions: Geological Society of America Special Paper 525, pp. 445-477.

Komárek, J., Jankovská, V., 2001. Review of the green algal genus Pediastrum: implications for pollen analytical research, J. Cramer, Berlin, Germany.

Kuhry, P., 1985. Transgressions of a raised bog across a coversand ridge originally covered with an oak-lime forest. Rev. Palaeobot. Palynol. 44, 313–353.

Lalayan, E., 1931. Mavzoleys' excavations in Soviet Armenia, Publication of Academy of Sciences of USSR, Yerevan. (In Armenian)

Lawrence, D., Philip, G., Hunt, H., Snape-Kennedy, L., Wilkinson, T.J., 2016. Correction: Long Term Population, City Size and Climate Trends in the Fertile Crescent: A First Approximation. PLoS ONE 11, e0157863. https://doi.org/10.1371/journal.pone.0157863

Lê, S., Josse, J., Husson, F., 2008. FactoMineR: An R Package for Multivariate Analysis. Journal of Statistical Software, 25(1), 1-18.

Lebreton, V., Messager, E., Marquer, L., Renault-Miskovsky, J., 2010. A neotaphonomic experiment in pollen oxidation and its implications for archaeopalynology. Review of Palaeobotany and Palynology 162, 29–38. https://doi.org/10.1016/j.revpalbo.2010.05.002

Lemcke, G., Sturm, M., 1997. δ18O and trace element measurements as proxy for the reconstruction of climate changes at Lake Van (Turkey): preliminary results, in: Dalfes, H.N., Kukla, G.,Weiss, H. (Eds.), Third Millennium BC Climate Change and Old World Collapse, NATO ASI Series 49, Springer, Berlin, pp. 653–678.

Leroy, S.A.G., Tudryn, A., Chalié, F., López-Merino, L., Gasse, F., 2013. From the Allerød to the mid-Holocene: palynological evidence from the south basin of the Caspian Sea. Quat. Sci. Rev. 78, 77–97. https://doi.org/10.1016/j.quascirev.2013.07.032

Leroyer, C., Joannin, S., Aoustin, D., Ali, A. A., Peyron, O., Ollivier, V., Tozalakyan, P., Karakhanyan, A., Fany, J., 2016. Mid Holocene vegetation reconstruction from Vanevan peat (south eastern shore of Lake Sevan, Armenia). Quaternary International, 395, 5-18. http://dx.doi.org/10.1016/j.quaint.2015.06.008

Li, Y., Xu, Q., Yang, X., Chen, H., Lu, X., 2005. Pollen-vegetation relationship and pollen preservation on the Northeastern Qinghai-Tibetan Plateau. Grana 44, 160–171. https://doi.org/10.1080/00173130500230608

Li, J., Pancost, R.D., Naafs, B.D.A., Yang, H., Zhao, C., Xie, S., 2016. Distribution of glycerol dialkyl glycerol tetraether (GDGT) lipids in a hypersaline lake system. Organic Geochemistry 99, 113–124. https://doi.org/10.1016/j.orggeochem.2016.06.007

Liaw, A., Wiener, M., 2002. Classification and regression by randomForest. R news 2, 18–22.

Lind, D., Taslakyan, L., 2005. Restoring the fallen blue sky: management issues and environmental legislation for Lake Sevan, Armenia. Environs 29, 29-103.

Lindsay, I., Smith, A.T., 2006. A History of Archaeology in the Republic of Armenia. Journal of Field Archaeology, 31(2), pp. 165-184

Loomis, S.E., Russell, J.M., Sinninghe Damsté, J.S., 2011. Distributions of branched GDGTs in soils and lake sediments from western Uganda: Implications for a lacustrine paleothermometer. Organic Geochemistry 42, 739–751. https://doi.org/10.1016/j.orggeochem.2011.06.004

Loomis, S.E., Russell, J.M., Ladd, B., Street-Perrott, F.A., Sinninghe Damsté, J.S., 2012. Calibration and application of the branched GDGT temperature proxy on East African lake sediments. Earth and Planetary Science Letters 357–358, 277–288. https://doi.org/10.1016/j.epsl.2012.09.031

Lytle, D.E., Wahl, E.R., 2005.Palaeoenvironmental reconstructions using the modern ana-logue technique: the effects of sample size and decision rules. The Holocene 15, 554–566. https://doi.org/10.1191/0959683605hl830rp

Ma, Y., Liu, K., Feng, Z., Sang, Y., Wang, W., Sun, A., 2008. A Survey of Modern Pollen and Vegetation along a South-North Transect in Mongolia. J. Biogeogr. 35, 1512–1532. https://doi.org/10.1111/j.1365-2699.2007.01871.x

Magny, M., Leuzinger, U., Bortenschlager, S., Haas, J.N., 2006. Tripartite climate reversal in Central Europe 5600–5300 years ago. Quat. res. 65, 3–19. https://doi.org/10.1016/j.yqres.2005.06.009

Martin, C., Ménot, G., Thouveny, N., Davtian, N., Andrieu-Ponel, V., Reille, M., Bard, E., 2019. Impact of human activities and vegetation changes on the tetraether sources in Lake St Front (Massif Central, France). Org. Geochem. 135, 38–52. https://doi.org/10.1016/j.orggeochem.2019.06.005

Martin, C., Ménot, G., Thouveny, N., Peyron, O., Andrieu-Ponel, V., Montade, V., Davtian, N., Reille, M., Bard, E., 2020. Early Holocene Thermal Maximum recorded by branched tetraethers and pollen in Western Europe (Massif Central, France). Quat. Sci. Rev. 228, 106109. https://doi.org/10.1016/j.quascirev.2019.106109

Martínez-Sosa, P., Tierney, J.E., Stefanescu, I.C., Dearing Crampton-Flood, E., Shuman, B.N., Routson, C., 2021. A global Bayesian temperature calibration for lacustrine brGDGTs. Geochimica et Cosmochimica Acta 305, 87–105. https://doi.org/10.1016/j.gca.2021.04.038

McGovern, P., Jalabadze, M., Batiuk, S., Callahan, M.P., Smith, K.E., Hall, G.R., Kvavadze, E., Maghradze, D., Rusishvili, N., Bouby, L., Failla, O., Cola, G., Mariani, L., Boaretto, E., Bacilieri, R., This, P., Wales, N., Lordkipanidze, D., 2017. Early Neolithic wine of Georgia in the South Caucasus. Proc Natl Acad Sci USA 114, E10309–E10318. https://doi.org/10.1073/pnas.1714728114

Meliksetian, K., Neill, I., Barfod, D.N., Milne, E.J.M., Waters, E.C., Navasardyan, G., Grigoryan, E., Olive, V., Odling, N., Karakhanian, A., 2021. Pleistocene-Holocene volcanism at the Karkar geothermal prospect, Armenia. Quaternary Geochronology, 66, 101201. https://doi.org/10.1016/j.quageo.2021.101201

Messager, E., Belmecheri, S., Von Grafenstein, U., Nomade, S., Ollivier, V., Voinchet, P., Puaud, S., Courtin-Nomade, A., Guillou, H., Mgeladze, A., Dumoulin, J.-P., Mazuy, A., Lordkipanidze, D., 2013. Late Quaternary record of the vegetation and catchment-related changes from Lake Paravani (Javakheti, South Caucasus). Quat. Sci. Rev. 77, 125–140. https://doi.org/10.1016/j.quascirev.2013.07.011

Messager, E., Nomade, S., Wilhelm, B., Joannin, S., Scao, V., Von Grafenstein, U., Martkoplishvili, I., Ollivier, V., Mgeladze, A., Dumoulin, J.-P., Mazuy, A., Belmecheri, S., Lordkipanidze, D., 2017. New pollen evidence from Nariani (Georgia) for delayed postglacial forest expansion in the South Caucasus. Quat. res. 87, 121–132. https://doi.org/10.1017/qua.2016.3

Mezhlumyan, S.K., 1972. Paleo-fauna of eneolith, bronze and iron periods in Armenia, Publication of Academy of Sciences of Armenia, Yerevan (In Russian).

Mnatsakanyan, H.H., 1952. Archaeological excavations in drained part of Lake Sevan, Publication of Academy of Sciences of Armenia, Yerevan (In Armenian).

Moore, P., Webb, J.A., Collinson, M.E., 1991. Pollen analysis, Blackwell Scientific Publications, London.

Moreno-Sanchez, R., Sayadyan, H.Y., 2005. Evaluation of the forest cover in Armenia. International Forestry Review 7, 113-127. https://doi.org/10.1505/ifor.2005.7.2.113

Mudie, P.J., Leroy, S.A.G., Marret, F., Gerasimenko, N.P., Kholeif, S.E.A., Sapelko, T., Filipova-Marinova, M., 2011. Nonpollen palynomorphs: Indicators of salinity and environmental change in the Caspian–Black Sea–Mediterranean corridor, in : Buynevich, I. , Yanko-Hombach, V., Gilbert, A.S, Martin, R.E. (Eds.), Geology and Geoarchaeology of the Black Sea Region: Beyond the Flood Hypothesis, Geological Society of America Special Paper 473, pp. 89-115.

Naafs, B.D.A., Gallego-Sala, A.V., Inglis, G.N., Pancost, R.D., 2017a. Refining the global branched glycerol dialkyl glycerol tetraether (brGDGT) soil temperature calibration. Org. Geochem. 106, 48–56. https://doi.org/10.1016/j.orggeochem.2017.01.009

Naafs, B.D.A., Inglis, G.N., Zheng, Y., Amesbury, M.J., Biester, H., Bindler, R., Blewett, J., Burrows, M.A., del Castillo Torres, D., Chambers, F.M., Cohen, A.D., Evershed, R.P., Feakins, S.J., Gałka, M., Gallego-Sala, A., Gandois, L., Gray, D.M., Hatcher, P.G., Honorio Coronado, E.N., Hughes, P.D.M., Huguet, A., Könönen, M., Laggoun-Défarge, F., Lähteenoja, O., Lamentowicz, M., Marchant, R., McClymont, E., Pontevedra-Pombal, X., Ponton, C., Pourmand, A., Rizzuti, A.M., Rochefort, L., Schellekens, J., De Vleeschouwer, F., Pancost, R.D., 2017b. Introducing global peat-specific temperature and pH calibrations based on brGDGT bacterial lipids. Geochimica et Cosmochimica Acta 208, 285–301. https://doi.org/10.1016/j.gca.2017.01.038

Ning, D., Zhang, E., Shulmeister, J., Chang, J., Sun, W., Ni, Z., 2019. Holocene mean annual air temperature (MAAT) reconstruction based on branched glycerol dialkyl glycerol tetraethers from Lake Ximenglongtan, southwestern China. Organic Geochemistry 133, 65–76. https://doi.org/10.1016/j.orggeochem.2019.05.003

Ollivier, V., Joannin, S., Roiron, P., Nahapetyan, S., Chataigner, C., 2011. Travertinization and Holocene morphogenesis in Armenia: A reading grid of rapid climatic changes impact on the landscape and societies between 9500-4000 cal. BP in the Circumcaspian regions? European Archaeologist 36, 26–31.

Ollivier V., Fontugne M., Hamon C., Decaix A., Hatté C., Jalabadze M., 2018. Neolithic water management and flooding in the Lesser Caucasus (Georgia). Quaternary Science Reviews 197, 267-287.

Ön, Z.B., Greaves, A.M., Akçer-Ön, S., Özeren, M.S., 2021. A Bayesian test for the 4.2 ka BP abrupt climatic change event in southeast Europe and southwest Asia using structural time series analysis of paleoclimate data. Climatic Change 165, 7. https://doi.org/10.1007/s10584-021-03010-6

Palmisano, A., Lawrence, D., de Gruchy, M.W., Bevan, A., Shennan, S., 2021. Holocene regional population dynamics and climatic trends in the Near East: A first comparison using archaeo-demographic proxies. Quat. Sci. Rev. 252, 106739. https://doi.org/10.1016/j.quascirev.2020.106739

Parmegiani, N., Poscolieri, M., 2003. DEM data processing for a landscape archaeology analysis (Lake Sevan-Armenia). International archives of photogrammetry remote sensing and spatial information sciences, 34, 255-258.

Pearson, E. J., Juggins, S., Talbot, H. M., Weckström, Jan., Rosén, P., Ryves, D. B., Roberts, S. J., and Schmidt, R., 2011. A lacustrine GDGT-temperature calibration from the Scandinavian Arctic to Antarctic: renewed potential for the application of GDGT-paleothermometry in lakes. Geochim. Cosmochim. Ac. 75, 6225–6238, https://doi.org/10.1016/j.gca.2011.07.042

Perşoiu, A., Ionita, M., Weiss, H., 2019. Atmospheric blocking induced by the strengthened Siberian High led to drying in west Asia during the 4.2 ka BP event – a hypothesis. Clim. Past 15, 781–793. https://doi.org/10.5194/cp-15-781-2019

Peyron, O., Magny, M., Goring, S., Joannin, S., de Beaulieu, J.-L., Brugiapaglia, E., Sadori, L., Garfi, G., Kouli, K., Ioakim, C., Combourieu-Nebout, N., 2013. Contrasting patterns of climatic changes during the Holocene across the Italian Peninsula reconstructed from pollen data. Clim. Past 9, 1233–1252. https://doi.org/10.5194/cp-9-1233-2013

Peyron, O., Combourieu-Nebout, N., Brayshaw, D., Goring, S., Andrieu-Ponel, V., Desprat, S., Fletcher, W., Gambin, B., Ioakim, C., Joannin, S., Kotthoff, U., Kouli, K., Montade, V., Pross, J., Sadori, L., Magny, M., 2017. Precipitation changes in the Mediterranean basin during the Holocene from terrestrial and marine pollen records: a model–data comparison. Clim. Past 13, 249–265. https://doi.org/10.5194/cp-13-249-2017

Prasad, A.M., Iverson, L.R. and Liaw, A., 2006. Newer classification and regression tree techniques: bagging and random forests for ecological prediction. Ecosystems 9(2), 181-199.

Prentice, I.C., 1985. Pollen representation, source area, and basin size: toward a unified theory of pollen analysis. Quaternary Research, 23(1), 76-86.

Prentice, C., Guiot, J., Huntley, B., Jolly, D., Cheddadi, R., 1996. Reconstructing biomes from palaeoecological data: a general method and its application to european pollen data at 0 and 6 ka. Climate Dynamics 12, 185–194.

Qian, H., Hongyan, L., Shilei, Y., Weihua, Y., Zhaoliang, S., 2019. Differentiated roles of mean climate and climate stability on post-glacial birch distributions in northern China. The Holocene 29, 1758–1766. https://doi.org/10.1177/0959683619862038

Ramezani, E., Marvie Mohadjer, M.R., Knapp, H.-D., Theuerkauf, M., Manthey, M., Joosten, H., 2013. Pollen–vegetation relationships in the central Caspian (Hyrcanian) forests of northern Iran. Review of Palaeobotany and Palynology 189, 38–49. https://doi.org/10.1016/j.revpalbo.2012.10.004

Reille, M., 1992-1998. Pollen et Spores d'Europe et d'Afrique du nord, Laboratoire de Botanique Historique et Palynologie, Universite d'Aix-Marseille, Marseille.

Reimer, P.J., Austin, W.E.N., Bard, E., Bayliss, A., Blackwell, P.G., Ramsey, C.B., Butzin, M., Cheng, H., Edwards, R.L., Friedrich, M., Grootes, P.M., Guilderson, T.P., Hajdas, I., Heaton, T.J., Hogg, A.G., Hughen, K.A., Kromer, B., Manning, S.W., Muscheler, R., Palmer, J.G., Pearson, C., vander Plicht, J., Reimer, R.W., Richards, D.A., Scott, E.M., Southon, J.R., Turney, C.S.M., Wacker, L., Adophi, F., Büntgen, U., Capano, M., Fahrni, S., Fogtmann-Schulz, A., Friedrich, R., Kudsk, S., Miyake, F., Olsen, J., Reinig, F., Sakamoto, M., Sookdeo, A., Talamo, S., 2020. The IntCal20Northern Hemisphere radiocarbon calibrationcurve (0–55 cal kBP). Radiocarbon 62 (4), 725–757. https://doi.org/10.1017/RDC.2020.41

Ricci, A., D'Anna, M.B., Lawrence, D., Helwing, B., Aliyev, T., 2018. Human mobility and early sedentism: the Late Neolithic landscape of southern Azerbaijan. Antiquity 92, 1445–1461. https://doi.org/10.15184/aqy.2018.230

Ritchie, K., Wouters, W., Mirtskhulava, G., Jokhadze, S., Zhvania, D., Abuladze, J., Hansen, S., 2021. Neolithic fishing in the South Caucasus as seen from Aruchlo I, Georgia. Archaeological Research in Asia 25, 100252. https://doi.org/10.1016/j.ara.2020.100252

Roberts, N., Reed, J.M., Leng, M.J., Kuzucuoğlu, C., Fontugne, M., Bertaux, J., Woldring, H., Bottema, S., Black, S., Hunt, E., Karabiyikoğlu, M., 2001. The tempo of Holocene climatic change in the eastern Mediterranean region: new high-resolution crater-lake sediment data from central Turkey. The Holocene 11, 721–736. https://doi.org/10.1191/09596830195744

Roberts, N., 2002. Did prehistoric landscape management retard the post-glacial spread of woodland in Southwest Asia? Antiquity 76, 1002–1010. https://doi.org/10.1017/S0003598X0009181X

Roberts, N., Eastwood, W.J., Kuzucuoğlu, C., Fiorentino, G., Caracuta, V., 2011. Climatic, vegetation and cultural change in the eastern Mediterranean during the mid-Holocene environmental transition. The Holocene 21, 147–162. https://doi.org/10.1177/0959683610386819

Roberts, C.N., Woodbridge, J., Palmisano, A., Bevan, A., Fyfe, R., Shennan, S., 2019. Mediterranean landscape change during the Holocene: Synthesis, comparison and regional trends in population, land cover and climate. The Holocene 29, 923–937. https://doi.org/10.1177/0959683619826697

Russell, J.M., Hopmans, E.C., Loomis, S.E., Liang, J., Sinninghe Damsté, J.S., 2018. Distributions of 5- and 6-methyl branched glycerol dialkyl glycerol tetraethers (brGDGTs) in East African lake sediment: Effects of temperature, pH, and new lacustrine paleotemperature calibrations. Organic Geochemistry 117, 56–69. https://doi.org/10.1016/j.orggeochem.2017.12.003

Ryabogina, N., Borisov, A., Idrisov, I., Bakushev, M., 2018. Holocene environmental history and populating of mountainous Dagestan (Eastern Caucasus, Russia). Quaternary International 516, 111–126. https://doi.org/10.1016/j.quaint.2018.06.020

Sagona, A., Kiguradze, T., 2003. On the origins of the Kura-Araxes cultural complex. Archaeology, in: Smith, T., Rubinson, K.S. (Eds.), Archaeology in the borderlands: investigations in Caucasia and beyond. Cotsen Institute of Archaeology, Los Angeles, pp. 38-94

Sagona, A., 2017. The Archaeology of the Caucasus: from Earliest Settlements to the Iron Age. Cambridge University Press, Cambridge.

St Jacques, J.M., Cumming, B.F., Sauchyn, D.J., Smol, J.P., 2015. The bias and signal attenuation present in conventional pollen-based climate reconstructions as assessedby early climate data from Minnesota, USA. PLoS One 10, 1–17. https://doi.org/10.1371/journal.pone.0113806

Salonen, J.S., Verster, A.J., Engels, S., Soininen, J., Trachsel, M., Luoto, M., 2016. Calibrating aquatic microfossil proxies with regression-tree ensembles: Cross-validation with modern chironomid and diatom data. The Holocene 26, 1040–1048. https://doi.org/10.1177/0959683616632881

Salonen, J.S., Korpela, M., Williams, J.W., Luoto, M., 2019. Machine-learning based reconstructions of primary and secondary climate variables from North American and European fossil pollen data. Scientific reports 9, 1–13.

Sayadyan, Y.V., Aleshinskaya, Z.V., Khanzadyan, E.V., 1977. Late glacial deposits and archaeology of the Sevan Lake, in: Sayadyan, Y.V. (Eds.), Geology of the Quaternary Period (Pleistocene), Akad. Nauk Arm. SSR, Yerevan, pp. 91-109 (in Russian).

Sayadyan, Y.V., 1978. Postglacial Times in Armenia and Adjacent Regions, vol. XII. Studia Geomorphologica Carpatho-Balcanica, Krakow, pp. 77-93.

Sayadyan, Y.V., 1983. Men and environment in postglacial period in Lake Sevan basin and neighbourhood areas. In: Problems of Quaternary Geology in Armenia. Yerevan, pp 67-73 (In Russian).

Sayadyan, Y.V., 2009. The Newest Geological History of Armenia. Gitutun publish, Nat. Acad. Sciences, Yerevan (In Russian).

Sayadyan, H.Y., 2011. Valuation of mountain forests: case study Armenia. Annals of agrarian science. Republic of Georgia, 9(1), 144-148.

Schouten, S., van der Meer, M. T., Hopmans, E. C., Rijpstra, W. I. C., Reysenbach, A.-L., Ward, D. M., Sinninghe Damsté, J.S., 2007. Archaeal and bacterial glycerol dialkyl glycerol tetraether lipids in hot springs of Yellowstone National Park. Applied and Environmental Microbiology 73(19), 6181–6191.

Shanahan, T.M., Hughen, K.A., Van Mooy, B.A.S., 2013. Temperature sensitivity of branched and isoprenoid GDGTs in Arctic lakes, Org. Geochem. 64, 119–128. https://doi.org/10.1016/j.orggeochem.2013.09.010

Sharifi, A., Pourmand, A., Canuel, E.A., Ferer-Tyler, E., Peterson, L.C., Aichner, B., Feakins, S.J., Daryaee, T., Djamali, M., Beni, A.N., Lahijani, H.A.K., Swart, P.K., 2015. Abrupt climate variability since the last deglaciation based on a high-resolution, multi-proxy peat record from NW Iran: The hand that rocked the Cradle of Civilization? Quat. Sci. Rev. 123, 215–230. https://doi.org/10.1016/j.quascirev.2015.07.006

Shumilovskikh, L.S., Tarasov, P., Arz, H.W., Fleitmann, D., Marret, F., Nowaczyk, N., Plessen, B., Schlütz, F., Behling, H., 2012. Vegetation and environmental dynamics in the southern Black Sea region since 18kyr BP derived from the marine core 22-GC3. Palaeogeography, Palaeoclimatology, Palaeoecology 337–338, 177–193. https://doi.org/10.1016/j.palaeo.2012.04.015

Sinninghe Damsté, J.S., Rijpstra, W.I.C., Foesel, B.U., Huber, K.J., Overmann, J., Nakagawa, S., Kim, J.J., Dunfield, P.F., Dedysh, S.N., Villanueva, L., 2018. An overview of the

occurrence of ether- and ester-linked iso-diabolic acid membrane lipids in microbial cultures of the Acidobacteria: Implications for brGDGT paleoproxies for temperature and pH. Organic Geochemistry 124, 63–76. https://doi.org/10.1016/j.orggeochem.2018.07.006

Smith, A.T., 2015. The Political Machine: Assembling Sovereignty in the Bronze Age Caucasus. Princeton University Press, Princeton.

Solomina, O.N., Bradley, R.S., Hodgson, D.A., Ivy-Ochs, S., Jomelli, V., Mackintosh, A.N., Nesje, A., Owen, L.A., Wanner, H., Wiles, G.C., Young, N.E., 2015. Holocene glacier fluctuations. Quat. Sci. Rev. 111, 9–34. https://doi.org/10.1016/j.quascirev.2014.11.018

Solomon, J.C., Shulkina, T.V., Schatz, G.E., 2014. Red List of the Endemic Plants of the Caucasus: Armenia, Azerbaijan, Georgia, Iran, Russia, and Turkey, Missouri Botanical Garden Press, Saint Louis.

Sosson, M., Rolland, Y., Müller, C., Danelian, T., Melkonyan, R., Kekelia, S., Adamia, S., Babazadeh, V., Kangarli, T., Avagyan, A., Galoyan, G., Mosar, J., 2010. Subductions, obduction and collision in the Lesser Caucasus (Armenia, Azerbaijan, Georgia), new insights, in: Sosson, M., Kaymakci, N., Stephenson, R., Bergerat, F., Starostenko, V. (Eds.), Sedimentary Basin Tectonics from the Black Sea and Caucasus to the Arabian Platform, Geological Society of London, Special Publication 340, pp. 329-352. https://doi.org/10.1144/SP340.14

St Jacques, J.M., Cumming, B.F., Sauchyn, D.J., Smol, J.P., 2015. The bias and signal attenuation present in conventional pollen-based climate reconstructions as assessed by early climate data from Minnesota, USA. PLoS One 10, 1-17. https://doi.org/10.1371/journal.pone.0113806.

Stanyukovich, K. V., 1973. Vegetation of the Mountains of the USSR. The Tadjik Academy of Sciences Presse, Dushanbe (in Russian).

Stevens, L.R., Wright, H.E., Ito, E., 2001. Proposed changes in seasonality of climate during the Lateglacial and Holocene at Lake Zeribar, Iran. The Holocene 11, 747–755. https://doi.org/10.1191/09596830195762

Stevens, L.R., Ito, E., Schwalb, A., Wright, H.E., 2006. Timing of Atmospheric Precipitation in the Zagros Mountains Inferred from a Multi-Proxy Record from Lake Mirabad, Iran. Quat. res. 66, 494–500. https://doi.org/10.1016/j.yqres.2006.06.008

Stockhecke, M., Bechtel, A., Peterse, F., Guillemot, T., Schubert, C.J., 2021. Temperature, precipitation, and vegetation changes in the Eastern Mediterranean over the last

deglaciation and Dansgaard-Oeschger events. Palaeogeography, Palaeoclimatology, Palaeoecology 577, 110535. https://doi.org/10.1016/j.palaeo.2021.110535

Sun, Q., Chu, G.Q., Liu, M.M., Xie, M.M., Li, S.Q., Ling, Y., Wang, X.H., Shi, L.M., Jia, G.D., Lü, H.Y., 2011. Distributions and temperature dependence of branched glycerol dialkyl glycerol tetraethers in recent lacustrine sediments from China and Nepal. J. Geophys. Res. 116, G01008. https://doi.org/10.1029/2010jg001365

Takhtajyan, A.L., 1941. Botanical-geographic overview of Armenia. Work Papers of Institute of Botany of Armenian Academy of Sciences/Branch of USSR Academy of Sciences 2, 180 (in Russian).

Telford, R.J., Birks, H.J.B., 2005. The secret assumption of transfer functions: problems with spatial autocorrelation in evaluating model performance. Quat. Sci. Rev. 24, 2173–2179. https://doi.org/10.1016/j.quascirev.2005.05.001

Telford, R.J., Birks, H.J.B., 2009. Evaluation of transfer functions in spatially structured environments. Quat. Sci. Rev. 28, 1309–1316. https://doi.org/10.1016/j.quascirev.2008.12.020

Telford, R.J., Birks, H.J.B., 2011. QSR Correspondence "is spatial autocorrelation introducing biases in the apparent accuracy of palaeoclimatic reconstructions?". Quat. Sci. Rev. 30, 3210–3213. https://doi.org/10.1016/j.quascirev.2011.07.019

Ter Braak, C.J.F., Van Dam, H., 1989. Inferring pH from diatoms: A comparison of old and new calibration methods. Hydrobiologia 178, 209–223.

Ter Braak, C.J.F., Juggins, S., Birks, H.J.B., Van der Voet, H., 1993. Weighted averaging partial least squares regression (WA-PLS): definition and comparison with other methods for species-environment calibration, chap. 25, Elsevier Science Publishers, Amsterdam, pp. 525–560.

Tumanyan, M.R., 1971. On the history of lake Sevan basin vegetation in holocene. Academy of Sciences of Armenian SSR, Biological Journal, T.XXIV 11, 57-61 (in Russian).

Tumajanov, I.I., Tumanyan, M.R., 1973. New data on the history of forest vegetation in Masrik plain in Holocene. Academy of Sciences of Armenian SSR, Biological Journal, T.XXVI 12, 24-28 (in Russian).

Turner, R., Roberts, N., Jones, M.D., 2008. Climatic pacing of Mediterranean fire histories from lake sedimentary microcharcoal. Global and Planetary Change 63, 317–324. https://doi.org/10.1016/j.gloplacha.2008.07.002

Turner, R., Roberts, N., Eastwood, W.J., Jenkins, E., Rosen, A., 2010. Fire, climate and the origins of agriculture: micro-charcoal records of biomass burning during the last glacial-

interglacial transition in Southwest Asia. J. Quaternary Sci. 25, 371–386. https://doi.org/10.1002/jqs.1332

Van Geel, B., van der Hammen, T., 1978. Zygnemataceae in Quaternary Colombian sediments. Rev. Palaeobot. Palynol. 25, 377–392.

Van Geel, B., Coope, G.R, van der Hammen, T., 1989. Palaeoecology and stratigraphy of the Lateglacial type section at Usselo (The Netherlands). Rev. Palaeobot. Palynol. 60, 25–129.

Van Geel, B., Grenfell, H.R., 1996. Spores of Zygnemataceae, in: Jansonius, J., McGregor D.C. (Eds.) Palynology: principles and applications, Am. Ass. Strat. Palynol. Found.,Vol. 1, pp. 173–179.

Van Geel, B., 2002. Non-Pollen Palynomorphs, in: Smol, J.P., Birks, H.J.B., Last, W.M., Bradley, R.S., Alverson, K. (Eds.), Tracking Environmental Change Using Lake Sediments. Developments in Paleoenvironmental Research. Springer, Dordrecht, pp. 99–119. https://doi.org/10.1007/0-306-47668-1_6

Van Geel, B., Heijnis, H., Charman, D.J., Thompson, G., Engels, S., 2014. Bog burst in the eastern Netherlands triggered by the 2.8 kyr BP climate event. The Holocene 24, 1465–1477. https://doi.org/10.1177/0959683614544066

Van Zeist, W., Woldring, H., Stapert, D., 1975. Late Quaternary vegetation and climate of southwestern Turkey. Palaeohistoria 17, 53–143.

Volodicheva, N., 2002. The Caucasus, in: Shahgedanova, M. (Eds.), The Physical Geography of Northern Eurasia. Oxford University Press, New York, pp. 350-376.

Wang, H. Y., Liu, W. G., Zhang, C. L., Wang, Z., Wang, J. X., Liu, Z. H., Dong, H. L., 2012. Distribution of glycerol dialkyl glycerol tetraethers in surface sediments of Lake Qinghai and surrounding soil, Org. Geochem. 47, 78–87. https://doi.org/10.1016/j.orggeochem.2012.03.008

Watson, B.I., Williams, J.W., Russell, J.M., Jackson, S.T., Shane, L., Lowell, T.V., 2018. Temperature variations in the southern Great Lakes during the last deglaciation: Comparison between pollen and GDGT proxies. Quaternary Science Reviews 182, 78–92. https://doi.org/10.1016/j.quascirev.2017.12.011

Weber, Y., Sinninghe Damsté, J.S., Zopfi, J., De Jonge, C., Gilli, A., Schubert, C.J., Lepori, F., Lehmann, M.F., Niemann, H., 2018. Redox-dependent niche differentiation provides evidence for multiple bacterial sources of glycerol tetraether lipids in lakes. Proc. Natl. Acad. Sci. USA 115, 10926–10931. https://doi.org/10.1073/pnas.1805186115

Wei, H., Zhao, Y., 2015. Surface pollen and its relationships with modern vegetation and climate in the Tianshan Mountains, northwestern China. Veget. Hist. Archaeobot. 25, 19–27. https://doi.org/10.1007/s00334-015-0530-2

Weijers, J.W., Schouten, S., Linden, M., Geel, B., Sinninghe Damsté, J.S., 2004. Water table related variations in the abundance of intact archaeal membrane lipids in a Swedish peat bog. FEMS Microbiology Letters 239, 51–56.

Weijers, J.W., Schouten, S., Hopmans, E.C., Geenevasen, J.A., David, O.R., Coleman, J.M., Pancost, R.D., Sinninghe Damsté, J.S., 2006. Membrane lipids of mesophilic anaerobic bacteria thriving in peats have typical archaeal traits. Environmental Microbiology 8(4), 648–657. https://doi.org/10.1111/j.1462-2920.2005.00941.x

Weijers, J.W., Schouten, S., van den Donker, J.C., Hopmans, E.C., Sinninghe Damsté, J.S., 2007. Environmental controls on bacterial tetraether membrane lipid distribution in soils. Geochem. Cosmochim. Acta 71, 703–713. https://doi.org/10.1016/j.gca.2006.10.003

Weiss, H., Courty, M.-A., Wetterstrom, W., Guichard, F., Senior, L., Meadow, R., Curnow, A., 1993. The genesis and collapse of third millennium north Mesopotamian civilization. Science 261, 995–1004.

Weiss, H., 2016. Global megadrought, societal collapse and resilience at 4.2–3.9 ka BP across the Mediterranean and west Asia. Magazine 24, 62–63. https://doi.org/10.22498/pages.24.2.62

Wick, L., Lemcke, G., Sturm, M., 2003. Evidence of Lateglacial and Holocene climatic change and human impact in eastern Anatolia: high-resolution pollen, charcoal, isotopic and geochemical records from the laminated sediments of Lake Van, Turkey. The Holocene 13, 665–675. https://doi.org/10.1191/0959683603hl653rp

Wright, H.E., Ammann, B., Stefanova, I., Atanassova, J., Margalitadze, N., Wick, L., Blyakharchuk, T., 2003. Late-glacial and Early-Holocene Dry Climates from the Balkan Peninsula to Southern Siberia, in: Tonkov, S. (Eds.), Aspects of Palynology and Palaeoecology – Festschrift in Honour of Elissaveta Bozilova. Pensoft Publishers, Sofia, pp. 127-136. https://doi.org/10.1016/j.quascirev.2009.02.001

Wu, W., Zheng, H., Hou, M., Ge, Q., 2018. The 5.5 cal ka BP climate event, population growth, circumscription and the emergence of the earliest complex societies in China. Sci. China Earth Sci. 61, 134–148. https://doi.org/10.1007/s11430-017-9157-1

Wünnemann, B., Demske, D., Tarasov, P., Kotlia, B.S., Reinhardt, C., Bloemendal, J., Diekmann, B., Hartmann, K., Krois, J., Riedel, F., Arya, N., 2010. Hydrological evolution during the last 15kyr in the Tso Kar lake basin (Ladakh, India), derived from

geomorphological, sedimentological and palynological records. Quat. Sci. Rev. 29, 1138-1155. https://doi.org/10.1016/j.quascirev.2010.02.017

Xiao, W., Wang, Y., Zhou, S., Hu, L., Yang, H., Xu, Y., 2016. Ubiquitous production of branched glycerol dialkyl glycerol tetraethers (brGDGTs) in global marine environments: a new source indicator for brGDGTs. Biogeosciences 13, 5883–5894. https://doi.org/10.5194/bg-13-5883-2016.

Xu, Q.H., Li, Y.C., Zhou, L.P., Li, Y.Y., Zhang, Z.Q., Lin, F.Y., 2007. Pollen flux and vertical dispersion in coniferous and deciduous broadleaved mixed forest in the Changbai Mountains. Chinese Science Bulletin 52 (11), 1540–1544.

Xu, Q., Li, Y., Tian, F., Cao, X., Yang, X., 2009. Pollen assemblages of tauber traps and surface soil samples in steppe areas of China and their relationships with vegetation and climate. Review of Palaeobotany and Palynology 153, 86–101. https://doi.org/10.1016/j.revpalbo.2008.07.003

Xu, Q., Cao, X., Tian, F., Zhang, S., Li, Y., Li, M., Li, J., Liu, Y., Liang, J., 2014. Relative pollen productivities of typical steppe species in northern China and their potential in past vegetation reconstruction. Sci. China Earth Sci. 57, 1254–1266. https://doi.org/10.1007/s11430-013-4738-7

Yang, H., Pancost, R.D., Dang, X., Zhou, X., Evershed, R.P., Xiao, G., Tang, C., Gao, L., Guo, Z., Xie, S., 2014. Correlations between microbial tetraether lipids and environmental variables in Chinese soils: Optimizing the paleo-reconstructions in semi-arid and arid regions. Geochimica et Cosmochimica Acta 126, 49–69. https://doi.org/10.1016/j.gca.2013.10.041

Yu, X., Zhou, W., Franzen, L.G., Xian, F., Cheng, P., Jull, A.J.T., 2006. High-resolution peat records for Holocene monsoon history in the eastern Tibetan Plateau. Sci. China 49, 615–621. https://doi.org/10.1007/s11430-006-0615-y

Zanchetta, G., Bar-Matthews, M., Drysdale, R.N., Lionello, P., Ayalon, A., Hellstrom, J.C., Isola, I., Regattieri, E., 2014. Coeval dry events in the central and eastern Mediterranean basin at 5.2 and 5.6ka recorded in Corchia (Italy) and Soreq caves (Israel) speleothems. Global and Planetary Change 122, 130–139. https://doi.org/10.1016/j.gloplacha.2014.07.013

Zanchetta, G., Regattieri, E., Isola, I., Drysdale, R. N., Bini, M., Baneschi, I., and Hellstrom, J. C., 2016. The so-called “4.2 event” in the central Mediterranean and its climatic teleconnections, Alp. Med. Quat. 29, 5–17.

Zhao, Y., Herzschuh, U., 2009. Modern pollen representation of source vegetation in the Qaidam Basin and surrounding mountains, north-eastern Tibetan Plateau. Veget. Hist. Archaeobot. 18, 245–260. https://doi.org/10.1007/s00334-008-0201-7

Zhao, Y., Yu, Z., Chen, F., 2009. Spatial and temporal patterns of Holocene vegetation and climate changes in arid and semi-arid China. Quaternary International 194, 6–18. https://doi.org/10.1016/j.quaint.2007.12.002

Zhang, Y.-J., Duo, L., Pang, Y.-Z., Felde, V.A., Birks, H.H., Birks, H.J.B., 2018. Modern pollen assemblages and their relationships to vegetation and climate in the Lhasa Valley, Tibetan Plateau, China. Quaternary International 467, 210–221. https://doi.org/10.1016/j.quaint.2018.01.040

Zheng, Z., Huang, K., Xu, Q., Lu, H., Cheddadi, R., Luo, Y., Beaudouin, C., Luo, C., Zheng, Y., Li, C., Wei, J., Du, C., 2008. Comparison of climatic threshold of geographical distribution between dominant plants and surface pollen in China. Sci. China Ser. D-Earth Sci. 51, 1107–1120. https://doi.org/10.1007/s11430-008-0080-x

Zielhofer, C., Fletcher, W.J., Mischke, S., De Batist, M., Campbell, J.F.E., Joannin, S., Tjallingii, R., El Hamouti, N., Junginger, A., Stele, A., Bussmann, J., Schneider, B., Lauer, T., Spitzer, K., Strupler, M., Brachert, T., Mikdad, A., 2017. Atlantic forcing of Western Mediterranean winter rain minima during the last 12,000 years, Quat. Sci. Rev. 157, 29–51, 2017. http://dx.doi.org/10.1016/j.quascirev.2016.11.037

Zink, K.-G., Vandergoes, M.J., Bauersachs, T., Newnham, R.M., Rees, A.B.H., Schwark, L., 2016. A refined paleotemperature calibration for New Zealand limnic environments using differentiation of branched glycerol dialkyl glycerol tetraether (brGDGT) sources. Journal of Quaternary Science 31, 823–835. https://doi.org/10.1002/jqs.2908

Appendix A. Supplementary data

Supplementary Table S1. Modern sites in Armenia along an altitudinal transect from the Ararat plain (808 m a.s.l.) to mountains at Lake Sevan (2699 m a.s.l.)

No.	Sample name	Lat.	Long.	Alt. (m)	Material	Botanical relevés
1	Armagh2	40.0704	45.2136	2699	Moss	X
2	Kataraj1	40.1983	45.9662	2641	Moss	X
3	Armagh3	40.0635	45.2074	2607	Moss	X
4	Arm31	40.6208	45.0865	2388	Moss	
5	Arm34	40.6434	45.1493	2358	Moss	
6	Arm33	40.6450	45.1497	2271	Moss	
7	Artanish4	40.4807	45.3204	2211	Moss	X
8	Armagh7	40.0706	45.2650	2202	Moss	X
9	Artanish3	40.4817	45.3203	2129	Moss	X
10	Armagh8	40.0928	45.2603	2128	Moss	X
11	Arm32	40.6286	45.0927	2101	Moss	
12	Artanish2	40.4848	45.3234	2019	Moss	X
13	Arm30	40.585	44.9731	1936	Moss	X
14	Artanish1	40.4897	45.3282	1925	Moss	X
15	Vanevan	40.2013	45.6805	1919	Moss	X
16	Arm18	40.2725	45.2226	1914	Moss	X
17	Dzknaget	40.6147	44.9652	1911	Moss	X
18	Norashen	40.5046	45.0404	1903	Moss	X
19	Sto11	39.8698	44.9504	1750	Soil	
20	Sto13	39.8606	44.9345	1545	Soil	
21	Sto4	39.8017	44.8487	1321	Moss	
22	Sto3	39.7982	44.84481	1248	Moss	
23	Sto20	39.8560	44.7669	1167	Soil	X
24	Sto15	39.9254	44.8118	1055	Moss	
25	Sto19	39.8525	44.7671	1049	Moss	X
26	Sto16	39.8398	44.7607	928	Moss	X
27	Sto17	39.8305	44.7424	840	Moss	X
28	Sto18	39.8081	44.7189	808	Moss	X

Supplementary Figure S2. Eurasian map with the location of the cold steppic modern samples.

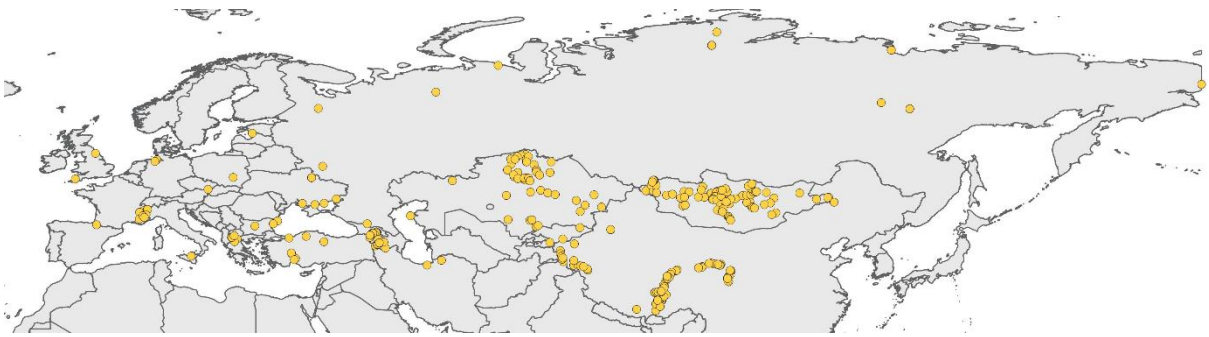

Supplementary Figure S3. Correlations between current climate parameters extracted from WorldClim 2 (Fick and Hijmans, 2017) and estimated climate parameters by each method (MAT, WAPLS, BRT and RF).

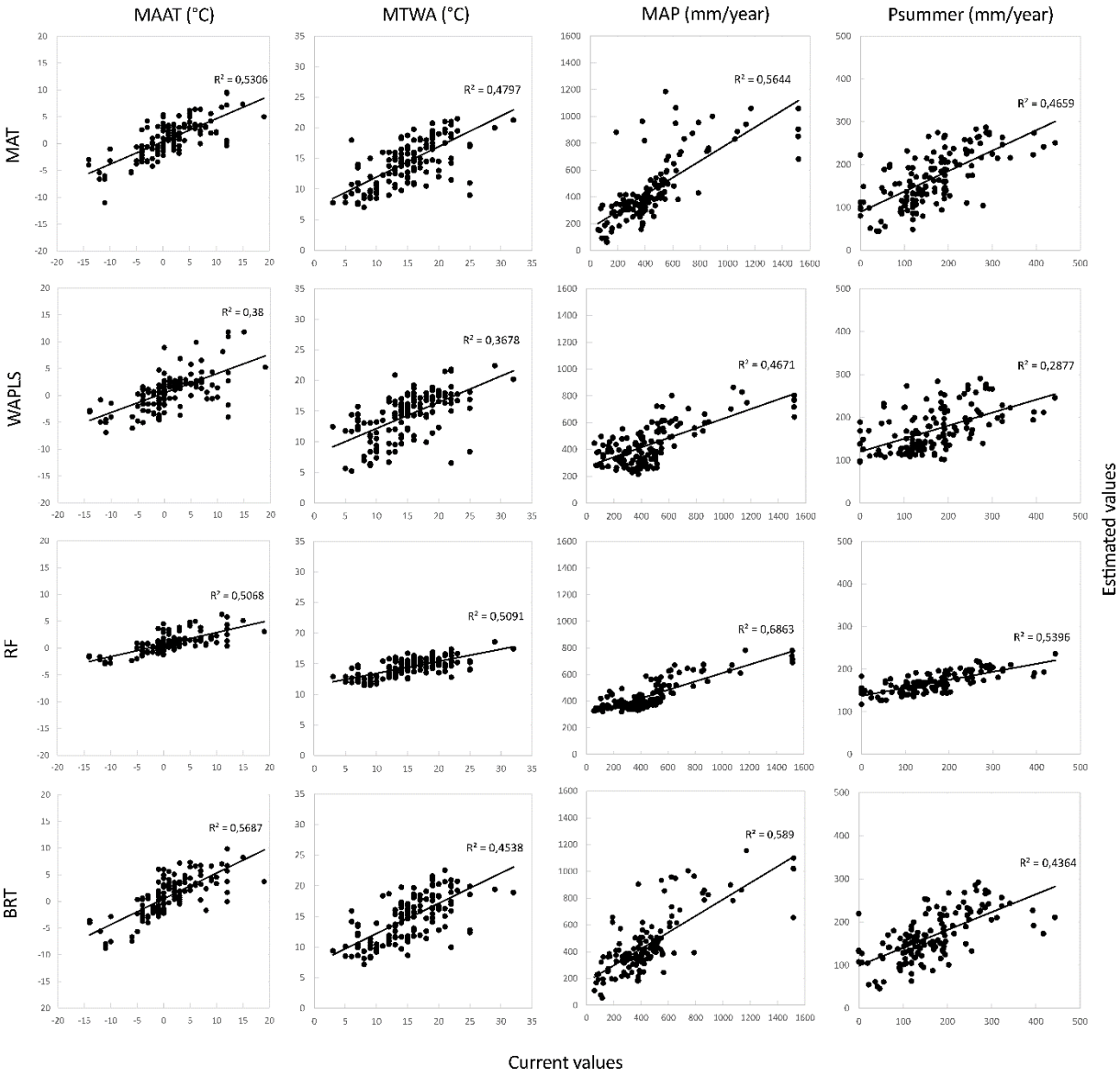

Supplementary Table S4. Statistical results of the MAT, WAPLS, BRT and RF methods as a result of using bootstrap technique on the modern "cold steppe" dataset.

Model	Climate parameter	R^2	RMSE
MAT	MAAT (°C)	0,64	3,65
	MTWA (°C)	0,60	3,67
	MAP (mm.year^{-1})	0,73	164,75
	P_{summer} (mm.year^{-1})	0,59	60,08
WAPLS	MAAT (°C)	0,50	3,89
	MTWA (°C)	0,48	3,88
	MAP (mm.year^{-1})	0,46	210,63
	P_{summer} (mm.year^{-1})	0,36	70,46
RF	MAAT (°C)	0,44	3,95
	MTWA (°C)	0,38	4,09
	MAP (mm.year^{-1})	0,47	191,75
	P_{summer} (mm.year^{-1})	0,33	68,40
BRT	MAAT (°C)	0,79	3,29
	MTWA (°C)	0,76	3,39
	MAP (mm.year^{-1})	0,79	156,03
	P_{summer} (mm.year^{-1})	0,74	57,97

Supplementary Table S5. Error ranges of the age-depth model of Vanevan (95% confidence intervals)

Depth (cm)	Min_95%	Max_95%
15-24	92	73
25-34	81	88
35-44	95	130
45-54	108	92
55-64	193	62
65-74	153	61
75-84	147	66
85-94	199	77
95-104	225	85
105-114	156	82
115-124	197	88
125-134	232	98
135-144	163	105
145-154	128	126
155-164	146	166
165-174	158	181
175-184	139	156
185-194	121	136
195-204	105	111
205-214	89	92
215-224	74	79
225-234	63	69
235-244	59	61
245-254	54	57
255-264	52	49
265-274	58	53
275-284	71	60
285-294	88	71
295-304	88	71
305-314	84	70
315-324	83	70
325-334	84	73
335-344	83	77
345-354	84	81
355-364	86	87
365-374	89	94
375-384	92	101
385-394	96	107
395-404	99	114
405-414	103	122
415-424	108	130
425-434	114	139
435-444	119	147
445-454	126	154
455-464	133	162
465-474	140	171
475-484	148	181
485-494	143	172
495-504	122	140
505-514	110	120
515-524	127	115
525-534	165	138
535-544	207	169
545-554	251	201
555-564	294	239
565-574	337	280
575-584	377	323
585-594	424	365
595-600	462	394

Supplementary Figure S6. Correspondence between VD2016 core (this study) and VD2011 core (Leroyer et al., 2016)

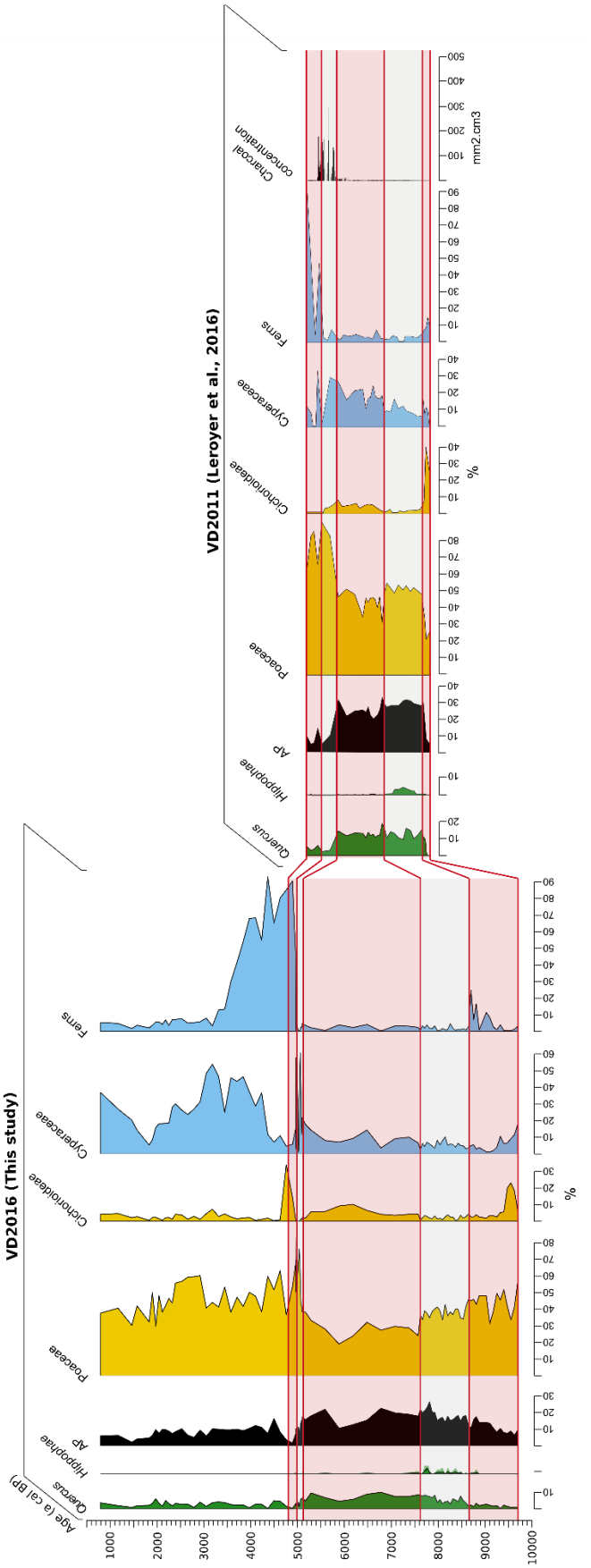

CHAPTER III - CLIMATE CHANGES DURING THE LATEGLACIAL IN SOUTH EUROPE: NEW INSIGHTS BASED ON POLLEN AND BRGDGTS OF LAKE MATESE IN ITALY

Mary Robles[1,2], Odile Peyron[2], Guillemette Ménot[3], Elisabetta Brugiapaglia[1], Sabine Wulf[4], Oona Appelt[5], Marion Blache[2], Boris Vannière[6,7], Lucas Dugerdil[2], Bruno Paura[1], Salomé Ansanay-Alex[3], Amy Cromartie[8], Laurent Charlet[9], Stephane Guédron[9], Jacques-Louis de Beaulieu[10], Sébastien Joannin[2,4]

[1] Univ. Molise, Department of Agricultural, Environmental and Food Sciences, Campobasso, Italy
[2] Univ. Montpellier, CNRS, IRD, EPHE, UMR 5554 ISEM, Montpellier, France
[3] Univ. Lyon, ENSL, UCBL, UJM, CNRS, LGL-TPE, F-69007 Lyon, France
[4] Univ. Portsmouth, School of the Environment, Geography and Geosciences, Portsmouth, United Kingdom
[5] Helmholtz Centre Potsdam, GFZ German Research Centre of Geosciences, Section 3.6, Telegrafenberg, Potsdam, Germany
[6] Chrono-Environnement, CNRS, Université Bourgogne Franche-Comté, Besançon, France
[7] MSHE Ledoux, CNRS, Université Bourgogne Franche-Comté, Besançon, France
[8] Cornell Univ., Department of Anthropology, Ithaca, NY, USA
[9] Univ. Grenoble Alpes, Univ. Savoie Mont Blanc, CNRS, IRD, IFSTTAR, ISTerre, Grenoble, France
[10] Aix-Marseille Univ., CNRS, IRD, UMR 7263 & 237 IMBE, Aix-en-Provence, France

Accepted in
Climate of the past
https://cp.copernicus.org/preprints/cp-2022-54/

Short Abstract

Quantitative climate reconstructions based on pollen and brGDGTs reveal, for the Lateglacial, a warm Bølling–Allerød and a marked cold Younger Dryas in Italy, showing no latitudinal differences in terms of temperatures across Italy. In terms of precipitation, no latitudinal differences are recorded during the Bølling–Allerød whereas the latitudes 40-42°N appear as a key junction point between wetter conditions in Southern Italy and drier conditions in Northern Italy during the Younger Dryas.

Abstract

The Lateglacial (14,700-11,700 cal BP) is a key climate period marked by rapid but contrasted changes in the Northern Hemisphere. Indeed, regional climate differences have been evidenced during the Lateglacial in Europe and the Northern Mediterranean areas. However, past climate patterns are still debated since temperature and precipitation changes are poorly investigated towards the lower European latitudes. Lake Matese in Southern Italy is a key site in the Central Mediterranean to investigate climate patterns during the Lateglacial. This study aims to reconstruct climate changes and their impacts at Matese using a multi-proxy approach including magnetic susceptibility, geochemistry (XRF core scanning), pollen data and molecular biomarkers like branched Glycerol Dialkyl Glycerol Tetraethers (brGDGTs). Palaeotemperatures and -precipitation patterns are quantitatively inferred from pollen assemblages (multi-method approach: Modern Analogue Technique, Weighted Averaging Partial Least Squares regression, Random Forest, and Boosted Regression Trees) and brGDGTs calibrations. The results are compared to a latitudinal selection of regional climate reconstructions in Italy to better understand climate processes in Europe and in the circum-Mediterranean region. A warm Bølling–Allerød and a marked cold Younger Dryas are revealed in all climate reconstructions inferred from various proxies (chironomids, ostracods, speleothems, pollen, brGDGTs), showing no latitudinal differences in terms of temperatures across Italy. During the Bølling–Allerød, no significant changes in terms of precipitation are recorded, however, a contrasted pattern is visible during the Younger Dryas. Slightly wetter conditions are recorded south of latitude 42°N whereas dry conditions are recorded north of latitude 42°N. During the Younger Dryas, cold conditions can be attributed to the southward position of North Atlantic sea-ice and of the Polar Frontal JetStream whereas the increase of precipitation is Southern Italy seems to be linked to relocation of Atlantic storm tracks into the Mediterranean, induced by the Fennoscandian ice sheet and the North European Plain. By contrast, during the Bølling–Allerød warm conditions can be linked to the northward position of North Atlantic sea-ice and of the Polar Frontal JetStream.

Keywords: Mediterranean region; Palynology; Molecular Biomarker; Paleoclimate; Transfer functions; Tephra; Younger Dryas; Bølling–Allerød; Lateglacial

Résumé

Le Tardiglaciaire (14,700-11,700 cal BP) est une période climatique clé marquée par des changements rapides mais contrastés dans l'hémisphère nord. En effet, des différences climatiques régionales ont été mises en évidence au cours du Tardiglaciaire en Europe et dans les régions du nord de la Méditerranée. Cependant, les tendances climatiques passés sont encore débattus car les changements de température et de précipitations sont peu étudiés vers les basses latitudes. Le lac Matese, dans le sud de l'Italie, est un site clé en Méditerranée centrale pour l'étude du climat au cours du Tardiglaciaire. Cette étude utilise une approche multi-proxy incluant la susceptibilité magnétique, la géochimie (XRF), les données polliniques et les biomarqueurs moléculaires comme les Glycerol Dialkyl Glyc-erol Tetraethers (brGDGT) pour reconstruire les changements climatiques et leurs impacts à Matese. Les paléotempératures et les précipitations sont reconstruits quantitativement à partir des assemblages polliniques (approche multi-méthodes : Modern Analogue Technique, Weighted Averaging Partial Least Squares regression, Random Forest, and Boosted Regression Trees) et des calibrations brGDGT. Les résultats sont comparés à une sélection latitudinale d'autres reconstructions climatiques en Italie afin de mieux comprendre les processus climatiques en Europe et dans la région circum-Méditerranéenne. Un Bølling-Allerød chaud et un Dryas récent froid et marqué sont à nouveau révélés dans toutes les reconstructions climatiques obtenues à partir de différents proxies (chironomes, ostracodes, spéléothèmes, pollen, brGDGT), ne montrant aucune différence latitudinale en termes de températures à travers l'Italie. Pendant le Bølling-Allerød, aucun changement significatif en termes de précipitations n'est enregistré, cependant, un modèle contrasté est visible pendant le Dryas récent. Des conditions légèrement humides sont enregistrées au sud de la latitude 42°N, tandis que des conditions sèches sont enregistrées au nord de cette même latitude. Pendant le Dryas récent, les conditions froides peuvent être attribuées à la position vers le sud de glaces marines dans l'Atlantique Nord et du JetStream Polaire, tandis que l'augmentation des précipitations dans le sud de l'Italie semble être liée au déplacement de trajectoires des tempêtes Atlantiques vers la Méditerranée, induit par la calotte glaciaire de Fennoscandie et la plaine nord-européenne. Au contraire, pendant le Bølling-Allerød, les conditions chaudes peuvent être liées à la position vers le nord des glaces marines de l'Atlantique Nord et du JetStream Polaire.

Mots clés : Région méditerranéenne ; Palynologie ; Biomarqueur moléculaire ; Paléoclimat ; Fonctions de transfert ; Téphra ; Dryas récent ; Bølling-Allerød ; Tardiglaciaire

1. Introduction

In the Northern Hemisphere, the Lateglacial (ca. 14,700-11,700 cal BP) is a period of special climatic interest characterized by contrasted and rapid climate changes, associated with the successive steps of the deglaciation and changes in atmospheric and ocean circulation patterns (e.g., Walker et al., 2012; Rehfeld et al., 2018). Following the cold Oldest Dryas (OD) period, the Bølling–Allerød (B/A) or Greenland Interstadial-1 (GI-1) began abruptly at 14,700 cal BP with warmer conditions. At 12,900–11,700 cal BP, the Younger Dryas (YD) or Greenland Stadial-1 (GS-1) was the last main millennial-scale cold event in Europe during the Lateglacial (Greenland ice-core records; Rasmussen et al., 2014). The YD is characterized by extreme cold, relative dry and windy climate conditions in northern-central Europe (Hepp et al., 2019). Climate became distinctly warmer at 11,700 cal BP with the onset of the Holocene Interglacial (Rasmussen et al., 2014). These rapid and marked climate oscillations have been observed in the Greenland ice core records (Rasmussen et al., 2014) and in Europe from various proxies such as pollen, oxygen isotopes, molecular biomarkers, beetles, and chironomids (e.g. Coope and Lemdahl, 1995; Ammann et al., 2000; Coope and Lemdahl, 1995; Peyron et al., 2005; Lotter et al., 2012; Millet et al., 2012; Blaga et al., 2013; Moreno et al., 2014; Heiri et al., 2015; Ponel et al., 2022; Duprat-Oualid et al., 2022).

Regional climate differences have been evidenced during the Lateglacial, and temperature trends in Europe and the Mediterranean region are still a matter of active research and debate. The chironomid-based synthesis of Heiri et al. (2014) suggests that temperature variations during the Lateglacial tend to be more pronounced in Western Europe (British Isles, Norway) than in Southwestern Europe, Central and Southeastern regions. This is particularly true for the Younger Dryas cooling which is not well evidenced in East and Central Southern Europe (Heiri et al., 2014). These regional differences would be attributed to the changing position of the North Atlantic sea-ice and the Polar Frontal JetStream (Renssen and Isarin, 2001).

Diverging temperature trends are also reconstructed from different proxies during key periods of the Lateglacial. Studies suggest that (1) the OD was cooler than the YD in Southern and Central Europe in comparison with Northern Europe (Heiri et al., 2014; Moreno et al., 2014); (2) the Allerød period was warmer than the Bølling in Southwestern Europe and the Mediterranean area (Moreno et al., 2014); and (3) temperatures were more contrasted during the B/A and YD in the Northwest of Europe in comparison to the South of Europe (Renssen and Isarin, 2001; Moreno et al., 2014; Heiri et al., 2014). In contrast to temperature, the

precipitation signal is poorly known in Europe during the Lateglacial because few proxies are available to quantitatively reconstruct precipitation change. Climate models (GCMs) simulate significant hydrological changes during the B/A and contrasted North-South patterns during the YD (Renssen and Isarin, 2001; Rea et al., 2020). They simulate drier conditions in Northern Europe and wetter conditions in Southern Europe, i.e. in the South of Italy, the Dinaric Alps, and Northern Turkey (Rea et al., 2020). Climate changes during the YD are attributed to a weak Atlantic Meridional Overturning Circulation (AMOC) and a southward shift of the Polar Frontal JetStream (PFJS), linked to the elevation of the ice sheet, in particular the Laurentide ice sheet (Renssen and Isarin, 2001; Renssen et al., 2015; Rea et al., 2020). Rea et al. (2020) also explains the regional climate patterns in Europe by a relocation of Atlantic storm tracks along the western European margin and into the Mediterranean.

The understanding of climate processes in Europe and Mediterranean regions during the Lateglacial still needs to be improved. The majority of climate reconstructions are focused on temperatures, and changes in precipitation remain elusive. The "key" junction area between Northern and Southern Europe and regional climatic patterns also needs to be better defined. Moreover, the proxies used to reconstruct climate changes (e.g., coleoptera, chironomids, pollen, ostracods, speleothems) can show differences in terms of amplitudes or patterns which are not only affected by temperatures, but also by precipitation or effective moisture (Moreno et al., 2014; Samartin et al., 2017). For these reasons, more reliable temperature reconstructions, especially from Western Europe and the Mediterranean region are required to test diverging trends during the Lateglacial. The proxies largely used to quantitatively reconstruct past climate changes are often a single proxy approach (e.g. Heiri et al., 2015; Gandouin et al., 2016; Peyron et al., 2017; Marchegiano et al., 2020; Duprat-Oualid et al., 2022). Multiproxy approaches on the same sedimentary record, including independent climate proxies, are necessary to better understand the climate processes in Europe during the Lateglacial (Lotter et al., 2012; Ponel et al., 2022). Pollen-based reconstructions have the advantage of reconstructing temperatures, precipitation, and seasonality, however, the climate signal can be perturbed by other factors such as CO_2 changes and human impact influencing vegetation development (Peyron et al., 2005). Over the last decades, novel proxies based on molecular geochemistry have been developed and molecular biomarkers are being increasingly used to reconstruct temperatures and represent a complementary proxy for lake sediments (Castañeda and Schouten, 2011). In particular, branched Glycerol Dialkyl Glycerol Tetraethers (brGDGTs) are ubiquitous organic compounds synthesized by bacteria (Weijers et al., 2006) which have been useful for reconstructing environmental parameters. To date, the actual producers of brGDGTs remain

elusive although it is proposed they come from the phylum *Acidobacteria* (Weijers et al., 2009; Sinninghe Damsté et al., 2018). The relationship, however, between brGDGT distribution and environmental changes, in particular pH and temperature, are well established (Naafs et al., 2017b, 2017a; Dearing Crampton-Flood et al., 2020; Martínez-Sosa et al., 2021; Raberg et al., 2021). The degree of methylation of brGDGTs (MBT; methylation of branched GDGTs) varies depending on the mean annual air temperature (MAAT) and higher fractional abundance of hexa- (III) and penta- (II) methylated brGDGTs are recorded in colder environments (Weijers et al., 2007). Branched glycerol dialkyl glycerol tetraether (brGDGT) membrane lipids are increasingly used as a temperature proxy: in Europe, brGDGTs have been used to reconstruct the Mid to Late Holocene temperature changes in the Carpathians (Ramos-Román et al., 2022), the last 36,000 years in the Southern Iberian Peninsula (Rodrigo-Gámiz et al., 2022), the Holocene temperatures in France (Martin et al., 2020), and in the Eastern Mediterranean over the last deglaciation (Sanchi et al., 2014; Stockhecke et al., 2021). The association in the same core between brGDGTs and other proxies such as pollen for climate reconstructions are still rare (Watson et al., 2018; Panagiotopoulos et al., 2020; Martin et al., 2020; Dugerdil et al., 2021a, 2021b; Ramos-Román et al., 2022; Robles et al., 2022; Rodrigo-Gámiz et al., 2022) and no studies are yet available for the circum-Mediterranean region during the Lateglacial.

This study presents a high-resolution climate reconstruction for the Lateglacial period in South Central Europe, inferred from multi-proxy data of the Lake Matese sedimentary record (Southern Italy). In detail, the aims of this study are to:

1) establish reliable and independent quantitative climate reconstructions based on molecular biomarkers (brGDGTs) and pollen data to help identify potential biases of currently used proxies and thus improve the reliability of each proxy-inferred climate record;

2) compare these reconstructions with regional climate reconstructions and in the light of other South European records;

3) better understand the climate processes in Europe and Mediterranean during the Lateglacial period.

2. Study site

Lake Matese (41°24'33.3"N, 14°24'22.1"E, 1012 m a.s.l.) is located in the Caserta province in the Campania region, Southern Italy, approximately 60 km north of the city of Naples and the active Campanian volcanoes (Vesuvius, Campi Flegrei, Ischia) (Fig. 1). The lake is situated in the Matese karst massif in the Southern Apennines, which extends over 30 km from the NE to the SW and is composed of Late Triassic-Miocene limestones and dolomites (Fiorillo and Doglioni, 2010). The present formation of the massif was the result of an extension by strike-slip faults during the Quaternary, and several strong earthquakes were recorded in the massif (Ferranti et al., 2015; Ferrarini et al., 2017; Galli et al., 2017; Valente et al., 2019). Lake Matese is the highest karst lake of Italy and is surrounded by the two highest peaks of the massif, Mount Miletto (2050 m a.s.l.) and Mount Gallinola (1923 m a.s.l.), which feed the lake by their snowmelt. Along the southern side of the lake, two sinkholes named the "Brecce" and "Scennerato" are present (Fiorillo and Pagnozzi, 2015). In the 1920s, hydraulic works were conducted to isolate the bottom of the lake and the main sinkholes by earthen dams (Fiorillo and Pagnozzi, 2015). The water level of the lake improved from 1007-1009 m a.s.l. to 1012 m a.s.l. with a volume of 15 Mm^3 (Fiorillo and Pagnozzi, 2015). A part of the lake water is transported to the hydroelectric power station of Piedimonte Matese at the bottom of the mountain massif.

The Matese Mountains are characterized by a Mediterranean warm-temperate, humid climate (Aucelli et al., 2013). The southeastern part of the massif, including Lake Matese, have the highest precipitation with a maximum of 2167 mm at Campitello Matese (1400 m a.s.l.) (Fiorillo and Pagnozzi, 2015). Lake Matese shows an annual precipitation of 1808 mm with a maximum in November (~290 mm) and December (~260 mm) and a minimum in July (~50 mm) (Fiorillo and Pagnozzi, 2015). The annual temperatures correspond to 9.3°C with a minimum in January (2°C) and a maximum in July (19°C) (Fiorillo and Pagnozzi, 2015).

The vegetation of the Matese massif is dominated by deciduous *Quercus* and *Ostrya carpinofolia*, while the highest altitudes at the northern flank also show an exposure of *Fagus sylvatica* and the lower altitudes of the southern flank includes Mediterranean taxa such as *Quercus ilex* (Taffetani et al., 2012; Carranza et al., 2012; Guarino et al., 2015). The hygrophilous vegetation at Lake Matese is distinguished by the presence of woody (e.g. *Salix alba, S. caprea, S. cinerea* subsp. *cinerea, Populus nigra, P. alba*), helophytes (e.g. *Phragmites australis, Schoenoplectus lacustris, Typha angustifolia, T. latifolia*) and hydrophytes species (*Myriophyllum spicatum, Persicaria amphibia*).

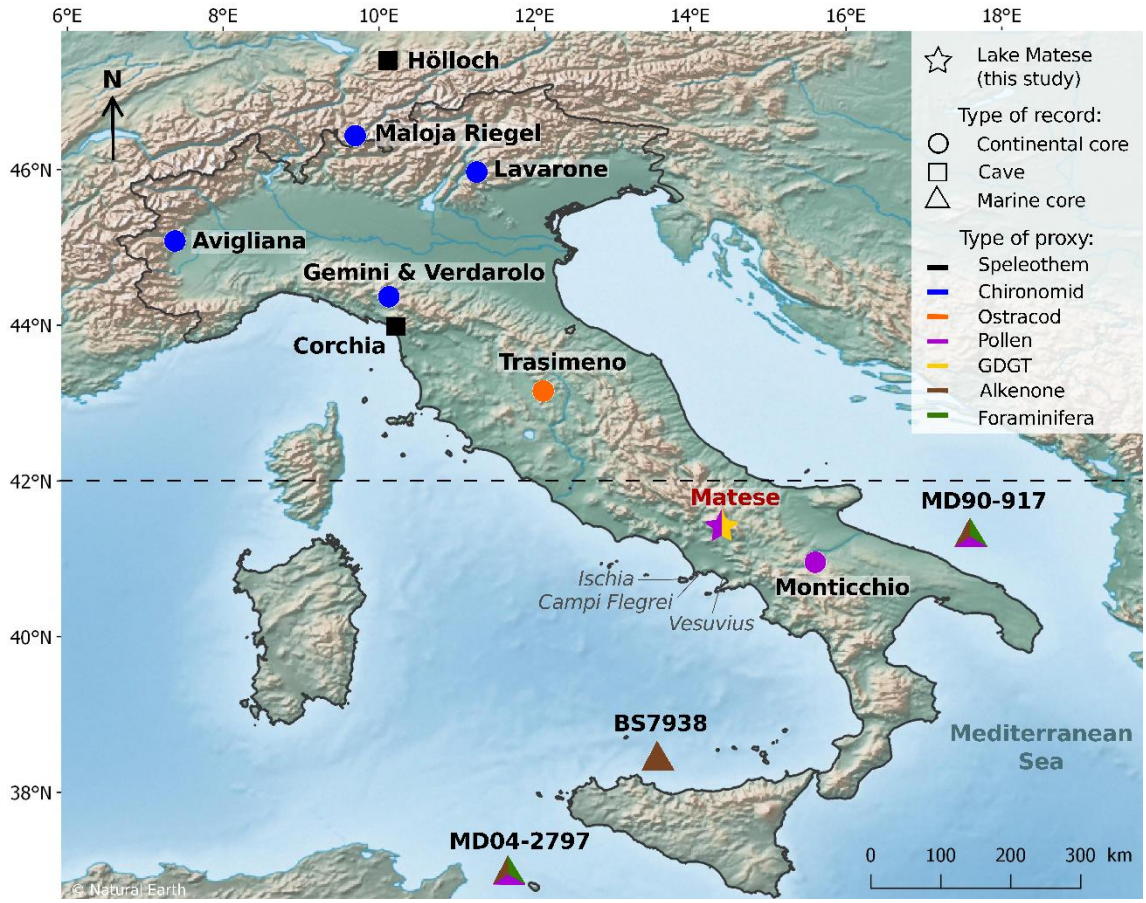

Figure III-1. Location of the Lake Matese and Lateglacial paleoclimate records : Hölloch (Li et al., 2021), Maloja Riegel (Heiri et al., 2014), Lago di Lavarone (Heiri et al., 2014), Lago Piccolo di Avigliana (Larocque and Finsinger, 2008), Lago Gemini (Samartin et al., 2017), Lago Verdarolo (Samartin et al., 2017), Corchia cave (Regattieri et al., 2014), Lake Trasimeno (Marchegiano et al., 2020), Lago Grande di Monticchio (Allen et al., 2002), MD90-917 (Combourieu-Nebout et al., 2013; Sicre et al., 2013), BS7938 (Sbaffi et al., 2004), MD04-2797 (Desprat et al., 2013; Sicre et al., 2013). Dotted line indicates latitude 42°N. Location of active Campanian volcanoes (Vesuvius, Campi Flegrei, Ischia).

3. Material and methods

3.1 Coring retrieval

Coring of Lake Matese was performed in July 2019 in the southwestern part of the lake (41°24'33.3"N, 14°24'22.1"E, 1012 m a.s.l.). Core occurred on a floating raft composed of *Salix* spp. and *Phragmites* spp., naturally present in the eastern part of the lake. Three parallel cores (cores A, B and C) were taken with a 1 m Russian corer with a chamber diameter of 6.3 cm. The composite core, measuring 535 cm, was constructed from sections of parallel cores and is based on the lithology and XRF data.

3.2 Chronology and age-depth model

Several methods have been used to build the chronology of the core including radiocarbon dating, and tephrochronology. The regional pollen stratigraphy is used to validate this age-depth model. Twelve accelerator mass spectrometry (AMS) ^{14}C dates were measured at Poznań Radiocarbon Laboratory and at the Radiocarbon Dating Center in Lyon. Plant macrofossils (plant fibers, wood) and charcoal were selected for four samples, and bulk sediment was used for eight samples according to the sediment type. Radiocarbon ages were calibrated in years cal BP using the *Calib 8.2* software with the IntCal20 calibration curve (Reimer et al., 2020).

Visible tephra layers and cryptotephra layers, detected by magnetic susceptibility and XRF core scanning data, were subsampled and processed for geochemical analysis. Cryptotephra was extracted using H_2O_2 and HCl to remove organic matter and carbonates, sieved at 20 and 100 microns, volcanic glass shards were embedded in resin, sectioned and polished for electron probe microanalysis. A JEOL-JXA8230 probe the Helmholtz Centre Potsdam (Germany) was used with a 15kV accelerating voltage, 10 nA beam current, and a 15 micron beam size. Analytical count times were 20 seconds for all elements except for K and Na, measured first at 10 s. International glass standards such as the Max Planck Institute (MPI-glasses) ATHO-G, StHs6/80 and GOR-132 (Jochum et al., 2006) and the natural Lipari obsidian (Hunt and Hill, 1996; Kuehn et al., 2011) were measured prior to sample analysis for data quality insurance. Glass geochemical data of Matese tephras are normalized on an anhydrous, volatile-free basis and compared with published tephra glass datasets (Wulf et al., 2008; Smith et al., 2011; Tomlinson et al., 2012).

The age-depth model based on based on one radiocarbon date and correlated tephra ages was constructed using an interpolated linear curve with the R 'Clam' program with 95% confidence intervals (Blaauw, 2010). In order to validate the age depth models, the pollen stratigraphy of the regional sites was compared with pollen data of Matese. The pollen stratigraphy of Pavullo di Frignano (Vescovi et al., 2010), Lakes Accesa (Drescher-Schneider et al., 2007), Albano (Mercuri et al., 2002), Mezzano (Sadori, 2018), Monticchio (Allen et al., 2002), and Trifoglietti (De Beaulieu et al., 2017) were used to identify the OD-B/A, B/A-YD and YD-Holocene transitions. We used the median age for each transition.

3.3 Magnetic susceptibility and geochemistry

Magnetic susceptibility (MS) was measured with a MS2E1 surface scanning sensor from Bartington Instruments on a Geotek Multi-Sensor Core logger based at the Chrono-environment laboratory (UMR CNRS - University of Franche-Comté). An interval of 3 mm or 5 mm was applied depending on the type of sediment.

Geochemical analyses were performed at high resolution by X-ray Fluorescence (XRF) with an AVAATECH core scanner at the EDYTEM laboratory (University Savoie Mont Blanc). A continuous 5 mm step measurement was applied with a run at 10 kV and 0.1 mA for 15 s to detect lightweight elements, such as Al, Si, K, Ca, Ti, Mn, Fe and a second run at 30 kV and 0.15 mA for 20 s to detect Br, Rb, Sr and Zr. The XRF core scanning provides an estimate of the geochemical composition, and the results are semi-quantitative and expressed as peak intensities counts i.e. counts per second (cps).

3.4 Pollen analyses

A total of 56 samples from the Matese core were collected at 4 cm or 6 cm resolution for pollen analysis. For each sample, 1 cm^3 of sediment was processed and 3 *Lycopodium* tablets were added to estimate pollen concentration. Samples were treated following the standard procedure (Faegri et al., 1989; Moore et al., 1991) including HCl, KOH, sieving, acetolysis and HF. The pollen concentrates were analyzed with a Leica DM1000 LED microscope at a standard magnification of 400x. Pollen taxa were identified using photo atlases (Beug, 2004; Reille, 1998; Van Geel, 2002) and a modern reference collection (ISEM, University of Montpellier). Each slide was counted with a minimum of 300 terrestrial pollen grains, excluding aquatic plants such as Cyperaceae, aquatic taxa, and fern spores. A simplified pollen diagram was constructed (Fig. 2) with the R package *Rioja* (Juggins and Juggins, 2020). This study presents the main pollen taxa and is not focused on variations of individual species.

3.5 Pollen-inferred climate reconstruction

A multi-method approach was used to reconstruct climate parameters from pollen data with greater reliability than reconstructions based on a single climate reconstruction method (Peyron et al., 2013, 2011, 2005; Salonen et al., 2019). We have selected here the Modern Analog Technique (MAT; Guiot, 1990), Weighted Averaging Partial Least Squares regression (WAPLS; ter Braak and van Dam, 1989; ter Braak and Juggins, 1993), and the most recent machine-learning methods : Random Forest (RF; Breiman, 2001; Prasad et al., 2006) and Boosted Regression Trees (BRT; De'ath, 2007; Elith et al., 2008).

The MAT is an assemblage approach, based on the measure of the degree of dissimilarity (squared chord distance) between fossil and modern pollen assemblages (Guiot, 1990). Fossil pollen assemblages are compared to a set of modern assemblages (modern dataset), each one associated with climate estimates. The closest modern samples are retained and averaged to estimate past climate conditions (annual and seasonal temperature and precipitation). WAPLS is a non-linear regression technique that models the relationships between the climate parameters and the pollen taxa from a modern pollen dataset, before applying these relationships to fossil pollen assemblages (ter Braak and Juggins, 1993; ter Braak and van Dam, 1989). WAPLS and MAT methods are applied with the R package *Rioja* (Juggins and Juggins, 2020). RF and BRT, based on machine learning, utilizes regression trees developed with ecological data, and has been used recently to reconstruct palaeoclimatic changes (Salonen et al., 2019; Robles et al., 2022). These classification trees are used to partition the data by separating the pollen assemblages based on the relative pollen percentages. RF is based on a large number of regression trees, each tree being estimated from a randomized ensemble of different subsets of the modern pollen dataset by bootstrapping (Breiman, 2001; Prasad et al., 2006). Finally, the RF prediction is applied to the fossil pollen record. BRT is also based on regression trees (De'ath, 2007; Elith et al., 2008); it differs from RF in the definition of the random modern datasets. In RF, each sample gets the same probability of being selected, while in BRT the samples that were insufficiently described in the previous tree get a higher probability of being selected. This approach is called 'boosting' and increases the performance of the model over the elements that are least well predicted (Breiman, 2001; Prasad et al., 2006; De'ath, 2007; Elith et al., 2008). RF is applied with the R package *randomForest* (Liaw and Wiener, 2002) and BRT with the R package *dismo* (Hijmans et al., 2021).

The modern pollen dataset (n = 3373 sites) used for the calibration of the methods is based on the large Eurasian/Mediterranean dataset compiled by Peyron et al. (2013, 2017) and completed by Dugerdil et al. (2021a) and Robles et al. (2022). In our study, we added pollen data of 92 surface lake sediments from Italy (Finsinger et al., 2007) and 15 moss polsters from the Matese massif (Robles, 2022). Then, a biome constraint (Guiot et al., 1993), based on the pollen-Plant Functional Type method and following the biomization procedure (Peyron et al., 1998; Prentice et al., 1996) was applied to modern and fossil pollen samples. The modern pollen dataset finally selected for the calibration of the different methods contains 1018 samples belonging to 3 biomes depicted in the fossil core: "warm mixed forest" (WAMX), "temperate deciduous" (TEDE) and "cold steppe" (COST). Performance of each method and calibration training was statistically tested (for more details, see Dugerdil et al., 2021a) to determining if

modern samples are suitable for quantitative climate reconstructions. The Root Mean Square Error (RMSE) and the R^2 are presented in the Supplementary Table S1. Five climate parameters were reconstructed, mean annual air temperature (MAAT), mean temperature of the warmest month (MTWA), mean temperature of the coldest month (MTCO), mean annual precipitation (PANN), and winter precipitation (P_{winter} = December, January, and February). For each climate parameter, the methods fitting with the higher R^2 and the lower RMSE were selected. Cyperaceae and ferns in the Matese record have been excluded because they are associated with local dynamics.

3.6 BrGDGT analyses

A total of 56 samples from the Matese core (4 cm or 6 cm resolution) were used for GDGT analysis (same as for pollen analysis). The samples were freeze-dried, powdered and subsampled (1 g for clay and 0.4 g for gyttja). Lipids were extracted from the sediment using a microwave oven (MARS 6; CEM) with dichloromethane:methanol (3:1). Then, the internal standard was added (C_{46} GDGT, Huguet et al., 2006). The total lipid extracts were separated into apolar and polar fractions using a silica SPE cartridge with hexane:DCM (1:1) and DCM:MeOH (1:1). The polar fractions containing brGDGTs were analyzed using a High-Performance Liquid Chromatography Mass Spectrometry (HPLC-APCI-MS, Agilent 1200) with detection via selective ion monitoring (SIM) of m/z 1050, 1048, 1046, 1036, 1034, 1032, 1022, 1020, and 1018 in the LGL-TPE of ENS Lyon (Hopmans et al., 2016; Davtian et al., 2018). GDGT concentrations were calculated based on the internal standard (C_{46} GDGT, Huguet et al., 2006). The analytic reproducibility was assessed by regularly processing a lab-internal sediment sample (Vaux Marsh; 45°57'21.1"N, 5°35'32.42"E). Analytical precision is based on duplicate injections of one sample of each Matese core lithological types (n=4). Respective analytical 1-sigma standard deviations are then applied to each measurement within one lithology.

3.7 GDGTs annual temperature reconstruction

The proportion of tetra- (I), penta- (II) and hexa- (III) methylated brGDGTs includes the fractional abundances of the 5-methyl (X), 6-methyl (X') and 7-methyl (X7) brGDGTs (Ding et al., 2016). The CBT (cyclization ratio of branched tetraethers) and MBT indexes were defined by Weijers et al. (2007) and the MBT'_{5me}, only based on the 5-methyl brGDGTs, by De Jonge et al. (2014). The Mean Annual Air Temperature (MAAT) was reconstructed with global (Sun et al., 2011) and East African (Russell et al., 2018) lacustrine calibrations. The mean

temperature of Months Above Freezing (MAF) was reconstructed with a lacustrine calibration based on Bayesian statistics (Martínez-Sosa et al., 2021; *https://github.com/jesstierney/BayMBT*) and a global lacustrine calibrations with revised compound fractional abundances based on methylation and cyclization number and methylation position (Raberg et al., 2021). Synthesis of the formulae for the main brGDGT indices are presented in Table 1. Modern MAAT and MAF of the Lake Matese corresponds to 9.3 °C.

The analytic reproducibility corresponds to ±0.040 for CBT, ±0.0167 for MBT, ±0.0206 for MBT'$_{5me}$, ±0.8566 °C for MAAT developed by Sun et al. (2011), ±0.6672 °C for MAAT developed by Russell et al. (2018), and ±0.5403 °C and ±1.1258 °C for MAF$_{Meth}$ and MAF$_{Full}$ developed by Raberg et al. (2021).

Table III-1. Synthesis of the formulae for the main brGDGT indices. For acronym explanation of MAF$_{Meth}$ and MAF$_{Full}$, see Raberg et al. (2021). For more information about the Bayesian statistics see Martínez-Sosa et al., 2021 and references therein.

Indice	Formula	Reference
$\%tetra$	$\frac{Ia + Ib + Ic}{\Sigma brGDGTs}$	Ding et al., 2016
$\%penta$	$\frac{IIa + IIa' + IIa_7 + IIb + IIb' + IIb_7 + IIc + IIc' + IIc_7}{\Sigma brGDGTs}$	Ding et al., 2016
$\%hexa$	$\frac{IIIa + IIIa' + IIIa_7 + IIIb + IIIb' + IIIb_7 + IIIc + IIIc' + IIIc_7}{\Sigma brGDGTs}$	Ding et al., 2016
CBT	$-log\frac{Ib + IIb}{Ia + IIa}$	Weijers et al., 2007
MBT	$\frac{Ia + Ib + Ic}{\Sigma brGDGTs}$	Weijers et al., 2007
MBT'_{5me}	$\frac{Ia + Ib + Ic}{Ia + Ib + Ic + IIa + IIb + IIc + IIIa}$	De Jonge et al., 2014
$MAAT\ (°C)$	$3.949 - 5.593 \times CBT\ + 38.213 \times MBT$ $(n = 100, R^2 = 0.73, RMSE = 4.27°C)$	Sun et al., 2011
$MAAT\ (°C)$	$-1{,}21 + 32.42 \times MBT'_{5me}$ $(n = 65, R^2 = 0.92, RMSE = 2.44\ °C)$	Russell et al., 2018
$MAF_{Meth}(°C)$	$92.9 + 63.84 \times fIb^2_{Meth} - 130.51 \times fIb_{Meth} - 28.77 \times fIIa^2_{Meth} - 72.28 \times fIIb^2_{Meth} - 5.88 \times fIIc^2_{Meth} + 20.89 \times fIIIa^2_{Meth} - 40.54 \times fIIIa_{Meth} - 80.47 \times fIIIb_{Meth}$ $(n = 182, R^2 = 0.90, RMSE = 2.14\ °C)$	Raberg et al., 2021

$MAF_{Full}(°C)$	$-8.06 + 37.52 \times fIa_{Full} - 266.83 \times fIb^2_{Full} + 133.42 \times fIb_{Full} + 100.85 \times fIIa'^2_{Full} + 58.15 \times fIIIa'^2_{Full} + 12.79 \times fIIIa_{Full}$ $(n = 182, R^2 = 0.91, RMSE = 1.97\ °C)$	Raberg et al., 2021
$MAF\ (°C)$	*Equation from the Bayesian model*: $MBT'_{5me} = 0.030(\pm 0.001)MAF + 0.075(\pm 0.012)$ $(R^2 = 0.82, RMSE = 2.9\ °C)$	Martínez-Sosa et al., 2021

4. Results

4.1 Lithology, magnetic susceptibility, XRF and pollen

The lithology of the Matese core (Fig. 2) is mainly composed of gray clay sediment with vivianite from the base to 350 cm, interrupted by an organic layer between 477-484 cm (sedimentary Unit 2) and a macroscopically visible tephra layer (Fig. 2) between 476-437 cm (sedimentary Unit 3). This part contains few plant fibers, which are essentially vertically oriented in the core. From 349 to 320 cm, the lithology is formed by a mix of clay sediment and gyttja (sedimentary Unit 5). This part is mostly composed by roots and fine rootlets.

Magnetic susceptibility (MS) and Potassium (K) peaks of XRF core scanning are used to detect tephra layers (Fig. 2). MS and Potassium contents show increased values at 516-502 cm, 482-437 cm and 366-338 cm, which correspond to the deposition of tephra material (macroscopic visible tephra and cryptotephra of primary and secondary deposition). Small peaks are also visible in MS between 430 and 360 cm but they are not associated with any observed tephra. Potassium content is also marked by an increase between 536-526 cm which corresponds to tephra of primary deposition. Titanium (Ti) content, on the other hand, is representative for terrigenous input which is prevailing in sedimentary Unit 4 (Fig. 2).

The main pollen taxa diagram (Fig. 2) shows the dominance of herbaceous taxa (Poaceae, *Artemisia*) and a small proportion of arboreal taxa at the base of the sequence. From 520 to 425 cm, the period is marked by three expansion phases of arboreal taxa, followed between 438 to 354 cm by a large increase of *Artemisia* and a drop of AP taxa starting at 422 cm. Finally, from 354 to 338 cm AP and Poaceae increase, whereas *Artemisia* significantly decline.

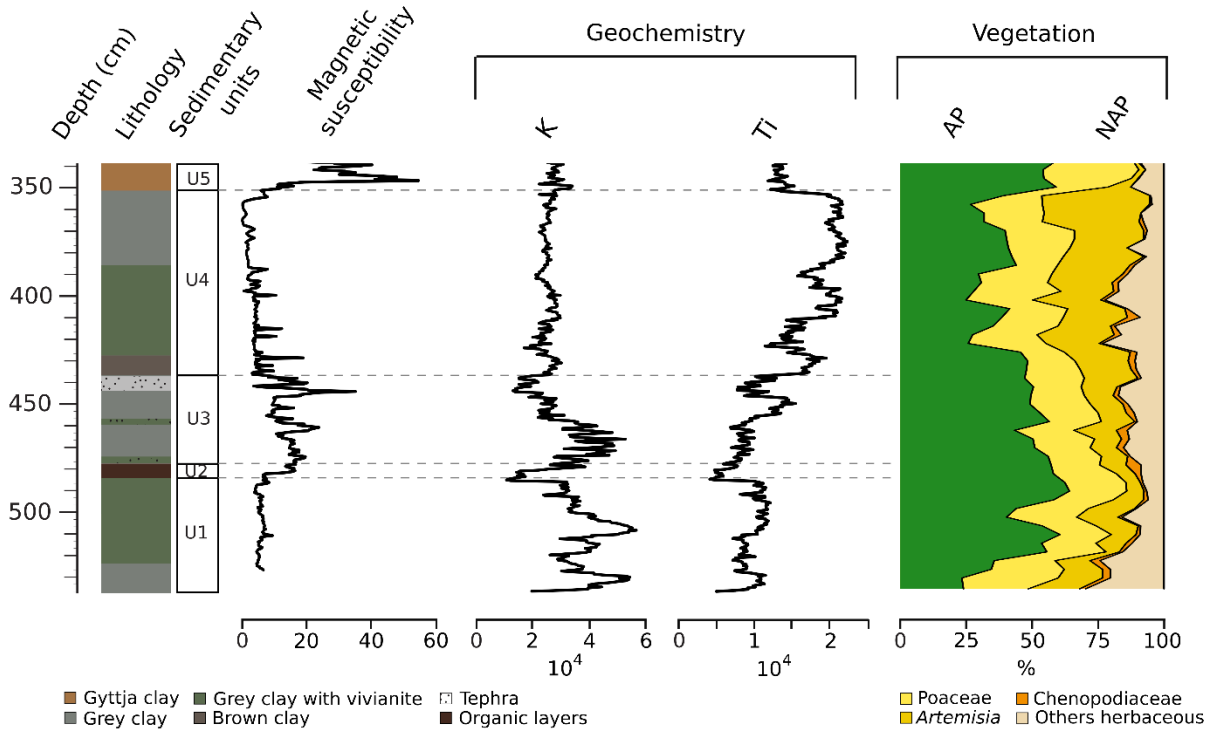

Figure III-2. Sediment lithology, magnetic susceptibility, geochemical data and selected terrestrial pollen taxa of Matese. Arboreal Pollen (AP; green) and Non Arboreal Pollen (NAP; yellow-orange) are expressed in percentages of total terrestrial pollen.

4.2 Age-depth model

The age-depth model is based on ^{14}C dates and tephrochronology, and then pollen stratigraphy was used to validate the age-depth model (Fig. 3). Based on their typical phono-trachytic and bimodal tephri-phonolitic to trachytic major element glass composition Matese tephras at 530 cm and 346 cm depth can be correlated with distal Monticchio tephras TM-8 and TM-6-2, respectively (Fig. 4; Table 2). Tephra TM-8 has been correlated with the Neapolitan Yellow Tuff (NYT) eruption (Wulf et al., 2004) which has an age of 14,194 ± 172 cal BP (Bronk Ramsey et al., 2015). The tephra layer at 530 cm corresponds to the primary deposition and secondary deposition of remobilised tephras that were identified at 510 cm and 475 cm. TM-6-2 most likely are derived from the Early Holocene Casale eruption from Campi Flegrei (Smith et al., 2011) which is varve dated in Monticchio at 11,210 ± 224 cal BP (Wulf et al., 2008). The tephra layer at 346 cm corresponds to a primary deposition.

The ages obtained with the regional pollen stratigraphy show an OD-B/A transition at 14,500 ± 93.7 cal BP, a B/A-YD transition at 12,800 ± 57.7 cal BP and a YD-Holocene transition at 11,575 ± 103.1 cal BP (Allen et al., 2002; Mercuri et al., 2002; Drescher-Schneider et al., 2007; Vescovi et al., 2010; De Beaulieu et al., 2017; Sadori, 2018). Pollen stratigraphy of

the regional sites were compared with pollen data of Matese and the ages obtained show a good correspondence with the ages of tephra samples but a poor correspondence with the ^{14}C dates. Therefore, most of the ^{14}C dates (Table 3) are not included in the age-depth model (except the date at the base of the core). The organic matter extracted from sediment was essentially composed of rootlets, that explains the rejuvenation of the ^{14}C ages.

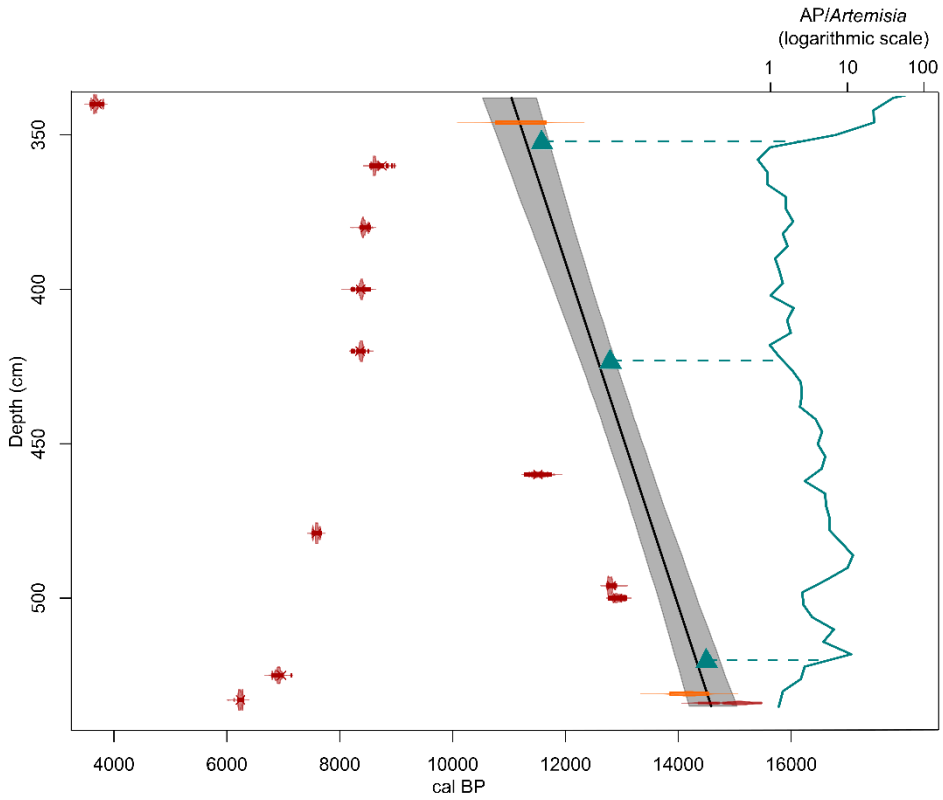

Figure III-3. Age-depth model is based on calibrated AMS radiocarbon dates (red points; Table 3) and tephra ages (orange points; Table 2). The grey band is the 95% confidence interval. Blue triangles are the median of ages of the vegetation transition compiled with the regional pollen stratigraphy. This pollen stratigraphy includes the sites of Pavullo di Frignano (Vescovi et al., 2010), Accesa (Drescher-Schneider et al., 2007), Albano (Mercuri et al., 2002), Mezzano (Sadori, 2018), Monticchio (Allen et al., 2002), and Trifoglietti (De Beaulieu et al., 2017). AP/Artemisia ratio (blue line) is expressed on a logarithmic scale. AP: Arboreal Pollen.

Table III-2. Tephra samples from Matese cores (MC) and correlation with tephra samples from Lago Grande di Monticchio (Wulf et al., 2008) and proximal eruptive sources.

Sample ID	Depth MC (cm)	Tephra Monticchio	Eruption	Age (cal BP)	Age reference
C1 96-97	346	TM-6-2	Casale	11,210 ± 224	Wulf et al., 2008
A5 75-77	475 (reworked)	TM-8	Neapolitan Yellow Tuff (NYT)	14,194 ± 172	Bronk Ramsey et al., 2015
C3 83-84	510 (reworked)				
B5 95-96	530				

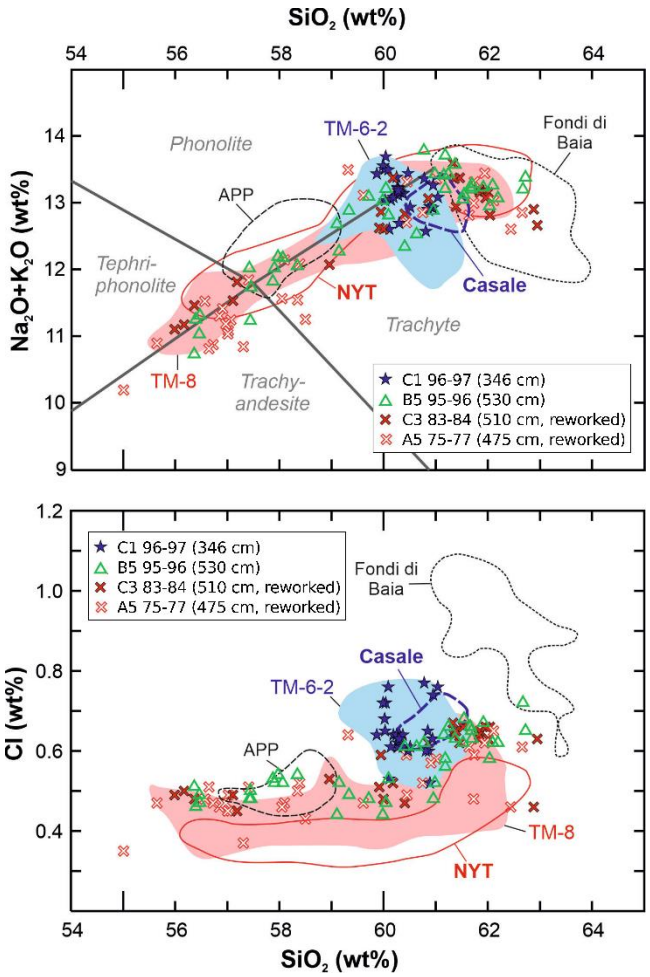

Figure III-4. Bivariate plot of selected major elements (SiO_2 vs. total alkalis and SiO_2 vs. Cl) of Matese tephras and potential proximal and Monticchio tephra correlatives. Data from: TM-6-2 (Monticchio, Wulf et al., 2008; this study); TM-8 (Monticchio, Tomlinson et al., 2012; this study); Casale, Fondi di Baia (proximal; Smith et al., 2011); APP/Agnano Pomici Principali and NYT/Neapolitan Yellow Tuff (proximal; Tomlinson et al., 2012).

Table III-3. AMS-radiocarbon dates (Radiocarbon Laboratory, Poznań), calibrated median ages, with 2 σ range of calibration from Matese cores (MC).

Sample ID	Depth MC (cm)	Lab code	Material	AMS ^{14}C age (BP)	Age (cal BP) (2 σ)	Median age (cal BP)
A4 40-41	340	Poz-128971	Bulk	3425 ± 30	3573 - 3822	3668
A4 60-61	360	Poz-138111	Bulk	7850 ± 40	8540 - 8968	8631
A4 80-81	380	Poz-138112	Bulk	7640 ± 50	8370 - 8541	8432
B4 50-51	400	Poz-128972	Bulk	7580 ± 60	8206 - 8519	8385
A5 20-21	420	Poz-138113	Bulk	7570 ± 50	8206 - 8512	8379
A5 60-61	460	Poz-128976	Bulk	10020 ± 50	11280 - 11743	11519
A6 52-53	479	Poz-119283	Plant fibers, wood fragments, charcoals	6730 ± 40	7513 - 7669	7596
A5 96-97	496	Poz-137155	Wood fragments	10870 ± 60	12728 - 12903	12799
B5 64-65	500	Poz-128973	Bulk	11000 ± 60	12769 - 13078	12925
A6 98-99	525	Poz-119284	Plant fibers	6060 ± 35	6795 - 7147	6912
B5 97-98	533	60747	Plant fibers	5430 ± 30	6190 - 6295	6236
B5 98-99	534	Poz-128975	Bulk	12650 ± 130	14331 - 15477	15027

4.3 Pollen-inferred climate reconstructions

Pollen-inferred climate reconstructions at Matese show similar trends for all methods (Fig. 5). The MAT and the BRT methods show higher sample-to-sample variability than the WAPLS, and RF appears as the less sensitive method. Statistical results of the model performance (Supplementary Table S1) show the better values for R^2 and RMSE for the BRT method (all climatic parameters).

Temperature trends show two cold periods (phases 1 and 3) and two warm periods (phases 2 and 4). The reconstructed values (MAAT and MTWA) during the warm periods are close to modern values whereas the values of MTCO are lower than the modern values. Annual precipitation (PANN) shows few variations and the values of PANN and P_{winter} are lower than modern values, with all methods. Phase 1 (535-530 cm; 14,600-14,500 cal BP) is characterized by cold conditions and low precipitation during winter. Phase 2 (530-436 cm; 14,500-12,800 cal BP) is a warm period characterized by strong warming and punctuated by three colder events at 14,000 cal BP, 13,500-13,350 cal BP and 13,000 cal BP. Mean annual precipitation shows little variation whereas P_{winter} shows higher values than during the phase 1. Phase 3 (436-367 cm; 12,800-11,570 cal BP) is a strong event marked by cold conditions, a slight decline in P_{winter} and few changes for PANN. At the transition with phase 4, a significant decrease in the precipitation parameters is recorded. Phase 4 (367-338 cm; 11,570-11,000 cal BP) is characterized by a well-marked temperature increase (MAAT and MTCO) associated with wet conditions (hydrological parameters reach their maximum value).

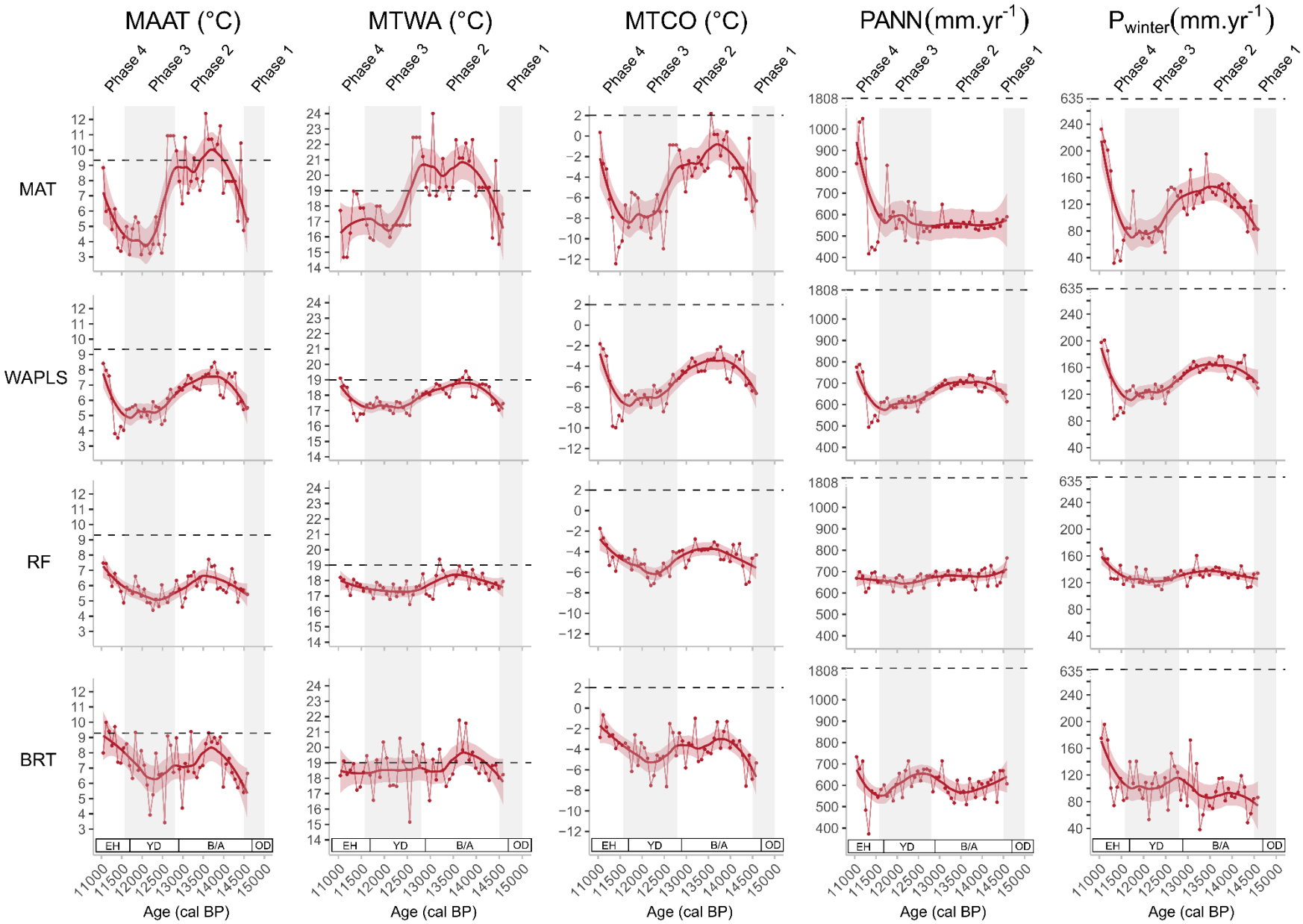
MAAT (°C)
MTWA (°C)
MTCO (°C)
PANN(mm.yr-1)
Pwinter(mm.yr-1)
Phase 4
Phase 3
Phase 2
Phase 1
MAT
WAPLS
RF
BRT
EH
YD
B/A
OD
Age (cal BP)

Figure III-5. Lake Matese pollen-inferred climate reconstruction based on four methods against age: MAT (Modern Analogue Technique), WAPLS (Weighted Averaging Partial Least Squares regression), RF (Random Forest) and BRT (Boosted Regression Trees). Large lines correspond to loess smoothed curves, shaded areas to the 95% confidence interval and dashed lines to modern climate values of Lake Matese. MAAT: mean annual air temperature. MTWA: mean temperature of the warmest month. MTCO: mean temperature of the coldest month. PANN: mean annual precipitation. P_{winter}: winter precipitation. OD: Oldest Dryas. B/A: Bølling–Allerød. YD: Younger Dryas. EH: Early Holocene.

4.3 BrGDGT-inferred climate reconstruction

4.3.1 Concentration and distribution of brGDGTs

The total concentration of brGDGTs ranges between 0.06 and 8.63 $\mu g.g^{-1}$ dry sediment. The fractional abundances of brGDGTs (Fig. 6A) show a dominance of pentamethylated brGDGTs (II, 46%), especially brGDGT IIa (23%), brGDGTs IIa' (7%) and brGDGTs IIb (6%). The relative abundance of tetramethylated brGDGTs (I, 33%) is mainly explained by brGDGT Ia (20%) and brGDGTs Ib (9%). The relative abundance of hexamethylated brGDGTs (III, 21%) is mainly explained by brGDGT IIIa (11%) and brGDGTs IIIa' (6%). The relative abundances of tetra, penta- and hexamethylated brGDGTs of Matese core are compared to global datasets (Fig. 6B). Sediment samples of the Matese core show a good correspondence with global lake and soil samples, except for some samples from sedimentary Unit 1 and 5. Samples of sedimentary Unit 5, characterized by a mix of clay and gyttja, are more similar to global soil and peat samples.

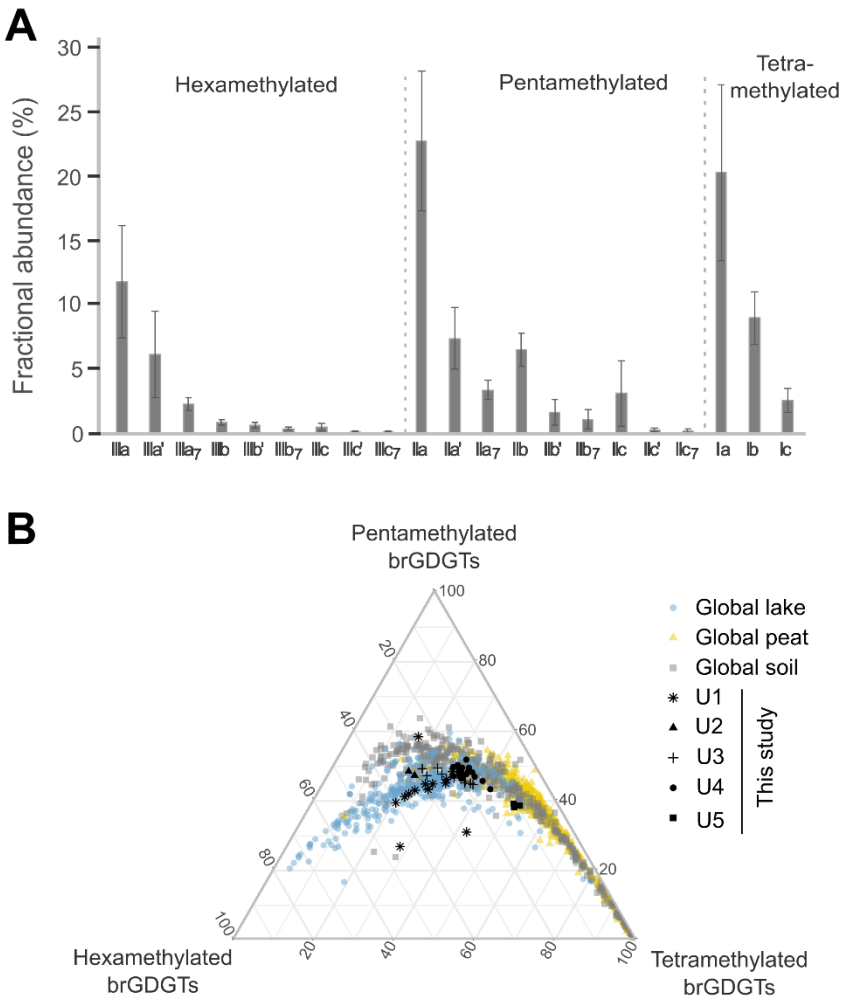

Figure III-6. A) Fractional abundance of tetra-, penta-, and hexamethylated brGDGTs for Matese core. B) Ternary diagram showing the fractional abundances of the tetra-, penta-, and hexamethylated brGDGTs for Matese core (black points) and global lake (blue points; Martínez-Sosa et al., 2021), peat (yellow circles; Naafs et al., 2017a), and soils (gray circles; Yang et al., 2014; Naafs et al., 2017b).

4.3.2 Indices of brGDGTs

The relative abundance of tetra-, penta-, and hexamethylated brGDGTs changes along Matese core (Fig. 7). The fractional abundance shows a dominance of pentamethylated brGDGTs except at 518 cm depth, and during the last phase (Phase 4). The fractional abundance of hexamethylated brGDGTs shows higher values between 535-502 cm and 490-466 cm and becomes dominant at 486 cm. The fractional abundance of tetramethylated brGDGTs shows higher values between 502-490 cm and 466-352 cm and is dominant at 518 cm and 352-338 cm (Phase 4).

The degree of methylation (MBT, MBT'$_{5Me}$) and the cyclisation ratio (CBT) also shows variation along Matese core (Fig. 7). The MBT and the MBT'$_{5Me}$ show similar trends but dif-

ferent absolute values; they vary between 0.17 and 0.52 and between 0.20 and 0.63, respectively. The degree of methylation remains relatively stable except during two phases of decrease between 534-522 cm and 486-458 cm, and two phases with higher values at 518 cm depth and during the Phase 4. The CBT varies between 0.27 and 0.74. Phase 1 (535-530 cm) is characterized by high values of CBT following by a decline until reaching a minimum between 494-482 cm. Then, the CBT slightly increases; at 382 cm a slow decline is recorded, and a strong increase marks Phase 4.

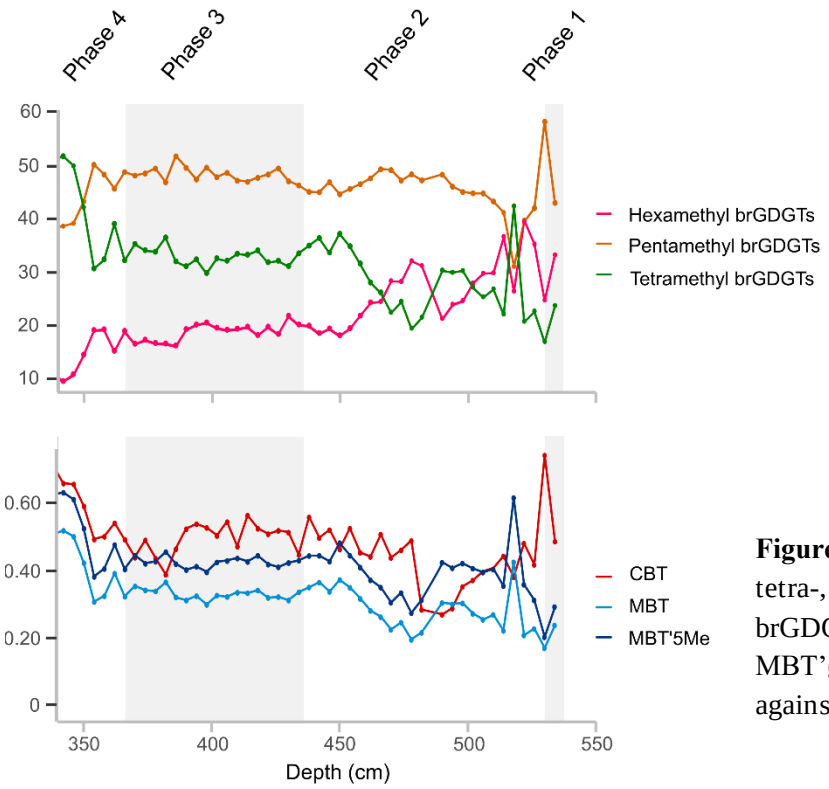

Figure III-7. Fractional abundance of tetra-, penta-, and hexamethylated brGDGTs degree of methylation (MBT, MBT'$_{5Me}$), cyclisation ratio (CBT) against depth for the Matese core.

4.3.3 Temperature reconstructions based on brGDGTs

The brGDGT inferred reconstructed MAAT using global (Sun et al., 2011) and East African (Russell et al., 2018) lacustrine calibrations show similar trends than MAF reconstructed using a Bayesian statistical model (Martínez-Sosa et al., 2021) and global (Raberg et al., 2021) lacustrine calibrations (Fig. 8). The values are higher than modern values, especially the values for the MAF_{Full} (Raberg et al., 2021). During Phase 1 (535-530 cm; 14,600-14,500 cal BP), all calibrations show cold temperatures. Phase 2 (530-436 cm; 14,500-12,800 cal BP) is marked by an abrupt temperature increase or a stabilization for MAF_{Meth} or a decline for MAF_{Full}. Between 13,700 and 13,200 cal BP, lower temperatures are recorded with all calibrations and from 13,100 cal BP, temperatures slowly decrease until 11,300 cal BP although a

slight increase is recorded between 11,900-11,500 cal BP. Phase 4 (367-338 cm; 11,570-11,000 cal BP) is characterized by a significant increase of temperature.

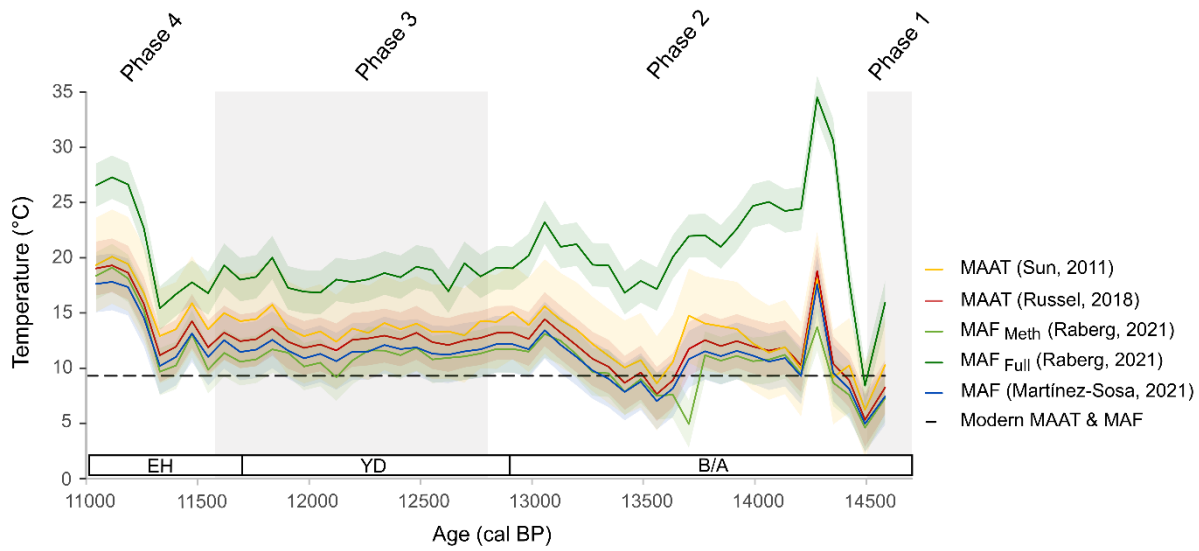

Figure III-8. Mean Annual Air Temperature (MAAT) based on global (Sun et al., 2011) and East African (Russell et al., 2018) lacustrine calibrations and Mean temperature of Months Above Freezing (MAF) based on Bayesian statistics (Martínez-Sosa et al., 2021) and global (Raberg et al., 2021) lacustrine calibrations against age for the Matese core. Shaded areas correspond to the error associated with calibrations and dashed lines correspond to modern climate values of Lake Matese. B/A: Bølling–Allerød. YD: Younger Dryas. EH: Early Holocene.

5. Discussion

5.1 Validation of age-depth model

The compilation of ages derived from the Italian pollen stratigraphy into the Matese age-model is based on the main vegetation changes identified in the area during the Lateglacial. In summary, the OD in Italian pollen records (and in the present study, Fig. 4) is characterized by an open vegetation dominated by Poaceae, *Artemisia,* with a few arboreal pollen such as *Pinus* and *Juniperus* appearing (Allen et al., 2002; Vescovi et al., 2010; Drescher-Schneider et al., 2007; De Beaulieu et al., 2017; Sadori, 2018). During the B/A, a significant increase of arboreal pollen taxa, including deciduous *Quercus* deciduous, is recorded, and in the majority of records *Betula* appears (Allen et al., 2002; Drescher-Schneider et al., 2007; Vescovi et al., 2010; Sadori, 2018; this study). During the YD, an increase of Poaceae and *Artemisia* (Allen et al., 2002; Mercuri et al., 2002; Drescher-Schneider et al., 2007; Vescovi et al., 2010) and an

overall decrease of arboreal pollen taxa, except in Southern Italy, (Allen et al., 2002; Beaulieu et al., 2017; this study) are documented.

The ages of tephra samples and ages constrained from the pollen stratigraphy are in good agreement, contrasting results from the ^{14}C dates which are randomly scattered and systematically too young (Fig. 2). The sediments of the Matese core are mainly composed of clay with only few plant fibers. Considering the recurrence of radiocarbon dates between 7570 and 7850 cal BP in the core interval between 420 and 360 cm depth (see Table 1), it is hypothesized that the dated organic matter may have partly originated from penetrating rootlets of plants growing during sedimentary Unit 5's deposition (Fig. 4). Indeed, aquatic plants of sedimentary Unit 5, identified with pollen, evidence a shallow water body and the development of tree species that typically grow in wetland.

Therefore, the overall age-depth model of the Matese core is based on imported, well-accepted tephra ages and one ^{14}C date of a bulk sediment sample from the bottom of the core at 534 cm (Fig. 2).

5.2 Influence of proxies and methods on climate reconstructions

5.2.1 Lake Matese climate signal reliability

Climate reconstructions are based both on pollen and brGDGTs, and some temperature discrepancies (absolute values or amplitudes) are depicted depending on the proxies (Fig. 9). The temperature amplitudes and absolute values are higher for brGDGTs (5-20°C) than the pollen (4-10°C) reconstructions. Pollen-inferred temperature values depend heavily on the quality of the modern pollen dataset including the number of samples, the diversity of samples in terms of biomes, and the similarity with the fossil samples (Chevalier et al., 2020). In our study, the modern database includes several modern samples from the Matese massif, and 95 samples from Italy were added to complete the dataset. Moreover, the spatial autocorrelation is low for MAT (Moran's I<0.34, p-value<0.01), and climate trends are consistent between methods. Reconstructed values for temperatures are close to modern values during the warmest periods, however, precipitation is largely underestimated by all methods for the recent time period (Fig. 5). The same observation was made in Calabria in Southern Italy (Trifoglietti; Joannin et al., 2012), a region also characterized by precipitation above 1700 mm. The underestimation of precipitation is certainly linked to the lack of modern samples located in very wet Mediterranean areas. Considering the brGDGT climate signal, the reconstructed temperatures are overestimated in comparison with modern values (Fig. 8). For shallow

temperate lakes (< 20 m), like Lake Matese, our brGDGT reconstructions suggest values anomalously higher than the expected temperature due to thermal variability (seasonal and diurnal; Martínez-Sosa et al., 2021). Lake Matese is located at an altitude of 1012 m a.s.l. and the strong seasonal variability may have influenced the brGDGT distribution. Moreover, the Lake Matese climate reconstructions are based on several global lacustrine calibration datasets, which may not be well adapted to reconstruct paleotemperatures in the Mediterranean region. According to Dugerdil et al. (2021a), local calibrations perform better to reconstruct more reliable absolute values. Unfortunately, at date, only a few global lacustrine calibrations are available, and a local calibration dataset for the Mediterranean region is still missing.

5.2.2 Regional climate signal reliability depending on the proxy

Climate reconstructions inferred from Lake Matese are compared to key terrestrial and marine temperature and precipitation records (Fig. 9, 10) in a latitudinal transect in central Mediterranean. These reconstructions for the Mediterranean region are based on different proxies. Most of those are indicators of annual temperatures, but some of them are indicators of seasonal temperature changes. For example, transfer functions based on chironomid assemblages provide estimates of mean July air temperatures (Larocque and Finsinger, 2008; Heiri et al., 2014; Samartin et al., 2017), while ostracod assemblages allow quantitative reconstruction of both January and July palaeotemperatures (Marchegiano et al., 2020). Planktonic foraminifera provide estimates of spring and autumn sea surface temperatures (SST) (Sicre et al., 2013). Depending on the production and deposition settings, molecular biomarkers are considered as indicators of annual or seasonal temperatures like brGDGTs or alkenones (Sbaffi et al., 2004; Sicre et al., 2013; Zhang et al., 2013; Max et al., 2020; Martínez-Sosa et al., 2021). For precipitation (Fig. 10), fewer reconstructions are available and they are mainly based on records of pollen (Combourieu-Nebout et al., 2013), $\delta^{18}O$ *G. bulloides* in marine sediments (Sicre et al., 2013), and $\delta^{18}O$ in speleothems (Regattieri et al., 2014). Pollen enable the reconstruction of both annual and seasonal temperatures and precipitation (e.g. Allen et al., 2002; Tarroso et al., 2016).

The comparison between climate reconstructions inferred from different proxies allows us to identify reliable regional climate signals and to reduce the bias linked to each proxy. Indeed, differences may appear for the timing or amplitudes of changes according to the type of proxy. These differences may be amplified by the proxy provenance, either marine or continental. In Figure 9, the temperature reconstructions above 42°N are mainly based on chironomids,

and the climate signal reconstructed is consistent between the sites. In South Italy, at Monticchio, climate reconstructions are based on three pollen records from the same site and differences in terms of amplitude and trend are clearly evidenced (Fig. 9I). These differences are linked to the differences in the core location in the lake and the pollen sample resolution (Allen et al., 2002). The closer the core to the center of the lake (dark blue, Fig. 9I), the better the regional vegetation record and therewith a possible regional climate signal (Peyron et al., 2005). Between latitude 41°N and 36°N, sea-surface temperatures (SSTs) were reconstructed from foraminifera and/or alkenones analyzed from marine cores (Sbaffi et al., 2004; Sicre et al., 2013). Alkenone-based SSTs show a low amplitude of 2-3°C between the B/A and the YD periods, whereas foraminifera-based reconstruction of seasonal temperature show differences of 5-10°C between the B/A and the YD. The differences are linked to their respective methods: For alkenones, the estimation of SSTs are based on the molecular biomarker as the C_{37} alkenone unsaturation ($U_{37}^{K'}$), whereas, for foraminifera, they are calculated with the MAT method and depend on the occurrence of modern analogues (Sicre et al., 2013).

5.3 Climate changes during the Lateglacial in Italy

5.3.1 Bølling–Allerød warming

The age of transition between the OD and the Bølling–Allerød Interstadial is estimated at around 14,700 cal BP based on the NGRIP ice-core chronology (Rasmussen et al., 2014). In Italy, an abrupt warming is evidenced at ca 14,700 cal BP (Fig. 9). The differences between the different reconstructions seem related to the type of proxy used rather than latitude. The transition is not obvious in the temperature reconstructions based on alkenones (Fig. 9MO; Sbaffi et al., 2004; Sicre et al., 2013), whereas it is well marked in reconstructions based on foraminifera (Fig. 9N; Sicre et al., 2013) and pollen assemblages (Desprat et al., 2013) from the same cores. According to Sicre et al. (2013), alkenones-inferred SSTs could be biased during the Early deglaciation due to water stratification inducing warming of the thin surface water layers where small size nanophytoplankton grow. Except for temperature reconstructions based on alkenones, all the records show an increase of the temperature at the transition OD-B/A (Larocque and Finsinger, 2008; Sicre et al., 2013; Heiri et al., 2014; Marchegiano et al., 2020). The transition, although marked, seems more progressive in the Italian records than in Greenland ice-core but the low resolution of some records can favor this trend. In terms of precipitation (Fig. 10), few records are available in Italy but no significant changes are recorded around

14,700 cal BP by $\delta^{18}O$ *G. bulloides* (Sicre et al., 2013) and pollen transfer functions (Desprat et al., 2013; this study).

The Bølling–Allerød interstadial is a warm interstadial period interrupted by several cold climate oscillations (Rasmussen et al., 2014). According to the synthesis by Moreno et al. (2014), the Bølling was cooler than the Allerød in the Southern Mediterranean compared to the warmer Northern Mediterranean. In Italy, above 42°N, temperature trends are complex to interpret: some records show an increase of temperature (Fig. 9B; Heiri et al., 2014) whereas other records show a decline (Fig. 9CE; Larocque and Finsinger, 2008; Marchegiano et al., 2020). At Matese, pollen and brGDGTs inferred temperatures decrease (Fig. 9F-H), whereas in the southern part of Italy, there are no significant changes during the B/A (Fig. 9I-O; Allen et al., 2002; Sbaffi et al., 2004; Sicre et al., 2013). Temperature reconstructions in Italy show no distinct difference between the Bølling and the Allerød with respect to the latitude. In terms of amplitude, several studies (Renssen and Isarin, 2001; Heiri et al., 2014; Moreno et al., 2014) suggests that there were less contrasts in temperatures during the B/A in Southern Europe in comparison with Northern Europe. Once again, this difference is not clear in Italy (Fig. 9). At Matese, a significant decrease of brGDGTs-inferred temperature is recorded at 13,700-13,200 cal BP cal BP (Fig. 9H). This change could be attributed to a colder period such as the Older Dryas or the Inter-Allerød cold period, two short periods characterized by colder conditions in the Greenland ice-core records at 14,000 and 13,100 cal BP, respectively (Rasmussen et al., 2014). However, this cooling event do not appear at the same time in the Matese climate curve based on pollen, and it is only vaguely recorded in other Italian records (Fig. 9). We suggest that this change could be attributed to changes of local conditions that are visible in a lithology change (sedimentary Unit 2, Fig. 4). Indeed, brGDGT distribution and origin can differ according to the type of wetland, water level or vegetation changes (Martínez-Sosa et al., 2021; Robles et al., 2022). In terms of precipitation (Fig. 10), no significant changes occur during the B/A in Italy as suggested previously by Renssen and Isarin (2001) for Southern Europe. The Alpine region seems instead to record wetter conditions during the B/A (Barton et al., 2018; Li et al., 2021).

5.3.2 A marked Younger Dryas cold event throughout Italy

The onset of the YD is estimated around 12,900 cal BP according to the Greenland ice-core chronology (Rasmussen et al., 2014). In Italy, above 42°N, the transition between the B/A and the YD is progressive in terms of temperatures except for chironomid records (Fig. 9B;

Heiri et al., 2014). At Matese, pollen-based reconstructions show a progressive decline of temperatures with all methods except the MAT (Fig. 9FG). For this method, the transition is more abrupt, but this difference can be attributed to the application of the biome constraint. BrGDGT-based reconstructions record a steady decrease during the YD or no significant changes according to the calibrations used (Fig. 9H). For southern Italian records, the transition is more abrupt and particularly marked in the foraminifera record in contrast to alkenones-based reconstructions (Fig. 9J-O; Sbaffi et al., 2004; Sicre et al., 2013). In terms of precipitation (Fig. 10), the northern Italian speleothems records show an abrupt transition (Regattieri et al., 2014; Li et al., 2021) whereas the southern Italian pollen and isotopes records do not reveal significant changes (Sicre et al., 2013; Combourieu-Nebout et al., 2013; Desprat et al., 2013).

The YD is characterized by cold conditions in the Northern Hemisphere from 12,900 to 11,700 cal BP (Rasmussen et al., 2014). As previously mentioned for the B/A, several studies (Renssen and Isarin, 2001; Heiri et al., 2014; Moreno et al., 2014) suggest that temperatures during the YD are less contrasted in the South of Europe in comparison with the North. In Italy as a whole (Fig. 9), a decline in temperatures is recorded in all records.

At Matese, a decrease of temperatures is evidenced by the pollen-based reconstructions, but it is less clear from the brGDGT-based reconstructions. The difference of climate signals may be related to different sources between both proxies. Pollen record local, extra-local and regional vegetation (Jacobson and Bradshaw, 1981). The basin size of the Lake Matese is larger than 5 hectares, which suggest a signal of regional vegetation rather than local (Jacobson and Bradshaw, 1981). Moreover, the YD is marked by a large proportion of herbaceous taxa (Fig. 4) and favors the catching of regional pollen (Jacobson and Bradshaw, 1981). By contrast, brGDGTs are produced in the lake or in the catchment area (Russell et al., 2018; Martin et al., 2019) and thus are local contributors. Moreover, the YD is characterized by high erosion rates in the catchment (Fig. 4), which could favor greater soil-derived brGDGTs and induce a warm bias in temperatures (Martínez-Sosa et al., 2021). Indeed, the distribution of brGDGTs differ according to sample type and could differ between lake sediments and catchment soils (Loomis et al., 2011, 2014; Buckles et al., 2014; Russell et al., 2018; Martin et al., 2019; Martínez-Sosa et al., 2021; Raberg et al., 2022). Soil sediments generally exhibit less hexamethylated brGDGTs and more tetramethylated brGDGTs than lake sediments (Loomis et al., 2011, 2014; Buckles et al., 2014; Russell et al., 2018; Martin et al., 2019; Martínez-Sosa et al., 2021). However, an increase of tetramethylated brGDGTs is mainly associated with an increase in temperatures in soils and lake sediments (Russell et al., 2018). At Matese, the YD is characterized by a decrease in hexamethylated brGDGTs and a slight increase in

tetramethylated brGDGTs. These differences may have affected the annual temperature reconstructions by inducing a warm bias in temperatures during the YD. Furthermore, soil-derived brGDGTs may also be affected by changes in pH, moisture, soil compounds and vegetation in the catchment of Lake Matese (Davtian et al., 2016; Martin et al., 2019; Liang et al., 2019; Dugerdil et al., 2021a). Furthermore soil samples without vegetation cover are more sensitive to seasonal changes than that of soil samples with grass and forest cover (Liang et al., 2019). Therefore, soils with vegetation cover allow a better reconstruction of global temperatures (Liang et al., 2019). Since at Matese, the YD is characterized by an open vegetation, soil-derived brGDGTs could also have been affected by seasonal temperature changes due to a sparse vegetation and this effect is superimposed to changes in the sources of brGDGTs in lake sediments.

Contrasted patterns are also recorded at Monticchio (Fig. 9I) by the three different climate variables used for pollen-based temperature reconstructions: a decrease in winter temperature is reconstructed for two lake cores, while a fen core external to the lake, which should record the local vegetation signal, does not reveal the temperature decline during the YD (Allen et al., 2002). However, the two other cores clearly show a temperature decrease, that is why we consider a winter temperature decrease during the YD at Monticchio. In Southern Italian records, temperature reconstructions based on alkenones, foraminifera and pollen (Sbaffi et al., 2004; Desprat et al., 2013; Sicre et al., 2013) show a shorter YD than in the north. For alkenones-based reconstructions, even an increase of temperatures is recorded at the end of the YD. In continental records of South Italy (Allen et al., 2002), this trend is only recorded at Monticchio (one core only) and does not appear at Matese. Nonetheless, this hypothesis is only based on marine records and should be investigated through continental records in Southern Italy.

In terms of precipitation, the marine sequences located south of latitude 42°N record a slight increase for proxies based on pollen (Fig. 9GH; Combourieu-Nebout et al., 2013) and on $\delta^{18}O$ *G. bulloides* data (Fig. 9FI; Sicre et al., 2013) during the YD. However, no significant change occurs at Matese for PANN (Fig. 10D), and on the contrary a low decline is recorded for P_{winter} towards the end of the YD (Fig. 10E). Above latitude 42°N, a precipitation decrease during the YD is recorded by two sites at Hölloch and Corchia caves (Fig. 10BC; Regattieri et al., 2014; Li et al., 2021). According to the model outputs of Rea et al. (2020), drier conditions occurred in Northern Europe whereas wetter conditions prevailed in Southern Europe, mainly during winter and in the South of Italy, the Dinaric Alps and Northern Turkey. This pattern is

consistent with our reconstruction but the limit between the North and the South is closer to latitude 42°N.

The transition between the YD and the Holocene is recorded around 11,700 cal BP by Greenland ice-core records (Rasmussen et al., 2014). In Italy, an important increase of temperature is recorded in all records (Fig. 9) which appears earlier (700-400 years) in southern sites (Sbaffi et al., 2004; Sicre et al., 2013). In terms of precipitation, marine records south of latitude 42°N continue to record a slight increase of precipitation (Fig. 10F-I; Combourieu-Nebout et al., 2013; Sicre et al., 2013), and in northern sites an increase of precipitation is recorded (Fig. 10B-E; Regattieri et al., 2014; Li et al., 2021; this study).

5.4 Atmospheric processes during the Lateglacial in central Mediterranean

According to several studies, climate changes during the Lateglacial show differences in temperatures between Southern and Central Europe (Heiri et al., 2014; Moreno et al., 2014; Renssen and Isarin, 2001). In Italy (Fig. 9), climate reconstructions do not show latitudinal differences in terms of temperature. The B/A is marked by warm conditions and the YD by cold conditions even in Southern Italy. Climate reconstructions for East-Central Southern Europe from Heiri et al. (2014) are not consistent with our results probably because while two of their chironomid records are located in North Italy and one in Bulgaria none consider Southern Italy. In the study of Moreno et al. (2014), only the record of Monticchio is used for the South of Italy during the Lateglacial, which may explain the differences in our study. Considering precipitation, several studies suggest no significant changes during the B/A but drier conditions in Northern Europe and wetter conditions in Southern Europe during the YD. In Italy (Fig. 10), we observe the same dynamics during the B/A and the YD.

Several studies (Renssen and Isarin, 2001; Moreno et al., 2014; Rea et al., 2020) explain that during cold periods of the Lateglacial (OD, YD) the Polar Frontal JetStream moved southward with a weak Atlantic Meridional Overturning Circulation (AMOC) (Moreno et al., 2014; Rea et al., 2020; Renssen and Isarin, 2001). The incursion of cold air masses is recorded until the South of Italy, however, during the YD, dry conditions are not reconstructed for this region. According to Rea et al. (2020), a relocation of Atlantic storm tracks in the Mediterranean is induced by the Fennoscandian ice sheet and the North European Plain which created a topographic barrier and a high pressure region during the YD. The presence of Atlantic storm tracks into the Mediterranean could have favored wetter conditions in the South of Italy during the YD. Our study suggests a limit around latitude 42°N, with drier conditions in Northern Italy and slightly wetter conditions in Southern Italy during the YD. A latitude limit at 40°N was

previously discussed by Magny et al. (2013) for the Holocene. These echoing limits over time in Italy inevitably reinforce Italy's key position to archive proxies catching atmospheric patterns.

By contrast, during the B/A, the North Atlantic sea-ice has a more northerly position inducing a northward shift of the Polar Frontal JetStream (Renssen and Isarin, 2001). The incursion of warm air masses is recorded in all of Italy, however, no significant changes in annual precipitation occur. Our study does not suggest the location of Atlantic storm tracks in Italy during the B/A, although at Matese winter precipitation was higher in most pollen-based climate reconstructions. However, very few records and climatic models reconstructing precipitation are available in Europe and the Mediterranean region for this period. Further investigations are necessary to fully understand the atmospheric processes and precipitation dynamic in Europe, mainly during the B/A.

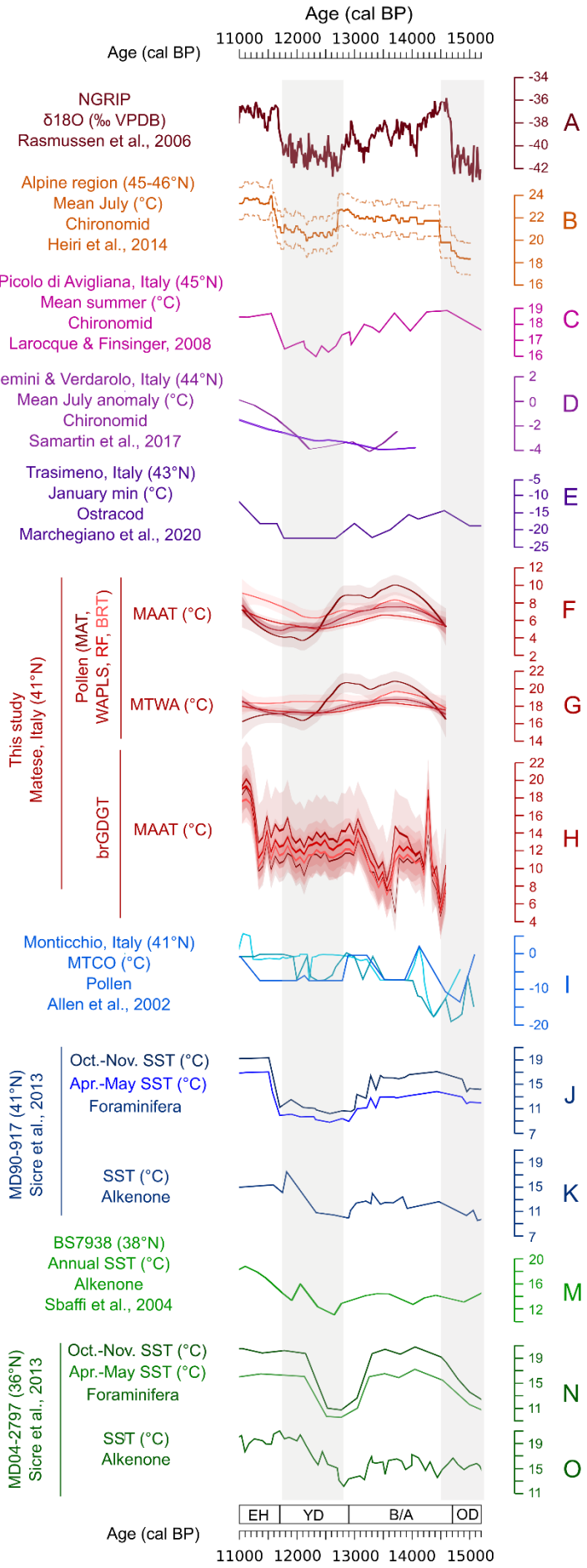
Age (cal BP)
11000 12000 13000 14000 15000
NGRIP
δ18O (‰ VPDB)
Rasmussen et al., 2006
-34
-36
-38
-40
-42
A
Alpine region (45-46°N)
Mean July (°C)
Chironomid
Heiri et al., 2014
24
22
20
18
16
B
Picolo di Avigliana, Italy (45°N)
Mean summer (°C)
Chironomid
Larocque & Finsinger, 2008
19
18
17
16
C
Gemini & Verdarolo, Italy (44°N)
Mean July anomaly (°C)
Chironomid
Samartin et al., 2017
2
0
-2
-4
D
Trasimeno, Italy (43°N)
January min (°C)
Ostracod
Marchegiano et al., 2020
-5
-10
-15
-20
-25
E
This study
Matese, Italy (41°N)
Pollen (MAT, WAPLS, RF, BRT)
MAAT (°C)
12
10
8
6
4
2
F
MTWA (°C)
22
20
18
16
14
G
brGDGT
MAAT (°C)
22
20
18
16
14
12
10
8
6
4
H
Monticchio, Italy (41°N)
MTCO (°C)
Pollen
Allen et al., 2002
0
-10
-20
I
MD90-917 (41°N)
Sicre et al., 2013
Oct.-Nov. SST (°C)
Apr.-May SST (°C)
Foraminifera
19
15
11
7
J
SST (°C)
Alkenone
19
15
11
7
K
BS7938 (38°N)
Annual SST (°C)
Alkenone
Sbaffi et al., 2004
20
16
12
M
MD04-2797 (36°N)
Sicre et al., 2013
Oct.-Nov. SST (°C)
Apr.-May SST (°C)
Foraminifera
19
15
11
N
SST (°C)
Alkenone
19
15
11
O
EH
YD
B/A
OD
Age (cal BP)
11000 12000 13000 14000 15000

Figure III-9. Synthesis of temperature records inferred from different proxies in Italy from 15,000 to 11,000 cal BP and comparison with the NGRIP ice core record. MAAT: mean annual air temperature. MTWA: mean temperature of the warmest month. MTCO: mean temperature of the coldest month. OD: Oldest Dryas. B/A: Bølling–Allerød. YD: Younger Dryas. EH: Early Holocene.

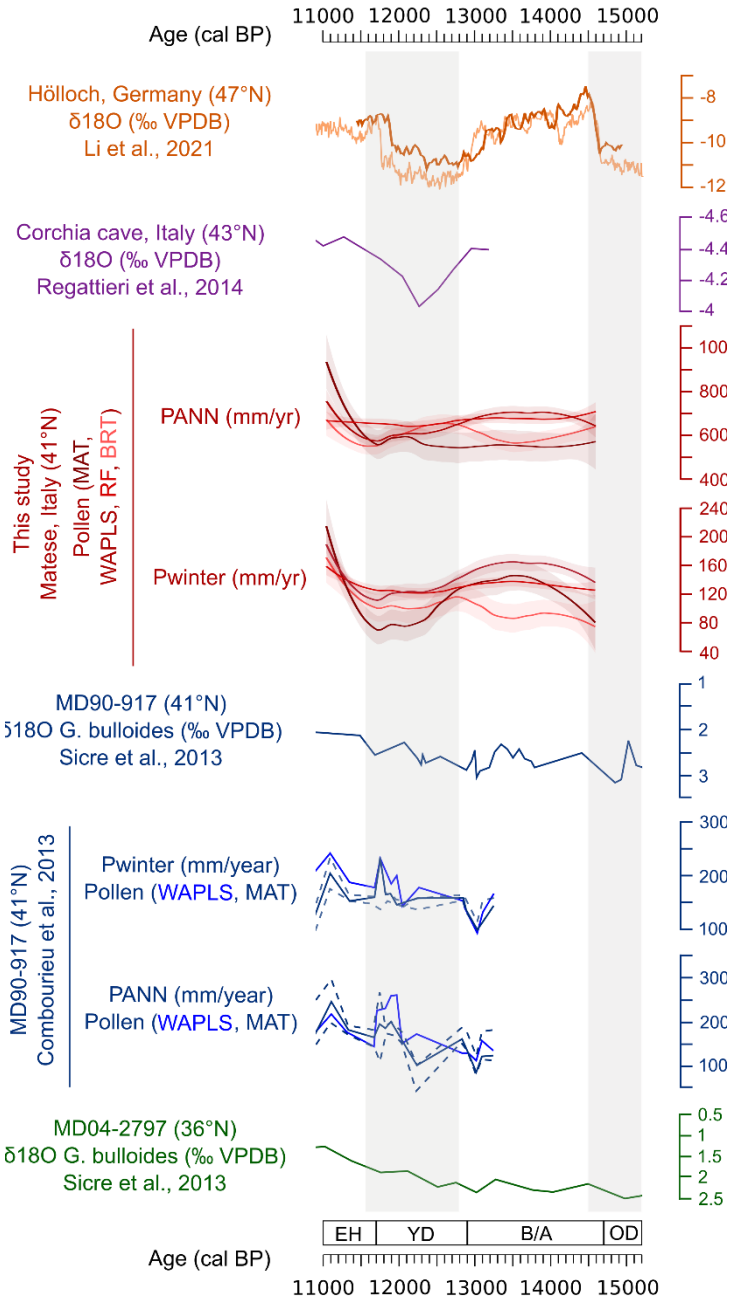

Figure III-10. Synthesis of precipitation records inferred from different proxies in Italy 15,000 to 11,000 cal BP. PANN: mean annual precipitation. P_{winter}: winter precipitation. OD: Oldest Dryas. B/A: Bølling–Allerød. YD: Younger Dryas. EH: Early Holocene.

6. Conclusions

This study provides a quantitative climate reconstruction for the Lateglacial period in Central-Southern Europe, inferred from a multi-proxy and multi-method approach based on the Lake Matese record. The comparison of the Lake Matese climate reconstructions based on brGDGTs and pollen and their comparison with regional terrestrial/marine climate reconstructions show the following:

- For the first time, pollen and brGDGTs were combined to reconstruct climate changes in the Mediterranean region during the Lateglacial. Temperature trends reconstructed with these proxies are consistent except during the YD. Both proxies show a marked cold OD, an increase of temperatures during the B/A, and an abrupt transition to warmer conditions for the Holocene. During the YD, pollen-based reconstructions show a decrease of temperatures, whereas brGDGT-based reconstructions show no significant changes.
- Comparison with regional climate records of Italy reveals that there are no latitudinal differences during the B/A and the YD in terms of temperatures. The B/A is marked by an increase of temperature and the YD is characterized by cold conditions in all Italy. By contrast, precipitation does not show changes during the B/A, and a slight increase of precipitation during the YD is recorded in Southern Italy below latitude 42°N.
- Cold conditions during the YD in Italy may be linked to the southward position of North Atlantic sea-ice and of the Polar Frontal JetStream. The low increase of precipitation during the YD may be linked to relocation of Atlantic storm tracks into the Mediterranean, induced by the Fennoscandian ice sheet and the North European Plain. We identified the latitude 42°N as a limit between dry conditions in northern Italy and slightly wetter conditions in Southern Italy during the YD. By contrast, warm conditions during the B/A may be linked to the northward position of North Atlantic sea-ice and of the Polar Frontal JetStream.

In summary, this study allowed us to document and discuss past climate changes in Italy while contributing to the debate about the atmospheric processes in Southern Europe. The latitudes 40-42°N appear as a key junction point between wetter conditions in Southern Italy and drier conditions in Northern Italy during the YD but also during the Early-Mid Holocene (Magny et al., 2013). However, further robust paleoclimate studies are needed to provide 1) high-resolution reconstructions based on several proxies in Northern Italy, 2) new records for

central Italy (between 41-43°N), 3) new continental records for Southern Italy (below 41°N) and 4) more model outputs at regional scales with transient simulations, if possible, mainly during the B/A and the YD.

Author contribution

MR: Conceptualization, Field work, Laboratory work, Formal analysis, Writing draft manuscript, Review, Funding acquisition. SJ, OP and EB: Conceptualization, Field work, Supervision, Review, Funding acquisition. GM: Conceptualization, Supervision, Review, Funding acquisition. SW: Laboratory work, Formal analysis, Review, Funding acquisition. OA and MB: Laboratory work. BV: Supervision of laboratory work, Review. BP: Field work. SAA: Coordination of laboratory work. LC and SG: Conceptualization, Review. J-LB, LD and AC: Review.

Declaration of competing interest

The authors declare that they have no known competing financial interests or personal relationships that could have appeared to influence the work reported in this paper.

Funding

This research was co-founded by the International PhD course "Agriculture Technologies and Biotechnologies" (34° Cycle, Code: DOT1339335). Financial support for this study was provided by EFFICACE project from EC2CO INSU CNRS (PI: Odile Peyron) and ERJ ClimMatese from LabEx CeMEB (PI: Mary Robles). The travels between Italy and France were financed by VINCI founding of the Università Italo Francese (UIF). The conference funding was provided by the Association des Palynologues de Langue Française (APLF).

Acknowledgements

The authors would like to thank Julien Didier for magnetic susceptibility measurements, Laurent Bouby and Isabelle Figueral for seed and wood identifications used for radiocarbon dating. The authors would like to express their appreciation to Gwenaël Magne, Thierry Pastor and Benoît Brossier for logistical support during fieldwork, and Anne-Lise Develle and Claire Blanchet for help during XRF analysis. We would like to thank Sandrine Canal and Sylvie Rouland for support during pollen sample preparation. This is an ISEM contribution N° ISEM 2022-266.

References

Allen, J.R.M., Watts, W.A., McGee, E., Huntley, B., 2002. Holocene environmental variability-the record from Lago Grande di Monticchio, Italy. Quaternary International 88, 69–80.

Ammann, B., Birks, H.J.B., Brooks, S.J., Eicher, U., von Grafenstein, U., Hofmann, W., Lemdahl, G., Schwander, J., Tobolski, K., Wick, L., 2000. Quantification of biotic responses to rapid climatic changes around the Younger Dryas — a synthesis. Palaeogeography, Palaeoclimatology, Palaeoecology 159, 313–347. https://doi.org/10.1016/S0031-0182(00)00092-4

Aucelli, P.P.C., Cesarano, M., Di Paola, G., Filocamo, F., Rosskopf, C.M., 2013. Geomorphological map of the central sector of the Matese Mountains (Southern Italy): an example of complex landscape evolution in a Mediterranean mountain environment. Journal of Maps 9, 604–616. https://doi.org/10.1080/17445647.2013.840054

Barton, C.M., Aura Tortosa, J.E., Garcia-Puchol, O., Riel-Salvatore, J.G., Gauthier, N., Vadillo Conesa, M., Pothier Bouchard, G., 2018. Risk and resilience in the late glacial: A case study from the western Mediterranean. Quaternary Science Reviews 184, 68–84. https://doi.org/10.1016/j.quascirev.2017.09.015

Beug, H.-J., 2004. Leitfaden der Pollenbestimmung für Mitteleuropa und angrenzende Gebiete. Friedrich Pfeil, München.

Blaauw, M., 2010. Methods and code for 'classical' age-modelling of radiocarbon sequences. Quaternary Geochronology 5, 512–518. https://doi.org/10.1016/j.quageo.2010.01.002

Blaga, C.I., Reichart, G.-J., Lotter, A.F., Anselmetti, F.S., Sinninghe Damsté, J.S., 2013. A TEX 86 lake record suggests simultaneous shifts in temperature in Central Europe and Greenland during the last deglaciation: A SWISS TEX 86 LAKE RECORD. Geophys. Res. Lett. 40, 948–953. https://doi.org/10.1002/grl.50181

Breiman, L., 2001. Random Forests. Machine Learning 45, 5–32. https://doi.org/10.1023/A:1010933404324

Bronk Ramsey, C., Albert, P.G., Blockley, S.P.E., Hardiman, M., Housley, R.A., Lane, C.S., Lee, S., Matthews, I.P., Smith, V.C., Lowe, J.J., 2015. Improved age estimates for key Late Quaternary European tephra horizons in the RESET lattice. Quaternary Science Reviews 118, 18–32. https://doi.org/10.1016/j.quascirev.2014.11.007

Buckles, L.K., Weijers, J.W.H., Verschuren, D., Sinninghe Damsté, J.S., 2014. Sources of core and intact branched tetraether membrane lipids in the lacustrine environment: Anatomy of

Lake Challa and its catchment, equatorial East Africa. Geochimica et Cosmochimica Acta 140, 106–126. https://doi.org/10.1016/j.gca.2014.04.042

Carranza, M.L., Frate, L., Paura, B., 2012. Structure, ecology and plant richness patterns in fragmented beech forests. Plant Ecology & Diversity 5, 541–551. https://doi.org/10.1080/17550874.2012.740509

Castañeda, I.S., Schouten, S., 2011. A review of molecular organic proxies for examining modern and ancient lacustrine environments. Quaternary Science Reviews 30, 2851–2891. https://doi.org/10.1016/j.quascirev.2011.07.009

Chevalier, M., Davis, B.A.S., Heiri, O., Seppä, H., Chase, B.M., Gajewski, K., Lacourse, T., Telford, R.J., Finsinger, W., Guiot, J., Kühl, N., Maezumi, S.Y., Tipton, J.R., Carter, V.A., Brussel, T., Phelps, L.N., Dawson, A., Zanon, M., Vallé, F., Nolan, C., Mauri, A., de Vernal, A., Izumi, K., Holmström, L., Marsicek, J., Goring, S., Sommer, P.S., Chaput, M., Kupriyanov, D., 2020. Pollen-based climate reconstruction techniques for late Quaternary studies. Earth-Science Reviews 210, 103384. https://doi.org/10.1016/j.earscirev.2020.103384

Combourieu-Nebout, N., Peyron, O., Bout-Roumazeilles, V., Goring, S., Dormoy, I., Joannin, S., Sadori, L., Siani, G., Magny, M., 2013. Holocene vegetation and climate changes in the central Mediterranean inferred from a high-resolution marine pollen record (Adriatic Sea). Clim. Past 9, 2023–2042. https://doi.org/10.5194/cp-9-2023-2013

Coope, G.R., Lemdahl, G., 1995. Regional differences in the Lateglacial climate of northern Europe based on coleopteran analysis. Journal of Quaternary Science 10, 391–395. https://doi.org/10.1002/jqs.3390100409

Davtian, N., Bard, E., Ménot, G., Fagault, Y., 2018. The importance of mass accuracy in selected ion monitoring analysis of branched and isoprenoid tetraethers. Organic Geochemistry 118, 58–62. https://doi.org/10.1016/j.orggeochem.2018.01.007

Davtian, N., Ménot, G., Bard, E., Poulenard, J., Podwojewski, P., 2016. Consideration of soil types for the calibration of molecular proxies for soil pH and temperature using global soil datasets and Vietnamese soil profiles. Organic Geochemistry 101, 140–153. https://doi.org/10.1016/j.orggeochem.2016.09.002

De Beaulieu, J.-L., Brugiapaglia, E., Joannin, S., Guiter, F., Zanchetta, G., Wulf, S., Peyron, O., Bernardo, L., Didier, J., Stock, A., Rius, D., Magny, M., 2017. Lateglacial-Holocene abrupt vegetation changes at Lago Trifoglietti in Calabria, Southern Italy: The setting of ecosystems in a refugial zone. Quaternary Science Reviews 158, 44–57. https://doi.org/10.1016/j.quascirev.2016.12.013

De Jonge, C., Stadnitskaia, A., Hopmans, E.C., Cherkashov, G., Fedotov, A., Sinninghe Damsté, J.S., 2014. In situ produced branched glycerol dialkyl glycerol tetraethers in suspended particulate matter from the Yenisei River, Eastern Siberia. Geochimica et Cosmochimica Acta 125, 476–491. https://doi.org/10.1016/j.gca.2013.10.031

Dearing Crampton-Flood, E., Tierney, J.E., Peterse, F., Kirkels, F.M.S.A., Sinninghe Damsté, J.S., 2020. BayMBT: A Bayesian calibration model for branched glycerol dialkyl glycerol tetraethers in soils and peats. Geochimica et Cosmochimica Acta 268, 142–159. https://doi.org/10.1016/j.gca.2019.09.043

De'ath, G., 2007. Boosted trees for ecological modeling and prediction. Ecology 88, 243–251. https://doi.org/10.1890/0012-9658(2007)88[243:BTFEMA]2.0.CO;2

Desprat, S., Combourieu-Nebout, N., Essallami, L., Sicre, M.A., Dormoy, I., Peyron, O., Siani, G., Bout Roumazeilles, V., Turon, J.L., 2013. Deglacial and Holocene vegetation and climatic changes in the southern Central Mediterranean from a direct land–sea correlation. Clim. Past 9, 767–787. https://doi.org/10.5194/cp-9-767-2013

Ding, S., Schwab, V.F., Ueberschaar, N., Roth, V.-N., Lange, M., Xu, Y., Gleixner, G., Pohnert, G., 2016. Identification of novel 7-methyl and cyclopentanyl branched glycerol dialkyl glycerol tetraethers in lake sediments. Organic Geochemistry 102, 52–58. https://doi.org/10.1016/j.orggeochem.2016.09.009

Drescher-Schneider, R., de Beaulieu, J.-L., Magny, M., Walter-Simonnet, A.-V., Bossuet, G., Millet, L., Brugiapaglia, E., Drescher, A., 2007. Vegetation history, climate and human impact over the last 15,000 years at Lago dell'Accesa (Tuscany, Central Italy). Veget Hist Archaeobot 16, 279–299. https://doi.org/10.1007/s00334-006-0089-z

Dugerdil, L., Joannin, S., Peyron, O., Jouffroy-Bapicot, I., Vannière, B., Boldgiv, B., Unkelbach, J., Behling, H., Ménot, G., 2021a. Climate reconstructions based on GDGT and pollen surface datasets from Mongolia and Baikal area: calibrations and applicability to extremely cold–dry environments over the Late Holocene. Clim. Past 17, 1199–1226. https://doi.org/10.5194/cp-17-1199-2021

Dugerdil, L., Ménot, G., Peyron, O., Jouffroy-Bapicot, I., Ansanay-Alex, S., Antheaume, I., Behling, H., Boldgiv, B., Develle, A.-L., Grossi, V., Magail, J., Makou, M., Robles, M., Unkelbach, J., Vannière, B., Joannin, S., 2021b. Late Holocene Mongolian climate and environment reconstructions from brGDGTs, NPPs and pollen transfer functions for Lake Ayrag: Paleoclimate implications for Arid Central Asia. Quaternary Science Reviews 273, 107235. https://doi.org/10.1016/j.quascirev.2021.107235

Duprat-Oualid, F., Bégeot, C., Peyron, O., Rius, D., Millet, L., Magny, M., 2022. High-frequency vegetation and climatic changes during the Lateglacial inferred from the Lapsou pollen record (Cantal, southern Massif Central, France). Quaternary International S1040618222001537. https://doi.org/10.1016/j.quaint.2022.04.012

Elith, J., Leathwick, J.R., Hastie, T., 2008. A working guide to boosted regression trees. J Anim Ecology 77, 802–813. https://doi.org/10.1111/j.1365-2656.2008.01390.x

Faegri, K., Kaland, P.E., Krzywinski, K., 1989. Textbook of pollen analysis. John Wiley & Sons, Chichester.

Ferranti, L., Milano, G., Burrato, P., Palano, M., Cannavò, F., 2015. The seismogenic structure of the 2013–2014 Matese seismic sequence, Southern Italy: implication for the geometry of the Apennines active extensional belt. Geophysical Journal International 201, 823–837. https://doi.org/10.1093/gji/ggv053

Ferrarini, F., Boncio, P., de Nardis, R., Pappone, G., Cesarano, M., Aucelli, P.P.C., Lavecchia, G., 2017. Segmentation pattern and structural complexities in seismogenic extensional settings: The North Matese Fault System (Central Italy). Journal of Structural Geology 95, 93–112. https://doi.org/10.1016/j.jsg.2016.11.006

Finsinger, W., Heiri, O., Valsecchi, V., Tinner, W., Lotter, A.F., 2007. Modern pollen assemblages as climate indicators in southern Europe. Global Ecology and Biogeography 16, 567–582. https://doi.org/10.1111/j.1466-8238.2007.00313.x

Fiorillo, F., Doglioni, A., 2010. The relation between karst spring discharge and rainfall by cross-correlation analysis (Campania, southern Italy). Hydrogeol J 18, 1881–1895. https://doi.org/10.1007/s10040-010-0666-1

Fiorillo, F., Pagnozzi, M., 2015. Recharge processes of Matese karst massif (southern Italy). Environ Earth Sci 74, 7557–7570. https://doi.org/10.1007/s12665-015-4678-y

Galli, P., Giaccio, B., Messina, P., Peronace, E., Amato, V., Naso, G., Nomade, S., Pereira, A., Piscitelli, S., Bellanova, J., Billi, A., Blamart, D., Galderisi, A., Giocoli, A., Stabile, T., Thil, F., 2017. Middle to Late Pleistocene activity of the northern Matese fault system (southern Apennines, Italy). Tectonophysics 699, 61–81. https://doi.org/10.1016/j.tecto.2017.01.007

Gandouin, E., Rioual, P., Pailles, C., Brooks, S.J., Ponel, P., Guiter, F., Djamali, M., Andrieu-Ponel, V., Birks, H.J.B., Leydet, M., Belkacem, D., Haas, J.N., Van der Putten, N., de Beaulieu, J.L., 2016. Environmental and climate reconstruction of the late-glacial-Holocene transition from a lake sediment sequence in Aubrac, French Massif Central:

Chironomid and diatom evidence. Palaeogeography, Palaeoclimatology, Palaeoecology 461, 292–309. https://doi.org/10.1016/j.palaeo.2016.08.039

Guarino, R., Bazan, G., Paura, B., 2015. Downy-Oak Woods of Italy: Phytogeographical Remarks on a Controversial Taxonomic and Ecologic Issue, in: Box, E.O., Fujiwara, K. (Eds.), Warm-Temperate Deciduous Forests around the Northern Hemisphere, Geobotany Studies. Springer International Publishing, Cham, pp. 139–151. https://doi.org/10.1007/978-3-319-01261-2_7

Guiot, J., 1990. Methodology of the last climatic cycle reconstruction in France from pollen data. Palaeogeography, Palaeoclimatology, Palaeoecology, Methods for the Study of Stratigraphical Records 80, 49–69. https://doi.org/10.1016/0031-0182(90)90033-4

Guiot, J., de Beaulieu, J.L., Cheddadi, R., David, F., Ponel, P., Reille, M., 1993. The climate in Western Europe during the last Glacial/Interglacial cycle derived from pollen and insect remains. Palaeogeography, Palaeoclimatology, Palaeoecology 103, 73–93. https://doi.org/10.1016/0031-0182(93)90053-L

Heiri, O., Brooks, S.J., Renssen, H., Bedford, A., Hazekamp, M., Ilyashuk, B., Jeffers, E.S., Lang, B., Kirilova, E., Kuiper, S., Millet, L., Samartin, S., Toth, M., Verbruggen, F., Watson, J.E., van Asch, N., Lammertsma, E., Amon, L., Birks, H.H., Birks, H.J.B., Mortensen, M.F., Hoek, W.Z., Magyari, E., Muñoz Sobrino, C., Seppä, H., Tinner, W., Tonkov, S., Veski, S., Lotter, A.F., 2014. Validation of climate model-inferred regional temperature change for late-glacial Europe. Nat Commun 5, 4914. https://doi.org/10.1038/ncomms5914

Heiri, O., Ilyashuk, B., Millet, L., Samartin, S., Lotter, A.F., 2015. Stacking of discontinuous regional palaeoclimate records: Chironomid-based summer temperatures from the Alpine region. The Holocene 25, 137–149. https://doi.org/10.1177/0959683614556382

Hepp, J., Wüthrich, L., Bromm, T., Bliedtner, M., Schäfer, I.K., Glaser, B., Rozanski, K., Sirocko, F., Zech, R., Zech, M., 2019. How dry was the Younger Dryas? Evidence from a coupled δ2H–δ18O biomarker paleohygrometer applied to the Gemündener Maar sediments, Western Eifel, Germany. Climate of the Past 15, 713–733. https://doi.org/10.5194/cp-15-713-2019

Hijmans, R.J., Phillips, S., Elith, J.L. and J., 2021. dismo: Species Distribution Modeling.

Hopmans, E.C., Schouten, S., Sinninghe Damsté, J.S., 2016. The effect of improved chromatography on GDGT-based palaeoproxies. Organic Geochemistry 93, 1–6. https://doi.org/10.1016/j.orggeochem.2015.12.006

Huguet, C., Hopmans, E.C., Febo-Ayala, W., Thompson, D.H., Sinninghe Damsté, J.S., Schouten, S., 2006. An improved method to determine the absolute abundance of glycerol dibiphytanyl glycerol tetraether lipids. Organic Geochemistry 37, 1036–1041. https://doi.org/10.1016/j.orggeochem.2006.05.008

Hunt, J.B., Hill, P.G., 1996. An inter-laboratory comparison of the electron probe microanalysis of glass geochemistry. Quaternary International 34–36, 229–241. https://doi.org/10.1016/1040-6182(95)00088-7

Jacobson, G.L., Bradshaw, R.H.W., 1981. The Selection of Sites for Paleovegetational Studies. Quat. res. 16, 80–96. https://doi.org/10.1016/0033-5894(81)90129-0

Joannin, S., Brugiapaglia, E., Vanniere, B., 2012. Pollen-based reconstruction of Holocene vegetation and climate in southern Italy: the case of Lago Trifoglietti. Clim. Past 24.

Jochum, K.P., Stoll, B., Herwig, K., Willbold, M., Hofmann, A.W., Amini, M., Aarburg, S., Abouchami, W., Hellebrand, E., Mocek, B., Raczek, I., Stracke, A., Alard, O., Bouman, C., Becker, S., Dücking, M., Brätz, H., Klemd, R., de Bruin, D., Canil, D., Cornell, D., de Hoog, C.-J., Dalpé, C., Danyushevsky, L., Eisenhauer, A., Gao, Y., Snow, J.E., Groschopf, N., Günther, D., Latkoczy, C., Guillong, M., Hauri, E.H., Höfer, H.E., Lahaye, Y., Horz, K., Jacob, D.E., Kasemann, S.A., Kent, A.J.R., Ludwig, T., Zack, T., Mason, P.R.D., Meixner, A., Rosner, M., Misawa, K., Nash, B.P., Pfänder, J., Premo, W.R., Sun, W.D., Tiepolo, M., Vannucci, R., Vennemann, T., Wayne, D., Woodhead, J.D., 2006. MPI-DING reference glasses for in situ microanalysis: New reference values for element concentrations and isotope ratios: MPI-DING REFERENCE GLASSES. Geochem. Geophys. Geosyst. 7, n/a-n/a. https://doi.org/10.1029/2005GC001060

Juggins, S., Juggins, M.S., 2020. Package 'rioja.'

Kuehn, S.C., Froese, D.G., Shane, P.A.R., 2011. The INTAV intercomparison of electron-beam microanalysis of glass by tephrochronology laboratories: Results and recommendations. Quaternary International, Enhancing tephrochronology and its application (INTREPID Project): Hiroshi Machida commemorative volume 246, 19–47. https://doi.org/10.1016/j.quaint.2011.08.022

Larocque, I., Finsinger, W., 2008. Late-glacial chironomid-based temperature reconstructions for Lago Piccolo di Avigliana in the southwestern Alps (Italy). Palaeogeography, Palaeoclimatology, Palaeoecology 257, 207–223. https://doi.org/10.1016/j.palaeo.2007.10.021

Li, H., Spötl, C., Cheng, H., 2021. A high-resolution speleothem proxy record of the Late Glacial in the European Alps: extending the NALPS19 record until the beginning of the Holocene. J. Quaternary Sci 36, 29–39. https://doi.org/10.1002/jqs.3255

Liang, J., Russell, J.M., Xie, H., Lupien, R.L., Si, G., Wang, J., Hou, J., Zhang, G., 2019. Vegetation effects on temperature calibrations of branched glycerol dialkyl glycerol tetraether (brGDGTs) in soils. Organic Geochemistry 127, 1–11. https://doi.org/10.1016/j.orggeochem.2018.10.010

Liaw, A., Wiener, M., 2002. Classification and Regression by randomForest 2, 5.

Loomis, S.E., Russell, J.M., Heureux, A.M., D'Andrea, W.J., Sinninghe Damsté, J.S., 2014. Seasonal variability of branched glycerol dialkyl glycerol tetraethers (brGDGTs) in a temperate lake system. Geochimica et Cosmochimica Acta 144, 173–187. https://doi.org/10.1016/j.gca.2014.08.027

Loomis, S.E., Russell, J.M., Sinninghe Damsté, J.S., 2011. Distributions of branched GDGTs in soils and lake sediments from western Uganda: Implications for a lacustrine paleothermometer. Organic Geochemistry 42, 739–751. https://doi.org/10.1016/j.orggeochem.2011.06.004

Lotter, A.F., Heiri, O., Brooks, S., van Leeuwen, J.F.N., Eicher, U., Ammann, B., 2012. Rapid summer temperature changes during Termination 1a: high-resolution multi-proxy climate reconstructions from Gerzensee (Switzerland). Quaternary Science Reviews, The INTegration of Ice core, Marine and TErrestrial records of the last termination (INTIMATE) 60,000 to 8000 BP 36, 103–113. https://doi.org/10.1016/j.quascirev.2010.06.022

Magny, M., Combourieu-Nebout, N., de Beaulieu, J.-L., Bout-Roumazeilles, V., Colombaroli, D., Desprat, S., Francke, A., Joannin, S., Ortu, E., Peyron, O., Revel, M., Sadori, L., Siani, G., Sicre, M.A., Samartin, S., Simonneau, A., Tinner, W., Vanniere, B., Wagner, B., Zanchetta, G., Anselmetti, F., Brugiapaglia, E., Chapron, E., Debret, M., Didier, J., Essallami, L., Galop, D., Gilli, A., Kallel, N., Millet, L., Stock, A., Turon, J.L., Wirth, S., 2013. North-south palaeohydrological contrasts in the central Mediterranean during the Holocene: tentative synthesis and working hypotheses. Clim. Past 30.

Marchegiano, M., Horne, D.J., Gliozzi, E., Francke, A., Wagner, B., Ariztegui, D., 2020. Rapid Late Pleistocene climate change reconstructed from a lacustrine ostracod record in central Italy (Lake Trasimeno, Umbria). Boreas 49, 739–750. https://doi.org/10.1111/bor.12450

Martin, C., Ménot, G., Thouveny, N., Davtian, N., Andrieu-Ponel, V., Reille, M., Bard, E., 2019. Impact of human activities and vegetation changes on the tetraether sources in Lake St Front (Massif Central, France). Organic Geochemistry 135, 38–52.

Martin, C., Ménot, G., Thouveny, N., Peyron, O., Andrieu-Ponel, V., Montade, V., Davtian, N., Reille, M., Bard, E., 2020. Early Holocene Thermal Maximum recorded by branched tetraethers and pollen in Western Europe (Massif Central, France). Quaternary Science Reviews 228, 106109. https://doi.org/10.1016/j.quascirev.2019.106109

Martínez-Sosa, P., Tierney, J.E., Stefanescu, I.C., Dearing Crampton-Flood, E., Shuman, B.N., Routson, C., 2021. A global Bayesian temperature calibration for lacustrine brGDGTs. Geochimica et Cosmochimica Acta 305, 87–105. https://doi.org/10.1016/j.gca.2021.04.038

Max, L., Lembke-Jene, L., Zou, J., Shi, X., Tiedemann, R., 2020. Evaluation of reconstructed sea surface temperatures based on U37k′ from sediment surface samples of the North Pacific. Quaternary Science Reviews 243, 106496. https://doi.org/10.1016/j.quascirev.2020.106496

Mercuri, A.M., Accorsi, C.A., Bandini Mazzanti, M., 2002. The long history of Cannabis and its cultivation by the Romans in central Italy, shown by pollen records from Lago Albano and Lago di Nemi. Veget Hist Archaeobot 11, 263–276. https://doi.org/10.1007/s003340200039

Millet, L., Rius, D., Galop, D., Heiri, O., Brooks, S.J., 2012. Chironomid-based reconstruction of Lateglacial summer temperatures from the Ech palaeolake record (French western Pyrenees). Palaeogeography, Palaeoclimatology, Palaeoecology 315–316, 86–99. https://doi.org/10.1016/j.palaeo.2011.11.014

Moore, P.D., Webb, J.A., Collinson, M.E., 1991. Pollen Analysis, Subsequent edition. ed. Blackwell Science Inc, Oxford.

Moreno, A., Svensson, A., Brooks, S.J., Connor, S., Engels, S., Fletcher, W., Genty, D., Heiri, O., Labuhn, I., Perşoiu, A., Peyron, O., Sadori, L., Valero-Garcés, B., Wulf, S., Zanchetta, G., 2014. A compilation of Western European terrestrial records 60–8 ka BP: towards an understanding of latitudinal climatic gradients. Quaternary Science Reviews 106, 167–185. https://doi.org/10.1016/j.quascirev.2014.06.030

Naafs, B.D.A., Gallego-Sala, A.V., Inglis, G.N., Pancost, R.D., 2017a. Refining the global branched glycerol dialkyl glycerol tetraether (brGDGT) soil temperature calibration. Organic Geochemistry 106, 48–56. https://doi.org/10.1016/j.orggeochem.2017.01.009

Naafs, B.D.A., Inglis, G.N., Zheng, Y., Amesbury, M.J., Biester, H., Bindler, R., Blewett, J., Burrows, M.A., del Castillo Torres, D., Chambers, F.M., Cohen, A.D., Evershed, R.P., Feakins, S.J., Gałka, M., Gallego-Sala, A., Gandois, L., Gray, D.M., Hatcher, P.G., Honorio Coronado, E.N., Hughes, P.D.M., Huguet, A., Könönen, M., Laggoun-Défarge, F., Lähteenoja, O., Lamentowicz, M., Marchant, R., McClymont, E., Pontevedra-Pombal, X., Ponton, C., Pourmand, A., Rizzuti, A.M., Rochefort, L., Schellekens, J., De Vleeschouwer, F., Pancost, R.D., 2017b. Introducing global peat-specific temperature and pH calibrations based on brGDGT bacterial lipids. Geochimica et Cosmochimica Acta 208, 285–301. https://doi.org/10.1016/j.gca.2017.01.038

Panagiotopoulos, K., Holtvoeth, J., Kouli, K., Marinova, E., Francke, A., Cvetkoska, A., Jovanovska, E., Lacey, J.H., Lyons, E.T., Buckel, C., Bertini, A., Donders, T., Just, J., Leicher, N., Leng, M.J., Melles, M., Pancost, R.D., Sadori, L., Tauber, P., Vogel, H., Wagner, B., Wilke, T., 2020. Insights into the evolution of the young Lake Ohrid ecosystem and vegetation succession from a southern European refugium during the Early Pleistocene. Quaternary Science Reviews 227, 106044. https://doi.org/10.1016/j.quascirev.2019.106044

Peyron, O., Bégeot, C., Brewer, S., Heiri, O., Magny, M., Millet, L., Ruffaldi, P., Van Campo, E., Yu, G., 2005. Late-Glacial climatic changes in Eastern France (Lake Lautrey) from pollen, lake-levels, and chironomids. Quat. res. 64, 197–211. https://doi.org/10.1016/j.yqres.2005.01.006

Peyron, O., Combourieu-Nebout, N., Brayshaw, D., Goring, S., Andrieu-Ponel, V., Desprat, S., Fletcher, W., Gambin, B., Ioakim, C., Joannin, S., Kotthoff, U., Kouli, K., Montade, V., Pross, J., Sadori, L., Magny, M., 2017. Precipitation changes in the Mediterranean basin during the Holocene from terrestrial and marine pollen records: a model–data comparison. Clim. Past 13, 249–265. https://doi.org/10.5194/cp-13-249-2017

Peyron, O., Goring, S., Dormoy, I., Kotthoff, U., Pross, J., de Beaulieu, J.-L., Drescher-Schneider, R., Vannière, B., Magny, M., 2011. Holocene seasonality changes in the central Mediterranean region reconstructed from the pollen sequences of Lake Accesa (Italy) and Tenaghi Philippon (Greece). The Holocene 21, 131–146. https://doi.org/10.1177/0959683610384162

Peyron, O., Guiot, J., Cheddadi, R., Tarasov, P., Reille, M., de Beaulieu, J.-L., Bottema, S., Andrieu, V., 1998. Climatic Reconstruction in Europe for 18,000 YR B.P. from Pollen Data. Quat. res. 49, 183–196. https://doi.org/10.1006/qres.1997.1961

Peyron, O., Magny, M., Goring, S., Joannin, S., de Beaulieu, J.-L., Brugiapaglia, E., Sadori, L., Garfi, G., Kouli, K., Ioakim, C., Combourieu-Nebout, N., 2013. Contrasting patterns of climatic changes during the Holocene across the Italian Peninsula reconstructed from pollen data. Clim. Past 9, 1233–1252. https://doi.org/10.5194/cp-9-1233-2013

Ponel, P., Guiter, F., Gandouin, E., Peyron, O., de Beaulieu, J.-L., 2022. Late-Glacial palaeotemperatures and palaeoprecipitations in the Aubrac Mountains (French Massif Central) reconstructed from multiproxy analyses (Coleoptera, chironomids and pollen). Quaternary International. https://doi.org/10.1016/j.quaint.2022.02.005

Prasad, A.M., Iverson, L.R., Liaw, A., 2006. Newer Classification and Regression Tree Techniques: Bagging and Random Forests for Ecological Prediction. Ecosystems 9, 181–199. https://doi.org/10.1007/s10021-005-0054-1

Prentice, C., Guiot, J., Huntley, B., Jolly, D., Cheddadi, R., 1996. Reconstructing biomes from palaeoecological data: a general method and its application to European pollen data at 0 and 6 ka. Climate Dynamics 12, 185–194. https://doi.org/10.1007/BF00211617

Raberg, J.H., Flores, E., Crump, S.E., de Wet, G., Dildar, N., Miller, G.H., Geirsdóttir, Á., Sepúlveda, J., 2022. Intact Polar brGDGTs in Arctic Lake Catchments: Implications for Lipid Sources and Paleoclimate Applications. Journal of Geophysical Research: Biogeosciences 127, e2022JG006969. https://doi.org/10.1029/2022JG006969

Raberg, J.H., Harning, D.J., Crump, S.E., de Wet, G., Blumm, A., Kopf, S., Geirsdóttir, Á., Miller, G.H., Sepúlveda, J., 2021. Revised fractional abundances and warm-season temperatures substantially improve brGDGT calibrations in lake sediments. Biogeosciences 18, 3579–3603. https://doi.org/10.5194/bg-2021-16

Ramos-Román, M.J., De Jonge, C., Magyari, E., Veres, D., Ilvonen, L., Develle, A.-L., Seppä, H., 2022. Lipid biomarker (brGDGT)- and pollen-based reconstruction of temperature change during the Middle to Late Holocene transition in the Carpathians. Global and Planetary Change 215, 103859. https://doi.org/10.1016/j.gloplacha.2022.103859

Rasmussen, S.O., Bigler, M., Blockley, S.P., Blunier, T., Buchardt, S.L., Clausen, H.B., Cvijanovic, I., Dahl-Jensen, D., Johnsen, S.J., Fischer, H., Gkinis, V., Guillevic, M., Hoek, W.Z., Lowe, J.J., Pedro, J.B., Popp, T., Seierstad, I.K., Steffensen, J.P., Svensson, A.M., Vallelonga, P., Vinther, B.M., Walker, M.J.C., Wheatley, J.J., Winstrup, M., 2014. A stratigraphic framework for abrupt climatic changes during the Last Glacial period based on three synchronized Greenland ice-core records: refining and extending the INTIMATE event stratigraphy. Quaternary Science Reviews 106, 14–28. https://doi.org/10.1016/j.quascirev.2014.09.007

Rea, B.R., Pellitero, R., Spagnolo, M., Hughes, P., Ivy-Ochs, S., Renssen, H., Ribolini, A., Bakke, J., Lukas, S., Braithwaite, R.J., 2020. Atmospheric circulation over Europe during the Younger Dryas. Sci. Adv. 6, eaba4844. https://doi.org/10.1126/sciadv.aba4844

Regattieri, E., Zanchetta, G., Drysdale, R.N., Isola, I., Hellstrom, J.C., Dallai, L., 2014. Lateglacial to Holocene trace element record (Ba, Mg, Sr) from Corchia Cave (Apuan Alps, central Italy): paleoenvironmental implications: Trace element record from Corchia Cave, central Italy. J. Quaternary Sci. 29, 381–392. https://doi.org/10.1002/jqs.2712

Rehfeld, K., Münch, T., Ho, S.L., Laepple, T., 2018. Global patterns of declining temperature variability from the Last Glacial Maximum to the Holocene. Nature 554, 356–359. https://doi.org/10.1038/nature25454

Reille, M., 1998. Reille, Maurice, 1995. Pollen et spores d'Europe et d'Afrique du Nord, Supplément 1 . Éditions du Laboratoire de botanique historique et palynologie, Marseille, 327 p., 800 FF. / Reille, Maurice, 1998. Pollen et spores d'Europe et d'Afrique du Nord, Supplément 2 . Éditions du Laboratoire de botanique historique et palynologie, Marseille, 530 p., 1600 FF. gpq 52, 0–0. https://doi.org/10.7202/004885ar

Reimer, P.J., Austin, W.E.N., Bard, E., Bayliss, A., Blackwell, P.G., Ramsey, C.B., Butzin, M., Cheng, H., Edwards, R.L., Friedrich, M., Grootes, P.M., Guilderson, T.P., Hajdas, I., Heaton, T.J., Hogg, A.G., Hughen, K.A., Kromer, B., Manning, S.W., Muscheler, R., Palmer, J.G., Pearson, C., Plicht, J. van der, Reimer, R.W., Richards, D.A., Scott, E.M., Southon, J.R., Turney, C.S.M., Wacker, L., Adolphi, F., Büntgen, U., Capano, M., Fahrni, S.M., Fogtmann-Schulz, A., Friedrich, R., Köhler, P., Kudsk, S., Miyake, F., Olsen, J., Reinig, F., Sakamoto, M., Sookdeo, A., Talamo, S., 2020. The IntCal20 Northern Hemisphere Radiocarbon Age Calibration Curve (0–55 cal kBP). Radiocarbon 62, 725–757. https://doi.org/10.1017/RDC.2020.41

Renssen, H., Isarin, R.F.B., 2001. The two major warming phases of the last deglaciation at ~14.7 and ~11.5 ka cal BP in Europe: climate reconstructions and AGCM experiments. Global and Planetary Change 30, 117–153. https://doi.org/10.1016/S0921-8181(01)00082-0

Renssen, H., Mairesse, A., Goosse, H., Mathiot, P., Heiri, O., Roche, D.M., Nisancioglu, K.H., Valdes, P.J., 2015. Multiple causes of the Younger Dryas cold period. Nature Geosci 8, 946–949. https://doi.org/10.1038/ngeo2557

Robles, M., 2022. Vegetation, climate, and human history of the Mediterranean basin: A Late-Glacial to Holocene reconstruction from Italy (Lake Matese) to Armenia (Lake Sevan)

inferred from a multi-proxy approach (pollen, NPPs, brGDGTs, XRF) (PhD thesis). University of Molise, University of Montpellier, Campobasso, Montpellier.

Robles, M., Peyron, O., Brugiapaglia, E., Ménot, G., Dugerdil, L., Ollivier, V., Ansanay-Alex, S., Develle, A.-L., Tozalakyan, P., Meliksetian, K., Sahakyan, K., Sahakyan, L., Perello, B., Badalyan, R., Colombié, C., Joannin, S., 2022. Impact of climate changes on vegetation and human societies during the Holocene in the South Caucasus (Vanevan, Armenia): A multiproxy approach including pollen, NPPs and brGDGTs. Quaternary Science Reviews 277, 107297. https://doi.org/10.1016/j.quascirev.2021.107297

Rodrigo-Gámiz, M., García-Alix, A., Jiménez-Moreno, G., Ramos-Román, M.J., Camuera, J., Toney, J.L., Sachse, D., Anderson, R.S., Sinninghe Damsté, J.S., 2022. Paleoclimate reconstruction of the last 36 kyr based on branched glycerol dialkyl glycerol tetraethers in the Padul palaeolake record (Sierra Nevada, southern Iberian Peninsula). Quaternary Science Reviews 281, 107434. https://doi.org/10.1016/j.quascirev.2022.107434

Russell, J.M., Hopmans, E.C., Loomis, S.E., Liang, J., Sinninghe Damsté, J.S., 2018. Distributions of 5- and 6-methyl branched glycerol dialkyl glycerol tetraethers (brGDGTs) in East African lake sediment: Effects of temperature, pH, and new lacustrine paleotemperature calibrations. Organic Geochemistry 117, 56–69. https://doi.org/10.1016/j.orggeochem.2017.12.003

Sadori, L., 2018. The Lateglacial and Holocene vegetation and climate history of Lago di Mezzano (central Italy). Quaternary Science Reviews 202, 30–44. https://doi.org/10.1016/j.quascirev.2018.09.004

Salonen, J.S., Korpela, M., Williams, J.W., Luoto, M., 2019. Machine-learning based reconstructions of primary and secondary climate variables from North American and European fossil pollen data. Sci Rep 9, 15805. https://doi.org/10.1038/s41598-019-52293-4

Samartin, S., Heiri, O., Joos, F., Renssen, H., Franke, J., Brönnimann, S., Tinner, W., 2017. Warm Mediterranean mid-Holocene summers inferred from fossil midge assemblages. Nature Geosci 10, 207–212. https://doi.org/10.1038/ngeo2891

Sanchi, L., Ménot, G., Bard, E., 2014. Insights into continental temperatures in the northwestern Black Sea area during the Last Glacial period using branched tetraether lipids. Quaternary Science Reviews 84, 98–108. https://doi.org/10.1016/j.quascirev.2013.11.013

Sbaffi, L., Wezel, F.C., Curzi, G., Zoppi, U., 2004. Millennial- to centennial-scale palaeoclimatic variations during Termination I and the Holocene in the central

Mediterranean Sea. Global and Planetary Change 40, 201–217. https://doi.org/10.1016/S0921-8181(03)00111-5

Sicre, M.-A., Siani, G., Genty, D., Kallel, N., Essallami, L., 2013. Seemingly divergent sea surface temperature proxy records in the central Mediterranean during the last deglacial. Climate of the Past 9, 1375–1383. https://doi.org/10.5194/cpd-9-683-2013

Sinninghe Damsté, J.S., Rijpstra, W.I.C., Foesel, B.U., Huber, K.J., Overmann, J., Nakagawa, S., Kim, J.J., Dunfield, P.F., Dedysh, S.N., Villanueva, L., 2018. An overview of the occurrence of ether- and ester-linked iso-diabolic acid membrane lipids in microbial cultures of the Acidobacteria: Implications for brGDGT paleoproxies for temperature and pH. Organic Geochemistry 124, 63–76. https://doi.org/10.1016/j.orggeochem.2018.07.006

Smith, V.C., Isaia, R., Pearce, N.J.G., 2011. Tephrostratigraphy and glass compositions of post-15 kyr Campi Flegrei eruptions: implications for eruption history and chronostratigraphic markers. Quaternary Science Reviews 30, 3638–3660. https://doi.org/10.1016/j.quascirev.2011.07.012

Stockhecke, M., Bechtel, A., Peterse, F., Guillemot, T., Schubert, C.J., 2021. Temperature, precipitation, and vegetation changes in the Eastern Mediterranean over the last deglaciation and Dansgaard-Oeschger events. Palaeogeography, Palaeoclimatology, Palaeoecology 577, 110535. https://doi.org/10.1016/j.palaeo.2021.110535

Sun, Q., Chu, G., Liu, M., Xie, M., Li, S., Ling, Y., Wang, X., Shi, L., Jia, G., Lü, H., 2011. Distributions and temperature dependence of branched glycerol dialkyl glycerol tetraethers in recent lacustrine sediments from China and Nepal. J. Geophys. Res. 116, G01008. https://doi.org/10.1029/2010JG001365

Taffetani, F., Catorci, A., Ciaschetti, G., Cutini, M., Di Martino, L., Frattaroli, A.R., Paura, B., Pirone, G., Rismondo, M., Zitti, S., 2012. The Quercus cerris woods of the alliance Carpinion orientalis Horvat 1958 in Italy. Plant Biosystems - An International Journal Dealing with all Aspects of Plant Biology 146, 918–953. https://doi.org/10.1080/11263504.2012.682613

Tarroso, P., Carrión, J., Dorado-Valiño, M., Queiroz, P., Santos, L., Valdeolmillos-Rodríguez, A., Célio Alves, P., Brito, J.C., Cheddadi, R., 2016. Spatial climate dynamics in the Iberian Peninsula since 15 000 yr BP. Climate of the Past 12, 1137–1149. https://doi.org/10.5194/cp-12-1137-2016

ter Braak, C.J.F., Juggins, S., 1993. Weighted averaging partial least squares regression (WA-PLS): an improved method for reconstructing environmental variables from species assemblages 18.

ter Braak, C.J.F., van Dam, H., 1989. Inferring pH from diatoms: a comparison of old and new calibration methods. Hydrobiologia 178, 209–223. https://doi.org/10.1007/BF00006028

Tomlinson, E.L., Arienzo, I., Civetta, L., Wulf, S., Smith, V.C., Hardiman, M., Lane, C.S., Carandente, A., Orsi, G., Rosi, M., Müller, W., Menzies, M.A., 2012. Geochemistry of the Phlegraean Fields (Italy) proximal sources for major Mediterranean tephras: Implications for the dispersal of Plinian and co-ignimbritic components of explosive eruptions. Geochimica et Cosmochimica Acta 93, 102–128. https://doi.org/10.1016/j.gca.2012.05.043

Valente, E., Buscher, J.T., Jourdan, F., Petrosino, P., Reddy, S.M., Tavani, S., Corradetti, A., Ascione, A., 2019. Constraining mountain front tectonic activity in extensional setting from geomorphology and Quaternary stratigraphy: A case study from the Matese ridge, southern Apennines. Quaternary Science Reviews 219, 47–67. https://doi.org/10.1016/j.quascirev.2019.07.001

Van Geel, B., 2002. Non-Pollen Palynomorphs, in: Smol, J.P., Birks, H.J.B., Last, W.M., Bradley, R.S., Alverson, K. (Eds.), Tracking Environmental Change Using Lake Sediments, Developments in Paleoenvironmental Research. Springer Netherlands, Dordrecht, pp. 99–119. https://doi.org/10.1007/0-306-47668-1_6

Vescovi, E., Kaltenrieder, P., Tinner, W., 2010. Late-Glacial and Holocene vegetation history of Pavullo nel Frignano (Northern Apennines, Italy). Review of Palaeobotany and Palynology 160, 32–45. https://doi.org/10.1016/j.revpalbo.2010.01.002

Walker, M., Lowe, J., Blockley, S.P.E., Bryant, C., Coombes, P., Davies, S., Hardiman, M., Turney, C.S.M., Watson, J., 2012. Lateglacial and early Holocene palaeoenvironmental 'events' in Sluggan Bog, Northern Ireland: comparisons with the Greenland NGRIP GICC05 event stratigraphy. Quaternary Science Reviews 36, 124–138. https://doi.org/10.1016/j.quascirev.2011.09.008

Watson, B.I., Williams, J.W., Russell, J.M., Jackson, S.T., Shane, L., Lowell, T.V., 2018. Temperature variations in the southern Great Lakes during the last deglaciation: Comparison between pollen and GDGT proxies. Quaternary Science Reviews 182, 78–92. https://doi.org/10.1016/j.quascirev.2017.12.011

Weijers, J.W.H., Panoto, E., van Bleijswijk, J., Schouten, S., Rijpstra, W.I.C., Balk, M., Stams, A.J.M., Damsté, J.S.S., 2009. Constraints on the Biological Source(s) of the Orphan

Branched Tetraether Membrane Lipids. Geomicrobiology Journal 26, 402–414. https://doi.org/10.1080/01490450902937293

Weijers, J.W.H., Schouten, S., Spaargaren, O.C., Sinninghe Damsté, J.S., 2006. Occurrence and distribution of tetraether membrane lipids in soils: Implications for the use of the TEX86 proxy and the BIT index. Organic Geochemistry 37, 1680–1693. https://doi.org/10.1016/j.orggeochem.2006.07.018

Weijers, J.W.H., Schouten, S., van den Donker, J.C., Hopmans, E.C., Sinninghe Damsté, J.S., 2007. Environmental controls on bacterial tetraether membrane lipid distribution in soils. Geochimica et Cosmochimica Acta 71, 703–713. https://doi.org/10.1016/j.gca.2006.10.003

Wulf, S., Kraml, M., Brauer, A., Keller, J., Negendank, J.F.W., 2004. Tephrochronology of the 100ka lacustrine sediment record of Lago Grande di Monticchio (southern Italy). Quaternary International 122, 7–30. https://doi.org/10.1016/j.quaint.2004.01.028

Wulf, S., Kraml, M., Keller, J., 2008. Towards a detailed distal tephrostratigraphy in the Central Mediterranean: The last 20,000 yrs record of Lago Grande di Monticchio. Journal of Volcanology and Geothermal Research 177, 118–132. https://doi.org/10.1016/j.jvolgeores.2007.10.009

Yang, H., Pancost, R.D., Dang, X., Zhou, X., Evershed, R.P., Xiao, G., Tang, C., Gao, L., Guo, Z., Xie, S., 2014. Correlations between microbial tetraether lipids and environmental variables in Chinese soils: Optimizing the paleo-reconstructions in semi-arid and arid regions. Geochimica et Cosmochimica Acta 126, 49–69. https://doi.org/10.1016/j.gca.2013.10.041

Zhang, J., Bai, Y., Xu, S., Lei, F., Jia, G., 2013. Alkenone and tetraether lipids reflect different seasonal seawater temperatures in the coastal northern South China Sea. Organic Geochemistry 58, 115–120. https://doi.org/10.1016/j.orggeochem.2013.02.012

Supplementary data

Supplementary Table S1. Statistical results of the MAT, WAPLS, BRT and RF methods applied on the modern "warm mixed forest" (WAMX), "temperature deciduous" (TEDE) and "cold steppe" (COST) datasets.

Model	Climate parameter	R^2	RMSE
MAT	MAAT (°C)	0,78	3,09
	MTWA (°C)	0,65	3,01
	MTCO (°C)	0,85	3,88
	PANN (mm.year^{-1})	0,75	183,11
	P_{winter} (mm.year^{-1})	0,71	76,76
WAPLS	MAAT (°C)	0,66	3,51
	MTWA (°C)	0,49	3,36
	MTCO (°C)	0,73	4,84
	PANN (mm.year^{-1})	0,55	220,36
	P_{winter} (mm.year^{-1})	0,51	90,95
RF	MAAT (°C)	0,61	3,72
	MTWA (°C)	0,42	3,52
	MTCO (°C)	0,71	4,94
	PANN (mm.year^{-1})	0,56	212,27
	P_{winter} (mm.year^{-1})	0,53	87,14
BRT	MAAT (°C)	0,87	2,97
	MTWA (°C)	0,77	2,94
	MTCO (°C)	0,91	3,77
	PANN (mm.year^{-1})	0,87	160,43
	P_{winter} (mm.year^{-1})	0,84	70,37

CHAPTER IV - VEGETATION, CLIMATE CHANGES AND HUMAN PRACTICES DURING THE LAST 15,000 YEARS RECORDED AT LAKE MATESE, IN ITALY

Mary Robles[1,2], Elisabetta Brugiapaglia[1], Odile Peyron[2], Guillemette Ménot[3], Bruno Paura[1], Sabine Wulf[4], Oona Appelt[5], Jacques-Louis de Beaulieu[6], Sébastien Joannin[2]

[1] Univ. Molise, Department Agriculture, Environment and Alimentation, Italy
[2] Univ. Montpellier, CNRS, IRD, EPHE, UMR 5554 ISEM, Montpellier, France
[3] Univ. Lyon, ENSL, UCBL, UJM, CNRS, LGL-TPE, F-69007 Lyon, France
[4] Univ. Portsmouth, Geography and Geosciences, School of the Environment, Portsmouth, United Kingdom
[5] Helmholtz Centre Potsdam, GFZ German Research Centre of Geosciences, Section 3.6, Telegrafenberg, Potsdam, Germany
[6] Aix-Marseille Univ., CNRS, IRD, UMR 7263 & 237 IMBE, Aix-en-Provence, France


Lake Matese, Italy, M.Robles

Abstract

Southern Italy a key area to study relationships between vegetation, climate and human activities during the Lateglacial and the Holocene : (1) vegetation history is poorly documented at mid- and high elevations, (2) human impacts must be present since a long time (8150 years), and (3) it is a transitional zone between atmospheric processes.Our study proposes to (1) evaluate the modern pollen rain in the Matese massifs, (2) reconstruct vegetation, human activities and climate changes in the Southern Italy during the Lateglacial and the Holocene from the sequence of Lake Matese. We used a multi-proxy approach including magnetic susceptibility, geochemistry (XRF), pollen, Non-Pollen Palynomorphs (NPPs), and molecular biomarkers (brGDGTs) to document the last 15,000 years. Climate reconstructions are based on brGDGTs, and pollen transfer functions associated with a multi-method approach: Modern Analogue Technique, Weighted Averaging Partial Least Squares regression, Random Forest, and Boosted Regression Trees. Modern pollen rain is dominated by Mediterranean evergreen taxa at low elevation and by deciduous arboreal taxa at higher elevations, except on the Lake Matese catchment with southern exposure where Poaceae is dominant. Important water level changes in Lake Matese are recorded with higher water level during the Lateglacial (maximum during the Younger Dryas) in comparison to the Holocene (minimum during the Early Holocene). Past vegetation shows a large proportion of Poaceae and *Artemisia* during the Lateglacial with an increase of deciduous arboreal taxa during the Bølling–Allerød. The Holocene begins with the persistence of Poaceae and then the development of *Fagus* during the Mid-Late Holocene. Deciduous *Quercus* remains abundant throughout the sequence. The first clear evidences of human activities appear relatively recently with the emergence of *Juglans* and they become more intense when cereals and *Olea* are recorded and that regional arboreal taxa decline. Climate reconstructions based on brGDGTs and pollen are rather consistent during the Lateglacial whereas they diverge during the Holocene. Our study suggests a significant impact of climate changes on vegetation dynamic and a recent impact of human activities. Moreover, the trend in water-level changes seems not directly linked to climate changes.

Keywords: Mediterranean Basin; Paleoclimate; Magnetic susceptibility; XRF; Pollen; NPPs; brGDGTs; Transfer functions; Lateglacial; Holocene; Water level changes

Résumé

L'Italie méridionale est une région clé pour étudier les relations entre la végétation, le climat et les activités humaines au cours du Tardiglaciaire et de l'Holocène : (1) l'histoire de la végétation est peu documentée à moyenne et haute altitude, (2) les impacts humains doivent être présents depuis longtemps (8150 ans), et (3) c'est une zone de transition entre les processus atmosphériques. Notre étude propose (1) d'évaluer la pluie pollinique moderne dans le Massif du Matese, (2) de reconstruire la végétation, les activités humaines et les changements climatiques dans le sud de l'Italie pendant le Tardiglaciaire et l'Holocène à partir de la séquence du lac Matese. Nous avons utilisé une approche multi-proxy comprenant la susceptibilité magnétique, la géochimie (XRF), les pollen, les Palynomorphes Non Polliniques (NPP) et les biomarqueurs moléculaires (brGDGT) pour documenter les 15,000 dernières années. Les reconstructions climatiques sont basées sur les brGDGT, et les fonctions de transfert du pollen associées à une approche multi-méthodes : Modern Analogue Technique, Weighted Averaging Partial Least Squares regression, Random Forest, and Boosted Regression Trees. La pluie pollinique moderne est dominée par des taxons méditerranéens à feuilles persistantes à basse altitude et par des taxons arborés décidus à plus haute altitude, sauf sur le bassin versant du lac Matese exposé au sud où les Poaceae sont dominantes. D'importants changements de niveau d'eau dans le lac Matese sont enregistrés, avec un niveau d'eau plus élevé pendant le Tardiglaciaire (maximum pendant le Dryas récent) par rapport à l'Holocène (minimum pendant l'Holocène inférieur). La végétation passée montre une grande proportion de Poaceae et d'*Artemisia* pendant le Tardiglaciaire avec une augmentation des taxons arborés décidus pendant le Bølling-Allerød. L'Holocène commence avec la persistance des Poaceae puis le développement de *Fagus* pendant l'Holocène moyen-supérieur. *Quercus* décidu reste abondant tout au long de la séquence. Les premières évidences d'activités humaines apparaissent relativement récemment avec l'émergence de J*uglans* et elles deviennent plus intenses lorsque les céréales et *Olea* sont enregistrées et que les taxons arborés régionaux diminuent. Les reconstructions climatiques basées sur les brGDGT et le pollen sont plutôt cohérentes durant le Tardiglaciaire alors qu'elles divergent durant l'Holocène. Notre étude suggère un impact significatif des changements climatiques sur les dynamiques de végétation et un impact récent des activités humaines. Par ailleurs, la tendance des changements de niveau d'eau ne semble pas directement liée aux changements climatiques.

Mots clés : Bassin méditerranéen ; Paléoclimat ; Susceptibilité magnétique ; XRF ; Pollen ; NPP ; brGDGT ; Fonctions de transfert ; Tardiglaciaire ; Holocène ; Changements de niveau d'eau

1. Introduction

The Mediterranean Basin is a key area to study interactions between vegetation dynamics, human activities and climate changes during the Lateglacial and the Holocene. The Mediterranean peninsulas are recognized as a "hotspot" of biodiversity and had played an important role as refugial zone during glacial periods (Magri, 2008; Hewitt, 2011). Their mountainous topography, favoring the presence of microclimates, is essential for the survival of species through the glacial periods (Hewitt, 2011). However, the spatial range of refugia is mostly limited, and many paleoecological studies are necessary to fully understand their distribution and species dynamics along the time. The Mediterranean Basin is also characterized by a widespread of human practices since the Neolithic, which could have an impact on the vegetation dynamics (Guilaine, 2003). Moreover, the Mediterranean Basin is highly sensitive to climate changes and recent studies have revealed a complex picture of spatio-temporal climate variability throughout the Holocene (Peyron et al., 2017; Di Rita et al., 2018; Marriner et al., 2022). In this context, it is sometimes difficult to distinguish the respective impact of human activities and climate changes on vegetation dynamics in paleoecological records. Indeed, human activities (e.g. agriculture, pastoralism, sylviculture) can modify vegetation structure, composition and diversity which impact pollen-climate relationships (Chevalier et al., 2020). Pollen-based climate reconstructions from records with a strong human impact need to be interpreted with caution and compared with independent climate reconstructions based on other proxies.

More specifically, the Southern Italy is a key region to investigate the links between agropastoral systems, climate changes and paleoenvironmental conditions. This region represents an important area by the presence of refugia during glacial periods (Magri, 2008; Hewitt, 2011). Studying vegetation dynamics allow to understand the localization of species and their expansion along the time. For example, several species are mostly recorded in the South of Italy during the Lateglacial such as deciduous *Quercus* or *Fagus sylvatica* (Magri, 2008; De Beaulieu et al., 2017). However, in contrast to the Northern and Central Italy, the Southern Italy is a region with few palynological records and its vegetation history during the Lateglacial and the Holocene is not totally understood. Only two terrestrial records documented both the Lateglacial and the Holocene: Lago Grande di Monticchio (Allen et al., 2002) and Lago Trifoglietti (Joannin et al., 2012; De Beaulieu et al., 2017). Moreover, the majority of palynological records are located at low elevation in the plains and only three records are located at mid-elevation: Lago Grande di Monticchio (656 m a.s.l.; Allen et al., 2002), Lago Trifoglietti (1048 m a.s.l.;

Joannin et al., 2012; De Beaulieu et al., 2017) and Lago Pergusa (667 m a.s.l; Sadori and Narcisi, 2001). Southern Italy is also an interesting area from the climatic point of view because it is located in a transitional zone between several climatic systems including the North Atlantic Oscillation (NAO) and the North African anticyclone (Magny et al., 2013; Peyron et al., 2013; Di Rita et al., 2018). Concerning human activities, the first traces of farmers in Italy is recorded in Southern Italy around 8150 cal BP and then practices were spread within the entire country (Palmisano et al., 2021). In this context, well-known proxies associated with independent proxies from vegetation are needed to distinguish the impact of humans and climate on vegetation changes. Pollen-based climate reconstructions are commonly used and perform well when human impact is absent or little affect the regional vegetation. However, it is recommended to use a multimethod approach to avoid method-dependance (Peyron et al., 2013). Molecular biomarkers are an emerging and promising proxy that allow quantitative temperature reconstructions independently from vegetation. In particular, branched Glycerol Dialkyl Glycerol Tetraethers (brGDGTs), also called glycerol tetraethers, are ubiquitous organic compounds synthesized by bacteria (Weijers et al., 2006; Sinninghe Damsté et al., 2018). Bacteria that produced brGDGTs are still largely unknown but the relationship between brGDGT distribution and temperature is well established (Naafs et al., 2017b, 2017a; Raberg et al., 2021; Martínez-Sosa et al., 2021). To date, very few studies associate pollen with brGDGTs to reconstruct climate variability over time (Watson, 2018; Martin et al., 2020; Dugerdil et al., 2021b, 2021a; Robles et al., 2022).

This study aims to improve the understanding of vegetation, human practices and climate history in Southern Italy during the Lateglacial and the Holocene from the Lake Matese. We propose here a multi-proxy approach including the study of magnetic susceptibility, XRF, pollen, Non-Pollen Palynomorphs (NPPs), and molecular biomarkers (brGDGTs) to document the last 15,000 years in the Southern Italy. We expect to better understand the relationships between vegetation, human societies and climate in this key area of the Mediterranean region. Our study goals are to:

1) understand the modern pollen rain in the Matese massifs and enhance the reliability of pollen-based climate reconstructions by the addition of new samples.
2) estimate the water level changes and ecological processes of the Lake Matese during the Lateglacial and the Holocene with XRF data, aquatic pollen taxa and NPPs.
3) reconstruct vegetation dynamics during the Lateglacial and the Holocene with pollen data.

4) identify human activities during the last 8000 years with pollen and NPPs and understand their impact on the environment
5) provide quantitative climate reconstructions based on brGDGTs and pollen which are associated with a multi-method approach including MAT (Modern Analogue Technique), WAPLS (Weighted Averaging Partial Least Squares regression), RF (Random Forest) and BRT (Boosted Regression Forest) methods.
6) finally infer relationships between vegetation dynamics, climate changes, and human practices at a local scale and discuss these results at a regional scale (Southern Italy).

2. Study site

2.1 Geological and geographical setting Hydrological

The Apennines Mountains are located in Italy between the Tyrrhenian, Adriatic and Ionian Sea. They extend over 1200 km from the Alps to northern Sicily. They were formed by the Alpine orogeny. The Matese Massif is situated in the South of Apennines, in the Campania region and in the Caserta province (Fig. 1). The Lake Matese (41°24'33.3"N, 14°24'22.1"E, 1012 m a.s.l.) is located in the Matese karst massif which extends over 30 km from NE to SW and composed of calcareous and calcareous-dolomite series dated to the Late Triassic-Miocene (Fiorillo and Doglioni, 2010). The present formation of the massif results of extension by strike-slip faults during the Quaternary and several strong earthquakes were recorded in the massif (Ferranti et al., 2015; Ferrarini et al., 2017; Galli et al., 2017; Valente et al., 2019). The lake Matese is the highest karst lake of Italy and it is located in the high ground elevated sector of the Matese massif. The lake is surrounded by the two highest peaks of the massif, the Mount Miletto (2050 m a.s.l.) and the Mount Gallinola (1923 m a.s.l.), whose the melting snow feeding the lake. Along the southern side of the lake, two sinkholes named the ''Brecce'' and ''Scennerato'' are present (Fiorillo and Pagnozzi, 2015). In the twenties, hydraulic works was realized to isolate the bottom of the lake and the main sinkholes by earth dams (Fiorillo and Pagnozzi, 2015). The water level of the lake improved from 1007-1009 m a.s.l. to 1012 m a.s.l. with a volume of 15 mm^3 (Fiorillo and Pagnozzi, 2015). A part of the lake water is transported until the hydroelectric power station of Piedimonte Matese, at the base of the massif.

2.2 Modern climate and vegetation

The Matese Mountains are characterized by a Mediterranean, warm-temperate humid climate (Aucelli et al., 2013). The southwestern part of the massif, including the Lake Matese, have the heaviest precipitation with a maximum at Campitello Matese (1400 m a.s.l.) (Fiorillo and Pagnozzi, 2015). The Lake Matese shows annual precipitation of 1808 mm with a maximum in November (~290 mm) and December (~260 mm) and a minimum in July (~50 mm) (Fiorillo and Pagnozzi, 2015). The annual temperatures correspond to 9.3°C with a minimum in January (2°C) and a maximum in July (19°C) (Fiorillo and Pagnozzi, 2015). The precipitation is less important in the southeastern part of the massif due to the Atlantic origin of storms and orographic effect of mountains (Fiorillo and Pagnozzi, 2015).

The forest landscape of the Matese massif is characterized by a succession of distinct vegetation belts. From the base of the massif up to 1000 meters above sea level, there are forests dominated by deciduous oaks (*Quercus cerris, Q. pubescens, Q. frainetto, Q. petraea*), sclerophyllous oaks (*Quercus ilex*) or dominated by hornbeam (*Ostrya carpinifolia*) (Taffetani et al., 2012; Guarino et al., 2015). At the highest altitudes, on the north-east facing slopes, the presence of beech (*Fagus sylvatica*) becomes massive (Carranza et al., 2012) while limited to gorge environments, mixed forests with lime trees (*Tilia plathyphyllos, T. cordata*) or maples (*Acer obtusatum, A. pseudoplatanus, A. platanoides, Acer cappadocicum subsp. lobelii*) are scattered (Paura and Cutini, 2006). The herbaceous vegetation is mainly composed of Poaceae that characterizes the still active pastures, the abandoned ones and the former cultivated fields. These are communities dominated by *Bromus erectus, Phleum ambiguum, Brachypodium rupestre* and *Festuca sp. pl.* replaced in the high-altitude aspects by grasslands with *Festuca violacea* subsp. *italica* (Giancola and Stanisci, 2006). The hygrophilous vegetation of the Lake Matese is distinguished by the presence of woody (e.g. *Salix alba, S. caprea, S. cinerea* subsp. *cinerea, Populus nigra, P. alba*), helophytes (e.g. *Phragmites australis, Schoenoplectus lacustris, Typha angustifolia, T. latifolia*) and hydrophytes species (*Myriophyllum spicatum, Persicaria amphibia*).

2.3 Archeology and modern human activities

The recent studies of Palmisano et al. (2021) and Parkinson et al. (2021) have synthesized the archeological data in Italy from the Mesolithic to the Iron Age. During the Mesolithic, hunter-gatherers lived in caves and rock shelters located in the plains, and along the coast and they established seasonal hunting camp in the Apennines. The Neolithic (8150-5650 cal BP) is marked by the development of farmers, firstly in south-east Italy (Apulia) and then in all Italy.

During the Early Neolithic, settlements were mainly based in subcoastal areas and lowlands on the shores of rivers and lakes whereas the Middle, Late Neolithic and the Cooper Age are characterized by the establishment of settlement in the Apennines and an intensification of agriculture and pastoralism. The Bronze Age (4150-2950 cal BP) is defined by development in social and political complexity in Italy. At this period, communities occupied upland and lowland and settled on naturally defensible locations. They intensified agricultural practices and they began the culture of tress/vines. The Iron Age is characterized by an increasing presence of Phoenician and Greek colonies in southern Italy. Around the Lake Matese, Soricelli (2013) shows the presence of pre-Roman and Roman settlements (2150 and 1550 cal BP) in the archeological site Capo di Campo located in the southeastern shore of the lake. The site was occupied by Samnites, a group of peoples and communities, with Greek origin, that in pre-Roman period occupied a large and mostly mountainous area of central-southern Italy (Farney and Bradley, 2018). They were mobile and interacted with other Mediterranean peoples (Etruscan, Picentes, South of France, Greek, Tunisia). They were divided into several populations and their economy was based on agriculture and livestock mainly in mountain areas (Farney and Bradley, 2018). The Pentri population occupied the Matese Massif and they bred cattles (work animals), horses, sheeps/goats (wool, dairy products) and pigs (meat). Several conflicts opposed Samnites and Rome and at the end of the war a period of peace and relative prosperity appears in the former territory of Pentri. Today, the human activities around the Lake Matese are based on pastoralism and agriculture on the flat areas around the lake.

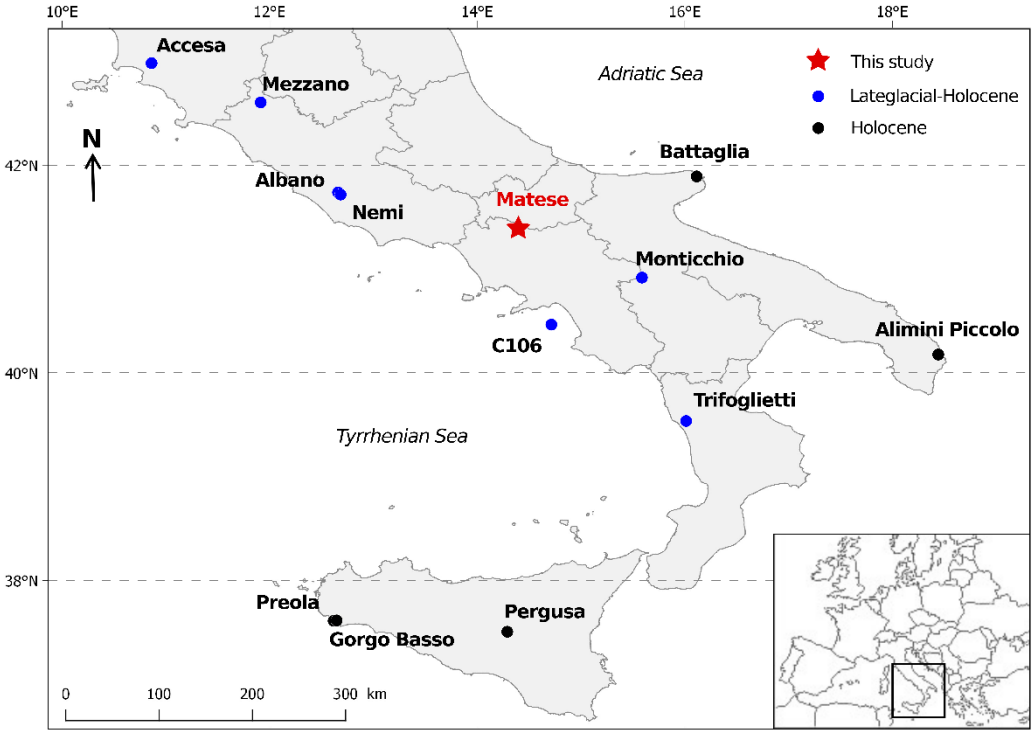

Figure IV-1. Location of the Lake Matese and selected pollen records in Central and Southern Italy covering all or part of the last 15,000 cal BP : Accesa (Drescher-Schneider et al., 2007; 157 m a.s.l.), Mezzano (Sadori, 2018; 452 m a.s.l.), Battaglia (Caroli and Caldara, 2007), Albano (Mercuri et al., 2002; 293 m a.s.l.), Nemi (Mercuri et al., 2002; 320 m a.s.l.), Monticchio (Allen et al., 2002 ; 656 m a.s.l.), C106 (Ermolli and di Pasquale, 2002), Alimini Piccolo (Di Rita and Magri, 2009; 1 m a.s.l.), Trifoglietti (Joannin et al., 2012; De Beaulieu et al., 2017; 1048 m a.s.l.), Preola (Magny et al., 2011; 4 m a.s.l.), Gorgo Basso (Tinner et al., 2009; 4 m a.s.l.), Pergusa (Sadori and Narcisi, 2001; 667 m a.s.l.).

3. Material and Methods

3.1 Core retrieval and modern samples

Coring of the Lake Matese was performed in July 2019 in the southeastern part of the lake (41°24'33.3"N, 14°24'22.1"E, 1012 m a.s.l.). This area was selected because of a higher sediment accumulation expected thanks to the dense hygrophilous vegetation. Coring was realized on a floating raft composed of *Salix* spp. and *Phragmites australis*. Three parallel cores (cores A, B and C) were taken with a 1 m Russian corer. The diameter chamber of the corer was adapted according to the type of sediment and corresponds to 8 cm or 6.3 cm. An additional core was retrieved with a UWITEC piston corer beside the floating raft in order to obtain the undisturbed surface water-sediment interface. The master core of Matese was constructed from sections of parallel cores and based on the lithology and XRF data. The complete continuous sequence measures 535 cm in total.

A total of 15 modern pollen samples along an altitudinal transect from 540 to 1620 m a.s.l were collected in July 2019. This transect records the vegetation across mixed forests, beech forests and meadows. In each sampling site, 3-5 moss polsters were collected within a radius of 5 m and then combined into one sample. The modern climate data were calculated with the *New_LocClim 1.10* software (Grieser et al., 2006) and then corrected according to the site elevation.

3.2 Lithology, magnetic susceptibility and geochemistry

Lithology was defined upon visual differences. Magnetic susceptibility (MS) was measured at high resolution with a Geotek Multi-Sensor Core logger in Chrono-environment laboratory (University of Franche Comté). An interval of 3 mm or 5 mm was applied according to the type of sediment. Geochemical analyses were performed at high resolution by X-ray Fluorescence (XRF) with an AVAATECH core scanner in EDYTEM laboratory (University Savoie Mont Blanc). A continuous 5 mm step measurement was applied with a run at 10 kV and 0.1 mA for 15 s to detect lightweight elements, such as Al, Si, K, Ca, Ti, Mn, Fe and a second run at 30 kV and 0.15 mA for 20 s to detect Br, Rb, Sr and Zr. The XRF core scanning provides an estimate of the geochemical composition, and the results are semi-quantitative and expressed as peak intensities counting (cps). Principal component analysis (PCA) was performed on XRF data with *FactoMineR 2.4* package (Lê et al., 2008).

3.3 Pollen analyses

A total of 77 samples from the Matese core were collected at 4 cm or 6 cm resolution for pollen analysis. For each sample, 1 cm^3 of sediment was processed and 3 *Lycopodium* tablets were added to estimate pollen concentration. Samples were treated following the standard procedure (Faegri et al., 1989; Moore et al., 1991) including HCl, KOH, sieving, acetolysis and HF. The pollen counts were analyzed with a Leica DM1000 LED microscope at a standard magnification of 400x. Pollen taxa were identified using photo atlases (Beug, 2004; Reille, 1998; Van Geel, 2002) and a modern reference collection (ISEM, University of Montpellier). Each slide was counted with a minimum of 300 terrestrial pollen grains, excluding aquatic plants such as Cyperaceae, aquatic taxa, fern spores. Grass pollen grains greater than 40 µm were classified as *Cerealia*-type (Beug, 2004). Aquatic taxa, fern spores, and NPPs (algae and fungal spores) were counted alongside pollen. The pollen diagrams were constructed with the R package *Rioja* (Juggins and Juggins, 2020).

3.4 Pollen-inferred climate reconstruction

A multi-method approach is used to reconstruct climate parameters from pollen data, including the Modern Analog Technique (MAT; Guiot, 1990), the Weighted Averaging Partial Least Squares regression (WAPLS; ter Braak and van Dam, 1989; ter Braak and Juggins, 1993), and the recent machine-learning methods : Random Forest (RF; Breiman, 2001; Prasad et al., 2006) and Boosted Regression Trees (BRT; De'ath, 2007; Elith et al., 2008). The description of methods is available in Robles et al., in prep (Chap. III).

Each method requires a modern pollen dataset. The modern pollen dataset (n = 3373 sites) used for the calibration of the methods is based on the large Eurasian/Mediterranean dataset compiled by Peyron et al. (2013, 2017) and completed by Dugerdil et al. (2021a), Robles et al. (2022) and Robles et al., in prep. A biome constraint (Guiot et al., 1993), based on the pollen-Plant Functional Type method and following the biomization procedure (Peyron et al., 1998; Prentice et al., 1996) was applied to modern and fossil pollen samples to better distinguish the warm and cold steppes. The modern pollen dataset finally selected for the calibration of the different methods contains 1018 samples belonging to 3 biomes depicted in the fossil core: "warm mixed forest" (WAMX), "temperature deciduous" (TEDE) and "cold steppe" (COST). For the MAT method, only the modern samples of COST (n = 385) were selected for the fossil samples corresponding to this biome. Performance of each method and calibration training was statistically tested (for more details, see Dugerdil et al., 2021a) to determining if modern samples are suitable for quantitative climate reconstructions. The Root Mean Square Error (RMSE) and the R^2 are presented in the Supplementary Table S1. Five climate parameters were reconstructed, mean annual air temperature (MAAT), mean temperature of the warmest month (MTWA), mean temperature of the coldest month (MTCO), mean annual precipitation (PANN), and winter precipitation (P_{winter} = December, January, and February). For each climate parameter, the methods fitting with the higher R^2 and the lower RMSE were selected. Cyperaceae and ferns of Matese record have been excluded because they are associated with local dynamics.

3.6 BrGDGTs extraction analyses

A total of 75 samples from the Matese core (4 cm or 6 cm resolution) were used for GDGT analysis. The samples were freeze-dried, powdered and subsampled (1 g for clay and 0.4 g for gyttja). Lipids were extracted from the sediment using a Microwave oven (MARS 6; CEM) with dichloromethane:methanol (3:1). Then, the internal standard was added (C_{46}

GDGT, Huguet et al., 2006). The total lipid extracts were separated into apolar and polar fractions using a silica SPE cartridge with hexane:DCM (1:1) and DCM:MeOH (1:1). The polar fractions containing brGDGTs were analyzed using a High-Performance Liquid Chromatography Mass Spectrometry (HPLC-APCI-MS, Agilent 1200) with detection via selective ion monitoring (SIM) of m/z 1050, 1048, 1046, 1036, 1034, 1032, 1022, 1020, and 1018 in the LGL-TPE of ENS Lyon (Davtian et al., 2018; Hopmans et al., 2016). GDGT concentrations were calculated based on the internal standard. The analytic reproducibility was assessed based on an internal standard sediment.

3.7 GDGTs annual temperature reconstruction

The proportion of tetra- (I), penta- (II) and hexa- (III) methylated brGDGTs includes the fractional abundances of the 5-methyl (X), 6-methyl (X') and 7-methyl (X7) brGDGTs (Ding et al., 2016). The CBT and MBT indexes were defined by Weijers et al., (2007) and the MBT'5me, only based on the 5-methyl brGDGTs, by De Jonge et al. (2014). The Mean Annual Air Temperature (MAAT) was reconstructed with global (Sun et al., 2011) and East African (Russell et al., 2018) lacustrine calibrations. The mean temperature of Months Above Freezing (MAF) was reconstructed with Bayesian (Martínez-Sosa et al., 2021) and high latitudes (Raberg et al., 2021) lacustrine calibrations. All the formulae are presented in Table 1.

Table IV-1. Synthesis of the formulae for the main brGDGT indices.

Indice	Formula	Reference
$\%tetra$	$\frac{Ia + Ib + Ic}{\Sigma brGDGTs}$	Ding et al., 2016
$\%penta$	$\frac{IIa + IIa' + IIa_7 + IIb + IIb' + IIb_7 + IIc + IIc' + IIc_7}{\Sigma brGDGTs}$	Ding et al., 2016
$\%hexa$	$\frac{IIIa + IIIa' + IIIa_7 + IIIb + IIIb' + IIIb_7 + IIIc + IIIc' + IIIc_7}{\Sigma brGDGTs}$	Ding et al., 2016
CBT	$-log\frac{Ib + IIb}{Ia + IIa}$	Weijers et al., 2007
MBT	$\frac{Ia + Ib + Ic}{\Sigma brGDGTs}$	Weijers et al., 2007
MBT'_{5me}	$\frac{Ia + Ib + Ic}{Ia + Ib + Ic + IIa + IIb + IIc + IIIa}$	De Jonge et al., 2014
$MAAT\ (°C)$	$3.949 - 5.593 \times CBT\ + 38.213 \times MBT$ $(n = 100, R^2 = 0.73, RMSE = 4.27°C)$	Sun et al., 2011

$MAAT\ (°C)$	$-1{,}21 + 32.42 \times MBT'_{5me}$ $(n = 65, R^2 = 0.92, RMSE = 2.44\ °C)$	Russell et al., 2018
$MAF_{Meth}(°C)$	$92.9 + 63.84 \times fIb^2_{Meth} - 130.51 \times fIb_{Meth} - 28.77 \times fIIa^2_{Meth} - 72.28 \times fIIb^2_{Meth} - 5.88 \times fIIc^2_{Meth} + 20.89 \times fIIIa^2_{Meth} - 40.54 \times fIIIa_{Meth} - 80.47 \times fIIIb_{Meth}$ $(n = 182, R^2 = 0.90, RMSE = 2.14\ °C)$	Raberg et al., 2021
$MAF_{Full}(°C)$	$-8.06 + 37.52 \times fIa_{Full} - 266.83 \times fIb^2_{Full} + 133.42 \times fIb_{Full} + 100.85 \times fIIa'^2_{Full} + 58.15 \times fIIIa'^2_{Full} + 12.79 \times fIIIa_{Full}$ $(n = 182, R^2 = 0.91, RMSE = 1.97\ °C)$	Raberg et al., 2021

4. Results

4.1 Modern pollen assemblages

The altitudinal vegetation gradient is well recorded in the modern pollen rain (Fig. 2). Samples at lower elevations (600 m) with southern exposure show the presence of Mediterranean taxa such as *Quercus ilex* and *Olea.* Then, at higher elevation (800-1000 m) with southern exposure, modern samples record a dominance of *Quercus pubescens*-type or *Carpinus orientalis/Ostrya carpinifolia.* Between 1000 and 1200 m, the vegetation is characterized by beech forests located on the catchment of Lake Matese with northern exposure. For these samples, modern pollen rain shows the presence of *Quercus pubescens*-type (10%), *Fagus sylvatica* (8%) and Poaceae (12%). Between 1000 and 1600 m, modern pollen rain delivered by southern exposure shows a dominance of herbaceous taxa (74%) mainly represented by Poaceae (32%). There, we also detect the presence of pollen of cereals and ferns on the terrace area formerly cultivated. Although pastoral indicators are recorded by a very low proportion of *Plantago lanceolata*-type or *Rumex*-type, representing 1% and less than 1% respectively.

4.2 Lithology, magnetic susceptibility and geochemistry

The lithology of Matese core is divided into 6 units (Fig. 3). From the base to 350 cm, the core is mainly composed of gray clay sediment with vivianite, interrupted by organic layer between 477-484 cm (Unit 2) and macroscopic volcanic glasses between 476-437 cm (Unit 3). From 350 to 320 cm, the lithology is formed by a mix of clay sediment and gyttja (Unit 5). From 320 to the top (Unit 6), the core is composed of gyttja with layers more organic such as between 310-302 cm.

Major XRF elements are presented in Figure 3 and a principal component analysis (PCA) was performed on XRF data (Fig. 4). The sample map of PCA was colored according to the lithology units (Fig. 3). The first two dimensions (PCA 1_{XRF} and PCA 2_{XRF}) explain 77% of the variability, 59% and 18% respectively. The first dimension (PCA 1_{XRF}) shows the opposition between autochthonous sediments, determined by Bromine (Br) present in organic layers of Units 2, 5, 6 versus allochthonous sediments, mainly determined by terrigenous elements present in clay sediments (Units 1, 3, 4, 5). The second dimension (PCA 2_{XRF}) explains the opposition between sediments with high terrigenous inputs (Ti, Al, Fe, Si, Pb, Zr), present in the Unit 4, and the sediments with tephra layers in Units 1, 3, 5 where increase elements (K, Rb, Sr, Zn, Mn) The base of the core is also characterized by a peak of Calcium (Ca; Fig. 4).

Magnetic susceptibility (MS) and Potassium (K) content were mainly used to detect the tephra layers (Fig. 3). MS and Potassium content show two major changes, between 482-437 cm and 366-338 cm which correspond to tephra layers (macroscopic tephra and cryptotephra respectively). For more details about tephra of the Matese core, see Robles et al., in prep (Chap. III).

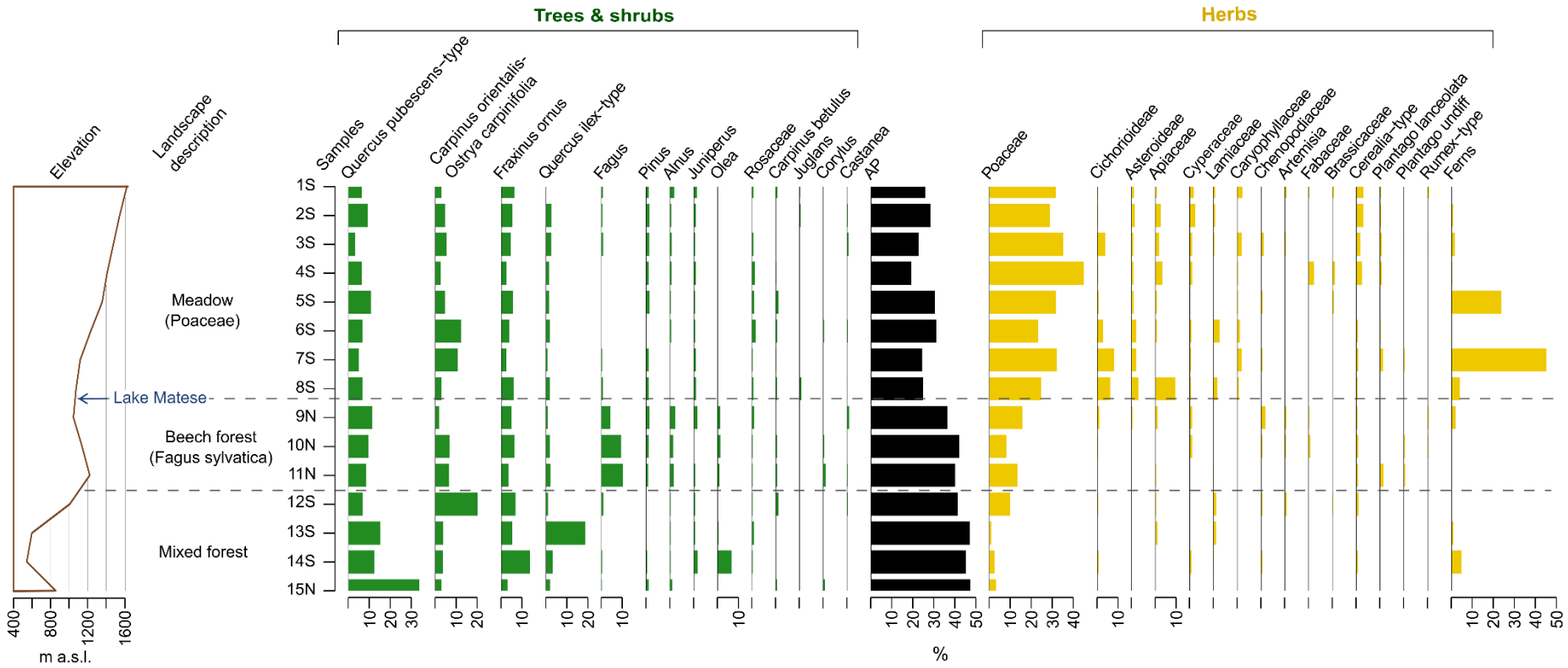

Figure IV-2. Modern pollen rain of selected taxa of the Lake Matese. S= southern exposure. N= northern exposure.

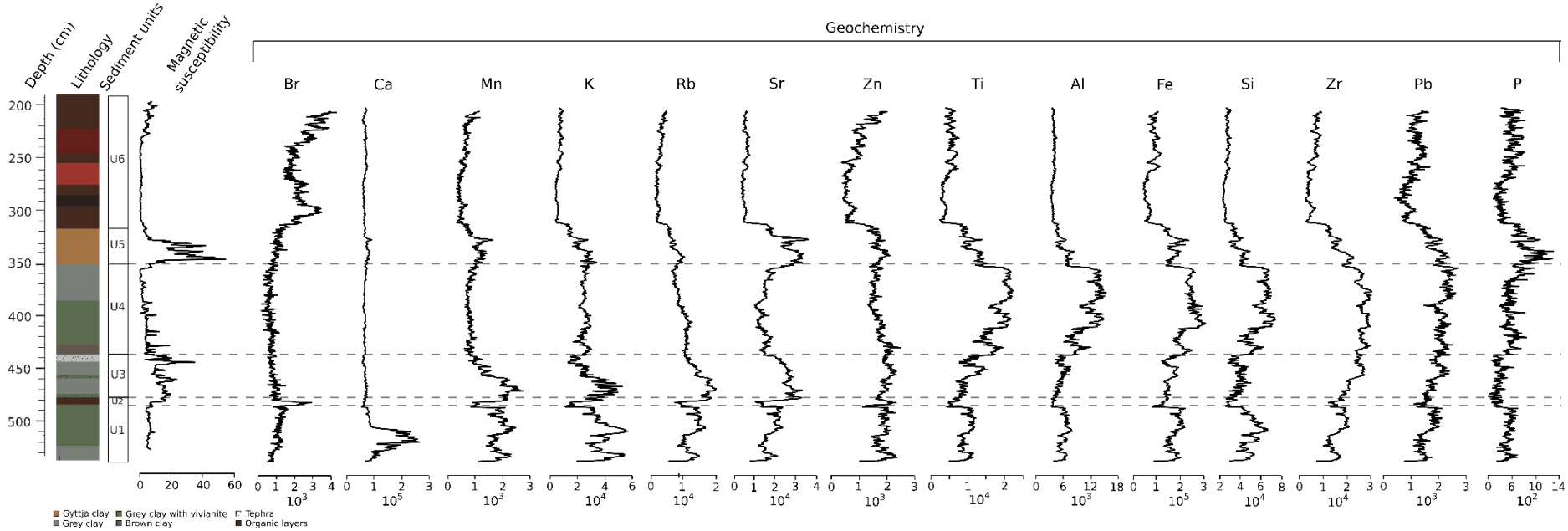

Figure IV-3. Lithology, magnetic susceptibility and XRF data of the Matese core against core depth.

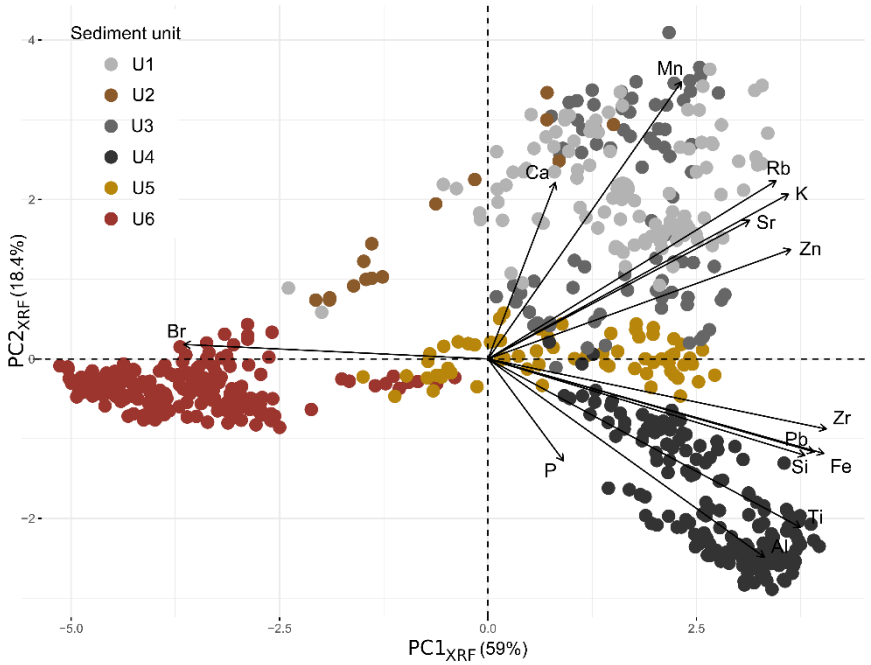

Figure IV-4. PCA analysis applied on XRF data of the Lake Matese and grouped according to the lithology.

4.3 Pollen sequence and terrestrial vegetation dynamics

A total of 95 terrestrial pollen taxa were identified in the Matese core. The pollen diagram includes a selection of the most abundant pollen taxa (Fig. 5) and it is divided into 6 pollen assemblage zones (PAZ) according to the CONISS method (Grimm, 1987).

PAZ 1 (535-520 cm) shows a dominance of herbaceous pollen taxa including Poaceae, *Artemisia*, Cichorioideae and *Rumex*-type. The arboreal pollen taxa (29%) are represented by *Quercus pubescens*-type, *Pinus*, *Betula, Carpinus orientalis/Ostrya carpinifolia* and *Corylus*.

PAZ 2 (520-440 cm) is characterized by a large increase of arboreal pollen taxa in terms of percentages (53%) and diversity. This period includes *Quercus pubescens*-type, *Pinus*, *Betula*, *Carpinus orientalis/Ostrya carpinifolia, Corylus* with the addition of *Fagus* at 485 cm. Considering herbaceous pollen taxa, their percentages decrease but Poaceae and *Artemisia* remains relatively abundant.

PAZ 3 (440-352 cm) is marked by an important drop in arboreal pollen taxa (19%), whereas the percentage of *Artemisia* steadily increases to a maximum of 41%. *Quercus pubescens*-type and *Carpinus orientalis/Ostrya carpinifolia* are recorded with a lesser percentage than in PAZ 2. *Pinus* increases slightly and Rosaceae appear at the end of the period. Herbaceous pollen taxa are dominated by *Artemisia,* Poaceae, Cichorioideae and Asteroideae whose percentage has increased.

PAZ 4 (352-312 cm) is characterized by an increase of arboreal pollen taxa (61%) and the abrupt decline of *Artemisia*. Considering arboreal pollen taxa, *Quercus pubescens*-type and *Carpinus orientalis/Ostrya carpinifolia* increase, *Fagus* appears and gradually increase, Rosaceae reach a peak at the beginning of this period and then are replaced by *Alnus glutinosa/incana.* The decrease of herbaceous pollen taxa at this period can be explained by the decline of *Artemisia*, however, the percentage of Poaceae remain stable.

PAZ 5 (312-216 cm) records the highest proportion of arboreal pollen taxa (77%) mainly explained by the high percentage of *Quercus pubescens*-type and *Fagus,* the increase of *Carpinus orientalis/Ostrya carpinifolia* and the appearance of *Fraxinus* and *Quercus ilex*-type. At this period, *Juglans* is also recorded between 267 and 243 cm. Considering herbaceous pollen taxa, Poaceae largely decrease. *Cerealia*-type mark the beginning of PAZ5 and then they are concomitantly recorded with *Secale* near 220 cm.

PAZ 6 (216-190 cm) shows a high percentage of arboreal pollen taxa (66%) mainly related to the appearance of *Salix* and the increase of *Fraxinus*, however *Quercus pubescens*-type and *Fagus* decrease. Herbaceous pollen taxa slightly increase due to the increase of Poaceae. *Cerealia*-type and *Secale* are still recorded and the presence of *Plantago lanceolota* is also visible.

4.4 Non-Pollen Palynomorphs and hygrophilous vegetation

The diagram of NPPs and hygrophilous pollen taxa (Fig. 6) is divided into 5 Non-Pollen Palynomorph assemblage zones (NPPAZ) according to the CONISS method (Grimm, 1987). The different CONISS zones are strongly associated with lithological changes.

NPPAZ 1 (535-484 cm) shows a dominance of the planktonic algae *Botryococcus* and the fungi *Sporormiella* is recorded between 514 and 502 cm.

NPPAZ 2 (484-440 cm) is characterized by a high percentage of Cyperaceae and the presence of the planktonic algae *Botryococcus* and *Pediastrum.*

NPPAZ 3 (440-352 cm) is marked by a high percentage of *Pediastrum* and from 400 cm the large increase of *Botryococcus* and the recording of *Sporormiella*.

NPPAZ 4 (352-312 cm) shows a high percentage of Cyperaceae, the development of ferns (monolete spores), the decline of *Pediastrum* and the drop in *Botryococcus*. A peak of *Zygnema* marks the transition with the following period.

NPPAZ 5 (312-190 cm) is primarily characterized by the high percentage of *Equisetum* and the presence of *Nymphaea* and *Myriophyllum spicatum*. Then, Cyperaceae increase again, and

on the contrary, *Equisetum* largely decrease. Finally, peaks of *Zygnema* and *Glomus* are recorded whereas Cyperaceae decrease again and will be replaced by *Equisetum*, *Myriophyllum spicatum*, *Potamogeton* and *Pediastrum*. Along all this period, *Botryococcus* and *Sporormiella* are recorded whereas *Sordaria* appears from 250 cm.

4.5 Pollen-inferred climate reconstructions

Pollen-inferred climate reconstructions corresponding to the Lateglacial period at Matese were partly discussed in Robles et al., in prep, that's why, we will describe only the results of the Phase 4 (Fig. 7). The results show similar trend except for the most recent period, between 260 and 190 cm where trends slightly diverge. Phase 4 is characterized by a strong increase of temperatures (MAAT, MTWA and MTCO). This phase contrasts to the cold phase 3 and is even warmer than the temperature Phase 2. However, MTWA values are close to the Phase 2 values (except for the MAT method). Considering hydrological parameters (PANN, P_{winter}), precipitation strongly increase until 300 cm and then their trends diverge according to the methods. The MAT shows an abrupt increase, the RF and BRT a slight increase whereas the WAPLS shows a decrease of precipitation. A decline in temperatures and precipitation seems depicted by all methods between 249 and 237 cm.

.

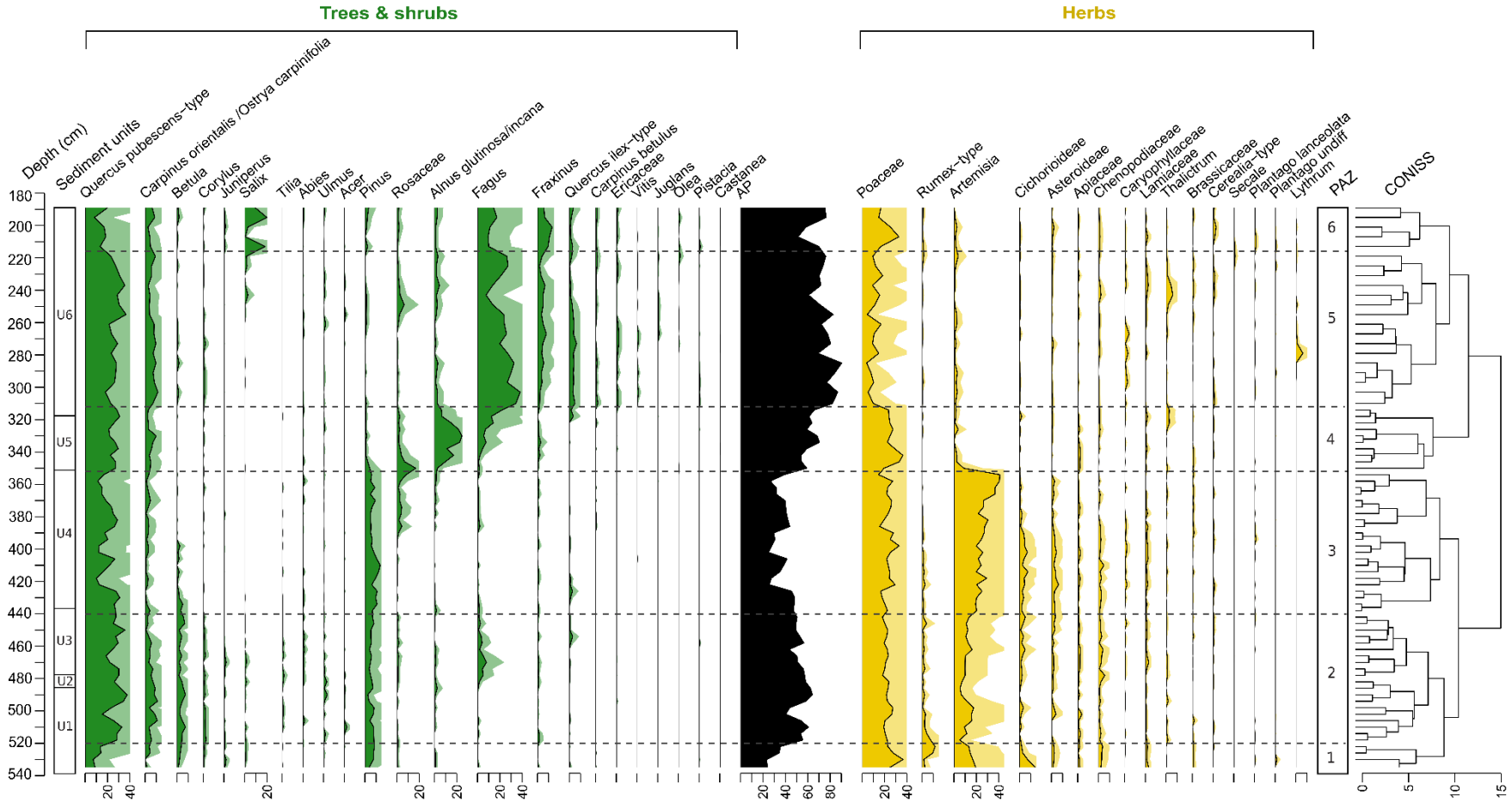

Figure IV-5. Selected terrestrial pollen taxa of the Lake Matese against core depth. Tree, shrub, and herb pollen taxa are expressed in percentages of total terrestrial pollen. AP: Arboreal Pollen. PAZ: Pollen Assemblage Zones.

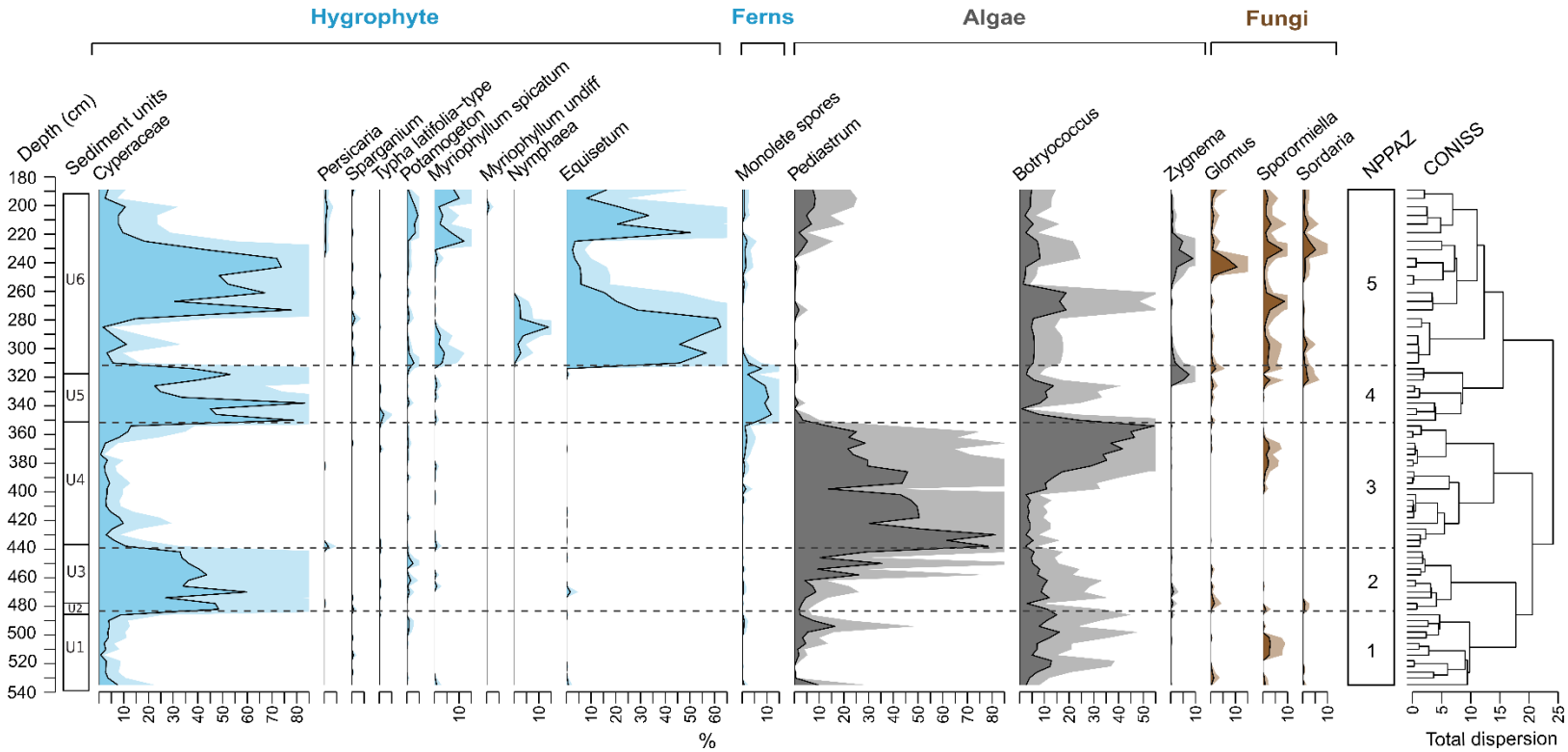

Figure IV-6. Selected pollen hygrophilous taxa and NPPs of the Lake Matese against core depth. Hygrophilous and aquatic pollen taxa are expressed in percentages of total pollen. Fern spores, algae and fungi are expressed in percentages of total terrestrial pollen and NPPs. NPPAZ: Non-Pollen Palynomorph Assemblage Zones.

.

4.6 GDGT climate reconstruction

The description of brGDGTs of the Matese core from 535 to 340 cm is discussed in Robles et al., in prep, that's why, we detail here the results between 340 and 190 cm (Fig. 8, 9 and 10).

The total concentration of brGDGTs ranges between 0.06 and 15 µg.g-1 dry sediment. The fractional abundances of brGDGTs (Fig. 8) still show a dominance of pentamethylated brGDGTs (II, 46%), followed by tetramethylated brGDGTs (I, 33%) and then hexamethylated brGDGTs (III, 21%). Samples of Unit 5 and 6 show a good correspondence with global lake and soil samples, except for one sample in Unit 5. Samples of lithologic Unit 5 seem more closed to global soil and peat samples than global lake samples.

The relative abundance of tetra-, penta-, hexamethylated brGDGTs, shows important changes during the Phase 4 (Fig. 9). Two periods (352-312 cm and 295-222 cm) show a large increase of tetramethylated brGDGTs whereas the relative abundance of penta- and hexamethylated brGDGTs decrease. Conversely, the two other periods (312-95 cm and 222-190 cm) are marked by a large decrease of tetramethylated brGDGTs, an increase of hexamethylated brGDGTs whereas the relative abundance pentamethylated brGDGTs are similar with the previous phase.

The degree of methylation (MBT, MBT'5Me) and the cyclisation ratio (CBT) also show large variation (Fig. 9). Two periods (352-312 cm and 295-222 cm) show an increase of all ratios whereas the two other periods (312-95 cm and 222-190 cm) show a decrease of all ratios.

The MAAT reconstructed using global (Sun et al., 2011) and East African (Russell et al., 2018) lacustrine calibrations and the MAF reconstructed using Bayesian (Martínez-Sosa et al., 2021) and high latitudes (Raberg et al., 2021) lacustrine calibrations show close trends and large variation along the Phase 4 (Fig. 10). Once again, two periods (352-312 cm and 295-222 cm) show an increase of temperatures for all calibrations whereas the two other periods (312-95 cm and 222-190 cm) show a decrease of temperatures for all calibrations.

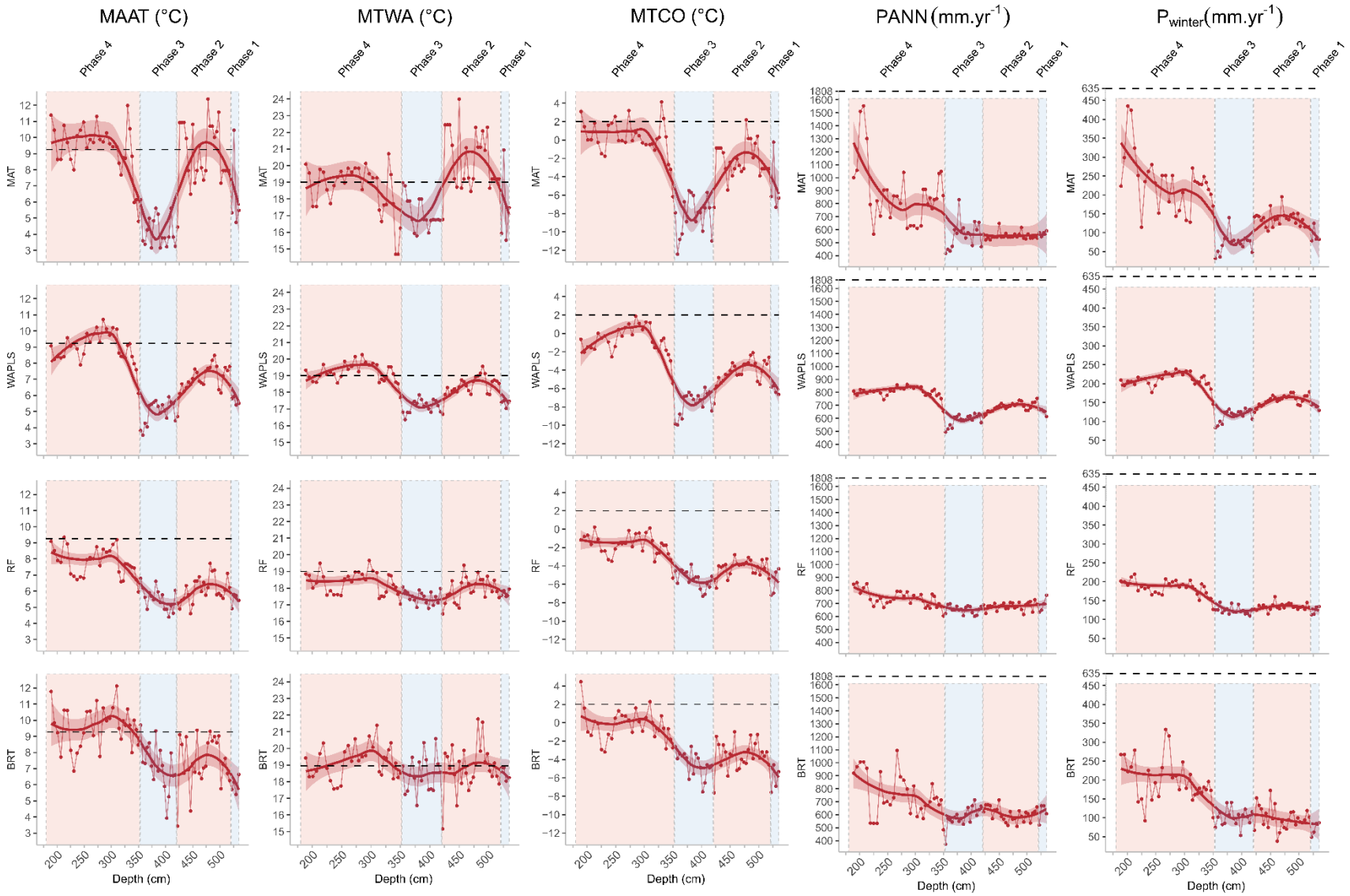
MAAT (°C)
MTWA (°C)
MTCO (°C)
PANN (mm.yr-1)
Pwinter (mm.yr-1)
Phase 4
Phase 3
Phase 2
Phase 1
MAT
WAPLS
RF
BRT
Depth (cm)

Figure IV-7. Pollen-inferred climate changes estimated using four methods: MAT (Modern Analogue Technique), WAPLS (Weighted Averaging Partial Least Squares regression), RF (Random Forest) and BRT (Boosted Regression Trees). Large lines correspond to loess smoothed curves, shaded areas to the 95% confidence interval and dotted lines to modern climate values of Lake Matese. MAAT: mean annual air temperature. MTWA: mean temperature of the warmest month. MAP: mean annual precipitation. P_{summer}: summer precipitation.

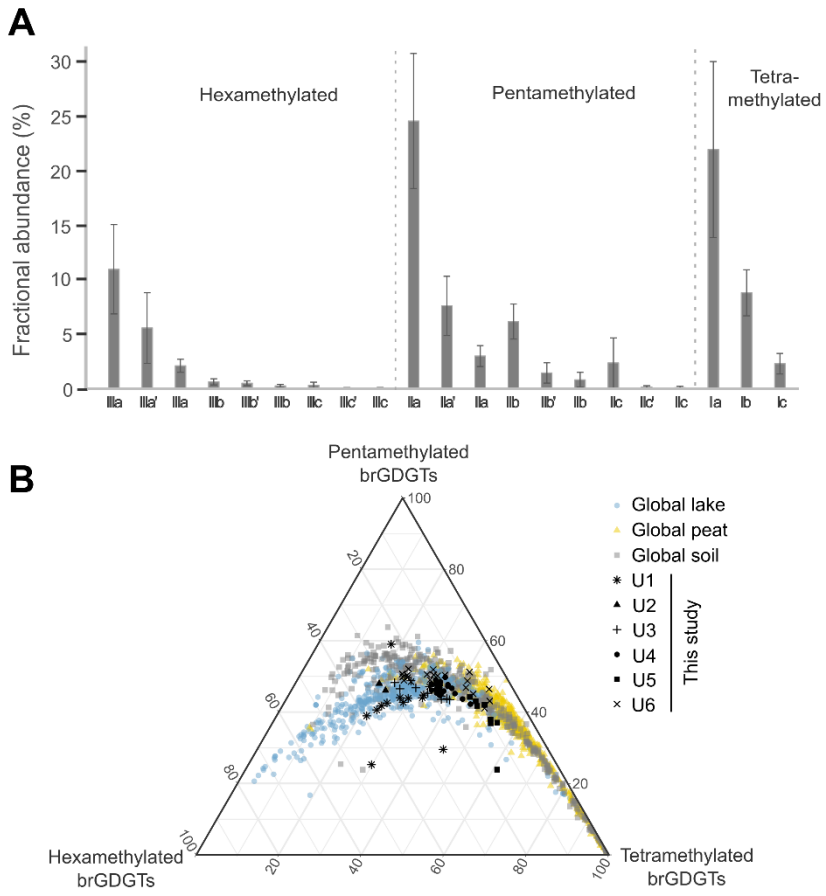

Figure IV-8. A) Fractional abundance of tetra-, penta-, and hexamethylated brGDGTs for Matese core. B) Ternary diagram showing the fractional abundances of the tetra-, penta-, and hexamethylated brGDGTs for Matese core (black points) and global lake (blue points; Martínez-Sosa et al., 2021), peat (yellow circles; Naafs et al., 2017a), and soils (gray circles; Yang et al., 2014; Naafs et al., 2017b).

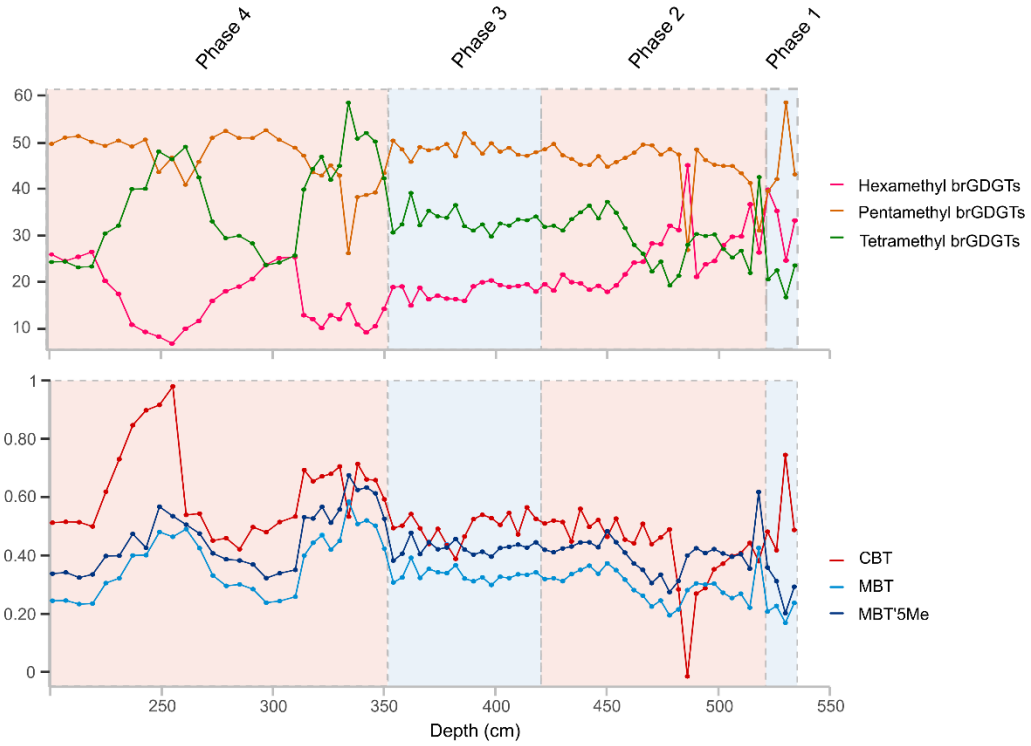

Figure IV-9. Fractional abundance of tetra-, penta-, and hexamethylated brGDGTs degree of methylation (MBT, MBT'5Me), cyclisation ratio (CBT) against depth for Matese core.

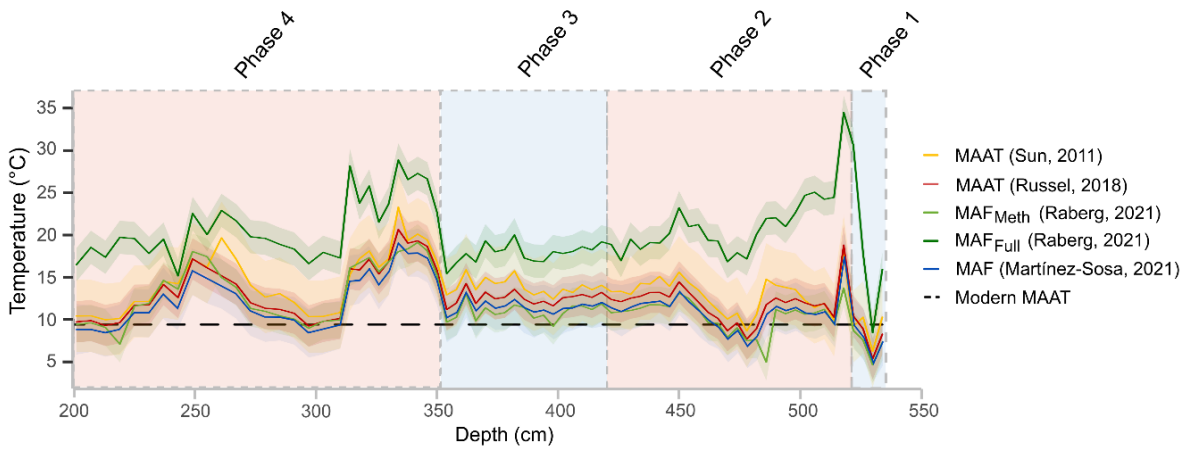

Figure IV-10. Temperature reconstructions based on brGDGTs against depth for Matese core. MAAT: mean annual air temperature. MAF: Months Above Freezing.

5. Discussion

5.1 Modern pollen rain in Matese Massifs

Modern pollen rain in Matese Massifs differs according to the altitude and the exposure of each site (Fig. 2). Botanical relevés were realized for each site, they will be used for the discussion and will soon be integrated in the results. Concerning arboreal pollen taxa, *Quercus pubescens*-type is not present in the local vegetation, except for the site n°15, and is very sparse in today's of the catchment of the Lake Matese. However, this taxon is recorded up to 15% which shows an over-representation and an input of regional vegetation close to the lake. Beech dense forests are present on slopes with northern exposure around the Lake Matese, however, *Fagus* represents only 10% of the pollen signal. Observed trees are young suggesting a low pollination. Considering samples located on the slopes with a southern exposure of the Lake Matese, they are surrounding by an open vegetation, however, modern pollen rain records arboreal pollen taxa and *Cerealia*-type. Trees are present around the lake and on the slopes with northern exposure whereas crops for agriculture locate only present around the lake. The open vegetation has certainly favored the long-distance transport of pollen (Jacobson and Bradshaw, 1981). Ferns are also present on the terraces formerly cultivated on the slopes with a southern exposure of the Lake Matese. Ferns are recorded in the modern pollen rain, however, spores seems short-distance transported and they represent mainly the local vegetation. Finally, very few markers of pastoralism are recorded in the modern pollen rain although the presence of extensive breeding is observed today around the Lake Matese.

5.2 Age-depth model of Matese core

The age-depth model was established for the levels between 535 and 340 cm by the previous study of Robles et al., in prep which was focusing on the climate changes during the Lateglacial and the beginning of the Holocene. It is based on one ^{14}C date and several tephra samples which were detected using magnetic susceptibility (MS) and Potassium (K) content. In the PCA of XRF data (Fig. 4), Potassium is also associated with Rubidium (Rb), Strontium (Sr) and Zinc (Zn) which show the same variations along the sequence (Fig. 5). K, Rb and Sr can be used and associated with tephra layers (Damaschke et al., 2013; Wulf et al., 2013). From 340 cm to the top of the core, the ^{14}C dates are not correct and appear too young, certainly due to the predominance of roots in the sediment. An age model only based on the ^{14}C dates appears as not reliable for the Lake Matese sequence.

Therefore, we are still in the process to detect and identify cryptotephra samples in gyttja sediment to propose an age model for the Holocene period. Meanwhile, several key pollen taxa observed at Matese can give indirect but valuable information on chronology and we can also try to check the appearance of these key taxa observed in other well-dated Italian pollen sequences to correlate them with the Matese record. For example, the Early Holocene is characterized by high proportion of Poaceae and the Mid-Holocene begins with the decline in Poaceae, the large increase of *Fagus* and the apparition of *Cerealia*-type (Palmisano et al., 2021). *Juglans* is also a key taxon for human impact, it appears between 3500-2500 cal BP in Central and South Italy (Allen et al., 2002; Mercuri et al., 2002; Sadori, 2018). An opening of forested environments is also recorded in southern Italy around 2600-2800 cal BP (Allen et al., 2002; Magny et al., 2011). Vegetation changes are described in detail in the following discussion (part 5.4).

5.3 Water level changes and ecological processes

Aquatic taxa, fern spores, and NPP changes are used altogether as an environmental indicators of lake dynamic and water-level changes. Following the previous study of Joannin et al. (2012) and Robles et al. (2022), we applied a ratio comprising algae (*Pediastrum, Botryococcus*), semi-aquatic plants (Cyperaceae, *Sparganium, Typha latifolia*) and ferns (*Asplenium, Botrychium, Pteropsida, Davallia, Polypodium, Selaginella*, monolete spores) to estimate water level changes (Fig. 11). The first division of CONISS applied on aquatic taxa, fern spores and NPPs oppose the Lateglacial to the Holocene (Fig. 6), indicating important changes between both period.

Major water level changes during the Lateglacial

The Oldest Dryas (OD) and the Bølling (NPPAZ 1) are characterized by a low development of semi-aquatic plants and the presence of *Botryococcus* showing a relative low water-level (Fig. 6). A high proportion of Calcium (Ca) is also recorded and may be derived from evaporative concentration or biogenic production (Cohen, 2003). Despite, an increase of precipitation at Matese during the Bølling in comparison with the OD (Robles et al., in prep), no significant water level changes are visible.

During the Older Dryas (Unit 2, NPPAZ 2), the sediment abruptly changes to become organic, and it is associated with a decrease in terrigenous inputs (Fig. 11). Cyperaceae developed and planktonic algae (*Botryococcus, Pediastrum*) largely decrease (Fig. 6) suggesting a reduction of water level. The Older Dryas is also marked by a low water level at Lake Accesa in Italy (Magny et al., 2006) whereas higher lake level is recorded in west-central Europe

(Magny, 2001). The Older Dryas event is not recorded in all sequence of the Mediterranean Basin, it corresponds to cold conditions in Northern Hemisphere (Rasmussen et al., 2014) and sometimes drier conditions around the Mediterranean area (Dormoy et al., 2009). At Matese, reconstructed precipitation based on pollen show no changes at this period (Robles et al., in prep).

The Allerød (NPPAZ 2) is characterized by a high proportion of Cyperaceae, the presence of *Botryococcus* and the progressive increase of *Pediastrum* showing an increase of water level during this period. Climate reconstructions of Italy show an increase of precipitation during the Allerød and a similar trend is recorded at Matese (Sbaffi et al., 2004; Larocque and Finsinger, 2008; Sicre et al., 2013; Heiri et al., 2014; Marchegiano et al., 2020; Robles et al., in prep).

The Younger Dryas (NPPAZ 3) is characterized by a high proportion of planktonic algae and on the contrary a low development of semi-aquatic plants suggesting a high level water. The most important water level of the sequence occurs at the beginning of the Younger Dryas and then it slighty decreases during this period although the level remains high. In Central Italy, the Lake Accesa also shows a high water level and a progressive decrease during this period (Magny et al., 2006). Concerning climate changes, a decline in temperatures is recorded in all Italy and a contrasted pattern occurs in terms of precipitation (Robles et al., in prep). A slight increase of precipitation is recorded in Southern Italy below latitude 42°N whereas drier conditions are recorded in Central and North Italy . At Matese, climate reconstructions based on pollen do not show changes in precipitation (Robles et al., in prep).

During the Lateglacial, water level changes of Lake Matese do not correlate with climate changes. This independancy migth well be linked to internal karstic system of the Matese'massif.

Ecological processes in shallow water during the Holocene

The Early Holocene (NPPAZ 4) is characterized by a major and abrupt decline in planktonic algae and the development of Cyperaceae and ferns, indicating a major decline in water level. A low pollen concentration is also recorded and could be linked to tephra which are recorded during this period. Indeed, tephra fall can induce a reduced vegetation productivity causing lower pollen accumulation rates (Allen and Huntley, 2018). In the South of Italy, the beginning of the Holocene is also marked by a low level water at Trifoglietti in Calabria (Joannin et al., 2012) and at Lake Pergusa in Sicily (Magny et al., 2011) whereas an increase of the water level is recorded from 11,000-10,500 cal BP in both sites. According to climate

reconstructions, the beginning of the Holocene is marked by dry conditions in southern Italy which is consistent with low water level (Joannin et al., 2012; Peyron et al., 2013).

The Mid and Late Holocene (NPPAZ 5) are marked by a low level of water with either a dominance of Cyperaceae or *Equisetum*. This is in accord with the site of Trifoglietti, where a low level water is also recorded (Joannin et al., 2012), but differs with the site of Lake Preola where a high level water is recorded during the Mid Holocene and a low water level during the Late Holocene (Magny et al., 2011). The last period at Matese (PAZ 6) shows the development of *Salix* and certainly the recent installation of the floating rafting, which is still present on the Lake Matese.

5.4 Vegetation dynamics in Southern Italy

Vegetation changes (Fig. 6) indicate marked environmental changes during the Lateglacial and the Holocene. The first division of CONISS applied on terrestrial pollen oppose the Lateglacial to the Holocene, indicating major vegetation change between both period.

Poaceae-Artemisia dominance during the Oldest Dryas

At Matese, the Oldest Dryas (PAZ 1) is characterized by an open vegetation dominated by Poaceae, *Artemisia* and secondly by *Rumex*-type and Cichorioideae (Fig. 5). During this period, open vegetation dominated by Poaceae and *Artemisia* is also recorded in Southern Italy (Monticchio, Allen et al., 2002; Trifoglietti, De Beaulieu et al., 2017), Central Italy (Accesa, Drescher-Schneider et al., 2007; Mezzano, Sadori, 2018) and Northern Italy (Pavullo nel Frignano; Vescovi et al., 2010). *Pinus* is also recorded in the pollen records, associated to *Juniperus* in some northern and central sites (Drescher-Schneider et al., 2007; Vescovi et al., 2010) and *Quercus pubescens*-type in southern sites (De Beaulieu et al., 2017; this study). Modern pollen samples located in the catchment of Lake Matese (Samples 1-11) show that *Quercus pubescens*-type could represent up to 15% even if there is only few trees in the catchment (Fig. 2). During the OD, *Quercus pubescens*-type represents less than 15%, indicating that it was certainly not present in the catchment of the Lake Matese but in the regional vegetation.

Afforestation during the Bølling-Allerød (14,700-12,900 cal BP)

The Bølling-Allerød (520-423 cm) is characterized, at Matese, by a large increase of *Quercus pubescens*-type and a diversification of arboreal pollen taxa including *Betula* and *Fagus*. At this period, *Artemisia* largely decrease whereas the proportion of Poaceae remains

abundant (Fig. 5). In several Italian records (Allen et al., 2002; Drescher-Schneider et al., 2007; Vescovi et al., 2010; De Beaulieu et al., 2017; Sadori, 2018), an increase of arboreal taxa is also recorded and they show the presence of deciduous and thermophilous taxa *Quercus, Betula, Corylus, Tilia* and *Ulmus* as at Matese. A decline in *Artemisia* and a maintaining of Poaceae is also visible in the majority of records (Allen et al., 2002; Drescher-Schneider et al., 2007; Vescovi et al., 2010; Sadori, 2018). However, only the sites located in southern Italy records *Fagus* (Allen et al., 2002; De Beaulieu et al., 2017; this study). Modern pollen samples located in the catchment of Lake Matese (Samples 9-11) show that *Fagus* could represent less than 10% even if samples are located in beech forest. During the Bølling-Allerød, deciduous *Quercus* and *Fagus* and grassland were probably present both in the catchment of the Lake Matese and in the regional vegetation. During this period, climate reconstructions based on several and independant proxies reveal warmer and wetter conditions in all Italy (Robles et al., in prep). These climate changes are consistent with vegetation dynamics which are very close in the different italian records. The presence of *Fagus* in southern Italy could be linked to the closer locality of refugia in this area during the Lateglacial (Magri, 2008).

Contrasted vegetation during the Younger Dryas (12,900-11,700 cal BP)

The vegetation during the Younger Dryas (423-352 cm) at Matese is marked by the increase of *Artemisia*, Cichorioideae and Asteroideae and a large decrease of arboreal taxa (Fig. 6). At this period, the surrounding vegetation in the catchment of the Lake Matese was certainly largely open. An increase of *Artemisia* and Poaceae is also recorded in the Central (Drescher-Schneider et al., 2007; Sadori, 2018) and Southern Italy (Allen et al., 2002; Ermolli and di Pasquale, 2002; this study). However, this increase is less important or not visible in southern sites (Monticchio, Trifoglietti) and it is not accompanied by a decrease of arboreal taxa (Allen et al., 2002; De Beaulieu et al., 2017). Climate reconstructions based on different proxies show that the Younger Dryas was cold for the entire Italy and that a slight increase in precipitation is recorded in southern Italy (south of 42°N) whereas drier conditions are recorded in northern sites (north of 42°) (Robles et al., in prep). Wetter conditions have certainly allowed deciduous trees to persist in southern Italy despite colder conditions contrary to other sites where a large decline of arboreal taxa is recorded.

Mixed grassland and woodland environment during the Early Holocene

At Matese, the Early Holocene (PAZ 4) is characterized by a large increase of arboreal taxa, mainly linked to the surrounding vegetation of the lake (Fig. 5). Rosaceae firstly develop and then they are replaced by *Alnus* and ferns (Fig. 5-6). At this period, *Artemisia* abruptly disappears whereas Poaceae remains abundant as for the majority of records in Italy (Allen et al., 2002; Tinner et al., 2009; Vescovi et al., 2010; Joannin et al., 2012; Sadori, 2018). Deciduous taxa such as *Fagus* and *Quercus* also increase during this period in Italy (Sadori and Narcisi, 2001; Joannin et al., 2012; this study) however their expansion remains limited at the beginning of the Early Holocene. In the littoral sites of Sicily, a dominance of sclerophyllous shrubs are recorded and they are associated with a low water level (Tinner et al., 2009; Magny et al., 2011). The beginning of the Holocene is marked by dry conditions in southern Italy (Joannin et al., 2012; Peyron et al., 2013) which have certainly favored the maintenance of Poaceae and limited the expansion of deciduous forests. However, the end of the Early Holocene is characterized by wet and warm conditions allowing trees development (Joannin et al., 2012; Peyron et al., 2013).

Predominance of forests during the Mid-Late Holocene

At Matese, the Mid and Late Holocene (PAZ 5) is marked by the increase of arboreal pollen taxa including *Fagus*, *Fraxinus* but also Mediterranean taxa such as *Quercus ilex*-type (Fig. 5). Pollen of *Vitis* are also recorded during the maximum of arboreal taxa but it is certainly wild because *Vitis* is not cultivated during the Neolithic in the South of Italy. The majority of records in southern Italy show a large proportion of arboreal pollen taxa during the Mid Holocene (Allen et al., 2002; Ermolli and di Pasquale, 2002; Caroli and Caldara, 2007; Tinner et al., 2009; Joannin et al., 2012). The expansion of forest occurs during a period which corresponds to the climate optimum. At 243 cm, a rapid change seems to occur with the large decrease of *Fagus* and the emergence of Rosaceae. However, the resolution is not optimal for this part of the pollen diagram and at date, we don't have reliable dates to correctly interpret this event.

The last period (PAZ 6) is marked by the decrease of regional arboreal taxa such as *Fagus* and *Quercus pubescent*-type. The opening of the forested environments is also recorded in Southern Italy, at Preola and at Monticchio around 2600-2800 cal BP (Allen et al., 2002; Magny et al., 2011).

5.5 Human impact

Human impact can be discussed through the presence of several pollen taxa associated to human activities in Matese record (Fig. 5). The first potential anthropogenic signal is an increase of *Cerealia*-type which we associate with the beginning of the Mid Holocene. The development of agriculture in Italy corresponds to the Neolithic. It is evidenced, primarily in lowland and then at higher elevations, in the Appenines (Palmisano et al., 2021). The Early Neolithic is particularly marked by a significant increase of demography in Southern Italy (Palmisano et al., 2021). However, the percentages of pollen of cereals remains low and it should be noted that wild Poaceae, such as *Glyceria*, can correspond to *Cerealia*-type (van Zeist and Bottema, 1975; Muller et al., 2022). For the moment, no archeological data are available for this period to confirm or refute the presence of agriculture around the Lake Matese.

Then, *Juglans* is recorded between 267 and 243 cm at Matese. *Juglans* is a taxon, cultivated by humans in the Mediterranean area for its high-quality wood and nuts (Pollegioni et al., 2017). Its current distribution results from its exploitation by humans over the last 5000 years around the Mediterranean Basin (Pollegioni et al., 2017). In Central and Southern Italy, *Juglans* is recorded in pollen sequences from 3500-2500 cal BP (Allen et al., 2002; Mercuri et al., 2002; Sadori, 2018). This period corresponds to the Bronze Age and the Early Iron Age and it is characterized by a large increase of population in Southern Italy with the presence of settlements in lowland and upland areas (Palmisano et al., 2021). At this period, populations intensified cereal cultivated and they began the culture of tress/vines such as *Olea*, *Juglans*, *Castanea* and *Vitis* (Palmisano et al., 2021). At Matese, only *Juglans* seems recorded during this period and this taxon disappears at 243 cm when a rapid climate change seems to occur (Fig. 7).

Finally, *Cerealia*-type and *Secale* are recorded from 250 cm, accompanied by *Olea* and a large decline in arboreal pollen taxa (Fig. 5). *Olea* is cultivated for its fruits and it appears tardively at Matese in comparison with some sites (Caroli and Caldara, 2007; Tinner et al., 2009). *Cerealia*-type and *Secale* are certainly indicator of agricultural practices around the lake. This period could be consistent with the presence of pre-Roman and Roman settlements (2150 and 1550 cal BP) around the Lake Matese (Soricelli, 2013). An opening of forested environments is also recorded at Preola and Monticchio around 2800-2600 cal BP (Allen et al., 2002; Magny et al., 2011). This change has an anthropogenic origin and would be linked to the Greek colonisation in Italy (Magny et al., 2011).

5.6 Climate changes in Central-Southern Italy

Pollen-based and GDGT-based temperature reconstructions of Lake Matese are roughly in agreement for the Lateglacial period (Fig. 11). The accuracy and the interpretation of the climate reconstructions for the Lateglacial is discussed in detail in Robles et al. (in prep).

In contrast to the Lateglacial, the pollen-inferred temperatures reconstructed for the Holocene are very different from those based on GDGTs which evidence more marked climate changes (Fig. 11). The advantage of GDGTs is that GDGTs are considered as a climate proxy independent to the vegetation changes, unlike pollen data which can be influenced by human impact, especially during the late Holocene. However, other factors (water level, lithological changes, erosion…) can also influence the GDGTs distribution, and then the temperature reconstruction. The differences between pollen and GDGTs at Matese will be investigated in detail but we first need a reliable age model for the Holocene period to be able to compare the Lake Matese temperature reconstructions with the climate patterns based on other proxies. When the uncertainties related to the Lake Matese age model will be clarified, our results will certainly help to answer the following questions on the Holocene climate changes.

Holocene temperature reconstructions are key to placing industrial-era warming into the perspective of natural climatic variability. The Central-Southern Italy is a region highly sensitive to climate changes, and recent studies reveal a very complex picture of climate variability within this region for the Holocene. For example, the northern and southern regions of Italy have been under the prevalent influence of different climate patterns (around 40°N), producing opposite hydrological regimes and consequent vegetation dynamics (Magny et al., 2013; Peyron et al., 2013). Moreover, recurrent forest declines and dry events are recorded in the south-central Mediterranean (Italy) while an opposite pattern is suggested for the south-western Mediterranean, indicating a spatio-temporal hydrological pattern opposite to the south-central Mediterranean and suggesting that different expressions of climate modes occurred in the two regions at the same time (Di Rita et al., 2018). The Holocene also exhibits a millennial-scale climate variability (Azuara et al., 2020; Marriner et al., 2022) and abrupt events as the 7.5 ka (Joannin et al., 2012) or the 4.2 ka (e.g. Bini et al., 2019, 2019; Kaniewski et al., 2019). These spatio-temporal patterns and underlying processes during the Holocene are not fully deciphered yet. Lake Matese is located in a key region close to 40°N: a better understanding of the climate signal obtained at Matese will allow to go further in the knowledge of these spatio-temporal patterns and underlying processes during the Holocene in the Central Mediterranean.

Many studies suggest large discrepancies for the Mediterranean region between pollen-based temperature reconstructions and climate patterns inferred from other proxies or from climate models for the Mid Holocene:

- The global-scale pollen-inferred climate reconstructions indicate cooler-than-present Mid Holocene summers in the Mediterranean area (Cheddadi et al., 1998; Davis et al., 2003; Mauri et al., 2014). This pattern contrasts with the thermal maximum reconstructed at 9000-5000 yrs BP from chironomids assemblages (Samartin et al., 2017), and with the thermal maximum evidenced by Marriner et al. (2022) 8000-6000 years ago (SSTs changes).

- The cooler-than-present climate pattern reconstructed from pollen data is also different than the climate models (GCMs) simulations which indicate warmer conditions than today (e.g. Mauri et al., 2014, 2015).

Most pollen-based climate reconstructions have been done using the best analogue method, and the results may have been different with another method. Our results show, however, that for Lake Matese the four methods show very consistent results for the Holocene.

Pollen records are abundant in the Mediterranean while GDGT and chironomid data are very scarce: more GDGTs and chironomids sequences are needed to better understand the reconstructed temperature signal (annual and summer) and the climatic processes (North Atlantic Oscillation, high pressures...) during the Holocene in the Central Mediterranean.

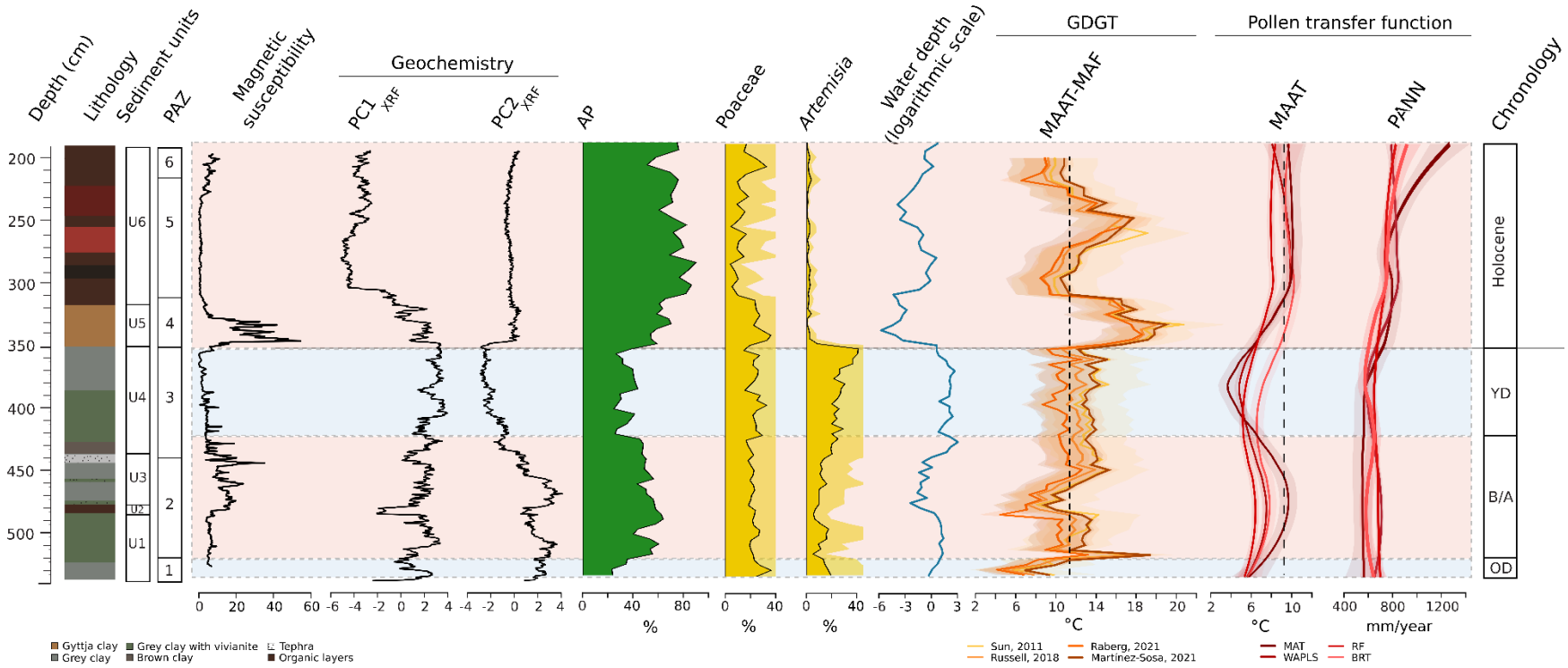

Figure IV-11. Synthesis of the main data, including lithology, magnetic susceptibility, XRF data, pollen, water depth, climate reconstructions based on pollen and brGDGTs of the lake Matese against depth. Water depth = (Algae+1)/(semi-aquatic plants+1))/(ferns +1) plotted on a logarithmic scale: algae (*Pediastrum*, *Botryococcus*), semi-aquatic plants (Cyperaceae, *Sparganium*, *Typha latifolia*) and ferns (*Asplenium*, *Botrychium*, *Pteropsida*, *Davallia*, *Polypodium*, *Selaginella*, monolete spores) to estimate water level changes.

6. Conclusions

This multiproxy study has enabled the reconstruction of environmental dynamic, human activities and climate changes during the last 15,000 years from the sequence of Lake Matese located in Italy. This study appears in the continuity of the previous study, Robles et al. (in prep), that was focusing on climate changes during the Lateglacial from the sequence of Lake Matese.

- Modern pollen rain of Matese Massifs records mediterranean evergreen taxa at low elevation (600 m), deciduous arboreal taxa at higher elevation (800-1000) and a dominance of Poaceae on Lake Matese catchment with southern exposure.
- Major paleohydrological changes are recorded at Matese during the last 15,000 years and they show a first opposition between the Lateglacial and the Holocene, which records a high/intermediate water level and a low water level respectively. More specifically, the Oldest Dryas and the Bølling–Allerød are characterized by an intermediate water level whereas the Younger Dryas records the highest water level of the sequence. The Early Holocene is marked by a very low water level whereas the Mid-Late Holocene are characterized by a low water level.
- The vegetation is dominated by Poaceae and *Artemisia* during the Lateglacial and an increase of deciduous arboreal taxa, including deciduous *Quercus* and *Betula*, marks the Bølling–Allerød. The Holocene is firstly characterized by the persistent of Poaceae and then the development of *Fagus* and some mediterranean taxa during the Mid-Late Holocene. Deciduous *Quercus* remains abundant throughout the sequence.
- Human activities are firstly recorded with the apparition of *Juglans* around 3500-2500 cal BP in Southern Italy and an intensification of human impact is observed when the forest opened around 2600-2800 cal BP, accompanied by the apparition of cereals and *Olea.*
- Climate reconstructions based on brGDGTs and pollen are rather consistent during the Lateglacial whereas the climate trends diverge during the Holocene. Our study suggests a dominant impact of climate changes on vegetation dynamic and a recent human impact.

References

Allen, J.R.M., Huntley, B., 2018. Effects of tephra falls on vegetation: A Late-Quaternary record from southern Italy. J Ecol 106, 2456–2472. https://doi.org/10.1111/1365-2745.12998

Allen, J.R.M., Watts, W.A., McGee, E., Huntley, B., 2002. Holocene environmental variability-the record from Lago Grande di Monticchio, Italy. Quaternary International 88, 69–80.

Aucelli, P.P.C., Cesarano, M., Di Paola, G., Filocamo, F., Rosskopf, C.M., 2013. Geomorphological map of the central sector of the Matese Mountains (Southern Italy): an example of complex landscape evolution in a Mediterranean mountain environment. Journal of Maps 9, 604–616. https://doi.org/10.1080/17445647.2013.840054

Azuara, J., Sabatier, P., Lebreton, V., Jalali, B., Sicre, M.-A., Dezileau, L., Bassetti, M.-A., Frigola, J., Combourieu-Nebout, N., 2020. Mid- to Late-Holocene Mediterranean climate variability: Contribution of multi-proxy and multi-sequence comparison using wavelet spectral analysis in the northwestern Mediterranean basin. Earth-Science Reviews 208, 103232. https://doi.org/10.1016/j.earscirev.2020.103232

Beug, H.-J., 2004. Leitfaden der Pollenbestimmung für Mitteleuropa und angrenzende Gebiete. Friedrich Pfeil, München.

Bini, M., Zanchetta, G., Persoiu, A., Cartier, R., Català, A., Cacho, I., Dean, J.R., Rita, F.D., Drysdale, R.N., Finnè, M., Isola, I., Jalali, B., Lirer, F., Magri, D., Masi, A., Marks, L., Mercuri, A.M., Peyron, O., Sadori, L., Sicre, M.-A., Welc, F., Zielhofer, C., Brisset, E., 2019. The 4.2 ka BP Event in the Mediterranean region: an overview. Clim. Past 23.

Breiman, L., 2001. Random Forests. Machine Learning 45, 5–32. https://doi.org/10.1023/A:1010933404324

Caroli, I., Caldara, M., 2007. Vegetation history of Lago Battaglia (eastern Gargano coast, Apulia, Italy) during the middle-late Holocene. Veget Hist Archaeobot 16, 317–327. https://doi.org/10.1007/s00334-006-0045-y

Carranza, M.L., Frate, L., Paura, B., 2012. Structure, ecology and plant richness patterns in fragmented beech forests. Plant Ecology & Diversity 5, 541–551. https://doi.org/10.1080/17550874.2012.740509

Cheddadi, R., Lamb, H.F., Guiot, J., van der Kaars, S., 1998. Holocene climatic change in Morocco: a quantitative reconstruction from pollen data. Climate Dynamics 14, 883–890. https://doi.org/10.1007/s003820050262

Chevalier, M., Davis, B.A.S., Heiri, O., Seppä, H., Chase, B.M., Gajewski, K., Lacourse, T., Telford, R.J., Finsinger, W., Guiot, J., Kühl, N., Maezumi, S.Y., Tipton, J.R., Carter,

V.A., Brussel, T., Phelps, L.N., Dawson, A., Zanon, M., Vallé, F., Nolan, C., Mauri, A., de Vernal, A., Izumi, K., Holmström, L., Marsicek, J., Goring, S., Sommer, P.S., Chaput, M., Kupriyanov, D., 2020. Pollen-based climate reconstruction techniques for late Quaternary studies. Earth-Science Reviews 210, 103384. https://doi.org/10.1016/j.earscirev.2020.103384

Cohen, A.S., 2003. Paleolimnology: the history and evolution of lake systems. Oxford University Press, New York.

Damaschke, M., Sulpizio, R., Zanchetta, G., Wagner, B., Böhm, A., Nowaczyk, N., Rethemeyer, J., Hilgers, A., 2013. Tephrostratigraphic studies on a sediment core from Lake Prespa in the Balkans. Climate of the Past 9, 267–287. https://doi.org/10.5194/cp-9-267-2013

Davis, B.A.S., Brewer, S., Stevenson, A.C., Guiot, J., 2003. The temperature of Europe during the Holocene reconstructed from pollen data. Quaternary Science Reviews 22, 1701–1716. https://doi.org/10.1016/S0277-3791(03)00173-2

Davtian, N., Bard, E., Ménot, G., Fagault, Y., 2018. The importance of mass accuracy in selected ion monitoring analysis of branched and isoprenoid tetraethers. Organic Geochemistry 118, 58–62. https://doi.org/10.1016/j.orggeochem.2018.01.007

De Beaulieu, J.-L., Brugiapaglia, E., Joannin, S., Guiter, F., Zanchetta, G., Wulf, S., Peyron, O., Bernardo, L., Didier, J., Stock, A., Rius, D., Magny, M., 2017. Lateglacial-Holocene abrupt vegetation changes at Lago Trifoglietti in Calabria, Southern Italy: The setting of ecosystems in a refugial zone. Quaternary Science Reviews 158, 44–57. https://doi.org/10.1016/j.quascirev.2016.12.013

De Jonge, C., Stadnitskaia, A., Hopmans, E.C., Cherkashov, G., Fedotov, A., Sinninghe Damsté, J.S., 2014. In situ produced branched glycerol dialkyl glycerol tetraethers in suspended particulate matter from the Yenisei River, Eastern Siberia. Geochimica et Cosmochimica Acta 125, 476–491. https://doi.org/10.1016/j.gca.2013.10.031

De'ath, G., 2007. Boosted trees for ecological modeling and prediction. Ecology 88, 243–251. https://doi.org/10.1890/0012-9658(2007)88[243:BTFEMA]2.0.CO;2

Di Rita, F., Fletcher, W.J., Aranbarri, J., Margaritelli, G., Lirer, F., Magri, D., 2018. Holocene forest dynamics in central and western Mediterranean: periodicity, spatio-temporal patterns and climate influence. Sci Rep 8, 8929. https://doi.org/10.1038/s41598-018-27056-2

Di Rita, F., Magri, D., 2009. Holocene drought, deforestation and evergreen vegetation development in the central Mediterranean: a 5500 year record from Lago Alimini

Piccolo, Apulia, southeast Italy. The Holocene 19, 295–306. https://doi.org/10.1177/0959683608100574

Ding, S., Schwab, V.F., Ueberschaar, N., Roth, V.-N., Lange, M., Xu, Y., Gleixner, G., Pohnert, G., 2016. Identification of novel 7-methyl and cyclopentanyl branched glycerol dialkyl glycerol tetraethers in lake sediments. Organic Geochemistry 102, 52–58. https://doi.org/10.1016/j.orggeochem.2016.09.009

Dormoy, I., Peyron, O., Nebout, N.C., Goring, S., Kotthoff, U., Magny, M., Pross, J., 2009. Terrestrial climate variability and seasonality changes in the Mediterranean region between 15 000 and 4000 years BP deduced from marine pollen records. Clim. Past 18.

Drescher-Schneider, R., de Beaulieu, J.-L., Magny, M., Walter-Simonnet, A.-V., Bossuet, G., Millet, L., Brugiapaglia, E., Drescher, A., 2007. Vegetation history, climate and human impact over the last 15,000 years at Lago dell'Accesa (Tuscany, Central Italy). Veget Hist Archaeobot 16, 279–299. https://doi.org/10.1007/s00334-006-0089-z

Dugerdil, L., Joannin, S., Peyron, O., Jouffroy-Bapicot, I., Vannière, B., Boldgiv, B., Unkelbach, J., Behling, H., Ménot, G., 2021a. Climate reconstructions based on GDGT and pollen surface datasets from Mongolia and Baikal area: calibrations and applicability to extremely cold–dry environments over the Late Holocene. Clim. Past 17, 1199–1226. https://doi.org/10.5194/cp-17-1199-2021

Dugerdil, L., Ménot, G., Peyron, O., Jouffroy-Bapicot, I., Ansanay-Alex, S., Antheaume, I., Behling, H., Boldgiv, B., Develle, A.-L., Grossi, V., Magail, J., Makou, M., Robles, M., Unkelbach, J., Vannière, B., Joannin, S., 2021b. Late Holocene Mongolian climate and environment reconstructions from brGDGTs, NPPs and pollen transfer functions for Lake Ayrag: Paleoclimate implications for Arid Central Asia. Quaternary Science Reviews 273, 107235. https://doi.org/10.1016/j.quascirev.2021.107235

Elith, J., Leathwick, J.R., Hastie, T., 2008. A working guide to boosted regression trees. J Anim Ecology 77, 802–813. https://doi.org/10.1111/j.1365-2656.2008.01390.x

Ermolli, E.R., di Pasquale, G., 2002. Vegetation dynamics of south-western Italy in the last 28 kyr inferred from pollen analysis of a Tyrrhenian Sea core. Veget Hist Archaeobot 11, 211–220. https://doi.org/10.1007/s003340200024

Faegri, K., Kaland, P.E., Krzywinski, K., 1989. Textbook of pollen analysis. John Wiley & Sons, Chichester.

Farney, G.D., Bradley, G., 2018. The peoples of ancient Italy. De Gruyter, Boston/Berlin.

Ferranti, L., Milano, G., Burrato, P., Palano, M., Cannavò, F., 2015. The seismogenic structure of the 2013–2014 Matese seismic sequence, Southern Italy: implication for the

geometry of the Apennines active extensional belt. Geophysical Journal International 201, 823–837. https://doi.org/10.1093/gji/ggv053

Ferrarini, F., Boncio, P., de Nardis, R., Pappone, G., Cesarano, M., Aucelli, P.P.C., Lavecchia, G., 2017. Segmentation pattern and structural complexities in seismogenic extensional settings: The North Matese Fault System (Central Italy). Journal of Structural Geology 95, 93–112. https://doi.org/10.1016/j.jsg.2016.11.006

Fiorillo, F., Doglioni, A., 2010. The relation between karst spring discharge and rainfall by cross-correlation analysis (Campania, southern Italy). Hydrogeol J 18, 1881–1895. https://doi.org/10.1007/s10040-010-0666-1

Fiorillo, F., Pagnozzi, M., 2015. Recharge processes of Matese karst massif (southern Italy). Environ Earth Sci 74, 7557–7570. https://doi.org/10.1007/s12665-015-4678-y

Galli, P., Giaccio, B., Messina, P., Peronace, E., Amato, V., Naso, G., Nomade, S., Pereira, A., Piscitelli, S., Bellanova, J., Billi, A., Blamart, D., Galderisi, A., Giocoli, A., Stabile, T., Thil, F., 2017. Middle to Late Pleistocene activity of the northern Matese fault system (southern Apennines, Italy). Tectonophysics 699, 61–81. https://doi.org/10.1016/j.tecto.2017.01.007

Giancola, C., Stanisci, A., 2006. La vegetazione delle rupi di altitudine del Molise. Fitosociologia 43, 9.

Grieser, J., Gommes, R., Bernardi, M., 2006. New LocClim - the Local Climate Estimator of FAO. Geophysical Research Abstracts 8, 2.

Grimm, E.C., 1987. CONISS: a FORTRAN 77 program for stratigraphically constrained cluster analysis by the method of incremental sum of squares. Computers & Geosciences 13, 13–35. https://doi.org/10.1016/0098-3004(87)90022-7

Guarino, R., Bazan, G., Paura, B., 2015. Downy-Oak Woods of Italy: Phytogeographical Remarks on a Controversial Taxonomic and Ecologic Issue, in: Box, E.O., Fujiwara, K. (Eds.), Warm-Temperate Deciduous Forests around the Northern Hemisphere, Geobotany Studies. Springer International Publishing, Cham, pp. 139–151. https://doi.org/10.1007/978-3-319-01261-2_7

Guilaine, J., 2003. De la vague à la tombe: la conquête néolithique de la Méditerranée, 8000-2000 avant J.-C. Seuil, Paris.

Guiot, J., 1990. Methodology of the last climatic cycle reconstruction in France from pollen data. Palaeogeography, Palaeoclimatology, Palaeoecology, Methods for the Study of Stratigraphical Records 80, 49–69. https://doi.org/10.1016/0031-0182(90)90033-4

Guiot, J., de Beaulieu, J.L., Cheddadi, R., David, F., Ponel, P., Reille, M., 1993. The climate in Western Europe during the last Glacial/Interglacial cycle derived from pollen and insect remains. Palaeogeography, Palaeoclimatology, Palaeoecology 103, 73–93. https://doi.org/10.1016/0031-0182(93)90053-L

Heiri, O., Brooks, S.J., Renssen, H., Bedford, A., Hazekamp, M., Ilyashuk, B., Jeffers, E.S., Lang, B., Kirilova, E., Kuiper, S., Millet, L., Samartin, S., Toth, M., Verbruggen, F., Watson, J.E., van Asch, N., Lammertsma, E., Amon, L., Birks, H.H., Birks, H.J.B., Mortensen, M.F., Hoek, W.Z., Magyari, E., Muñoz Sobrino, C., Seppä, H., Tinner, W., Tonkov, S., Veski, S., Lotter, A.F., 2014. Validation of climate model-inferred regional temperature change for late-glacial Europe. Nat Commun 5, 4914. https://doi.org/10.1038/ncomms5914

Hewitt, G.M., 2011. Mediterranean Peninsulas: The Evolution of Hotspots, in: Zachos, F.E., Habel, J.C. (Eds.), Biodiversity Hotspots: Distribution and Protection of Conservation Priority Areas. Springer, Berlin, Heidelberg, pp. 123–147. https://doi.org/10.1007/978-3-642-20992-5_7

Hopmans, E.C., Schouten, S., Sinninghe Damsté, J.S., 2016. The effect of improved chromatography on GDGT-based palaeoproxies. Organic Geochemistry 93, 1–6. https://doi.org/10.1016/j.orggeochem.2015.12.006

Huguet, C., Hopmans, E.C., Febo-Ayala, W., Thompson, D.H., Sinninghe Damsté, J.S., Schouten, S., 2006. An improved method to determine the absolute abundance of glycerol dibiphytanyl glycerol tetraether lipids. Organic Geochemistry 37, 1036–1041. https://doi.org/10.1016/j.orggeochem.2006.05.008

Jacobson, G.L., Bradshaw, R.H.W., 1981. The Selection of Sites for Paleovegetational Studies. Quat. res. 16, 80–96. https://doi.org/10.1016/0033-5894(81)90129-0

Joannin, S., Brugiapaglia, E., de Beaulieu, J.-L., Bernardo, L., Magny, M., Peyron, O., Goring, S., Vannière, B., 2012. Pollen-based reconstruction of Holocene vegetation and climate in southern Italy: the case of Lago Trifoglietti. Clim. Past 8, 1973–1996. https://doi.org/10.5194/cp-8-1973-2012

Juggins, S., Juggins, M.S., 2020. Package 'rioja.'

Kaniewski, D., Marriner, N., Bretschneider, J., Jans, G., Morhange, C., Cheddadi, R., Otto, T., Luce, F., Van Campo, E., 2019. 300-year drought frames Late Bronze Age to Early Iron Age transition in the Near East: new paleoecological data from Cyprus and Syria. Reg Environ Change 19, 2287–2297. https://doi.org/10.1007/s10113-018-01460-w

Larocque, I., Finsinger, W., 2008. Late-glacial chironomid-based temperature reconstructions for Lago Piccolo di Avigliana in the southwestern Alps (Italy). Palaeogeography, Palaeoclimatology, Palaeoecology 257, 207–223. https://doi.org/10.1016/j.palaeo.2007.10.021

Lê, S., Josse, J., Husson, F., 2008. FactoMineR: An R Package for Multivariate Analysis. Journal of Statistical Software 25, 1–18. https://doi.org/10.18637/jss.v025.i01

Magny, M., 2001. Palaeohydrological changes as reflected by lake-level fluctuations in the Swiss Plateau, the Jura Mountains and the northern French Pre-Alps during the Last Glacial–Holocene transition: a regional synthesis. Global and Planetary Change, The last deglaciation: climate modeling and data analysis 30, 85–101. https://doi.org/10.1016/S0921-8181(01)00080-7

Magny, M., Combourieu-Nebout, N., de Beaulieu, J.-L., Bout-Roumazeilles, V., Colombaroli, D., Desprat, S., Francke, A., Joannin, S., Ortu, E., Peyron, O., Revel, M., Sadori, L., Siani, G., Sicre, M.A., Samartin, S., Simonneau, A., Tinner, W., Vanniere, B., Wagner, B., Zanchetta, G., Anselmetti, F., Brugiapaglia, E., Chapron, E., Debret, M., Didier, J., Essallami, L., Galop, D., Gilli, A., Kallel, N., Millet, L., Stock, A., Turon, J.L., Wirth, S., 2013. North-south palaeohydrological contrasts in the central Mediterranean during the Holocene: tentative synthesis and working hypotheses. Clim. Past 30.

Magny, M., de Beaulieu, J.-L., Drescher-Schneider, R., Vannière, B., Walter-Simonnet, A.-V., Millet, L., Bossuet, G., Peyron, O., 2006. Climatic oscillations in central Italy during the Last Glacial–Holocene transition: the record from Lake Accesa. J. Quaternary Sci. 21, 311–320. https://doi.org/10.1002/jqs.999

Magny, M., Vannière, B., Calo, C., Millet, L., Leroux, A., Peyron, O., Zanchetta, G., La Mantia, T., Tinner, W., 2011. Holocene hydrological changes in south-western Mediterranean as recorded by lake-level fluctuations at Lago Preola, a coastal lake in southern Sicily, Italy. Quaternary Science Reviews 30, 2459–2475. https://doi.org/10.1016/j.quascirev.2011.05.018

Magri, D., 2008. Patterns of post-glacial spread and the extent of glacial refugia of European beech (Fagus sylvatica). Journal of Biogeography 35, 450–463. https://doi.org/10.1111/j.1365-2699.2007.01803.x

Marchegiano, M., Horne, D.J., Gliozzi, E., Francke, A., Wagner, B., Ariztegui, D., 2020. Rapid Late Pleistocene climate change reconstructed from a lacustrine ostracod record in central Italy (Lake Trasimeno, Umbria). Boreas 49, 739–750. https://doi.org/10.1111/bor.12450

Marriner, N., Kaniewski, D., Pourkerman, M., Devillers, B., 2022. Anthropocene tipping point reverses long-term Holocene cooling of the Mediterranean Sea: A meta-analysis of the basin's Sea Surface Temperature records. Earth-Science Reviews 227, 103986. https://doi.org/10.1016/j.earscirev.2022.103986

Martin, C., Ménot, G., Thouveny, N., Peyron, O., Andrieu-Ponel, V., Montade, V., Davtian, N., Reille, M., Bard, E., 2020. Early Holocene Thermal Maximum recorded by branched tetraethers and pollen in Western Europe (Massif Central, France). Quaternary Science Reviews 228, 106109. https://doi.org/10.1016/j.quascirev.2019.106109

Martínez-Sosa, P., Tierney, J.E., Stefanescu, I.C., Dearing Crampton-Flood, E., Shuman, B.N., Routson, C., 2021. A global Bayesian temperature calibration for lacustrine brGDGTs. Geochimica et Cosmochimica Acta 305, 87–105. https://doi.org/10.1016/j.gca.2021.04.038

Mauri, A., Davis, B. a. S., Collins, P.M., Kaplan, J.O., 2014. The influence of atmospheric circulation on the mid-Holocene climate of Europe: a data–model comparison. Climate of the Past 10, 1925–1938. https://doi.org/10.5194/cp-10-1925-2014

Mauri, A., Davis, B.A.S., Collins, P.M., Kaplan, J.O., 2015. The climate of Europe during the Holocene: a gridded pollen-based reconstruction and its multi-proxy evaluation. Quaternary Science Reviews 112, 109–127. https://doi.org/10.1016/j.quascirev.2015.01.013

Mercuri, A.M., Accorsi, C.A., Bandini Mazzanti, M., 2002. The long history of Cannabis and its cultivation by the Romans in central Italy, shown by pollen records from Lago Albano and Lago di Nemi. Veget Hist Archaeobot 11, 263–276. https://doi.org/10.1007/s003340200039

Moore, P.D., Webb, J.A., Collinson, M.E., 1991. Pollen Analysis, Subsequent edition. ed. Blackwell Science Inc, Oxford.

Muller, S.D., Daoud-Bouattour, A., Fauquette, S., Bottollier-Curtet, M., Rifai, N., Robles, M., Saber, E.-R., El Madihi, M., Moukrim, S., Rhazi, L., 2022. Holocene history of peatland communities of central Rif (Northern Morocco). Geobios S0016699522000018. https://doi.org/10.1016/j.geobios.2021.12.001

Naafs, B.D.A., Gallego-Sala, A.V., Inglis, G.N., Pancost, R.D., 2017a. Refining the global branched glycerol dialkyl glycerol tetraether (brGDGT) soil temperature calibration. Organic Geochemistry 106, 48–56. https://doi.org/10.1016/j.orggeochem.2017.01.009

Naafs, B.D.A., Inglis, G.N., Zheng, Y., Amesbury, M.J., Biester, H., Bindler, R., Blewett, J., Burrows, M.A., del Castillo Torres, D., Chambers, F.M., Cohen, A.D., Evershed, R.P.,

Feakins, S.J., Gałka, M., Gallego-Sala, A., Gandois, L., Gray, D.M., Hatcher, P.G., Honorio Coronado, E.N., Hughes, P.D.M., Huguet, A., Könönen, M., Laggoun-Défarge, F., Lähteenoja, O., Lamentowicz, M., Marchant, R., McClymont, E., Pontevedra-Pombal, X., Ponton, C., Pourmand, A., Rizzuti, A.M., Rochefort, L., Schellekens, J., De Vleeschouwer, F., Pancost, R.D., 2017b. Introducing global peat-specific temperature and pH calibrations based on brGDGT bacterial lipids. Geochimica et Cosmochimica Acta 208, 285–301. https://doi.org/10.1016/j.gca.2017.01.038

Palmisano, A., Lawrence, D., de Gruchy, M.W., Bevan, A., Shennan, S., 2021. Holocene regional population dynamics and climatic trends in the Near East: A first comparison using archaeo-demographic proxies. Quaternary Science Reviews 252, 106739. https://doi.org/10.1016/j.quascirev.2020.106739

Parkinson, E.W., McLaughlin, T.R., Esposito, C., Stoddart, S., Malone, C., 2021. Radiocarbon Dated Trends and Central Mediterranean Prehistory. J World Prehist 34, 317–379. https://doi.org/10.1007/s10963-021-09158-4

Paura, B., Cutini, M., 2006. Sull'ecologia delle foreste del Tilio-Acerion Klika 1955 in Molise e considerazioni sui caratteri cenologici e fitogeografici dei boschi di forra dell'Appennino centro-meridionale (Italia centrale e meridionale). https://doi.org/10.1080/00837792.2006.10670798

Peyron, O., Combourieu-Nebout, N., Brayshaw, D., Goring, S., Andrieu-Ponel, V., Desprat, S., Fletcher, W., Gambin, B., Ioakim, C., Joannin, S., Kotthoff, U., Kouli, K., Montade, V., Pross, J., Sadori, L., Magny, M., 2017. Precipitation changes in the Mediterranean basin during the Holocene from terrestrial and marine pollen records: a model–data comparison. Clim. Past 13, 249–265. https://doi.org/10.5194/cp-13-249-2017

Peyron, O., Guiot, J., Cheddadi, R., Tarasov, P., Reille, M., de Beaulieu, J.-L., Bottema, S., Andrieu, V., 1998. Climatic Reconstruction in Europe for 18,000 YR B.P. from Pollen Data. Quat. res. 49, 183–196. https://doi.org/10.1006/qres.1997.1961

Peyron, O., Magny, M., Goring, S., Joannin, S., de Beaulieu, J.-L., Brugiapaglia, E., Sadori, L., Garfi, G., Kouli, K., Ioakim, C., Combourieu-Nebout, N., 2013. Contrasting patterns of climatic changes during the Holocene across the Italian Peninsula reconstructed from pollen data. Clim. Past 9, 1233–1252. https://doi.org/10.5194/cp-9-1233-2013

Pollegioni, P., Woeste, K., Chiocchini, F., Lungo, S.D., Ciolfi, M., Olimpieri, I., Tortolano, V., Clark, J., Hemery, G.E., Mapelli, S., Malvolti, M.E., 2017. Rethinking the history of common walnut (Juglans regia L.) in Europe: Its origins and human interactions. PLOS ONE 12, e0172541. https://doi.org/10.1371/journal.pone.0172541

Prasad, A.M., Iverson, L.R., Liaw, A., 2006. Newer Classification and Regression Tree Techniques: Bagging and Random Forests for Ecological Prediction. Ecosystems 9, 181–199. https://doi.org/10.1007/s10021-005-0054-1

Prentice, C., Guiot, J., Huntley, B., Jolly, D., Cheddadi, R., 1996. Reconstructing biomes from paleoecological data: a general method and its application to European pollen data at 0 and 6 ka. Climate Dynamics 12, 185–194. https://doi.org/10.1007/BF00211617

Raberg, J.H., Harning, D.J., Crump, S.E., de Wet, G., Blumm, A., Kopf, S., Geirsdóttir, Á., Miller, G.H., Sepúlveda, J., 2021. Revised fractional abundances and warm-season temperatures substantially improve brGDGT calibrations in lake sediments (preprint). Biogeochemistry: Organic Biogeochemistry. https://doi.org/10.5194/bg-2021-16

Rasmussen, S.O., Bigler, M., Blockley, S.P., Blunier, T., Buchardt, S.L., Clausen, H.B., Cvijanovic, I., Dahl-Jensen, D., Johnsen, S.J., Fischer, H., Gkinis, V., Guillevic, M., Hoek, W.Z., Lowe, J.J., Pedro, J.B., Popp, T., Seierstad, I.K., Steffensen, J.P., Svensson, A.M., Vallelonga, P., Vinther, B.M., Walker, M.J.C., Wheatley, J.J., Winstrup, M., 2014. A stratigraphic framework for abrupt climatic changes during the Last Glacial period based on three synchronized Greenland ice-core records: refining and extending the INTIMATE event stratigraphy. Quaternary Science Reviews 106, 14–28. https://doi.org/10.1016/j.quascirev.2014.09.007

Reille, M., 1998. Reille, Maurice, 1995. Pollen et spores d'Europe et d'Afrique du Nord, Supplément 1 . Éditions du Laboratoire de botanique historique et palynologie, Marseille, 327 p., 800 FF. / Reille, Maurice, 1998. Pollen et spores d'Europe et d'Afrique du Nord, Supplément 2 . Éditions du Laboratoire de botanique historique et palynologie, Marseille, 530 p., 1600 FF. gpq 52, 0–0. https://doi.org/10.7202/004885ar

Robles, M., Peyron, O., Brugiapaglia, E., Ménot, G., Dugerdil, L., Ollivier, V., Ansanay-Alex, S., Develle, A.-L., Tozalakyan, P., Meliksetian, K., Sahakyan, K., Sahakyan, L., Perello, B., Badalyan, R., Colombié, C., Joannin, S., 2022. Impact of climate changes on vegetation and human societies during the Holocene in the South Caucasus (Vanevan, Armenia): A multiproxy approach including pollen, NPPs and brGDGTs. Quaternary Science Reviews 277, 107297. https://doi.org/10.1016/j.quascirev.2021.107297

Robles, M., Peyron, O., Ménot, G., Brugiapaglia, E., Wulf, S., Appelt, O., Blache, M., Vannière, B., Dugerdil, L., Paura, B., Charlet, L., Guédron, S., De Beaulieu, J.-L., Joannin, S., in prep. Climate changes during the Late-Glacial in South Europe: new insights based on pollen and brGDGTs of Lake Matese in Italy.

Russell, J.M., Hopmans, E.C., Loomis, S.E., Liang, J., Sinninghe Damsté, J.S., 2018. Distributions of 5- and 6-methyl branched glycerol dialkyl glycerol tetraethers (brGDGTs) in East African lake sediment: Effects of temperature, pH, and new lacustrine paleotemperature calibrations. Organic Geochemistry 117, 56–69. https://doi.org/10.1016/j.orggeochem.2017.12.003

Sadori, L., 2018. The Lateglacial and Holocene vegetation and climate history of Lago di Mezzano (central Italy). Quaternary Science Reviews 202, 30–44. https://doi.org/10.1016/j.quascirev.2018.09.004

Sadori, L., Narcisi, B., 2001. The Postglacial record of environmental history from Lago di Pergusa, Sicily. The Holocene 11, 655–671. https://doi.org/10.1191/09596830195681

Samartin, S., Heiri, O., Joos, F., Renssen, H., Franke, J., Brönnimann, S., Tinner, W., 2017. Warm Mediterranean mid-Holocene summers inferred from fossil midge assemblages. Nature Geosci 10, 207–212. https://doi.org/10.1038/ngeo2891

Sbaffi, L., Wezel, F.C., Curzi, G., Zoppi, U., 2004. Millennial- to centennial-scale palaeoclimatic variations during Termination I and the Holocene in the central Mediterranean Sea. Global and Planetary Change 40, 201–217. https://doi.org/10.1016/S0921-8181(03)00111-5

Sicre, M.-A., Siani, G., Genty, D., Kallel, N., Essallami, L., 2013. Seemingly divergent sea surface temperature proxy records in the central Mediterranean during the last deglacial. Climate of the Past 9, 1375-1383. https://doi.org/10.5194/cpd-9-683-2013

Sinninghe Damsté, J.S., Rijpstra, W.I.C., Foesel, B.U., Huber, K.J., Overmann, J., Nakagawa, S., Kim, J.J., Dunfield, P.F., Dedysh, S.N., Villanueva, L., 2018. An overview of the occurrence of ether- and ester-linked iso-diabolic acid membrane lipids in microbial cultures of the Acidobacteria: Implications for brGDGT paleoproxies for temperature and pH. Organic Geochemistry 124, 63–76. https://doi.org/10.1016/j.orggeochem.2018.07.006

Soricelli, G., 2013. Atlante tematico di topografia antica : ATTA : Rivista di Studi di Topografia Antica, Atlante tematico di topografia antica. "L'Erma" di Bretschneider, Roma.

Sun, Q., Chu, G., Liu, M., Xie, M., Li, S., Ling, Y., Wang, X., Shi, L., Jia, G., Lü, H., 2011. Distributions and temperature dependence of branched glycerol dialkyl glycerol tetraethers in recent lacustrine sediments from China and Nepal. J. Geophys. Res. 116, G01008. https://doi.org/10.1029/2010JG001365

Taffetani, F., Catorci, A., Ciaschetti, G., Cutini, M., Di Martino, L., Frattaroli, A.R., Paura, B., Pirone, G., Rismondo, M., Zitti, S., 2012. The Quercus cerris woods of the alliance

Carpinion orientalis Horvat 1958 in Italy. Plant Biosystems - An International Journal Dealing with all Aspects of Plant Biology 146, 918–953. https://doi.org/10.1080/11263504.2012.682613

Ter Braak, C.J.F., Juggins, S., 1993. Weighted averaging partial least squares regression (WA-PLS): an improved method for reconstructing environmental variables from species assemblages 18.

Ter Braak, C.J.F., van Dam, H., 1989. Inferring pH from diatoms: a comparison of old and new calibration methods. Hydrobiologia 178, 209–223. https://doi.org/10.1007/BF00006028

Tinner, W., van Leeuwen, J.F.N., Colombaroli, D., Vescovi, E., van der Knaap, W.O., Henne, P.D., Pasta, S., D'Angelo, S., La Mantia, T., 2009. Holocene environmental and climatic changes at Gorgo Basso, a coastal lake in southern Sicily, Italy. Quaternary Science Reviews 28, 1498–1510. https://doi.org/10.1016/j.quascirev.2009.02.001

Valente, E., Buscher, J.T., Jourdan, F., Petrosino, P., Reddy, S.M., Tavani, S., Corradetti, A., Ascione, A., 2019. Constraining mountain front tectonic activity in extensional setting from geomorphology and Quaternary stratigraphy: A case study from the Matese ridge, southern Apennines. Quaternary Science Reviews 219, 47–67. https://doi.org/10.1016/j.quascirev.2019.07.001

Van Geel, B., 2002. Non-Pollen Palynomorphs, in: Smol, J.P., Birks, H.J.B., Last, W.M., Bradley, R.S., Alverson, K. (Eds.), Tracking Environmental Change Using Lake Sediments, Developments in Paleoenvironmental Research. Springer Netherlands, Dordrecht, pp. 99–119. https://doi.org/10.1007/0-306-47668-1_6

Van Zeist, W., Bottema, S., 1975. Palynological investigations in western iran 67.

Vescovi, E., Ammann, B., Ravazzi, C., Tinner, W., 2010. A new Late-glacial and Holocene record of vegetation and fire history from Lago del Greppo, northern Apennines, Italy. Veget Hist Archaeobot 19, 219–233. https://doi.org/10.1007/s00334-010-0243-5

Watson, B.I., 2018. Temperature variations in the southern Great Lakes during the last deglaciation: Comparison between pollen and GDGT proxies. Quaternary Science Reviews 15.

Weijers, J.W.H., Schouten, S., Spaargaren, O.C., Sinninghe Damsté, J.S., 2006. Occurrence and distribution of tetraether membrane lipids in soils: Implications for the use of the TEX86 proxy and the BIT index. Organic Geochemistry 37, 1680–1693. https://doi.org/10.1016/j.orggeochem.2006.07.018

Weijers, J.W.H., Schouten, S., van den Donker, J.C., Hopmans, E.C., Sinninghe Damsté, J.S., 2007. Environmental controls on bacterial tetraether membrane lipid distribution in soils. Geochimica et Cosmochimica Acta 71, 703–713. https://doi.org/10.1016/j.gca.2006.10.003

Wulf, S., Ott, F., Słowiński, M., Noryśkiewicz, A.M., Dräger, N., Martin-Puertas, C., Czymzik, M., Neugebauer, I., Dulski, P., Bourne, A.J., Błaszkiewicz, M., Brauer, A., 2013. Tracing the Laacher See Tephra in the varved sediment record of the Trzechowskie palaeolake in central Northern Poland. Quaternary Science Reviews 76, 129–139. https://doi.org/10.1016/j.quascirev.2013.07.010

Supplementary data

Supplementary Table S1. Statistical results of the MAT, WAPLS, BRT and RF methods applied on the modern "warm mixed forest" (WAMX), "temperature deciduous" (TEDE) and "cold steppe" (COST) datasets.

Model	Climate parameter	R^2	RMSE
MAT	MAAT (°C)	0,78	3,09
	MTWA (°C)	0,65	3,01
	MTCO (°C)	0,85	3,88
	PANN (mm.year^{-1})	0,75	183,11
	P_{winter} (mm.year^{-1})	0,71	76,76
WAPLS	MAAT (°C)	0,66	3,51
	MTWA (°C)	0,49	3,36
	MTCO (°C)	0,73	4,84
	PANN (mm.year^{-1})	0,55	220,36
	P_{winter} (mm.year^{-1})	0,51	90,95
RF	MAAT (°C)	0,61	3,72
	MTWA (°C)	0,42	3,52
	MTCO (°C)	0,71	4,94
	PANN (mm.year^{-1})	0,56	212,27
	P_{winter} (mm.year^{-1})	0,53	87,14
BRT	MAAT (°C)	0,87	2,97
	MTWA (°C)	0,77	2,94
	MTCO (°C)	0,91	3,77
	PANN (mm.year^{-1})	0,87	160,43
	P_{winter} (mm.year^{-1})	0,84	70,37

CHAPTER V - DISCUSSION

Lake Sevan, Armenia, M.Robles

Two mountainous sites have been studied: the Vanevan peat located in the Lesser Caucasus, and the Lake Matese located in the Southern Italy. They are both situated at a latitude of 41°N. A multiproxy approach has been applied to both cores: it includes sediment geochemistry, pollen, Non-Pollen Palynomorphs (NPPs), molecular biomarkers (brGDGTs) and quantitative climate reconstructions. Based on the same methodology during the field and the laboratory work, the study of the sequences of Vanevan and Lake Matese allowed us to highlight and discuss in detail several lessons from the past.

1. Local ecological processes: comparison between Vanevan peat and Lake Matese

The reconstruction of local ecological processes has revealed important changes associated with major water level changes along the time in both sites (Chap. II, IV). Water level changes are reconstructed in both sequences using the same ratio which includes aquatic pollen taxa, fern spores and NPPs. The taxa of aquatic pollen taxa and NPPs are comparable between both studied sites.

Lithological description of both sites are firstly characterized by clay sediments formed by inputs of detrital elements (Ti, Al, Fe, Si, Pb, Zr) coming from the catchment area (allochthonous deposits). Indeed, Titanium (Ti) content is considered as a terrigenous indicator because it is weakly affected by weathering and redox conditions (Arnaud et al., 2012). Clay sediments at Vanevan sequence is deposited between 9700 and 5100 cal BP, and, at Matese sequence during the Lateglacial. NPP content in this sediment has a high proportion of freshwater algae (*Botryococcus* and *Pediastrum*) and the semi-aquatic vegetation is poorly developed. These are good indicators of high level water in the two sites with the exception of the beginning of each sequence where a low or intermediate water-level associated to a high proportion of Calcium (Ca) is recorded.

Then, a transitional phase, interpreted as a major drop in water level, is characterized by a sediment becoming organic and the development of Cyperaceae and ferns in both sites. This phase which extends between 5100 and 4950 cal BP at Vanevan, is also characterized by high proportions of calcium, sulfur and phosphorus which have been linked to high fire activity (Leroyer et al., 2016; Robles et al., 2022). The fire activity seems to have burned Cyperaceae sedges or grassland and favored developments of ferns and Poaceae. The same vegetation dynamic was recorded at Shenkani in Armenia when a fire event burned the wetland vegetation itself (Cromartie et al., 2020). At Vanevan, the ecological perturbation of fire also results in an abrupt and major increase of Cichorioideae which suggests a local development on perturbed

soil or a drying phase leading to an over-representation of the resistant pollen taxa (Lebreton et al., 2010). These major changes are associated to the 5.2 ka event, characterized by drier conditions around the Mediterranean Basin (Magny et al., 2006). This arid event is well marked in the Caucasus (Connor and Kvavadze, 2008; Joannin et al., 2014; Cromartie et al., 2020) and the Near East (Stevens et al., 2001, 2006; Eastwood et al., 2007) and seems associated to cold conditions (Solomina et al., 2015; Robles et al., 2022). This period is also characterized by major vegetation changes and the development of human activities in the region. At Matese, the transitional phase extends during the Early Holocene (in the actual knowledge of sediment ages) and is characterized by an increase of potassium, rubidium and strontium contents, associated to tephra layers. For this site, we do not have charcoal record, and XRF data do not seem to indicate fire activity (Croudace and Rothwell, 2015). However, tephra layers are recorded and their deposition can impact vegetation and induces a reduction of vegetation productivity causing lower pollen accumulation rates in sediments (Allen and Huntley, 2018).

In the two sites, this transition phase ends with organic sediment, and the development of semi-aquatic vegetation. Although water levels slightly increase after the transition phase, they remain low until the most recent periods for both sites. The semi-aquatic vegetation is mainly composed of Cyperaceae for the Vanevan peat whereas it is composed by alternating *Equisetum* or Cyperaceae for the Lake Matese. The low water levels are consistent with high variation in the distribution of brGDGTs. Bacterial communities are more sensitive to wetland changes when the water level is low whereas the climate signal is more visible for high water level. In shallow lakes, the impacts of seasonal and diurnal temperature changes are also more important (Martínez-Sosa et al., 2021).

Water level changes are well associated with climate changes at Vanevan whereas they seem more dissociated from the climate at Matese, or maybe linked with seasonal climate changes or internal karstic draining of the Matese's massif (Chap. IV).

2. Modern pollen rain and vegetation dynamics along the time

2.1 Contribution of the modern pollen-vegetation relationship analysis

The relationship between pollen and vegetation can differ according to several factors such as topography, surrounding vegetation, the size of the water body or microclimatic parameters (Jacobson and Bradshaw, 1981). Modern pollen samples provided from mosses were taken according to an altitudinal distribution in different environments of Armenia and the Matese Massif. Understanding modern pollen-vegetation relationship was essential to

accurately interpret the reconstructions of past vegetation around the Lake Sevan and the Lake Matese, two sites surrounded by mountains.

At Vanevan (Chap. II), *Quercus* pollen represent up to 15% of the signal for modern pollen samples located around the Lake Sevan, even if no trees are not present in the catchment. During the Mid Holocene, the *Quercus* percentage remained lower than 10%, indicating that oak forest was not present on the slopes of Lake Sevan. Thanks to the modern pollen-vegetation relationship, it has been possible to requestion the older palynological studies which have suggested the presence of deciduous forests on the slopes of Lake Sevan during the Mid Holocene (Moreno-Sanchez and Sayadyan, 2005).

In the same way, at Matese (Chap. IV), *Quercus pubescens*-type pollen represents up to 15% even if there are only few oak trees in the catchment today. During the Oldest Dryas, *Quercus pubescens*-type represented less than 15%, indicating that it was certainly not present in the catchment of the Lake Matese but present in the regional vegetation at lower altitude. Considering anthropogenic pollen indicators, such as *Plantago lanceolata* and *Rumex*-type, very low percentages are recorded in the modern pollen rain of Armenia and the Matese Massif even if extensive pastoralism is present in these areas. Pastoralism activities are thus difficult to detect in the pollen assemblages of these two sequences.

In a climate point of view, the modern pollen samples analyzed in my PhD were added to the modern pollen database (Peyron et al., 2017; Dugerdil et al., 2021a) which is used to calibrate the transfer functions. The addition of this new modern pollen assemblages allows to improve the reliability of paleoclimatic reconstructions. Indeed, an adequate modern database and an understanding of modern processes in the climate system and in the proxies are important for reliable paleoclimate reconstructions (Dugerdil et al., 2021).

2.2 An attempt to better understand the vegetation dynamics around the Mediterranean Basin during the Lateglacial and the Holocene

Vegetation dynamics were reconstructed from pollen data around the Lake Sevan during the Holocene and around the Lake Matese during the Lateglacial and the Holocene (Chap. II, IV). Then, the reconstructed vegetation was compared with other regional sites of the Caucasus and the Near East and in Italy, respectively (Chap. II, IV). Vegetation changes will now be compared across the Mediterranean Basin with a selection of key sites which document the Lateglacial and the Holocene. Selected sites are located around latitude 41°N to match the latitude of Vanevan peat and Lake Matese records. Five geographical groups, including the Iberian Peninsula, Italy, the Balkans and the Caucasus and the Near East, were distinguished to

discuss the vegetation dynamics at the scale of the Mediterranean Basin around latitude 41°N (Fig. 1)

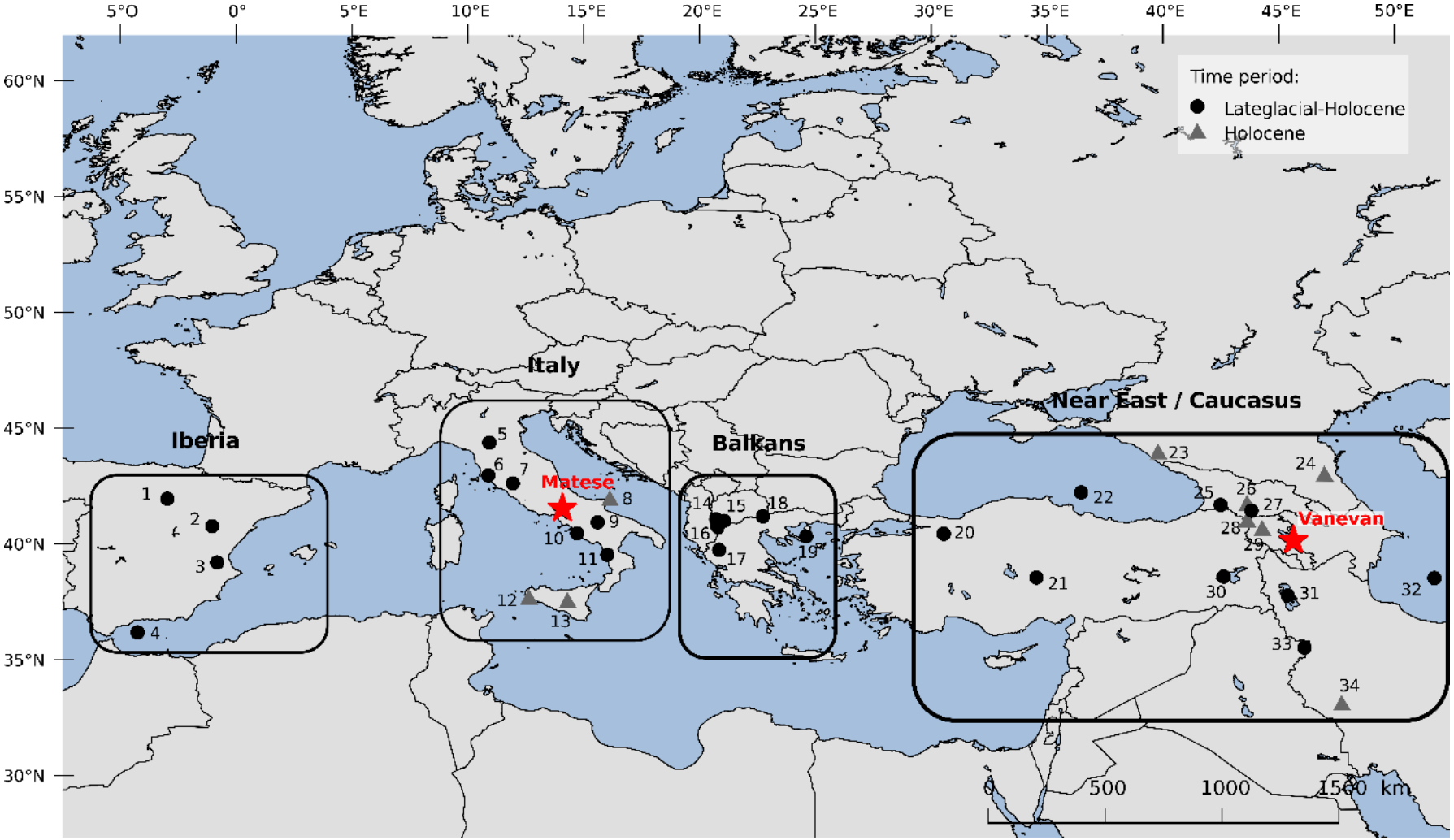
5°O
0°
5°E
10°E
15°E
20°E
25°E
30°E
35°E
40°E
45°E
50°E
60°N
55°N
50°N
45°N
40°N
35°N
30°N
Time period:
Lateglacial-Holocene
Holocene
Italy
Iberia
Balkans
Near East / Caucasus
Matese
Vanevan
0
500
1000
1500 km

Figure V-1. Location of the Lake Matese, the Vanevan peat and selected Lateglacial-Holocene palynological records: 1) Sierra de Cebollera (Gil García et al., 2002), 2) Villarquemado (Aranbarri et al., 2014), 3) Navarrés (Carrión and Van Geel, 1999), 4) ODP site 976 (Combourieu Nebout et al., 2009), 5) Pavullo nel Frignano (Vescovi et al., 2010), 6) Lago dell'Accesa (Drescher-Schneider et al., 2007), 7) Lago di Mezzano (Sadori, 2018), 8) Lago Battaglia (Caroli and Caldara, 2007), 9) Lago Grande di Monticchio (Allen et al., 2002), 10) C106 (Ermolli and di Pasquale, 2002), 11) Lago Trifoglietti (Joannin et al., 2012; De Beaulieu et al., 2017), 12) Gorgo Basso (Tinner et al., 2009), 13) Lago di Pergusa (Sadori and Narcisi, 2001), 14) Lake Ohrid (Sadori et al., 2016), 15) Lake Prespa (Panagiotopoulos et al., 2013) , 16) Lake Maliq (Denèfle et al., 2000; Bordon et al., 2009), 17) Ioannina (Lawson et al., 2004), 18) Lake Dojran (Masi et al., 2018), 19) SL 152 (Dormoy et al., 2009), 20) Lake Iznik (Miebach et al., 2016), 21) Eski Acigöl (Roberts et al., 2001), 22) 22-GC3 (Shumilovskikh et al., 2012), 23) Lake Khuko (Grachev et al., 2021), 24) Shotota swamp (Ryabogina et al., 2019), 25) Didachara Mire (Connor et al., 2018), 26) Nariani (Messager et al., 2017), 27) Lake Paravani (Messager et al., 2013), 28) Zarishat fen (Joannin et al., 2014), 29) Lake Shenkani (Cromartie et al., 2020), 30) Lake Van (Wick et al., 2003), 31) Lake Urmia (Djamali et al., 2008), 32) GS05 (Leroy et al., 2013), 33) Lake Zeribar (Stevens et al., 2001), 34) Lake Mirabad (Stevens et al., 2006)

2.2.1 Steppic or grassland vegetation during the Oldest Dryas

During the Oldest Dryas (OD), a steppic vegetation dominated by *Artemisia*, Chenopodiaceae and Poaceae is recorded in the Iberian margin (ODP site 976; Combourieu Nebout et al., 2009) and in Central and Northern Iberian Peninsula (Carrión and Van Geel, 1999; Gil García et al., 2002). *Pinus* is also largely documented by the majority of records, representing between 30 and 80 % of the pollen signal and deciduous *Quercus* is detected (Carrión and Van Geel, 1999; Gil García et al., 2002; Combourieu Nebout et al., 2009). In Italy, the vegetation is also characterized by an open vegetation dominated by Poaceae and *Artemisia* in southern (Monticchio, Allen et al., 2002; Trifoglietti, De Beaulieu et al., 2017), central (Accesa, Drescher-Schneider et al., 2007; Mezzano, Sadori, 2018) and northern regions (Pavullo nel Frignano; Vescovi et al., 2010). *Pinus* is also recorded (~ 15%), associated to *Juniperus* in some northern and central sites (Drescher-Schneider et al., 2007; Vescovi et al., 2010) and *Quercus pubescens*-type in southern sites (De Beaulieu et al., 2017; this study). In the Balkans, a steppic vegetation dominated by *Artemisia*, Poaceae and Chenopodiaceae is also recorded (Ioannina, Lawson et al., 2004; marine core SL 152, Dormoy et al., 2009; Lake Prespa, Panagiotopoulos et al., 2013; Lake Ohrid, Sadori et al., 2016). A high percentage of *Pinus* is recorded in this region and deciduous *Quercus* are detected (Lawson et al., 2004; Panagiotopoulos et al., 2013; Sadori et al., 2016). In the Western Near East, steppic vegetation is recorded and includes high percentages of *Artemisia* accompanied by Chenopodiaceae and Poaceae whereas *Pinus* represents only a low percentage (Eski Acıgöl, Roberts et al., 2001; 22-GC3, Shumilovskikh et al., 2012; Lake Iznik, Miebach et al., 2016). To summarize, steppic

vegetation accompanied by high percentages of *Pinus* (which can also partly be due to long-distance transport in open environments) are recorded in the Iberian Peninsula and in the Balkans whereas the Western Near East is only characterized by steppe vegetation and Italy by grassland vegetation accompanied by a low *Pinus* percentage.

2.2.2 Expansion of deciduous trees and open vegetation during the Bølling–Allerød (14,700-12,900 cal BP)

The Bølling–Allerød Interstadial (B/A) is characterized in the Iberic Peninsula by a decline of *Artemisia* and Poaceae and, on the contrary, by an increase of deciduous trees such as *Quercus* and *Betula* (Gil García et al., 2002; Combourieu Nebout et al., 2009). *Quercus ilex* is also recorded in the Southern Iberian Peninsula (Combourieu Nebout et al., 2009). In Italy, *Artemisia* declines whereas Poaceae remains stable (Allen et al., 2002; Drescher-Schneider et al., 2007; Vescovi et al., 2010; Sadori, 2018; this study) and an increase of deciduous and thermophilous arboreal taxa including *Quercus*, *Betula*, *Corylus*, *Tilia* and *Ulmus* is recorded. However, only the sites located in Southern Italy records *Fagus* (Allen et al., 2002; De Beaulieu et al., 2017; this study), probably linked to the closer locality of refugia in this area during the Lateglacial (Magri, 2008). In the Balkans, for the majority of records, Poaceae remain stable whereas *Artemisia* and Chenopodiaceae decrease (Bordon et al., 2009; Dormoy et al., 2009; Panagiotopoulos et al., 2013). However, for the most southern site, Ioannina in Greece, *Artemisia* and Poaceae remain stable and deciduous *Quercus* largely increases (Lawson et al., 2004). In the Near East, the majority of records show the maintenance of steppic vegetation although *Artemisia* can slightly decrease (Roberts et al., 2001; Stevens et al., 2001; Shumilovskikh et al., 2012) whereas a large increase of deciduous *Quercus* is recorded at Iznik, in the Northwestern Turkey (Miebach et al., 2016). To sum up, the development of deciduous arboreal is recorded in the Iberian Peninsula and in Italy although grasslands are still present in Italy. In the Balkans, the percentage of Poaceae remains important and the vegetation is steppic in the Near East (except in the extreme northwestern part of Turkey). A gradient seems to be present with more arboreal taxa in the western part of the Mediterranean Basin, followed by the presence of grasslands in the central part and finally a steppic vegetation in the Near East but more sites are needed to corroborate or not this assumption.

2.2.3 Steppic or grassland vegetation during the Younger Dryas (12,900-11,700 cal BP)

The Younger Dryas (YD) is marked in the Iberian Peninsula by a decline in deciduous arboreal taxa whereas steppe vegetation (Poaceae, *Artemisia*, Chenopodiaceae) develops (Carrión and Van Geel, 1999; Gil García et al., 2002; Combourieu Nebout et al., 2009). In Italy, an increase of *Artemisia* and Poaceae is recorded in Central (Drescher-Schneider et al., 2007; Sadori, 2018) and Southern Italy (Allen et al., 2002; Ermolli and di Pasquale, 2002; this study). However, this increase is less important or not visible in the southern sites (Monticchio, Trifoglietti) and it is not accompanied by a decrease of arboreal taxa (Allen et al., 2002; De Beaulieu et al., 2017). In the Balkans, the proportion of *Artemisia* and Chenopodiaceae becomes more important whereas *Pinus* largely declines (Maliq, Denèfle et al., 2000; SL 52, Dormoy et al., 2009; Lake Prespa, Panagiotopoulos et al., 2013; Lake Dojran, Masi et al., 2018). Finally, in the Near East, high percentages of *Artemisia* and Chenopodiaceae are documented in the majority of records (Roberts et al., 2001; Stevens et al., 2001; Shumilovskikh et al., 2012) whereas Poaceae increase at Iznik (Miebach et al., 2016). The YD is clearly marked by the opening of the vegetation and the emergence of steppic taxa from the Iberian Peninsula to the Near East.

2.2.4 Grassland vegetation and increase of deciduous trees during the Early Holocene (11,700-8200 cal BP)

During the Early Holocene (EH), different patterns occur in the Iberian Peninsula. In some records, Chenopodiaceae and *Artemisia* decrease whereas temperate arboreal taxa, including *Betula* and deciduous *Quercus*, increase (Gil García et al., 2002; Combourieu Nebout et al., 2009). However, in others records, *Artemisia* and Chenopodiaceae can remain abundant (Aranbarri et al., 2014) and the percentages of temperate arboreal taxa can remain low (Carrión and Van Geel, 1999). In the Southern Iberian Peninsula, *Quercus ilex* appears and will be recorded during all the Holocene (Combourieu Nebout et al., 2009). In Italy, *Artemisia* abruptly disappears whereas Poaceae remains abundant in the majority of records (Allen et al., 2002; Tinner et al., 2009; Vescovi et al., 2010; Joannin et al., 2012; Sadori, 2018) and deciduous taxa such as *Fagus* and *Quercus* also increase (Sadori and Narcisi, 2001; Joannin et al., 2012; this study). In the Balkans, a large drop in *Artemisia* and Chenopodiaceae is recorded whereas Poaceae remains stable and abundant. An increase of deciduous trees also appears, in terms of percentages (mainly *Quercus*) and of diversity (*Carpinus, Corylus, Ulmus, Tilia*) (Denèfle et al., 2000; Lawson et al., 2004; Panagiotopoulos et al., 2013; Masi et al., 2018). In the Near East and the Caucasus, the beggining of the Holocene is dominated by Chenopodiaceae steppe

before 10,000 cal BP (Wick et al., 2003; Messager et al., 2013; Joannin et al., 2014; Cromartie et al., 2020). Then, the vegetation remains largely open, but the dominant steppic taxa varies from (1) Poaceae (Roberts et al., 2001; Stevens et al., 2001; Wick et al., 2003; Stevens et al., 2006; Ryabogina et al., 2019; Cromartie et al., 2020) to (2) *Artemisia*, (Djamali et al., 2008; Joannin et al., 2014) or (3) Chenopodiaceae (Leroy et al., 2013; Messager et al., 2013) and *Betula* is also present in the regional vegetation. On the contrary, in the Northwest Caucasus, forested phases are recorded during this period (Connor, 2011; Shumilovskikh et al., 2012; Messager et al., 2017; Connor et al., 2018; Grachev et al., 2021). Thus, during the EH, the vegetation is still largely open and dominated by grassland, but the deciduous trees (mainly *Quercus* and sometimes *Corylus*) increase at this period in the Iberian Peninsula, Italy, the Balkans, the Near East and the Caucasus.

2.2.5 Dominance of deciduous forests during the Mid to Late Holocene (8200 cal BP-today)

During the Mid to Late Holocene, in the Iberian Peninsula, an increase of Mediterranean taxa is recorded, such as *Quercus ilex, Olea* or *Pistacia*, and on the contrary, Poaceae largely decline. A decrease of deciduous trees, in particular *Quercus*, is also recorded mainly during the last 5000 years (Carrión and Van Geel, 1999; Gil García et al., 2002; Combourieu Nebout et al., 2009; Aranbarri et al., 2014). In Italy, this period is marked by an increase of Mediterranean taxa, such as *Quercus ilex*, and deciduous arboreal taxa including *Quercus* and *Fagus* (Allen et al., 2002; Ermolli and di Pasquale, 2002; Caroli and Caldara, 2007; Tinner et al., 2009; Joannin et al., 2012; this study). Some abrupt forest declines are also evidenced in Italy and in the Iberian Peninsula (Di Rita et al., 2018). For example, from 2600-2800 cal BP, an opening of the forested environments is recorded in Southern Italy (Allen et al., 2002; Magny et al., 2011). In the Balkans, high percentages of arboreal taxa, including deciduous *Quercus* and *Fagus*, and a decrease of Poaceae characterizes the Mid Holocene (Denèfle et al., 2000; Lawson et al., 2004; Panagiotopoulos et al., 2013; Masi et al., 2018). Mediterranean taxa, including *Quercus ilex*, appear later, from 4500-4000 cal BP, during the Late Holocene (Denèfle et al., 2000; Lawson et al., 2004; Masi et al., 2018). The last 2000-1500 years are characterized, in the majority of sites, by a decline of arboreal taxa mainly deciduous *Quercus* and *Pinus* whereas Poaceae increase again (Lawson et al., 2004; Panagiotopoulos et al., 2013; Masi et al., 2018). However, this trend is not observed in all sequences, as is the case at Maliq (Denèfle et al., 2000). In the Near East and the Caucasus, different patterns are recorded according to the regions. In several sites of Turkey and Iran, an important increase of deciduous *Quercus* is recorded (Roberts et al., 2001; Stevens et al., 2001; Wick et al., 2003; Shumilovskikh

et al., 2012; Miebach et al., 2016) and can be accompanied by other deciduous trees such as *Fagus* in the Western Turkey (Roberts et al., 2001; Shumilovskikh et al., 2012; Miebach et al., 2016). In Armenia and Iran, grassland and scarce open woodlands composed the landscape during the Mid Holocene (Djamali et al., 2008; Joannin et al., 2014; Cromartie et al., 2020; this study). Then, a drop of arboreal taxa occurs from 5000 cal BP and Poaceae increase in Armenia (Joannin et al., 2014; Cromartie et al., 2020). To summarize, during the Mid-Late Holocene, deciduous trees are abundant, mainly *Quercus*, and Mediterranean taxa appears in the sequences of the Iberian Peninsula and Italy since the Mid Holocene and from 4500-4000 cal BP in the Balkans. In Turkey, an abundance of deciduous *Quercus* is also recorded whereas the vegetation remains open in Armenia. Between 5000 and 1000 cal BP, an opening of the deciduous forests is detected from the Iberian Peninsula to the Near East. The impact of human societies on the vegetation dynamics since the Late Holocene is discussed in the 3.1 part.

3. Relationship between vegetation, human activities and climate changes in the Mediterranean area

3.1 Human history, vegetation and climate changes in the Lesser Caucasus and in Italy

3.1.1 Human history and impact of abrupt climate events in the Lesser Caucasus

Around Vanevan peat (Chap. II), human activities are principally expressed through agricultural practices, identified by *Cerealia*-type pollen. Although, *Cerealia*-type pollen may come from Poaceae species or wild cereals commonly present in the Near East (Van Zeist et al., 1975), our record matches with archeological evidences around the Lake Sevan (Parmegiani and Poscolieri, 2003; Hovsepyan, 2013, 2017) and with the estimates of the population in the South Caucasus (Palmisano et al., 2021b). On the other hand, pastoralism is complex to detect in pollen records, as suggested by the study of modern samples of Armenia, despite the presence of extensive livestock production.

The first increase of *Cerealia*-type pollen occurs during Late Neolithic-Chalcolithic, but no archeological data are available around the Lake Sevan at this period. During the Neolithic archeological evidences of agriculture are centered on the Ararat plain (Badalyan et al., 2004; Hovsepyan and Willcox, 2008; Badalyan and Harutyunyan, 2014) and during the Middle Chalcolithic the presence of cereals is detected at Getahovit-2 in northeastern Armenia (Chataigner et al., 2020). Although several studies suggest a human impact on the environment since the Early Holocene in the Near East, by fostering the maintenance of steppic vegetation

with fires (Roberts et al., 2002; Turner et al., 2008, 2010), this hypothesis is not verified in the South Caucasus (Joannin et al., 2014; Messager et al., 2017) and no human activities which could impact on vegetation dynamic is detected around the Lake Sevan before 5200 cal BP.

Since 5200 cal BP, the percentages of *Cerealia*-type pollen become more important, and their presence is consistent with archeological remains around the Lake Sevan (Parmegiani and Poscolieri, 2003; Hovsepyan, 2013, 2017) and demography estimation in the South Caucasus (Palmisano et al., 2021b). At 5200 cal BP, an abrupt environmental event is evidenced in the South Caucasus (Connor and Kvavadze, 2008; Joannin et al., 2014; Cromartie et al., 2020). It resulted at Vanevan with an abrupt drop of water level and high fire activities. In terms of vegetation, a large decrease of arboreal taxa (*Quercus, Betula*) occurs in Armenia (Cromartie et al., 2020; Robles et al., 2022), Turkey (Wick et al., 2003), and at a larger scale in East Asia (Qian et al., 2019). However, this period is also marked by an abrupt dry and cold event which occurs at Vanevan and in the Near East (Stevens et al., 2001, 2006; Eastwood et al., 2007; Bar-Matthews and Ayalon, 2011). The '5.2 ka event' was defined by Magny et al., (2006) and is characterized by drier conditions. Hence, although agriculture practices are present around Vanevan peat since 5200 cal BP, the changes of vegetation and fire activity between 5200 and 4800 cal BP are regional, suggesting a stronger impact of the aridification event than human activities.

Then, *Cerealia*-type pollen increase and reach a maximum of 40 % during Antiquity and Medieval periods. The periods of increase or decrease of *Cerealia*-type pollen match the occupation and abandonment phases of archeological sites of Lake Sevan but also with demographic trends of the South Caucasus (Palmisano et al., 2021b). Our study also revealed a good correspondence between the declines in agricultural practices around the Lake Sevan and population demography in the South Caucasus (Palmisano et al., 2021b) with several abrupt climate events including, in addition to the 5.2 ka, the 4.2 ka and the 2.8 ka. The 4.2 ka climate event is characterized by arid conditions around the Mediterranean Basin (e.g.Kaniewski et al., 2018; Bini et al., 2019) associated to warm conditions in the Near East and the South Caucasus (Bini et al., 2019; Robles et al., 2022). The decline of agricultural practices is associated with the decline of local population (Hovsepyan, 2017, 2013) but it is difficult to say whether it is due to societal collapse or migrations of population in the South Caucasus and the Near East (Kaniewski et al., 2018; Palmisano et al., 2021b). The 2.8 ka event is defined by arid and cold conditions at a global scale (Ivy-Ochs et al., 2009; Fukumoto et al., 2012; van Geel et al., 2014) and in the Near East and the Caucasus (Bar-Matthews et al., 2003; Wick et al., 2003; Solomina et al., 2015; Robles et al., 2022). This climate event may have contributed to the decline of the

Urartian empire centered around Lake Sevan and it coincides with the arrival of the Persians in Armenia.

According to several studies focused on the Near East, the demographic trends become decoupled from climate from 4000-3500 cal BP because populations are more resilient due to the technological advancement (Lawrence et al., 2016; Roberts et al., 2019). Our study suggests on the contrary a significant impact of abrupt climate changes on populations even for the recent periods, at least for the South Caucasus.

3.1.2 Human history and vegetation changes in Southern Italy

At Matese (Chap. IV), the occurrence of anthropogenic pollen indicators is low, but several key pollen taxa can provide information on human activities. However, like in the Vanevan pollen record, pastoralism is difficult to detect in pollen records, as it is also the case for modern samples of Matese massif, despite the presence of extensive livestock production.

The first potential anthropogenic signal is an increase of *Cerealia*-type during the Neolithic. However, no archeological data are available for this period around the Lake Matese but a significant increase of demography in Southern Italy marks the Early Neolithic (Palmisano et al., 2021a). The first evidences of agriculture are recorded in south-east Italy (Apulia), firstly in lowland and then at higher elevations all over Italy (Palmisano et al., 2021a). Then, the tree *Juglans* (walnut) is recorded at Matese and in Southern Italy from the Bronze Age and the Early Iron Age (Allen et al., 2002; Mercuri et al., 2002; Sadori, 2018). At this period, a large increase of population in Southern Italy is recorded, the presence of settlements is attested in lowland and upland areas and an intensification of agricultural practices appear (Palmisano et al., 2021a). Finally, cereals and *Olea* develop during the general opening of the forest at Matese and in Southern Italy around 2800-2600 cal BP (Allen et al., 2002; Magny et al., 2011). During pre-Roman and Roman periods, settlements is attested on the shore of Lake Matese. Human activities seem to affect regional vegetation dynamics since this period through increases of agricultural practices and forest clearance.

According to Palmisano et al. (2021a), the Late Holocene is marked by a strong impact of human on the vegetation and a decoupling of demographic trends and climate in Italy. Population would be less vulnerable to climatic changes due to technological advancement (Roberts et al., 2019). On the contrary, Di Rita et al., (2018) suggests a good correspondence between forest fluctuations and climate changes, also identified by independent climate proxies, during the Late Holocene. In Southern Italy, a decrease of forests accompanied by an increase of anthropogenic pollen indicators are recorded since 2800-2600 cal BP (Allen et al., 2002;

Magny et al., 2011). Independent climate reconstructions in Southern Italy show few variations in terms of humidity conditions (Sbaffi et al., 2004; Sicre et al., 2013). The decrease of forests in Southern Italy could be linked to human practices during the last 2800-2600 cal BP.

3.2 Climate changes around the Mediterranean Basin during the Lateglacial and the Holocene

3.2.1 Reliability of climate reconstructions of Vanevan peat and Lake Matese

Climate reconstructions at Vanevan and Matese are based on both pollen and brGDGTs (Chap. II, III, IV). Concerns with pollen-inferred climate reconstructions may arise for the following reasons (1) results are often based on the use of a single method, which is not robust enough, (2) modern pollen datasets must be of high quality and contain sufficient modern samples to be representative of all ecosystems encountered in the past, (3) the taphonomy processes may biased the pollen assemblages and (3) for recent periods such as the Late Holocene, vegetation changes may be related to human impact rather than climate change or the synergy of the two. Here, to provide reliable climate reconstructions, we have developed an approach that takes into account each of these weaknesses: multi-method approach, improvement of the modern pollen dataset, and validation of the pollen-inferred climate signal by an independent temperature proxy: the brGDGTs.

Pollen-based reconstructions have the advantage to reconstruct temperatures, precipitation, and when possible the seasonality which is a key climate parameter in the Mediterranean area. Pollen-based climate reconstructions at Vanevan and Matese were obtained with a multi-method approach (Peyron et al., 2005, 2013) including commonly used transfer functions methods (WAPLS, MAT) and recent "machine-learning" methods (RF, BRT). The results of the four methods show a very good correspondence except for the most recent periods when human activities are important and impact regional vegetation dynamic. Pollen-based climate reconstructions diverge from 2300 cal BP, at Vanevan, when the percentages of *Cerealia*-type become important (19-44%) and from around 2500 cal BP, at Matese, when cereals and *Olea* are recorded, and a drop of arboreal taxa occurs. The impact of taphonomy processes is not negligible at Vanevan, where a large percentage of Cichorioideae is recorded at the base of the core and around 5000 cal BP, when the lithology and sediment composition are indicative of disruption in the dynamic. The overestimation of this resistant pollen taxa can be an indicator of taphonomy processes (deposition and conservation) and the poor conservation of pollen in sediments (Lebreton et al., 2010).

Considering the brGDGTs-inferred temperature signal obtained at Vanevan and Matese, the trends of reconstructions are closed to the pollen-based reconstructions except when the water level is estimated low. Indeed, the type of wetland (from open lake to peatland), the water level (from deep to shallow) and the belt vegetation may influence the brGDGT distribution and origins (catchment soils, rivers, in situ production in waters or sediments) (Martin et al., 2019; Martínez-Sosa et al., 2021). Changes in the water level and associated communities of aquatic plant may have largely impacted the brGDGT distribution.

3.2.2 Climate changes around the Mediterranean Basin during the Lateglacial

In the following sections, an attempt to provide a synthesis of climate changes around the Mediterranean Basin during the Lateglacial are presented according to a longitudinal transect from Spain to the Near East. As we are aware that providing such a synthesis is an extremely ambitious work, this synthesis does not pretend to be exhaustive. Selected sites are selected approximately the latitude 41°N as the Vanevan peat and the Lake Matese. Several geographical areas, including the Iberian Peninsula, Italy, the Balkans, the Caucasus and the Near East, have been distinguished (Fig. 2).

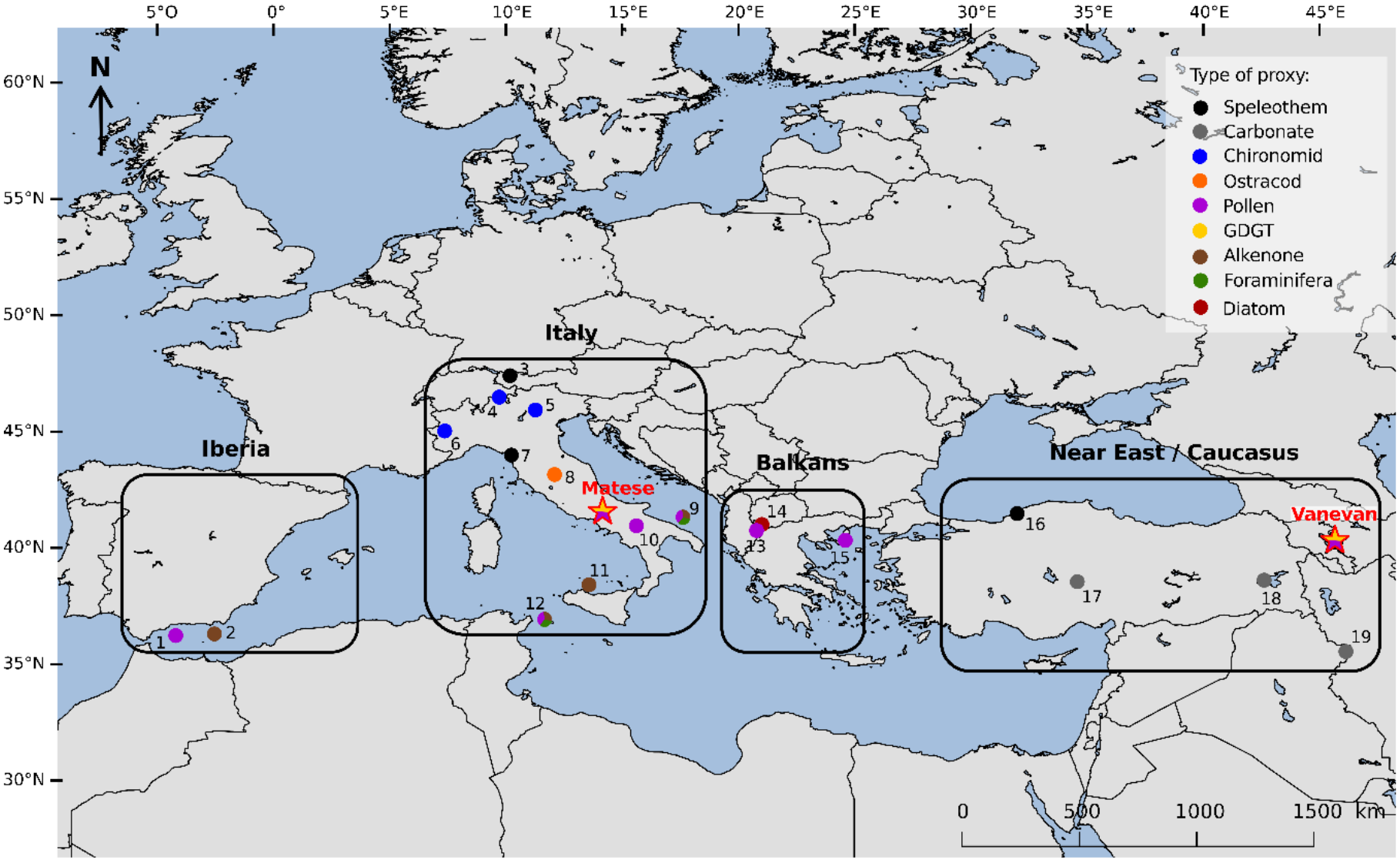
5°O
0°
5°E
10°E
15°E
20°E
25°E
30°E
35°E
40°E
45°E
60°N
55°N
50°N
45°N
40°N
35°N
30°N
N
Type of proxy:
Speleothem
Carbonate
Chironomid
Ostracod
Pollen
GDGT
Alkenone
Foraminifera
Diatom
Italy
Iberia
Balkans
Near East / Caucasus
Matese
Vanevan
1
2
3
4
5
6
7
8
9
10
11
12
13
14
15
16
17
18
19
0
500
1000
1500 km

Figure V-2. Location of the Lake Matese, the Vanevan peat and selected Lateglacial-Holocene paleoclimate records: 1) ODP site 976 (Combourieu Nebout et al., 2009), 2) MD95-2043 (Cacho et al., 2001), 3) Hölloch (Li et al., 2021), 4) Maloja Riegel (Heiri et al., 2014), 5) Lago di Lavarone (Heiri et al., 2014), 6) Lago Piccolo di Avigliana (Larocque and Finsinger, 2008), 7) Corchia cave (Regattieri et al., 2014), 8) Lake Trasimeno (Marchegiano et al., 2020), 9) MD90-917 (Combourieu-Nebout et al., 2013; Sicre et al., 2013) 10) Lago Grande di Monticchio (Allen et al., 2002), 11) BS7938 (Sbaffi et al., 2004), 12) MD04-2797 (Desprat et al., 2013; Sicre et al., 2013), 13) Lake Maliq (Bordon et al., 2009), 14) Lake Prespa (Cvetkoska et al., 2014), 15) SL-152 (Dormoy et al., 2009), 16) Sofular cave (Göktürk et al., 2011), 17) Eski Acigöl (Roberts et al., 2001), 18) Lake Van (Wick et al., 2003), 19) Lake Zeribar (Stevens et al., 2001).

Contrasting precipitation patterns during the Bølling–Allerød warming (14,700-12,900 cal BP)

The onset and the end of the Bølling–Allerød Interstadial (B/A) are estimated at 14,700 and 12,900 cal BP respectively by the NGRIP ice-core chronology (Rasmussen et al., 2014). In the Iberian margin, this period is characterized by an increase of temperatures and precipitation in comparison to the Oldest Dryas in the Alboran Sea (Cacho et al., 2001; Combourieu Nebout et al., 2009). In Italy (Chap. III), an increase of terrestrial temperatures and SSTs is also recorded by different proxies (Larocque and Finsinger, 2008; Heiri et al., 2014; Sicre et al., 2013; Marchegiano et al., 2020; this study). However, in terms of precipitation no significant changes occur for Italian sites (Sicre et al., 2013; this study) except in the Alpine region (Barton et al., 2018; Li et al., 2021). In the Balkans, an increase of temperatures and precipitation is reconstructed from pollen assemblages (Maliq, Bordon et al., 2009; SL152, Dormoy et al., 2009) and is consistent with the high lake-level reconstructed at Lake Prespa (Cvetkoska et al., 2014). In the Near East, high $\delta^{18}O$ values are recorded in the Western Turkey (Eski Acigöl, Roberts et al., 2001; Sofular cave, Göktürk et al., 2011) which can indicate lower water levels, suggesting drier conditions in the region. On the contrary, the Lake Zeribar in Iran show low $\delta^{18}O$ values (Stevens et al., 2001) which can indicate wetter conditions mainly during winter.

Thus, climate reconstructions show an increase of precipitation in the Iberian margin, the Alpine regions, the Balkans and in Iran whereas the Southern Italy and the Western Turkey show no significant changes or drier conditions. In terms of temperatures, the records show warm conditions, and the changes seems not more contrasted in northern studied region. Other high-resolution records based on different proxies are required to corroborate or not the hypothesis of more contrasted temperatures in the north-west of Europe in comparison to the south of Europe (Renssen and Isarin, 2001; Moreno et al., 2014; Heiri et al., 2014).

Contrasting climate patterns during the Younger Dryas cold period (12,900-11,700 cal BP)

The Younger Dryas (YD) chronology is estimated between 12,900 and 11,700 cal BP by the NGRIP ice-core chronology (Rasmussen et al., 2014). Climate reconstructions provided by marine cores located in the southeastern Iberian Peninsula (Alboran Sea) indicate a decrease in temperatures and precipitation (Cacho et al., 2001; Combourieu Nebout et al., 2009). This precipitation drop is particularly marked during winter whereas a slight increase is recorded during summer (Combourieu Nebout et al., 2009). In the Northern Iberian Peninsula, a decrease of temperatures accompanied by an increase of summer precipitation are also recorded (Peñalba et al., 1996). In Italy (Chap. III), a drop in temperatures is recorded in all records (Allen et al., 2002; Sbaffi et al., 2004; Larocque and Finsinger, 2008; Sicre et al., 2013; Heiri et al., 2014; Marchegiano et al., 2020; this study). A slight increase of precipitation during the YD appears in Southern Italy below latitude 42°N (Combourieu-Nebout et al., 2013; Sicre et al., 2013) whereas a decrease of precipitation occurs in Northern Italy (Li et al., 2021; Regattieri et al., 2014). In the Balkans, a precipitation decrease reconstructed from pollen assemblages of Lake Maliq and SL52 marine core (Bordon et al., 2009; Dormoy et al., 2009) is consistent with a drop in water level of Lake Prespa (Cvetkoska et al., 2014). In terms of temperatures, a decrease is observed at Maliq (Bordon et al., 2009) and no significant changes are recorded in the SL 152 marine core (Dormoy et al., 2009). In the Near East, low $\delta^{18}O$ values are recorded in Western part, in Turkey (Roberts et al., 2001; Göktürk et al., 2011), indicating wetter conditions, whereas high values are recorded in the Eastern part, in Turkey and Iran (Stevens et al., 2001; Wick et al., 2003), indicating drier conditions.

Most of these records show colder conditions during the YD and they do not record differences between the northwestern sites and the southern sites. The hypothesis of a more contrasted Younger Dryas in terms of temperatures between the north-west and the south of Europe (Renssen and Isarin, 2001; Moreno et al., 2014; Heiri et al., 2014) is not evidenced here between the latitudes 35-46°N. Considering precipitation, a decrease is recorded in the Iberian Peninsula, the Northern Italy, the Balkans and the eastern part of the Near East and, on the contrary, wetter conditions are recorded in the Southern Italy and the Western Turkey. This pattern is very consistent with the model output by Rea et al. (2020) which have simulated the atmospheric circulation changes over Europe and Mediterranean Basin during the Younger Dryas. Their simulations show wetter conditions in the Southern Italy and the Western Turkey in agreement with our results. Cold conditions during the YD may be explained by the southward position of the Polar Frontal JetStream and a weak Atlantic Meridional Overturning

Circulation (AMOC) (Moreno et al., 2014; Rea et al., 2020; Renssen and Isarin, 2001). The incursion of cold air masses is recorded until the South of Italy. Considering precipitation, Rea et al. (2020) explains that a relocation of Atlantic storm tracks into the Mediterranean is induced by the Fennoscandian ice sheet and the North European Plain which created a topographic barrier and a high pressure region during the YD. The presence of Atlantic storm tracks into the Mediterranean could have favored wetter conditions in the Southern Italy and the Western Turkey during the YD.

3.2.3 Climate changes around the Mediterranean Basin during the Holocene

We cannot present an attempt to synthesize the climate in the same way as for the Lateglacial period because it is an even more ambitious task than for the Lateglacial period. Recent studies have revealed a very complex picture of climate variability within the Mediterranean area for the Holocene: (1) The northern and southern regions in the central Mediterranean have been under the prevalent influence of different climate patterns (around 40°N), producing opposite hydrological regimes and consequent vegetation dynamics (Magny et al., 2013; Peyron et al., 2013, 2017); (2), recurrent forest declines lateand dry events are also recorded in several pollen and palaeohydrological proxy-records in the south-central Mediterranean while an opposite pattern is suggested for the south-western Mediterranean, indicating a spatio-temporal hydrological pattern opposite to the south-central Mediterranean and suggesting that different expressions of climate modes occurred in the two regions at the same time (Di Rita et al., 2018); (3) The Holocene also exhibits a millennial-scale climate variability (Azuara et al., 2020; Marriner et al., 2022) and abrupt events as the 7.5 ka (Joannin et al., 2012) or the 4.2 ka (Bini et al., 2019). These spatio-temporal patterns and underlying processes during the Holocene are not fully deciphered yet, particularly in the central and western Mediterranean and the question of the onset of the Mediterranean climate is still open.

As we could not yet obtain a reliable age model for Lake Matese, we can unfortunately go further in these interpretations and assumptions, particularly for central Mediterranean area (Magny and Di Rita assumptions).

CHAPTER VI - CONCLUSION AND PERSPECTIVES

Lake Matese, Italy, M.Robles

This study investigates environmental dynamics, climate changes and human practices during the Lateglacial and the Holocene around the Mediterranean Basin through a multiproxy approach including sediment geochemistry (XRF), pollen, NPPs and biomarkers molecular (brGDGTs). We investigate two mountainous areas poorly documented: the Lesser Caucasus with the Vanevan peat (Lake Sevan) and the Apennines in Southern Italy with the Lake Matese. These two sites share the same latitude.

- Modern pollen-vegetation relationships have been studied for the first time in Armenia and in the Matese massif located in the Southern Italy. We realized altitudinal transects to characterize the different ecosystems. Understanding modern pollen-vegetation relationships was essential to accurately interpret the reconstructions of past vegetation around the Lake Sevan and the Lake Matese. Moreover, the addition of these modern pollen samples from Armenia and Southern Italy in the modern pollen dataset used to calibrate the climate reconstructions methods has allowed to improve the reliability of the pollen-based climate reconstructions.
- Past vegetation dynamics were reconstructed around the Vanevan peat for the Holocene period and around the Lake Matese for the Lateglacial and the Holocene. At Vanevan, a steppic vegetation (Poaceae) is recorded during the last 9700 years. The surrounding vegetation of Lake Sevan was poorly forested, even during the Mid-Holocene and contrasts with the previous hypotheses which suggested the occurrence of a deciduous forest. At Matese, the vegetation was mainly steppic during the Lateglacial, although an increase of deciduous arboreal taxa was recorded during the Bølling–Allerød. The Younger Dryas event is well recorded in the Matese pollen sequence. The Holocene is firstly characterized by the persistence of Poaceae and then the development of *Fagus* and Mediterranean taxa during the Mid-Late Holocene. Finally, vegetation reconstructions were compared across the Mediterranean Basin with a transect West -East including the Iberian Peninsula, Italy, the Balkans, the Near East and the Caucasus in order to understand the vegetation changes at a larger scale.
- Major paleohydrological changes were recorded by aquatic plants and algae at Vanevan peat and Lake Matese. At Vanevan, from 9700 cal BP, a lake system was present following by a drying phase at 4950 cal BP associated with ferns and finally a peatland dominated by Cyperaceae developed. At Matese, the Oldest Dryas and the Bølling–Allerød are characterized by an intermediate water level whereas the Younger Dryas

records the highest water level of the sequence. The Early Holocene is marked by a very low water level whereas the Mid-Late Holocene are characterized by a low water level. Understanding the paleohydrological changes are an important step to correctly interpret the climate reconstructions based on brGDGTs, because their distribution is more variable when the water levels are low. The water level changes have been used as markers of climate changes in Armenia, but not for Italy where the changes seem rather related to internal karstic draining of the Matese's massif.

- Climate reconstructions are based on a comparative study including both brGDGTs and pollen data. For the first time in the Mediterranean region, this study provides a comparative approach including pollen and GDGTs to quantify climate variability over time. A multimethod approach (MAT, WAPLS, RF, BRT) has been tested on Vanevan and Lake Matese pollen records to provide robust estimates of temperature and precipitation, and recent brGDGTs calibrations have been tested on the same samples to provide estimates of annual temperature. Climate reconstructions are complementary and show roughly a good correspondence between the proxies. BrGDGTs-based reconstructions have the advantage to reconstruct the climate independently of the vegetation and consequently of anthropogenic activities. However, the signal can also be largely impacted by water level changes of the wetland, therefore it is essential to document the paleohydrological changes. At Vanevan, climate reconstructions show an arid and cold Early Holocene, a more humid and warmer Mid Holocene, and a more arid and cooler Late Holocene. This result gives a strong support to the precipitation regime shift happening at the Early-Mid Holocene transition, separating a climate dominated by north influences from the Siberian highs with today's conditions, i.e. westerly dominance over precipitation and mild climate (Wick et al., 2003; Chen et al., 2008; Joannin et al., 2014). Several abrupt events have been detected at 6.2 ka, 5.2 ka, 4.2 ka, 2.8 ka and allow us to highlight the atmospheric processes in the Caucasus and the Near East. The four climate events are arid and seem linked to weak westerlies associated to multi-centennial cyclicity (NAO-like). The 5.2 ka and 2.8 ka are characterized by cold conditions and could be associated to a strong Siberian High. On the contrary, the 4.2 ka is characterized by warm conditions and would be influenced by the northward migration of Arabian subtropical systems. At Matese, the Bølling–Allerød is characterized by warm and humid conditions whereas the Younger Dryas is marked by cold conditions. Then, the Holocene is firstly characterized by humid and

warmer conditions followed by a slight decrease of precipitation and temperature during the Mid-Late Holocene. Cold (or warm) conditions during the YD (or Bølling–Allerød) in Italy may be linked to the southward (or northward) position of North Atlantic sea-ice and of the Polar Frontal JetStream. The low increase of precipitation during the YD may be linked to relocation of Atlantic storm tracks into the Mediterranean, induced by the Fennoscandian ice sheet and the North European Plain.

- Our study reveals a significant impact of abrupt climate changes on populations in the Near East and the Caucasus even for the recent periods, and contrasts with several studies which concluded to the dissociation between demographic trends and climate from 4000-3500 cal BP in the Near East. In the South Caucasus, the different climate events are consistent with the population abandonment phases and the agricultural practices around the Lake Sevan. In our study, climate changes appear as one of the main drivers of vegetation and thus on demographic changes in the South Caucasus. In Southern Italy, the opening of forests is detected during the last 2800-2600 years and seem associated to human practices. According to several studies, the Late Holocene is marked by a strong impact of humans on the vegetation and a decoupling of demographic trends and climate in Italy. In Southern Italy, strong human impacts seem to appear more tardively.

This study documented vegetation dynamics, climate changes and human practices in regions still poorly documented of the Mediterranean regions. However, the understanding of their environmental, climatic and human histories can still be improved as follows:

- The age-depth model of Lake Matese will be improved particularly for the Holocene part which is not well dated with the ^{14}C dates. We propose to check the occurrence of tephras in the organic parts of the sediment (Holocene period) with a new tephra protocol thought to be more reliable to detect cryptotephras in organic samples.
- The pollen resolution of the Lake Matese for the Holocene part can be improved, in order to better evidence abrupt climate changes, or the events related to human societies.
- It will be interesting to study with more details the pollen of Cereals at Vanevan, in order to improve our knowledge on agricultural practices around the Lake Sevan during the Neolithic and the Chalcolithic even if no archeological data are currently available.

- Climate reconstructions based on brGDGTs were mostly overestimated in comparison to the modern values and the pollen-based climate reconstructions. It might be interesting to study the modern relationships between GDGTs and climate in order to create local calibrations to reliable reconstruct the absolute values around the Mediterranean Basin. A calibration for GDGTs in Armenia is being elaborated and will include soil samples collected during the field in May 2019.
- Finally, in our study, the multiproxy approach was essential to correctly reconstruct past environment and climate. Other proxies, mainly climatic, could be added in order to complete and better understand the climate changes along the time.

Conclusion et perspectives

Cette étude s'intéresse aux dynamiques environnementales, aux changements climatiques et aux pratiques humaines durant le Tardiglaciaire et l'Holocène autour du bassin méditerranéen à travers une approche multiproxy incluant la géochimie des sédiments (XRF), les pollen, les NPP et les biomarqueurs moléculaires (brGDGT). Deux zones montagneuses peu documentées ont été étudiées : le Petit Caucase avec la tourbière Vanevan (lac Sévan) et les Apennins en Italie du Sud avec le lac Matese. Ces deux sites partagent la même latitude.

- Les relations modernes pollen-végétation ont été étudiées pour la première fois en Arménie et dans le Massif du Matese situé dans le Sud de l'Italie. Nous avons réalisé des transects altitudinaux pour caractériser les différents écosystèmes. La compréhension des relations modernes pollen-végétation a été essentielle pour correctement interpréter les reconstructions de la végétation passée autour du lac Sévan et du lac Matese. De plus, l'ajout de ces échantillons polliniques modernes provenant d'Arménie et d'Italie du Sud dans l'ensemble des données polliniques modernes, utilisé pour calibrer les méthodes de reconstruction du climat, a permis d'améliorer la fiabilité des reconstructions climatiques basées sur le pollen.
- Les dynamiques de la végétation passée ont été reconstruites autour de la tourbière Vanevan pour l'Holocène et autour du lac Matese pour le Tardiglaciaire et l'Holocène. À Vanevan, une végétation steppique (Poaceae) est enregistrée durant les 9700 dernières années. La végétation environnante du lac Sévan était peu boisée, même pendant l'Ho-

locène moyen, ce qui contraste avec les hypothèses précédentes qui suggéraient l'existence de forêts décidues. À Matese, la végétation était principalement steppique pendant le Tardiglaciaire, bien qu'une augmentation des taxons arborées décidus ait été enregistrée pendant le Bølling-Allerød. L'événement du Dryas Récent est bien enregistré dans la séquence pollinique de Matese. L'Holocène est d'abord caractérisé par la persistance des Poaceae, puis par le développement de *Fagus* et de taxons méditerranéens au cours de l'Holocène moyen-supérieur. Enfin, les reconstructions de végétation ont été comparées à travers le bassin méditerranéen selon un transect ouest-est comprenant la Péninsule Ibérique, l'Italie, les Balkans, le Proche-Orient et le Caucase afin de comprendre les changements de végétation à une échelle plus large.

- Des changements paléohydrologiques majeurs ont été enregistrés par les plantes aquatiques et les algues de la tourbière Vanevan et du lac Matese. À Vanevan, à partir de 9700 cal BP, un système lacustre était présent, suivi d'une phase d'assèchement à 4950 cal BP associée à des fougères et finalement une tourbière dominée par des Cyperaceae s'est développée. À Matese, le Dryas ancien et le Bølling-Allerød sont caractérisés par un niveau d'eau intermédiaire tandis que le Dryas récent enregistre le niveau d'eau le plus élevé de la séquence. L'Holocène inférieur est marqué par un niveau d'eau très bas, tandis que l'Holocène moyen-supérieur est caractérisé par un faible niveau d'eau. La compréhension des changements paléohydrologiques est une étape importante pour correctement interpréter les reconstructions climatiques basées sur les brGDGT, car leur distribution est plus variable lorsque le niveau d'eau est bas. Les changements de niveau d'eau ont été utilisés comme marqueurs des changements climatiques en Arménie, mais pas pour l'Italie où les changements semblent plutôt liés au drainage karstique interne du Massif du Matese.
- Les reconstructions climatiques sont basées sur une étude comparative incluant à la fois des brGDGT et des données polliniques. Pour la première fois dans la région Méditerranéenne, cette étude fournit une approche comparative incluant des pollen et des GDGT pour quantifier la variabilité climatique au cours du temps. Une approche multi-méthode (MAT, WAPLS, RF, BRT) a été appliquée sur les enregistrements polliniques de Vanevan et du lac Matese pour fournir des estimations robustes des températures et des précipitations, et des calibrations récentes de brGDGT ont été utilisées sur les mêmes échantillons pour fournir une estimation des températures annuelles. Les reconstructions climatiques sont complémentaires et montrent une bonne correspondance entre

les proxies. Les reconstructions basées sur les brGDGT ont l'avantage de reconstruire le climat indépendamment de la végétation et donc des activités anthropiques. Cependant, le signal peut aussi être largement influencé par les changements de niveau d'eau de la zone humide, il est donc essentiel de documenter les changements paléohydrologiques. À Vanevan, les reconstructions climatiques montrent un Holocène inférieur aride et froid, un Holocène moyen plus humide et plus chaud, et un Holocène supérieur plus aride et plus frais. Ces résultats appuient fortement le changement de régime des précipitations qui s'est produit à la transition Holocène inférieur-moyen, séparant un climat dominé par les influences du nord (anticyclone Sibérien) avec des conditions actuelles dominée par les vents d'Ouest incluant des précipitations et un climat doux (Wick et al., 2003 ; Chen et al., 2008 ; Joannin et al., 2014). Plusieurs événements abrupts ont été détectés à 6.2 ka, 5.2 ka, 4.2 ka, 2.8 ka et permettent de mettre en évidence les processus atmosphériques dans le Caucase et le Proche-Orient. Les quatre événements climatiques sont arides et semblent liés à de faibles vents d'Ouest associés à une cyclicité multi-centennale (de type NAO). Les événements du 5.2 ka et 2.8 ka sont caractérisés par des conditions froides et pourraient être associés à un important anticyclone Sibérien. Au contraire, la période 4.2 ka est caractérisée par des conditions chaudes et serait influencée par la migration vers le nord des systèmes subtropicaux Arabes. À Matese, le Bølling-Allerød est caractérisé par des conditions chaudes et humides alors que le Dryas Récent est marqué par des conditions froides. Ensuite, l'Holocène est d'abord caractérisé par des conditions humides et plus chaudes, suivies d'une légère diminution des précipitations et des températures pendant l'Holocène moyen-supérieur. Les conditions froides (ou chaudes) durant le Dryas Récent (ou le Bølling-Allerød) en Italie peuvent être liées à la position vers le sud (ou vers le nord) des glaces marines de l'Atlantique Nord et du JetStream Polaire. La faible augmentation des précipitations pendant le Dryas Récent peut être liée à la relocalisation des trajectoires des tempêtes de l'Atlantique vers la Méditerranée, induite par la calotte glaciaire de Fennoscandie et la Plaine Nord-Européenne.

- Notre étude révèle un impact significatif des changements climatiques abrupts sur les populations du Proche-Orient et du Caucase, même pour les périodes récentes, et contraste avec plusieurs études qui ont conclu à la dissociation entre les tendances démographiques et le climat à partir de 4000-3500 cal BP au Proche-Orient. Dans le Petit

Caucase, les différents événements climatiques sont cohérents avec les phases d'abandon des populations et les pratiques agricoles autour du lac Sévan. Dans notre étude, les changements climatiques apparaissent comme l'un des principaux moteurs de la végétation et des changements démographiques dans le Sud du Caucase. En Italie du Sud, l'ouverture des forêts est détectée au cours des 2800-2600 dernières années et semble associée aux pratiques humaines. Selon plusieurs études, l'Holocène supérieur est marqué par un fort impact de l'homme sur la végétation et un découplage des tendances démographiques et climatiques en Italie. En Italie du Sud, un fort impact anthropique semble apparaître plus tardivement.

Cette étude a permis de documenter les dynamiques de végétation, les changements climatiques et les pratiques humaines dans des régions encore peu documentées de la région Méditerranéenne. Cependant, la compréhension de leur histoire environnementale, climatique et humaine peut encore être améliorée comme suit :

- Le modèle âge-profondeur du lac Matese doit être amélioré, en particulier pour la partie Holocène qui n'est pas bien datée avec les dates ^{14}C. Je propose de vérifier la présence de téphras dans les parties organiques des sédiments (période Holocène) à l'aide d'un nouveau protocole, considéré comme plus fiable pour détecter les cryptotéphras dans les échantillons organiques.
- La résolution pollinique du lac Matese pour la partie Holocène peut être améliorée, afin de mieux mettre en évidence les changements climatiques abrupts, ou les événements liés aux sociétés humaines.
- Il sera intéressant d'étudier plus en détail le pollen de Céréales à Vanevan, afin d'améliorer nos connaissances sur les pratiques agricoles autour du lac Sévan pendant le Néolithique et le Chalcolithique même si aucune donnée archéologique n'est actuellement disponible.
- Les reconstructions climatiques basées sur les brGDGT étaient pour la plupart surestimées par rapport aux valeurs modernes et aux reconstructions climatiques basées sur les pollen. Il pourrait être intéressant d'étudier les relations modernes entre les GDGT et le climat afin de créer des calibrations locales pour reconstruire de manière fiable les valeurs absolues autour du bassin méditerranéen. Une calibration pour les GDGT en Arménie est en cours d'élaboration et inclura des échantillons de sol collectés sur le terrain en Mai 2019.

- Enfin, dans notre étude, l'approche multi-proxy était essentielle pour reconstruire correctement l'environnement et le climat passé. D'autres proxies, principalement climatiques, pourraient être ajoutés afin de compléter et mieux comprendre les changements climatiques au cours du temps.

REFERENCES

Allen, J.R.M., Huntley, B., 2018. Effects of tephra falls on vegetation: A Late-Quaternary record from southern Italy. J Ecol 106, 2456–2472. https://doi.org/10.1111/1365-2745.12998

Allen, J.R.M., Watts, W.A., McGee, E., Huntley, B., 2002. Holocene environmental variability-the record from Lago Grande di Monticchio, Italy. Quaternary International 88, 69–80.

Aptroot, A., van Geel, B., 2006. Fungi of the colon of the Yukagir Mammoth and from stratigraphically related permafrost samples. Review of Palaeobotany and Palynology, Quaternary non-pollen palynomorphs 141, 225–230. https://doi.org/10.1016/j.revpalbo.2005.04.006

Aranbarri, J., González-Sampériz, P., Valero-Garcés, B., Moreno, A., Gil-Romera, G., Sevilla-Callejo, M., García-Prieto, E., Di Rita, F., Mata, M.P., Morellón, M., Magri, D., Rodríguez-Lázaro, J., Carrión, J.S., 2014. Rapid climatic changes and resilient vegetation during the Lateglacial and Holocene in a continental region of south-western Europe. Global and Planetary Change 114, 50–65. https://doi.org/10.1016/j.gloplacha.2014.01.003

Arnaud, F., Révillon, S., Debret, M., Revel, M., Chapron, E., Jacob, J., Giguet-Covex, C., Poulenard, J., Magny, M., 2012. Lake Bourget regional erosion patterns reconstruction reveals Holocene NW European Alps soil evolution and paleohydrology. Quaternary Science Reviews 51, 81–92. https://doi.org/10.1016/j.quascirev.2012.07.025

Azuara, J., Sabatier, P., Lebreton, V., Jalali, B., Sicre, M.-A., Dezileau, L., Bassetti, M.-A., Frigola, J., Combourieu-Nebout, N., 2020. Mid- to Late-Holocene Mediterranean climate variability: Contribution of multi-proxy and multi-sequence comparison using wavelet spectral analysis in the northwestern Mediterranean basin. Earth-Science Reviews 208, 103232. https://doi.org/10.1016/j.earscirev.2020.103232

Badalyan, R., Harutyunyan, A., 2014. Aknashen—the Late Neolithic Settlement of the Ararat Valley: Main Results and Prospects for the Research, in: Gasparyan, B., Arimura, M. (Eds.), Stone Age of Armenia: A Guide-Book to the Stone Age Archaeology in the Republic of Armenia, Monograph of the JSPS-Bilateral Joint Research Project. Center for Cultural Resource Studies, Kanazawa, pp. 161–177.

Badalyan, R., Lombard, P., Chataigner, C., Avetisyan, P., 2004. The Neolithic and Chalcolithic phases in the Ararat plain (Armenia): The view from Aratashen, in: Sagona, A. (Ed.), A

View from the Highlands: Archaeological Studies in Honour of Charles Burney, Ancient Near Eastern Studies. Peeters Press, Leuven ; Dudley, MA, pp. 399–420.

Bar-Matthews, M., Ayalon, A., 2011. Mid-Holocene climate variations revealed by high-resolution speleothem records from Soreq Cave, Israel and their correlation with cultural changes. The Holocene 21, 163–171. https://doi.org/10.1177/0959683610384165

Bar-Matthews, M., Ayalon, A., Gilmour, M., Matthews, A., Hawkesworth, C.J., 2003. Sea–land oxygen isotopic relationships from planktonic foraminifera and speleothems in the Eastern Mediterranean region and their implication for paleorainfall during interglacial intervals. Geochimica et Cosmochimica Acta 67, 3181–3199. https://doi.org/10.1016/S0016-7037(02)01031-1

Barton, C.M., Aura Tortosa, J.E., Garcia-Puchol, O., Riel-Salvatore, J.G., Gauthier, N., Vadillo Conesa, M., Pothier Bouchard, G., 2018. Risk and resilience in the late glacial: A case study from the western Mediterranean. Quaternary Science Reviews 184, 68–84. https://doi.org/10.1016/j.quascirev.2017.09.015

Bini, M., Zanchetta, G., Perşoiu, A., Cartier, R., Català, A., Cacho, I., Dean, J.R., Di Rita, F., Drysdale, R.N., Finnè, M., Isola, I., Jalali, B., Lirer, F., Magri, D., Masi, A., Marks, L., Mercuri, A.M., Peyron, O., Sadori, L., Sicre, M.-A., Welc, F., Zielhofer, C., Brisset, E., 2019. The 4.2 ka BP Event in the Mediterranean region: an overview. Clim. Past 15, 555–577. https://doi.org/10.5194/cp-15-555-2019

Blaga, C.I., Reichart, G.-J., Lotter, A.F., Anselmetti, F.S., Sinninghe Damsté, J.S., 2013. A TEX 86 lake record suggests simultaneous shifts in temperature in Central Europe and Greenland during the last deglaciation: A SWISS TEX 86 LAKE RECORD. Geophys. Res. Lett. 40, 948–953. https://doi.org/10.1002/grl.50181

Bordon, A., Peyron, O., Lézine, A.-M., Brewer, S., Fouache, E., 2009. Pollen-inferred Late-Glacial and Holocene climate in southern Balkans (Lake Maliq). Quaternary International 200, 19–30. https://doi.org/10.1016/j.quaint.2008.05.014

Bradley, R.S., 2015. Chapter 1 - Paleoclimatic Reconstruction, in: Bradley, R.S. (Ed.), Paleoclimatology (Third Edition). Academic Press, San Diego, pp. 1–11. https://doi.org/10.1016/B978-0-12-386913-5.00001-6

Cacho, I., Grimalt, J.O., Canals, M., Sbaffi, L., Shackleton, N.J., Schönfeld, J., Zahn, R., 2001. Variability of the western Mediterranean Sea surface temperature during the last 25,000 years and its connection with the Northern Hemisphere climatic changes. Paleoceanography 16, 40–52. https://doi.org/10.1029/2000PA000502

Caroli, I., Caldara, M., 2007. Vegetation history of Lago Battaglia (eastern Gargano coast, Apulia, Italy) during the middle-late Holocene. Veget Hist Archaeobot 16, 317–327. https://doi.org/10.1007/s00334-006-0045-y

Carrión, J.S., Van Geel, B., 1999. Fine-resolution Upper Weichselian and Holocene palynological record from Navarrés (Valencia, Spain) and a discussion about factors of Mediterranean forest succession. Review of Palaeobotany and Palynology 106, 209–236. https://doi.org/10.1016/S0034-6667(99)00009-3

Chataigner, C., Gratuze, B., Tardy, N., Abbès, F., Kalantaryan, I., Hovsepyan, R., Chahoud, J., Perello, B., 2020. Diachronic variability in obsidian procurement patterns and the role of the cave-sheepfold of Getahovit-2 (NE Armenia) during the Chalcolithic period. Quaternary International 550, 1–19. https://doi.org/10.1016/j.quaint.2020.02.010

Chen, F., Yu, Z., Yang, M., Ito, E., Wang, S., Madsen, D.B., Huang, X., Zhao, Y., Sato, T., John B. Birks, H., Boomer, I., Chen, J., An, C., Wünnemann, B., 2008. Holocene moisture evolution in arid central Asia and its out-of-phase relationship with Asian monsoon history. Quaternary Science Reviews 27, 351–364. https://doi.org/10.1016/j.quascirev.2007.10.017

Colledge, S., Conolly, J., Shennan, S., 2004. Archaeobotanical Evidence for the Spread of Farming in the Eastern Mediterranean. Current Anthropology 45, S35–S58. https://doi.org/10.1086/422086

Combourieu Nebout, N., Peyron, O., Dormoy, I., Desprat, S., Beaudouin, C., Kotthoff, U., Marret, F., 2009. Rapid climatic variability in the west Mediterranean during the last 25 000 years from high resolution pollen data. Clim. Past 19.

Combourieu-Nebout, N., Peyron, O., Bout-Roumazeilles, V., Goring, S., Dormoy, I., Joannin, S., Sadori, L., Siani, G., Magny, M., 2013. Holocene vegetation and climate changes in the central Mediterranean inferred from a high-resolution marine pollen record (Adriatic Sea). Clim. Past 9, 2023–2042. https://doi.org/10.5194/cp-9-2023-2013

Connor, S.E., 2011. A promethean legacy: late quaternary vegetation history of Southern Georgia, Caucasus (PhD thesis). University of Melbourne, Melbourne.

Connor, S.E., Colombaroli, D., Confortini, F., Gobet, E., Ilyashuk, B.P., Ilyashuk, E.A., van Leeuwen, J.F.N., Lamentowicz, M., van der Knaap, W.O., Malysheva, E., Marchetto, A., Margalitadze, N., Mazei, Y., Mitchell, E.A.D., Payne, R.J., Ammann, B., 2018. Long-term population dynamics: Theory and reality in a peatland ecosystem. J Ecol 106, 333–346. https://doi.org/10.1111/1365-2745.12865

Connor, S.E., Kvavadze, E.V., 2008. Modelling late Quaternary changes in plant distribution, vegetation and climate using pollen data from Georgia, Caucasus. Journal of Biogeography 36, 529–545. https://doi.org/10.1111/j.1365-2699.2008.02019.x

Coope, G.R., 2004. Several million years of stability among insect species because of, or in spite of, Ice Age climatic instability? Philosophical Transactions of the Royal Society of London. Series B: Biological Sciences 359, 209–214. https://doi.org/10.1098/rstb.2003.1393

Cromartie, A., Blanchet, C., Barhoumi, C., Messager, E., Peyron, O., Ollivier, V., Sabatier, P., Etienne, D., Karakhanyan, A., Khatchadourian, L., Smith, A.T., Badalyan, R., Perello, B., Lindsay, I., Joannin, S., 2020. The vegetation, climate, and fire history of a mountain steppe: A Holocene reconstruction from the South Caucasus, Shenkani, Armenia. Quaternary Science Reviews 246, 106485. https://doi.org/10.1016/j.quascirev.2020.106485

Croudace, I.W., Rothwell, R.G. (Eds.), 2015. Micro-XRF Studies of Sediment Cores: Applications of a non-destructive tool for the environmental sciences, Developments in Paleoenvironmental Research. Springer Netherlands, Dordrecht. https://doi.org/10.1007/978-94-017-9849-5

Cugny, C., Mazier, F., Galop, D., 2010. Modern and fossil non-pollen palynomorphs from the Basque mountains (western Pyrenees, France): the use of coprophilous fungi to reconstruct pastoral activity. Veget Hist Archaeobot 19, 391–408. https://doi.org/10.1007/s00334-010-0242-6

Cvetkoska, A., Levkov, Z., Reed, J.M., Wagner, B., 2014. Late Glacial to Holocene climate change and human impact in the Mediterranean: The last ca. 17ka diatom record of Lake Prespa (Macedonia/Albania/Greece). Palaeogeography, Palaeoclimatology, Palaeoecology 406, 22–32. https://doi.org/10.1016/j.palaeo.2014.04.010

De Beaulieu, J.-L., Brugiapaglia, E., Joannin, S., Guiter, F., Zanchetta, G., Wulf, S., Peyron, O., Bernardo, L., Didier, J., Stock, A., Rius, D., Magny, M., 2017. Lateglacial-Holocene abrupt vegetation changes at Lago Trifoglietti in Calabria, Southern Italy: The setting of ecosystems in a refugial zone. Quaternary Science Reviews 158, 44–57. https://doi.org/10.1016/j.quascirev.2016.12.013

De Jonge, C., Hopmans, E.C., Zell, C.I., Kim, J.-H., Schouten, S., Sinninghe Damsté, J.S., 2014. Occurrence and abundance of 6-methyl branched glycerol dialkyl glycerol tetraethers in soils: Implications for palaeoclimate reconstruction. Geochimica et Cosmochimica Acta 141, 97–112. https://doi.org/10.1016/j.gca.2014.06.013

Dearing Crampton-Flood, E., Peterse, F., Munsterman, D., Sinninghe Damsté, J.S., 2018. Using tetraether lipids archived in North Sea Basin sediments to extract North Western European Pliocene continental air temperatures. Earth and Planetary Science Letters 490, 193–205. https://doi.org/10.1016/j.epsl.2018.03.030

Dearing Crampton-Flood, E., Tierney, J.E., Peterse, F., Kirkels, F.M.S.A., Sinninghe Damsté, J.S., 2020. BayMBT: A Bayesian calibration model for branched glycerol dialkyl glycerol tetraethers in soils and peats. Geochimica et Cosmochimica Acta 268, 142–159. https://doi.org/10.1016/j.gca.2019.09.043

Denèfle, M., Lézine, A.-M., Fouache, E., Dufaure, J.-J., 2000. A 12,000-Year Pollen Record from Lake Maliq, Albania. Quaternary Research 54, 423–432. https://doi.org/10.1006/qres.2000.2179

Di Rita, F., Fletcher, W.J., Aranbarri, J., Margaritelli, G., Lirer, F., Magri, D., 2018. Holocene forest dynamics in central and western Mediterranean: periodicity, spatio-temporal patterns and climate influence. Sci Rep 8, 8929. https://doi.org/10.1038/s41598-018-27056-2

Ding, S., Schwab, V.F., Ueberschaar, N., Roth, V.-N., Lange, M., Xu, Y., Gleixner, G., Pohnert, G., 2016. Identification of novel 7-methyl and cyclopentanyl branched glycerol dialkyl glycerol tetraethers in lake sediments. Organic Geochemistry 102, 52–58. https://doi.org/10.1016/j.orggeochem.2016.09.009

Djamali, M., Akhani, H., Andrieu-Ponel, V., Braconnot, P., Brewer, S., de Beaulieu, J.-L., Fleitmann, D., Fleury, J., Gasse, F., Guibal, F., Jackson, S.T., Lézine, A.-M., Médail, F., Ponel, P., Roberts, N., Stevens, L., 2010. Indian Summer Monsoon variations could have affected the early-Holocene woodland expansion in the Near East. The Holocene 20, 813–820. https://doi.org/10.1177/0959683610362813

Djamali, M., de Beaulieu, J.-L., Shah-hosseini, M., Andrieu-Ponel, V., Ponel, P., Amini, A., Akhani, H., Leroy, S.A.G., Stevens, L., Lahijani, H., Brewer, S., 2008. A late Pleistocene long pollen record from Lake Urmia, Nw Iran. Quat. res. 69, 413–420. https://doi.org/10.1016/j.yqres.2008.03.004

Dormoy, I., Peyron, O., Nebout, N.C., Goring, S., Kotthoff, U., Magny, M., Pross, J., 2009. Terrestrial climate variability and seasonality changes in the Mediterranean region between 15 000 and 4000 years BP deduced from marine pollen records. Clim. Past 18.

Drescher-Schneider, R., de Beaulieu, J.-L., Magny, M., Walter-Simonnet, A.-V., Bossuet, G., Millet, L., Brugiapaglia, E., Drescher, A., 2007. Vegetation history, climate and human

impact over the last 15,000 years at Lago dell'Accesa (Tuscany, Central Italy). Veget Hist Archaeobot 16, 279–299. https://doi.org/10.1007/s00334-006-0089-z

Dugerdil, L., Joannin, S., Peyron, O., Jouffroy-Bapicot, I., Vannière, B., Boldgiv, B., Unkelbach, J., Behling, H., Ménot, G., 2021a. Climate reconstructions based on GDGT and pollen surface datasets from Mongolia and Baikal area: calibrations and applicability to extremely cold–dry environments over the Late Holocene. Clim. Past 17, 1199–1226. https://doi.org/10.5194/cp-17-1199-2021

Dugerdil, L., Ménot, G., Peyron, O., Jouffroy-Bapicot, I., Ansanay-Alex, S., Antheaume, I., Behling, H., Boldgiv, B., Develle, A.-L., Grossi, V., Magail, J., Makou, M., Robles, M., Unkelbach, J., Vannière, B., Joannin, S., 2021b. Late Holocene Mongolian climate and environment reconstructions from brGDGTs, NPPs and pollen transfer functions for Lake Ayrag: Paleoclimate implications for Arid Central Asia. Quaternary Science Reviews 273, 107235. https://doi.org/10.1016/j.quascirev.2021.107235

Eastwood, W.J., Leng, M.J., Roberts, N., Davis, B., 2007. Holocene climate change in the eastern Mediterranean region: a comparison of stable isotope and pollen data from Lake Gölhisar, southwest Turkey. J. Quaternary Sci. 22, 327–341. https://doi.org/10.1002/jqs.1062

Edwards, P.C., Meadows, J., Sayej, G.J., Westaway, M., 2004. From the PPNA to the PPNB : new views from the Southern Levant after excavations at Zahrat adh-Dhra' 2 in Jordan. Paléorient 30, 21–60. https://doi.org/10.3406/paleo.2004.1010

Ermolli, E.R., di Pasquale, G., 2002. Vegetation dynamics of south-western Italy in the last 28 kyr inferred from pollen analysis of a Tyrrhenian Sea core. Veget Hist Archaeobot 11, 211–220. https://doi.org/10.1007/s003340200024

Evans, M.N., Tolwinski-Ward, S.E., Thompson, D.M., Anchukaitis, K.J., 2013. Applications of proxy system modeling in high resolution paleoclimatology. Quaternary Science Reviews 76, 16–28. https://doi.org/10.1016/j.quascirev.2013.05.024

Faegri, K., Kaland, P.E., Krzywinski, K., 1989. Textbook of pollen analysis. John Wiley & Sons, Chichester.

Fukumoto, Y., Kashima, K., Orkhonselenge, A., Ganzorig, U., 2012. Holocene environmental changes in northern Mongolia inferred from diatom and pollen records of peat sediment. Quaternary International 254, 83–91. https://doi.org/10.1016/j.quaint.2011.10.014

Fuller, D.Q., 2007. Contrasting patterns in crop domestication and domestication rates: recent archaeobotanical insights from the Old World. Ann Bot 100, 903–924. https://doi.org/10.1093/aob/mcm048

Gil García, M.J., Valiño, M.D., Rodríguez, A.V., Zapata, M.B.R., 2002. Late-glacial and Holocene palaeoclimatic record from Sierra de Cebollera (northern Iberian Range, Spain). Quaternary International 93–94, 13–18. https://doi.org/10.1016/S1040-6182(02)00003-4

Göktürk, O.M., Fleitmann, D., Badertscher, S., Cheng, H., Edwards, R.L., Leuenberger, M., Fankhauser, A., Tüysüz, O., Kramers, J., 2011. Climate on the southern Black Sea coast during the Holocene: implications from the Sofular Cave record. Quaternary Science Reviews 30, 2433–2445. https://doi.org/10.1016/j.quascirev.2011.05.007

Grachev, A.M., Novenko, E.Y., Grabenko, E.A., Alexandrin, M.Y., Zazovskaya, E.P., Konstantinov, E.A., Shishkov, V.A., Lazukova, L.I., Chepurnaya, A.A., Kuderina, T.M., Ivanov, M.M., Kuzmenkova, N.V., Darin, A.V., Solomina, O.N., 2021. The Holocene paleoenvironmental history of Western Caucasus (Russia) reconstructed by multi-proxy analysis of the continuous sediment sequence from Lake Khuko. The Holocene 31, 368–379. https://doi.org/10.1177/0959683620972782

Guilaine, J., 2003. De la vague à la tombe, La conquête néolithique de la Méditerranée (8000-2000 avant J.-C.). Bulletin de la Société préhistorique française 100, 818–822.

Heiri, O., Brooks, S.J., Renssen, H., Bedford, A., Hazekamp, M., Ilyashuk, B., Jeffers, E.S., Lang, B., Kirilova, E., Kuiper, S., Millet, L., Samartin, S., Toth, M., Verbruggen, F., Watson, J.E., van Asch, N., Lammertsma, E., Amon, L., Birks, H.H., Birks, H.J.B., Mortensen, M.F., Hoek, W.Z., Magyari, E., Muñoz Sobrino, C., Seppä, H., Tinner, W., Tonkov, S., Veski, S., Lotter, A.F., 2014. Validation of climate model-inferred regional temperature change for late-glacial Europe. Nat Commun 5, 4914. https://doi.org/10.1038/ncomms5914

Heiri, O., Ilyashuk, B., Millet, L., Samartin, S., Lotter, A.F., 2015. Stacking of discontinuous regional palaeoclimate records: Chironomid-based summer temperatures from the Alpine region. The Holocene 25, 137–149. https://doi.org/10.1177/0959683614556382

Hillman, G., Hedges, R., Moore, A., Colledge, S., Pettitt, P., 2001. New evidence of Lateglacial cereal cultivation at Abu Hureyra on the Euphrates. The Holocene 11, 383–393. https://doi.org/10.1191/095968301678302823

Hovsepyan, R., 2017. New Data on Archaeobotany of the Lake Sevan Basin. Iran and the Caucasus 21, 251–276. https://doi.org/10.1163/1573384X-20170302

Hovsepyan, R., 2013. First archaeobotanical data from the basin of Lake Sevan. Archäologie in Armenien II 67, 93–108.

Hovsepyan, R., Willcox, G., 2008. The earliest finds of cultivated plants in Armenia: evidence from charred remains and crop processing residues in pisé from the Neolithic settlements of Aratashen and Aknashen. Veget Hist Archaeobot 17, 63–71. https://doi.org/10.1007/s00334-008-0158-6

Hurrell, J.W., 1995. Decadal Trends in the North Atlantic Oscillation: Regional Temperatures and Precipitation. Science 269, 676–679. https://doi.org/10.1126/science.269.5224.676

Ivy-Ochs, S., Kerschner, H., Maisch, M., Christl, M., Kubik, P.W., Schlüchter, C., 2009. Latest Pleistocene and Holocene glacier variations in the European Alps. Quaternary Science Reviews 28, 2137–2149. https://doi.org/10.1016/j.quascirev.2009.03.009

Jacobson, G.L., Bradshaw, R.H.W., 1981. The Selection of Sites for Paleovegetational Studies. Quat. res. 16, 80–96. https://doi.org/10.1016/0033-5894(81)90129-0

Jalut, G., Dedoubat, J.J., Fontugne, M., Otto, T., 2009. Holocene circum-Mediterranean vegetation changes: Climate forcing and human impact. Quaternary International 200, 4–18. https://doi.org/10.1016/j.quaint.2008.03.012

Joannin, S., Ali, A.A., Ollivier, V., Roiron, P., Peyron, O., Chevaux, S., Nahapetyan, S., Tozalakyan, P., Karakhanyan, A., Chataigner, C., 2014. Vegetation, fire and climate history of the Lesser Caucasus: a new Holocene record from Zarishat fen (Armenia): PALAEOENVIRONMENT AND PALAEOCLIMATE IN ARMENIA. J. Quaternary Sci. 29, 70–82. https://doi.org/10.1002/jqs.2679

Joannin, S., Brugiapaglia, E., de Beaulieu, J.-L., Bernardo, L., Magny, M., Peyron, O., Goring, S., Vannière, B., 2012. Pollen-based reconstruction of Holocene vegetation and climate in southern Italy: the case of Lago Trifoglietti. Clim. Past 8, 1973–1996. https://doi.org/10.5194/cp-8-1973-2012

Kaniewski, D., Marriner, N., Cheddadi, R., Guiot, J., Van Campo, E., 2018. The 4.2 ka BP event in the Levant. Clim. Past 14, 1529–1542. https://doi.org/10.5194/cp-14-1529-2018

Kuijt, I., Finlayson, B., 2009. Evidence for food storage and predomestication granaries 11,000 years ago in the Jordan Valley. Proc Natl Acad Sci U S A 106, 10966–10970. https://doi.org/10.1073/pnas.0812764106

Larocque, I., Finsinger, W., 2008. Late-glacial chironomid-based temperature reconstructions for Lago Piccolo di Avigliana in the southwestern Alps (Italy). Palaeogeography, Palaeoclimatology, Palaeoecology 257, 207–223. https://doi.org/10.1016/j.palaeo.2007.10.021

Lawrence, D., Philip, G., Hunt, H., Snape-Kennedy, L., Wilkinson, T.J., 2016. Correction: Long Term Population, City Size and Climate Trends in the Fertile Crescent: A First Approximation. PLoS ONE 11, e0157863. https://doi.org/10.1371/journal.pone.0157863

Lawson, I., Frogley, M., Bryant, C., Preece, R., Tzedakis, P., 2004. The Lateglacial and Holocene environmental history of the Ioannina basin, north-west Greece. Quaternary Science Reviews 23, 1599–1625. https://doi.org/10.1016/j.quascirev.2004.02.003

Lebreton, V., Messager, E., Marquer, L., Renault-Miskovsky, J., 2010. A neotaphonomic experiment in pollen oxidation and its implications for archaeopalynology. Review of Palaeobotany and Palynology 162, 29–38. https://doi.org/10.1016/j.revpalbo.2010.05.002

Leroy, S.A.G., Tudryn, A., Chalié, F., López-Merino, L., Gasse, F., 2013. From the Allerød to the mid-Holocene: palynological evidence from the south basin of the Caspian Sea. Quaternary Science Reviews 78, 77–97. https://doi.org/10.1016/j.quascirev.2013.07.032

Leroyer, C., Joannin, S., Aoustin, D., Ali, A.A., Peyron, O., Ollivier, V., Tozalakyan, P., Karakhanyan, A., Jude, F., 2016. Mid Holocene vegetation reconstruction from Vanevan peat (south-eastern shore of Lake Sevan, Armenia). Quaternary International, Environments and Societies in the Southern Caucasus during the Holocene 395, 5–18. https://doi.org/10.1016/j.quaint.2015.06.008

Li, H., Spötl, C., Cheng, H., 2021. A high-resolution speleothem proxy record of the Late Glacial in the European Alps: extending the NALPS19 record until the beginning of the Holocene. J. Quaternary Sci 36, 29–39. https://doi.org/10.1002/jqs.3255

Lionello, P. (Ed.), 2012. The climate of the Mediterranean region: from the past to the future, 1st ed. ed, Elsevier insights. Elsevier, London ; Waltham, MA.

Lionello, P., Malanotte-Rizzoli, P., Boscolo, R., Alpert, P., Artale, V., Li, L., Luterbacher, J., May, W., Trigo, R., Tsimplis, M., Ulbrich, U., Xoplaki, E., 2006. The Mediterranean climate: An overview of the main characteristics and issues, in: Developments in Earth and Environmental Sciences. Elsevier, pp. 1–26. https://doi.org/10.1016/S1571-9197(06)80003-0

Litt, T., Krastel, S., Sturm, M., Kipfer, R., Örcen, S., Heumann, G., Franz, S.O., Ülgen, U.B., Niessen, F., 2009. 'PALEOVAN', International Continental Scientific Drilling Program (ICDP): site survey results and perspectives. Quaternary Science Reviews 28, 1555–1567. https://doi.org/10.1016/j.quascirev.2009.03.002

Loomis, S.E., 2011. Distributions of branched GDGTs in soils and lake sediments from western Uganda: Implications for a lacustrine paleothermometer. Organic Geochemistry 13.

López-Merino, L., López-Sáez, J.A., Alba-Sánchez, F., Pérez-Díaz, S., Carrión, J.S., 2009. 2000 years of pastoralism and fire shaping high-altitude vegetation of Sierra de Gredos in central Spain. Review of Palaeobotany and Palynology 158, 42–51. https://doi.org/10.1016/j.revpalbo.2009.07.003

López-Moreno, J.I., Vicente-Serrano, S.M., Morán-Tejeda, E., Lorenzo-Lacruz, J., Kenawy, A., Beniston, M., 2011. Effects of the North Atlantic Oscillation (NAO) on combined temperature and precipitation winter modes in the Mediterranean mountains: Observed relationships and projections for the 21st century. Global and Planetary Change 77, 62–76. https://doi.org/10.1016/j.gloplacha.2011.03.003

Lu, H., Liu, W., Yang, H., Wang, H., Liu, Z., Leng, Q., Sun, Y., Zhou, W., An, Z., 2019. 800-kyr land temperature variations modulated by vegetation changes on Chinese Loess Plateau. Nat Commun 10, 1958. https://doi.org/10.1038/s41467-019-09978-1

Magny, M., Combourieu-Nebout, N., de Beaulieu, J.-L., Bout-Roumazeilles, V., Colombaroli, D., Desprat, S., Francke, A., Joannin, S., Ortu, E., Peyron, O., Revel, M., Sadori, L., Siani, G., Sicre, M.A., Samartin, S., Simonneau, A., Tinner, W., Vanniere, B., Wagner, B., Zanchetta, G., Anselmetti, F., Brugiapaglia, E., Chapron, E., Debret, M., Didier, J., Essallami, L., Galop, D., Gilli, A., Kallel, N., Millet, L., Stock, A., Turon, J.L., Wirth, S., 2013. North-south palaeohydrological contrasts in the central Mediterranean during the Holocene: tentative synthesis and working hypotheses. Clim. Past 30.

Magny, M., Leuzinger, U., Bortenschlager, S., Haas, J.N., 2006. Tripartite climate reversal in Central Europe 5600–5300 years ago. Quat. res. 65, 3–19. https://doi.org/10.1016/j.yqres.2005.06.009

Magny, M., Vannière, B., Calo, C., Millet, L., Leroux, A., Peyron, O., Zanchetta, G., La Mantia, T., Tinner, W., 2011. Holocene hydrological changes in south-western Mediterranean as recorded by lake-level fluctuations at Lago Preola, a coastal lake in southern Sicily, Italy. Quaternary Science Reviews 30, 2459–2475. https://doi.org/10.1016/j.quascirev.2011.05.018

Magri, D., 2008. Patterns of post-glacial spread and the extent of glacial refugia of European beech (Fagus sylvatica). Journal of Biogeography 35, 450–463. https://doi.org/10.1111/j.1365-2699.2007.01803.x

Marchegiano, M., Horne, D.J., Gliozzi, E., Francke, A., Wagner, B., Ariztegui, D., 2020. Rapid Late Pleistocene climate change reconstructed from a lacustrine ostracod record in

central Italy (Lake Trasimeno, Umbria). Boreas 49, 739–750. https://doi.org/10.1111/bor.12450

Marriner, N., Kaniewski, D., Pourkerman, M., Devillers, B., 2022. Anthropocene tipping point reverses long-term Holocene cooling of the Mediterranean Sea: A meta-analysis of the basin's Sea Surface Temperature records. Earth-Science Reviews 227, 103986. https://doi.org/10.1016/j.earscirev.2022.103986

Martin, C., Ménot, G., Thouveny, N., Davtian, N., Andrieu-Ponel, V., Reille, M., Bard, E., 2019. Impact of human activities and vegetation changes on the tetraether sources in Lake St Front (Massif Central, France). Organic Geochemistry 135, 38–52.

Martin, C., Ménot, G., Thouveny, N., Peyron, O., Andrieu-Ponel, V., Montade, V., Davtian, N., Reille, M., Bard, E., 2020. Early Holocene Thermal Maximum recorded by branched tetraethers and pollen in Western Europe (Massif Central, France). Quaternary Science Reviews 228, 106109. https://doi.org/10.1016/j.quascirev.2019.106109

Martínez-Sosa, P., Tierney, J.E., Stefanescu, I.C., Dearing Crampton-Flood, E., Shuman, B.N., Routson, C., 2021. A global Bayesian temperature calibration for lacustrine brGDGTs. Geochimica et Cosmochimica Acta 305, 87–105. https://doi.org/10.1016/j.gca.2021.04.038

Masi, A., Francke, A., Pepe, C., Thienemann, M., Wagner, B., Sadori, L., 2018. Vegetation history and paleoclimate at Lake Dojran (FYROM/Greece) during the Late Glacial and Holocene. Clim. Past 14, 351–367. https://doi.org/10.5194/cp-14-351-2018

Mauri, A., Davis, B. a. S., Collins, P.M., Kaplan, J.O., 2014. The influence of atmospheric circulation on the mid-Holocene climate of Europe: a data–model comparison. Climate of the Past 10, 1925–1938. https://doi.org/10.5194/cp-10-1925-2014

Mauri, A., Davis, B.A.S., Collins, P.M., Kaplan, J.O., 2015. The climate of Europe during the Holocene: a gridded pollen-based reconstruction and its multi-proxy evaluation. Quaternary Science Reviews 112, 109–127. https://doi.org/10.1016/j.quascirev.2015.01.013

McCormack, J., Viehberg, F., Akdemir, D., Immenhauser, A., Kwiecien, O., 2019. Ostracods as ecological and isotopic indicators of lake water salinity changes: the Lake Van example. Biogeosciences 16, 2095–2114. https://doi.org/10.5194/bg-16-2095-2019

Mercuri, A.M., Accorsi, C.A., Bandini Mazzanti, M., 2002. The long history of Cannabis and its cultivation by the Romans in central Italy, shown by pollen records from Lago Albano and Lago di Nemi. Veget Hist Archaeobot 11, 263–276. https://doi.org/10.1007/s003340200039

Messager, E., Belmecheri, S., Von Grafenstein, U., Nomade, S., Ollivier, V., Voinchet, P., Puaud, S., Courtin-Nomade, A., Guillou, H., Mgeladze, A., Dumoulin, J.-P., Mazuy, A., Lordkipanidze, D., 2013. Late Quaternary record of the vegetation and catchment-related changes from Lake Paravani (Javakheti, South Caucasus). Quaternary Science Reviews 77, 125–140. https://doi.org/10.1016/j.quascirev.2013.07.011

Messager, E., Nomade, S., Wilhelm, B., Joannin, S., Scao, V., Von Grafenstein, U., Martkoplishvili, I., Ollivier, V., Mgeladze, A., Dumoulin, J.-P., Mazuy, A., Belmecheri, S., Lordkipanidze, D., 2017. New pollen evidence from Nariani (Georgia) for delayed postglacial forest expansion in the South Caucasus. Quat. res. 87, 121–132. https://doi.org/10.1017/qua.2016.3

Miebach, A., Niestrath, P., Roeser, P., Litt, T., 2016. Impacts of climate and humans on the vegetation in northwestern Turkey: palynological insights from Lake Iznik since the Last Glacial. Clim. Past 12, 575–593. https://doi.org/10.5194/cp-12-575-2016

Moreno, A., Svensson, A., Brooks, S.J., Connor, S., Engels, S., Fletcher, W., Genty, D., Heiri, O., Labuhn, I., Perşoiu, A., Peyron, O., Sadori, L., Valero-Garcés, B., Wulf, S., Zanchetta, G., 2014. A compilation of Western European terrestrial records 60–8 ka BP: towards an understanding of latitudinal climatic gradients. Quaternary Science Reviews 106, 167–185. https://doi.org/10.1016/j.quascirev.2014.06.030

Moreno-Sanchez, R., Sayadyan, H.Y., 2005. Evolution of the forest cover in Armenia. int. forest. rev. 7, 113–127. https://doi.org/10.1505/ifor.2005.7.2.113

Naafs, B.D.A., Gallego-Sala, A.V., Inglis, G.N., Pancost, R.D., 2017a. Refining the global branched glycerol dialkyl glycerol tetraether (brGDGT) soil temperature calibration. Organic Geochemistry 106, 48–56. https://doi.org/10.1016/j.orggeochem.2017.01.009

Naafs, B.D.A., Inglis, G.N., Blewett, J., McClymont, E.L., Lauretano, V., Xie, S., Evershed, R.P., Pancost, R.D., 2019. The potential of biomarker proxies to trace climate, vegetation, and biogeochemical processes in peat: A review. Global and Planetary Change 179, 57–79. https://doi.org/10.1016/j.gloplacha.2019.05.006

Naafs, B.D.A., Inglis, G.N., Zheng, Y., Amesbury, M.J., Biester, H., Bindler, R., Blewett, J., Burrows, M.A., del Castillo Torres, D., Chambers, F.M., Cohen, A.D., Evershed, R.P., Feakins, S.J., Gałka, M., Gallego-Sala, A., Gandois, L., Gray, D.M., Hatcher, P.G., Honorio Coronado, E.N., Hughes, P.D.M., Huguet, A., Könönen, M., Laggoun-Défarge, F., Lähteenoja, O., Lamentowicz, M., Marchant, R., McClymont, E., Pontevedra-Pombal, X., Ponton, C., Pourmand, A., Rizzuti, A.M., Rochefort, L., Schellekens, J., De Vleeschouwer, F., Pancost, R.D., 2017b. Introducing global peat-

specific temperature and pH calibrations based on brGDGT bacterial lipids. Geochimica et Cosmochimica Acta 208, 285–301. https://doi.org/10.1016/j.gca.2017.01.038

Palmisano, A., Bevan, A., Kabelindde, A., Roberts, N., Shennan, S., 2021a. Long-Term Demographic Trends in Prehistoric Italy: Climate Impacts and Regionalised Socio-Ecological Trajectories. J World Prehist 34, 381–432. https://doi.org/10.1007/s10963-021-09159-3

Palmisano, A., Lawrence, D., de Gruchy, M.W., Bevan, A., Shennan, S., 2021b. Holocene regional population dynamics and climatic trends in the Near East: A first comparison using archaeo-demographic proxies. Quaternary Science Reviews 252, 106739. https://doi.org/10.1016/j.quascirev.2020.106739

Panagiotopoulos, K., Aufgebauer, A., Schäbitz, F., Wagner, B., 2013. Vegetation and climate history of the Lake Prespa region since the Lateglacial. Quaternary International 293, 157–169. https://doi.org/10.1016/j.quaint.2012.05.048

Parmegiani, N., Poscolieri, M., 2003. DEM data processing for a landscape archaeology analysis (Lake Sevan-Armenia). International archives of photogrammetry remote sensing and spatial information sciences 34, 255–258.

Peñalba, M.C., Arnold, M., Guiot, J., Duplessy, J.-C., De Beaulieu, J.-L., 1996. Termination of the Last Glaciation in the Iberian Peninsula Inferred from the Pollen Sequence of Quintanar de la Sierra. Quaternary Research 48, 205–214.

Peyron, O., Bégeot, C., Brewer, S., Heiri, O., Magny, M., Millet, L., Ruffaldi, P., Van Campo, E., Yu, G., 2005. Late-Glacial climatic changes in Eastern France (Lake Lautrey) from pollen, lake-levels, and chironomids. Quat. res. 64, 197–211. https://doi.org/10.1016/j.yqres.2005.01.006

Peyron, O., Combourieu-Nebout, N., Brayshaw, D., Goring, S., Andrieu-Ponel, V., Desprat, S., Fletcher, W., Gambin, B., Ioakim, C., Joannin, S., Kotthoff, U., Kouli, K., Montade, V., Pross, J., Sadori, L., Magny, M., 2017. Precipitation changes in the Mediterranean basin during the Holocene from terrestrial and marine pollen records: a model–data comparison. Clim. Past 13, 249–265. https://doi.org/10.5194/cp-13-249-2017

Peyron, O., Magny, M., Goring, S., Joannin, S., de Beaulieu, J.-L., Brugiapaglia, E., Sadori, L., Garfi, G., Kouli, K., Ioakim, C., Combourieu-Nebout, N., 2013. Contrasting patterns of climatic changes during the Holocene across the Italian Peninsula reconstructed from pollen data. Clim. Past 9, 1233–1252. https://doi.org/10.5194/cp-9-1233-2013

Qian, H., Hongyan, L., Shilei, Y., Weihua, Y., Zhaoliang, S., 2019. Differentiated roles of mean climate and climate stability on post-glacial birch distributions in northern China. The Holocene 29, 1758–1766. https://doi.org/10.1177/0959683619862038

Quereda Sala, J., Gil Olcina, A., Perez Cuevas, A., Olcina Cantos, J., Rico Amoros, A., Montón Chiva, E., 2000. Climatic Warming in the Spanish Mediterranean: Natural Trend or Urban Effect. Climatic Change 46, 473–483. https://doi.org/10.1023/A:1005688608044

Quézel, P., Médail, F., 2003. Ecologie et biogéographie des foréts du bassin méditerranéen, Environnment. Elsevier.

Raberg, J.H., Harning, D.J., Crump, S.E., de Wet, G., Blumm, A., Kopf, S., Geirsdóttir, Á., Miller, G.H., Sepúlveda, J., 2021. Revised fractional abundances and warm-season temperatures substantially improve brGDGT calibrations in lake sediments. Biogeosciences 18, 3579–3603. https://doi.org/10.5194/bg-2021-16

Rasmussen, S.O., Bigler, M., Blockley, S.P., Blunier, T., Buchardt, S.L., Clausen, H.B., Cvijanovic, I., Dahl-Jensen, D., Johnsen, S.J., Fischer, H., Gkinis, V., Guillevic, M., Hoek, W.Z., Lowe, J.J., Pedro, J.B., Popp, T., Seierstad, I.K., Steffensen, J.P., Svensson, A.M., Vallelonga, P., Vinther, B.M., Walker, M.J.C., Wheatley, J.J., Winstrup, M., 2014. A stratigraphic framework for abrupt climatic changes during the Last Glacial period based on three synchronized Greenland ice-core records: refining and extending the INTIMATE event stratigraphy. Quaternary Science Reviews 106, 14–28. https://doi.org/10.1016/j.quascirev.2014.09.007

Rea, B.R., Pellitero, R., Spagnolo, M., Hughes, P., Ivy-Ochs, S., Renssen, H., Ribolini, A., Bakke, J., Lukas, S., Braithwaite, R.J., 2020. Atmospheric circulation over Europe during the Younger Dryas. Sci. Adv. 6, eaba4844. https://doi.org/10.1126/sciadv.aba4844

Regattieri, E., Zanchetta, G., Drysdale, R.N., Isola, I., Hellstrom, J.C., Dallai, L., 2014. Lateglacial to Holocene trace element record (Ba, Mg, Sr) from Corchia Cave (Apuan Alps, central Italy): paleoenvironmental implications: Trace element record from Corchia Cave, central Italy. J. Quaternary Sci. 29, 381–392. https://doi.org/10.1002/jqs.2712

Renssen, H., Isarin, R.F.B., 2001. The two major warming phases of the last deglaciation at ~14.7 and ~11.5 ka cal BP in Europe: climate reconstructions and AGCM experiments. Global and Planetary Change 30, 117–153. https://doi.org/10.1016/S0921-8181(01)00082-0

Rhanem, M., 2008. Quelques résultats obtenus par l'analyse de l'information mutuelle sur les observations phyto-écologiques recueillies dans la vallée des Aït- Bou-Guemmez (Haut Atlas, Maroc). information ..., Quaderni di Botanica Ambientale e Applicata, 19, 183–201.

Roberts, C.N., Woodbridge, J., Palmisano, A., Bevan, A., Fyfe, R., Shennan, S., 2019. Mediterranean landscape change during the Holocene: Synthesis, comparison and regional trends in population, land cover and climate. The Holocene 29, 923–937. https://doi.org/10.1177/0959683619826697

Roberts, N., 2013. The Holocene: An Environmental History, Wiley-Blackwell. ed. Oxford.

Roberts, N., Eastwood, W.J., Kuzucuoğlu, C., Fiorentino, G., Caracuta, V., 2011. Climatic, vegetation and cultural change in the eastern Mediterranean during the mid-Holocene environmental transition. The Holocene 21, 147–162. https://doi.org/10.1177/0959683610386819

Roberts, N., Moreno, A., Valero-Garcés, B.L., Corella, J.P., Jones, M., Allcock, S., Woodbridge, J., Morellón, M., Luterbacher, J., Xoplaki, E., Türkeş, M., 2012. Palaeolimnological evidence for an east–west climate see-saw in the Mediterranean since AD 900. Global and Planetary Change, Perspectives on Climate in Medieval Time 84–85, 23–34. https://doi.org/10.1016/j.gloplacha.2011.11.002

Roberts, N., Reed, J.M., Leng, M.J., Kuzucuoğlu, C., Fontugne, M., Bertaux, J., Woldring, H., Bottema, S., Black, S., Hunt, E., Karabiyikoğlu, M., 2001. The tempo of Holocene climatic change in the eastern Mediterranean region: new high-resolution crater-lake sediment data from central Turkey. The Holocene 11, 721–736. https://doi.org/10.1191/09596830195744

Robles, M., Peyron, O., Brugiapaglia, E., Ménot, G., Dugerdil, L., Ollivier, V., Ansanay-Alex, S., Develle, A.-L., Tozalakyan, P., Meliksetian, K., Sahakyan, K., Sahakyan, L., Perello, B., Badalyan, R., Colombié, C., Joannin, S., 2022. Impact of climate changes on vegetation and human societies during the Holocene in the South Caucasus (Vanevan, Armenia): A multiproxy approach including pollen, NPPs and brGDGTs. Quaternary Science Reviews 277, 107297. https://doi.org/10.1016/j.quascirev.2021.107297

Russell, J.M., Hopmans, E.C., Loomis, S.E., Liang, J., Sinninghe Damsté, J.S., 2018. Distributions of 5- and 6-methyl branched glycerol dialkyl glycerol tetraethers (brGDGTs) in East African lake sediment: Effects of temperature, pH, and new lacustrine paleotemperature calibrations. Organic Geochemistry 117, 56–69. https://doi.org/10.1016/j.orggeochem.2017.12.003

Ryabogina, N., Borisov, A., Idrisov, I., Bakushev, M., 2019. Holocene environmental history and populating of mountainous Dagestan (Eastern Caucasus, Russia). Quaternary International 516, 111–126. https://doi.org/10.1016/j.quaint.2018.06.020

Sabatier, P., Dezileau, L., Colin, C., Briqueu, L., Bouchette, F., Martinez, P., Siani, G., Raynal, O., Grafenstein, U.V., 2012. 7000 years of paleostorm activity in the NW Mediterranean Sea in response to Holocene climate events. Quaternary Research 77, 1–11. https://doi.org/10.1016/j.yqres.2011.09.002

Sadori, L., 2018. The Lateglacial and Holocene vegetation and climate history of Lago di Mezzano (central Italy). Quaternary Science Reviews 202, 30–44. https://doi.org/10.1016/j.quascirev.2018.09.004

Sadori, L., Koutsodendris, A., Panagiotopoulos, K., Masi, A., Bertini, A., Combourieu-Nebout, N., Francke, A., Kouli, K., Joannin, S., Mercuri, A.M., Peyron, O., Torri, P., Wagner, B., Zanchetta, G., Sinopoli, G., Donders, T.H., 2016. Pollen-based paleoenvironmental and paleoclimatic change at Lake Ohrid (south-eastern Europe) during the past 500 ka. Biogeosciences 13, 1423–1437. https://doi.org/10.5194/bg-13-1423-2016

Sadori, L., Narcisi, B., 2001. The Postglacial record of environmental history from Lago di Pergusa, Sicily. The Holocene 11, 655–671. https://doi.org/10.1191/09596830195681

Sáenz, J., Rodríguez-Puebla, C., Fernández, J., Zubillaga, J., 2001. Interpretation of interannual winter temperature variations over southwestern Europe. Journal of Geophysical Research: Atmospheres 106, 20641–20651. https://doi.org/10.1029/2001JD900247

Sarmaja-Korjonen, K., Seppänen, A., Bennike, O., 2006. Pediastrum algae from the classic late glacial Bølling Sø site, Denmark: Response of aquatic biota to climate change. Review of Palaeobotany and Palynology 138, 95–107. https://doi.org/10.1016/j.revpalbo.2005.12.003

Sbaffi, L., Wezel, F.C., Curzi, G., Zoppi, U., 2004. Millennial- to centennial-scale palaeoclimatic variations during Termination I and the Holocene in the central Mediterranean Sea. Global and Planetary Change 40, 201–217. https://doi.org/10.1016/S0921-8181(03)00111-5

Sharkov, E., Lebedev, V., Chugaev, A., Zabarinskaya, L., Rodnikov, A., Sergeeva, N., Safonova, I., 2015. The Caucasian-Arabian segment of the Alpine-Himalayan collisional belt: Geology, volcanism and neotectonics. Geoscience Frontiers 6, 513–522. https://doi.org/10.1016/j.gsf.2014.07.001

Shumilovskikh, L.S., Tarasov, P., Arz, H.W., Fleitmann, D., Marret, F., Nowaczyk, N., Plessen, B., Schlütz, F., Behling, H., 2012. Vegetation and environmental dynamics in the

southern Black Sea region since 18kyr BP derived from the marine core 22-GC3. Palaeogeography, Palaeoclimatology, Palaeoecology 337–338, 177–193. https://doi.org/10.1016/j.palaeo.2012.04.015

Sicre, M.-A., Siani, G., Genty, D., Kallel, N., Essallami, L., 2013. Seemingly divergent sea surface temperature proxy records in the central Mediterranean during the last deglacial. Climate of the Past 9, 1375–1383. https://doi.org/10.5194/cpd-9-683-2013

Sinninghe Damsté, J.S., Rijpstra, W.I.C., Foesel, B.U., Huber, K.J., Overmann, J., Nakagawa, S., Kim, J.J., Dunfield, P.F., Dedysh, S.N., Villanueva, L., 2018. An overview of the occurrence of ether- and ester-linked iso-diabolic acid membrane lipids in microbial cultures of the Acidobacteria: Implications for brGDGT paleoproxies for temperature and pH. Organic Geochemistry 124, 63–76. https://doi.org/10.1016/j.orggeochem.2018.07.006

Sinninghe Damsté, J.S., C. Hopmans, E., D. Pancost, R., Schouten, S., J. Geenevasen, J.A., 2000. Newly discovered non-isoprenoid glycerol dialkyl glycerol tetraether lipids in sediments. Chemical Communications 0, 1683–1684. https://doi.org/10.1039/B004517I

Solomina, O.N., Bradley, R.S., Hodgson, D.A., Ivy-Ochs, S., Jomelli, V., Mackintosh, A.N., Nesje, A., Owen, L.A., Wanner, H., Wiles, G.C., Young, N.E., 2015. Holocene glacier fluctuations. Quaternary Science Reviews 111, 9–34. https://doi.org/10.1016/j.quascirev.2014.11.018

Sorrel, P., Mathis, M., 2016. Mid- to late-Holocene coastal vegetation patterns in Northern Levant (Tell Sukas, Syria): Olive tree cultivation history and climatic change. The Holocene 26, 858–873. https://doi.org/10.1177/0959683615622555

Stevens, L.R., Ito, E., Schwalb, A., Wright, H.E., 2006. Timing of Atmospheric Precipitation in the Zagros Mountains Inferred from a Multi-Proxy Record from Lake Mirabad, Iran. Quat. res. 66, 494–500. https://doi.org/10.1016/j.yqres.2006.06.008

Stevens, L.R., Wright, H.E., Ito, E., 2001. Proposed changes in seasonality of climate during the Lateglacial and Holocene at Lake Zeribar, Iran. The Holocene 11, 747–755. https://doi.org/10.1191/09596830195762

Stockhecke, M., Timmermann, A., Kipfer, R., Haug, G.H., Kwiecien, O., Friedrich, T., Menviel, L., Litt, T., Pickarski, N., Anselmetti, F.S., 2016. Millennial to orbital-scale variations of drought intensity in the Eastern Mediterranean. Quaternary Science Reviews 133, 77–95. https://doi.org/10.1016/j.quascirev.2015.12.016

Sun, Q., Chu, G., Liu, M., Xie, M., Li, S., Ling, Y., Wang, X., Shi, L., Jia, G., Lü, H., 2011. Distributions and temperature dependence of branched glycerol dialkyl glycerol

tetraethers in recent lacustrine sediments from China and Nepal. J. Geophys. Res. 116, G01008. https://doi.org/10.1029/2010JG001365

Tinner, W., van Leeuwen, J.F.N., Colombaroli, D., Vescovi, E., van der Knaap, W.O., Henne, P.D., Pasta, S., D'Angelo, S., La Mantia, T., 2009. Holocene environmental and climatic changes at Gorgo Basso, a coastal lake in southern Sicily, Italy. Quaternary Science Reviews 28, 1498–1510. https://doi.org/10.1016/j.quascirev.2009.02.001

Trigo, R.M., Pozo-Vázquez, D., Osborn, T.J., Castro-Díez, Y., Gámiz-Fortis, S., Esteban-Parra, M.J., 2004. North Atlantic oscillation influence on precipitation, river flow and water resources in the Iberian Peninsula. International Journal of Climatology 24, 925–944. https://doi.org/10.1002/joc.1048

Tzedakis, P.C., 2007. Seven ambiguities in the Mediterranean palaeoenvironmental narrative. Quaternary Science Reviews 26, 2042–2066. https://doi.org/10.1016/j.quascirev.2007.03.014

Van Geel, B., 2002. Non-Pollen Palynomorphs, in: Smol, J.P., Birks, H.J.B., Last, W.M., Bradley, R.S., Alverson, K. (Eds.), Tracking Environmental Change Using Lake Sediments, Developments in Paleoenvironmental Research. Springer Netherlands, Dordrecht, pp. 99–119. https://doi.org/10.1007/0-306-47668-1_6

Van Geel, B., Andersen, S.T., 1988. Fossil ascopores of the parasitic fungus Ustulina deusta in Eemian deposits in Denmark. Review of Palaeobotany and Palynology 56, 89–93. https://doi.org/10.1016/0034-6667(88)90076-0

van Geel, B., Heijnis, H., Charman, D.J., Thompson, G., Engels, S., 2014. Bog burst in the eastern Netherlands triggered by the 2.8 kyr BP climate event. The Holocene 24, 1465–1477. https://doi.org/10.1177/0959683614544066

Van Zeist, W., Bakker-Heeres, J. a. H., 1984. Archaeobotanical studies in the Levant. 3. Late-Palaeolithic Mureybit. Palaeohistoria 171–199.

Van Zeist, W., Woldring, H., Stapert, D., 1975. Late Quaternary vegetation and climate of southwestern Turkey. Palaeohistoria 17, 53–143.

Vescovi, E., Ammann, B., Ravazzi, C., Tinner, W., 2010. A new Late-glacial and Holocene record of vegetation and fire history from Lago del Greppo, northern Apennines, Italy. Veget Hist Archaeobot 19, 219–233. https://doi.org/10.1007/s00334-010-0243-5

Vogiatzakis, I., 2012. Mediterranean Mountain Environments, Wiley-Blackwell. ed. Chichester, UK.

Wallace, J.M., Gutzler, D.S., 1981. Teleconnections in the Geopotential Height Field during the Northern Hemisphere Winter. Monthly Weather Review 109, 784–812. https://doi.org/10.1175/1520-0493(1981)109<0784:TITGHF>2.0.CO;2

Watson, B.I., 2018. Temperature variations in the southern Great Lakes during the last deglaciation: Comparison between pollen and GDGT proxies. Quaternary Science Reviews 15.

Weijers, J.W.H., Schouten, S., Hopmans, E.C., Geenevasen, J.A.J., David, O.R.P., Coleman, J.M., Pancost, R.D., Sinninghe Damste, J.S., 2006a. Membrane lipids of mesophilic anaerobic bacteria thriving in peats have typical archaeal traits. Environ Microbiol 8, 648–657. https://doi.org/10.1111/j.1462-2920.2005.00941.x

Weijers, J.W.H., Schouten, S., Spaargaren, O.C., Sinninghe Damsté, J.S., 2006b. Occurrence and distribution of tetraether membrane lipids in soils: Implications for the use of the TEX86 proxy and the BIT index. Organic Geochemistry 37, 1680–1693. https://doi.org/10.1016/j.orggeochem.2006.07.018

Weijers, J.W.H., Schouten, S., van den Donker, J.C., Hopmans, E.C., Sinninghe Damsté, J.S., 2007. Environmental controls on bacterial tetraether membrane lipid distribution in soils. Geochimica et Cosmochimica Acta 71, 703–713. https://doi.org/10.1016/j.gca.2006.10.003

Weiss, E., Kislev, M.E., Hartmann, A., 2006. Autonomous Cultivation Before Domestication. Science 312, 1608.

White, C.E., Makarewicz, C.A., 2012. Harvesting practices and early Neolithic barley cultivation at el-Hemmeh, Jordan. Veget Hist Archaeobot 21, 85–94. https://doi.org/10.1007/s00334-011-0309-z

Wick, L., Lemcke, G., Sturm, M., 2003. Evidence of Lateglacial and Holocene climatic change and human impact in eastern Anatolia: high-resolution pollen, charcoal, isotopic and geochemical records from the laminated sediments of Lake Van, Turkey. The Holocene 13, 665–675. https://doi.org/10.1191/0959683603hl653rp

Willcox, G., Buxo, R., Herveux, L., 2009. Late Pleistocene and early Holocene climate and the beginnings of cultivation in northern Syria. The Holocene 19, 151–158. https://doi.org/10.1177/0959683608098961

Zeist, W. van, Roller, G.J. de, 1994. The plant husbandry of aceramic Çayönü, SE Turkey. Palaeohistoria 65–96.

Zhao, J., Huang, Y., Yao, Y., An, Z., Zhu, Y., Lu, H., Wang, Z., 2020. Calibrating branched GDGTs in bones to temperature and precipitation: Application to Alaska chronological

sequences. Quaternary Science Reviews 240, 106371. https://doi.org/10.1016/j.quascirev.2020.106371

Zielhofer, C., Fletcher, W.J., Mischke, S., De Batist, M., Campbell, J.F.E., Joannin, S., Tjallingii, R., El Hamouti, N., Junginger, A., Stele, A., Bussmann, J., Schneider, B., Lauer, T., Spitzer, K., Strupler, M., Brachert, T., Mikdad, A., 2017. Atlantic forcing of Western Mediterranean winter rain minima during the last 12,000 years. Quaternary Science Reviews 157, 29–51. https://doi.org/10.1016/j.quascirev.2016.11.037

APPENDIXES

Appendix 1. Detailed description of pollen data of Vanevan

Pollen sequence and terrestrial vegetation dynamics

PAZ 1 (600-566 cm; ca. 9700-9400 cal BP) records low pollen concentrations (ca. 1200-3200 grains.cm^{-3}) and an open-ground vegetation. Herbaceous pollen taxa are dominated by Poaceae, Cichorioideae and Chenopodiaceae. Other herbaceous pollen taxa occur with low percentages, such as *Artemisia,* Asteroideae, *Polygonum, Thalictrum*, Brassicaceae and Apiaceae. Arboreal vegetation represents 8% and is characterized by the occurrence of *Juniperus,* and mesophilous trees with *Betula*, *Carpinus betulus* and *Quercus*.

PAZ 2 (566-436 cm; ca. 9400-8600 cal BP) shows an increase of pollen concentration (ca. 10000-75000 grains.cm^{-3}) and an open steppic vegetation. Poaceae and Chenopodiaceae remains stable, *Artemisia* increases (ca. 10%) while Cichorioideae decreases. Among the herbaceous pollen taxa, *Polygonum* declines and Lamiaceae and Rosaceae develop. Concerning arboreal pollen taxa, *Carpinus betulus* disappears whereas *Quercus* remains steady. Noteworthy is that AP total increases thanks to *Betula* increase (ca. 5%), to the apparition of *Salix* followed by *Hippophae* at 8900 cal BP. The zone is also marked by the presence of shrubland taxa with *Juniperus* and *Ephedra distachya*-type.

PAZ 3 (436-153 cm; ca. 8600-5100 cal BP) corresponds to the maximum of arboreal pollen percentages with an average of 18%, and diversity. This zone is also characterized by a progressive decrease in Poaceae until 5900 cal BP, ranging from 38 to 19%. The pollen concentration increases up to around 58000 grains.cm^{-3}, then decline to 17000 grains.cm^{-3} at 5900 cal BP when percentages of trees and Poaceae also strongly decrease. The pollen concentration finally increases to reach 100000 grains.cm^{-3}. The zone is divided into 4 subzones.

PAZ 3a (436-326 cm; ca 8600-8000 cal BP) records a decrease of Poaceae, an increase of *Artemisia* while Chenopodiaceae remains stable. Concerning other herbaceous pollen taxa with low percentages (<5%), *Cerealia*-type and Caryophyllaceae appears. The proportion of shrubs decline with the disappearance of *Ephedra distachya*-type and the decrease of *Juniperus*.

In contrast, trees are in expansion, *Betula* remains steady, *Quercus* and *Ulmus* increase, *Fraxinus* appears followed by *Carpinus orientalis* at 8400 cal BP and finally *Hippophae* and *Pinus* also acquired a continuous record whereas *Salix* pollen is scarce.

PAZ 3b (326-256 cm; ca. 8000-7600 cal BP) shows a decrease of Poaceae, *Artemisia*, and Chenopodiaceae. Herbaceous pollen taxa present with low percentages (<5%), *Ranunculus*-type and *Rumex*-type appear. Arboreal pollen are well recorded: *Quercus*, *Juniperus* and *Fraxinus* increases, *Carpinus betulus* appears while the other arboreal taxa remain stable. In contrast, *Betula* starts to decline.

PAZ 3c (*256-169 cm; ca. 7600-5200 cal BP*) is marked by changes in herbaceous taxa. Poaceae regresses to a minimum until 5900 cal BP, while Chenopodiaceae, *Artemisia,* Cichorioideae and Asteroideae increase. Other herbs such as Brassicaceae, Caryophyllaceae and *Ranunculus*-type rise slightly. *Rumex*-type is still recorded and a peak of *Alchemilla* (7%) is attested around 5900 cal BP. At the end of this zone, Poaceae rebounds and expands with higher percentages than before. Considering trees, *Corylus* develops, *Ulmus* and *Fraxinus* decrease and *Hippophae* disappears. The other arboreal taxa remain steady, except at 5600 cal BP, when a significant drop occurs on all trees.

PAZ 3d (169-153 cm; ca. 5200-5100 cal BP) records an increase of Poaceae (ca. 40%), *Cerealia*-type (7%) and Apiaceae. In contrast, Chenopodiaceae, *Artemisia,* Cichorioideae, Asteroideae and Brassicaceae decrease. Other herbs disappear, such as Caryophyllaceae and *Rumex*-type. The zone is characterized by a decrease of arboreal taxa, primarily related to the reduction of *Quercus* and at the end to the decline of *Betula*. In contrast, *Carpinus betulus* increases.

PAZ 4 (153-98 cm; ca. 5100-4950 cal BP) records a maximum development of Poaceae, with an average of 65%, and a decrease of arboreal pollen taxa, which represent 8%. The pollen concentration declines at 5000 cal BP, reached 24000 grains.cm^{-3}, and then gradually increases to 170000 grains.cm^{-3}. A peak of *Cerealia*-type is attested at 4970 cal BP. Chenopodiaceae and *Artemisia* decrease except at 4990 and 4960 cal BP. Other herbs decline heavily or disappear, such as Cichorioideae, Asteroideae, *Ranunculus*-type, Brassicaceae, *Thalicthrum*, Caryophyllaceae and *Rumex*-type. Considering trees, *Quercus* and *Juniperus* decrease.

PAZ 5 (98-58 cm; ca. 4950- 2350 cal BP) is dominated by herbaceous pollen, especially by Poaceae (ca. 50%) and Chenopodiaceae (ca. 15%). For this zone, arboreal vegetation

represents 9%. The pollen concentration is approximately 94000 grains.cm^{-3}. The zone is divided into 3 subzones.

PAZ 5a (98-88 cm; ca 4950-4300 cal BP) is marked by a peak of Cichorioideae (reaching 34%), a decrease of Poaceae (ca. 53%) and *Cerealia*-type, an increase of Chenopodiaceae while *Artemisia* remains stable. Other herbaceous pollen taxa are present with low percentages, such as Asteroideae, Lamiaceae and *Thalictrum*. Arboreal vegetation is represented by *Quercus*, *Juniperus* and *Pinus.*

PAZ 5b (88-76 cm; ca 4300-3500 cal BP) records a decrease of Poaceae, a significant rise of Chenopodiaceae (ca. 23%) while *Artemisia* remains stable. *Cerealia*-type shows a peak (ca. 14%) at 3300 cal BP, then a drop, and finally a rebound at the end of the zone. Other herbaceous pollen taxa are present with low percentages, such as Asteroideae, Cichorioideae and Apiaceae. Considering trees, *Juniperus* increases slightly while *Quercus* and *Pinus* remain stable.

PAZ 5c (76-58 cm; ca 3500-2350 cal BP) shows an increase of Poaceae (ca. 52%), *Cerealia*-type (ca. 10%; followed by a decline at the end of the zone) and *Artemisia* while Chenopodiaceae diminishes. Herbaceous pollen taxa present with low percentages, Cichorioideae and Apiaceae increases. Considering trees, *Juniperus* decreases slightly and *Quercus* remains stable.

PAZ 6 (58-15 cm; ca. 2350-790 cal BP) records a decrease of Poaceae, Chenopodiaceae, *Artemisia* and a large rise of *Cerealia*-type (ca. 28%), mainly between 1850 and 1450 cal BP, when it reaches 40%. Other herbaceous pollen taxa are present with low percentages (Cichorioideae, Asteroideae, Apiaceae Rosaceae and *Ranunculus*-type). Arboreal vegetation represents 7% and is characterized by the presence of *Quercus*, *Carpinus betulus* and *Juniperus*. A drop in arboreal pollen is recorded around 1450 a cal BP.

Non-Pollen Palynomorphs and hygrophilous vegetation

NPPAZ 1 (600-556 cm; ca. 9700-9400 cal BP) is marked by a large rise of the arbuscular mycorrhizal fungi *Glomus*, and by the presence of Cyperaceae followed by *Myriophyllum spicatum*.

NPPAZ 2 (556-456 cm; ca. 9400-8700 cal BP) is dominated by *Myriophyllum spicatum* and monolete spores which increases progressively. Around 9200 cal BP a peak of Botryococcus *Glomus* and *Sparganium/Typha* is recorded. In contrast, Cyperaceae decreases.

NPPAZ 3 (456-216 cm; ca. 8700-5100 cal BP) is mainly dominated by planktonic Algae while Cyperaceae remains relatively stable. *Glomus* and monolete spores are present in low percentage (ca. 2%). The zone is divided into 3 subzones: *NPPAZ 3a (456-326 cm; 8700-8000 cal BP)* records the highest percentage of planktonic Algae, including *Pediastrum* and *Botryococcus*. *Botryococcus* is initially present and then *Pediastrum* becomes dominant after 8600 cal BP. *NPPAZ 3b (326-216 cm; 8000-6600 cal BP)* shows a decline of *Pediastrum* (ca. 6%) and *Botryococcus* (ca. 3%).

NPPAZ 3c (216-157 cm; ca 6600-5100 cal BP) still records a decrease of *Pediastrum* and *Botryococcus* while Cyperaceae increases slightly. At the end of this zone, *Sparganium/Typha* and *Myriophyllum spicatum* appear.

NPPAZ 4 (157-101 cm; ca. 5100-4950 cal BP) is marked by alternating episodes with/without Cyperaceae and the complete disappearance of *Pediastrum, Botryococcus* and *Glomus*. The first peak of Cyperaceae is accompanied by *Sparganium/Typha* and *Myriophyllum spicatum*. The second and the third peaks are accompanied by the fungi HdV-200. At the end of this zone, Cyperaceae drops and a peak of algae *Mougeotia* is recorded.

NPPAZ 5 (101-76 cm; ca. 4950-3500 cal BP) is largely dominated by monolete spores (ca. 64%). At the beginning of the zone, the percentage of Cyperaceae is low and *Typha latifolia*-type is present. Then, Cyperaceae increases to reach 45%.

NPPAZ 6 (76-15 cm; ca. 3500-790 cal BP) mostly records hygrophilous pollen such as Cyperaceae *Potamogeton, Sparganium/Typha* and *Typha latifolia*-Type. Monolete spore decreases to reach 6%.

ABSTRACT

The Mediterranean area is a key region to study relationships between vegetation dynamics, climate changes and human practices along the time. This region is characterized by high biodiversity, a significant sensitivity to climate changes and a complex and long human history. The Mediterranean Basin is thus a key region for understanding the respective impact of climate changes and human activities on ecosystems since the Holocene. The actual climate and biodiversity crisis raises this topic as a current and major issue that needs to be investigated and debated. This PhD study proposes to document environmental dynamics, climate changes and human practices during the last 15,000 years around the Mediterranean Basin through a multiproxy approach including sediment geochemistry (XRF), pollen, Non-Pollen Palynomorphs (NPPs) and biomarkers molecular (branched Glycerol Dialkyl Glycerol Tetraethers or brGDGTs). Two mountainous areas poorly documented have been studied: the Lesser Caucasus with the Vanevan peat (Armenia) and the Apennines in Southern Italy with the Lake Matese. We investigated (1) modern pollen-vegetation relationships in Armenia and in the Matese Massif, (2) changes in vegetation and human activity around the Vanevan peat and the Lake Matese, (3) climate changes with water-level changes, molecular biomarkers "brGDGTs", and pollen transfer functions (multi-method approach: Modern Analogue Technique, Weighted Averaging Partial Least Squares regression, Random Forest, and Boosted Regression Trees) and (4) relationships between vegetation dynamics, climate changes and human activities during the Lateglacial and the Holocene.

At Vanevan, steppic taxa dominated during the last 9700 years and few trees have grown on shores of the Lake Sevan, even during the Mid-Holocene. At Matese, the vegetation was mainly steppic during the Lateglacial and the Early Holocene, although an increase of deciduous arboreal taxa was recorded during the Bølling–Allerød and finally *Fagus* and Mediterranean taxa develop during the Mid-Late Holocene. The Younger Dryas is well recorded in the Matese pollen assemblages. Climate reconstructions based on pollen and brGDGTs are complementary and they each have their advantages and biases. At Vanevan, climate reconstructions show an arid and cold Early Holocene, a more humid and warmer Mid Holocene, and a more arid and cooler Late Holocene. Several abrupt events have been detected at 6.2 ka, 5.2 ka, 4.2 ka, 2.8 ka and allow us to highlight the atmospheric processes in the Caucasus and the Near East. At Matese, the Bølling–Allerød is characterized by warm and humid conditions whereas the Younger Dryas is marked by cold conditions. The Holocene is firstly characterized by humid and warmer conditions followed by a slight decrease of precipitation and temperatures during the Mid-Late Holocene. Our study reveals a significant impact of abrupt climate changes on populations in the Near East and the Caucasus even for the recent periods. In the South Caucasus, the arid climate events are consistent with the population abandonment phases and changes in the agricultural practices around the Lake Sevan. In Southern Italy, anthropogenic indicators are less important, and the opening of forests is detected during the last 2800-2600 years and seem associated to human practices.

Keywords: Paleoecology; Paleoclimate quantitative reconstructions; Pollen; molecular biomarkers brGDGTs, Water level changes; Human impact; Agriculture; Abrupt climate events; Lateglacial; Holocene